The Scientific World Journal

Recent Development in Partial Differential Equations and Their Applications

Guest Editors: Hossein Jafari, Chaudry M. Khalique, and Dumitru Baleanu

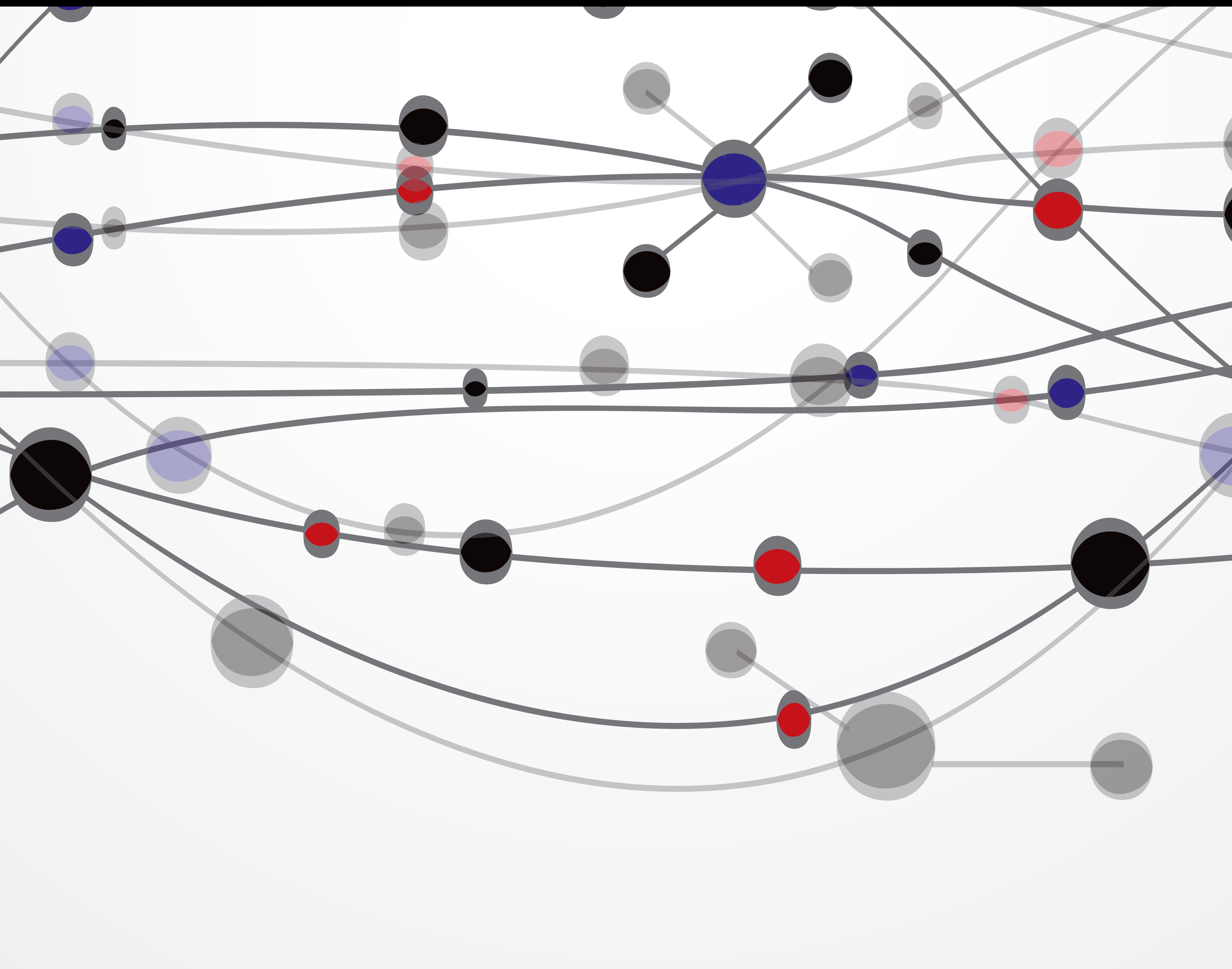

Recent Development in Partial Differential Equations and Their Applications

The Scientific World Journal

Recent Development in Partial Differential Equations and Their Applications

Guest Editors: Hossein Jafari, Chaudry M. Khalique, and Dumitru Baleanu

Contents

Hindawi Publishing Corporation
The Scientific World Journal
Volume 2014, Article ID 243461, 1 page
http://dx.doi.org/10.1155/2014/243461

Editorial

Recent Development in Partial Differential Equations and Their Applications

Hossein Jafari,[1] Chaudry M. Khalique,[2] and Dumitru Baleanu[3]

[1] *Department of Mathematics, University of Mazandaran, Babolsar 47416-95447, Iran*
[2] *International Institute for Symmetry Analysis and Mathematical Modelling, Department of Mathematical Sciences, North-West University, Mafikeng Campus, Private Bag Box X2046, Mmabatho 2735, South Africa*
[3] *Department of Mathematics, Çankaya University, Balgat, 06530 Ankara, Turkey*

Correspondence should be addressed to Hossein Jafari; jafari@umz.ac.ir

Received 8 May 2014; Accepted 8 May 2014; Published 25 June 2014

In recent years, the partial differential equations, both fractional and integer orders, have been recognized as a powerful modeling methodology. They are inspired by problems which arise in diverse fields such as biology, fluid dynamics, physics, differential geometry, control theory, materials science, and engineering.

The purpose of this special issue is to report and review some recent developments in methods and applications of partial differential equations. The majority of the papers contained in this special issue are based on areas of research ranging from functional analytic techniques and singularity methods as well as numerical methods that are applied to both partial and ordinary differential equations. There are papers which deal with fractional partial differential equations and in addition papers analyzing equations that arise in engineering as well as classical and fluid mechanics.

This special issue contains the papers addressing the recent theoretical advances and experimental results on the topics such as operational calculus and inverse differential operators, global existence and energy decay rates for a Kirchhoff-type wave equation, nonsymmetric system of Keyfitz-Kranzer type, different methods for numerical solution, recent progress on nonlinear Schrödinger systems with quadratic interactions, upper semicontinuity of pullback attractors, numerical modeling, mean-variance portfolio selection, a novel iterative scheme, and the iterative methods of linearization.

The guest editors very much hope that the papers published in this special issue will be useful to a large community of researchers and will arouse further research in the topics presented as well as in the connected fields.

Acknowledgments

The guest editors would like to express their gratitude to all authors who send their papers to our special issue. Also, we would like to thank to the referees for their valuable efforts. We would also like to thank the editorial board members of this journal for their support and help throughout the preparation of this special issue.

Hossein Jafari
Chaudry Masood Khalique
Dumitru Baleanu

Hindawi Publishing Corporation
The Scientific World Journal
Volume 2014, Article ID 417486, 15 pages
http://dx.doi.org/10.1155/2014/417486

Research Article

HPM-Based Dynamic Sparse Grid Approach for Perona-Malik Equation

Shu-Li Mei[1] and De-Hai Zhu[2]

[1] *College of Information and Electrical Engineering, China Agricultural University, Beijing 100083, China*
[2] *Key Laboratory of Agricultural Information Acquisition Technology, Ministry of Agriculture, China Agricultural University, Beijing 100083, China*

Correspondence should be addressed to Shu-Li Mei; meishuli@163.com

Received 24 January 2014; Accepted 2 March 2014; Published 23 June 2014

Academic Editors: D. Baleanu, H. Jafari, and C. M. Khalique

The Perona-Malik equation is a famous image edge-preserved denoising model, which is represented as a nonlinear 2-dimension partial differential equation. Based on the homotopy perturbation method (HPM) and the multiscale interpolation theory, a dynamic sparse grid method for Perona-Malik was constructed in this paper. Compared with the traditional multiscale numerical techniques, the proposed method is independent of the basis function. In this method, a dynamic choice scheme of external grid points is proposed to eliminate the artifacts introduced by the partitioning technique. In order to decrease the calculation amount introduced by the change of the external grid points, the Newton interpolation technique is employed instead of the traditional Lagrange interpolation operator, and the condition number of the discretized matrix different equations is taken into account of the choice of the external grid points. Using the new numerical scheme, the time complexity of the sparse grid method for the image denoising is decreased to $O(4^{J+2j})$ from $O(4^{3J})$, $(j \ll J)$. The experiment results show that the dynamic choice scheme of the external gird points can eliminate the boundary effect effectively and the efficiency can also be improved greatly comparing with the classical interval wavelets numerical methods.

1. Introduction

The nonlinear difference equation has been widely used in various fields in the past few decades such as the option pricing [1], stochastic analysis [2], hydrodynamics [3], and image processing [4]. Many powerful and efficient methods to find analytic solutions of nonlinear equation have drawn a lot of interest by a diverse group of scientists. These methods include the tanh-function method, the extended tanh-function method [5, 6], the sine-cosine method [7], the variational iteration method [8, 9], the homotopy perturbation method [10, 11], and Exp-function method [12].

As an excellent medical image processing model, the Perona-Malik model [4] has been widely used in image denoising in recent years. Perona-Malik model is a nonlinear 2-dimension partial differential equation in itself, which overcomes the drawback of the scale-space technique introduced by Witkin which involves generating coarser resolution images by convolving the original image with a Gaussian kernel. In this approach, a new definition of scale-space was suggested, and a class of algorithms was introduced; then accurately the locations of the "semantically meaningful" edges at coarse scales using a diffusion process can be obtained; that is, a high quality edge detector which successfully exploits global information was obtained with this new method.

It is very difficult to find the exact analytical solution of the Perona-Malik model as it is a nonlinear partial differential equation. Conventional methods for numerical solutions of partial differential equations mostly fall into three classes: finite difference methods, finite element methods, and spectral methods. Briefly, the finite difference method consists in defining the different unknowns by their values on a discrete grid and in replacing differential operators by difference operators using neighboring points. In the finite element method, the equations are integrated against a set of linear independent test functions with small compact support, and the solution is considered as a linear combination of this set of test functions. In spectral methods, the unknown functions are developed along a basis of functions having global support. This development is truncated to a finite number of terms which satisfy a system of coupled ordinary differential equations in time. The advantage of using either of the first two numerical techniques is the simplicity in adapting to complex geometries, while the main advantage of spectral methods is the greater accuracy [13, 14].

If the solution of a partial differential equation is regular, any of the three above-mentioned numerical techniques can be applied successfully. It is obvious that most of the images are irregular. This makes the Perona-Malik equation particularly difficult to resolve numerically using the above-mentioned methods. Spectral methods are not easily implemented because the irregularity of the solution causes the loss of high accuracy. Moreover, the global support of the basis function induces the well-known Gibbs phenomenon, which appears as the artifacts in images. Wavelet analysis is a new numerical concept which allows one to represent a function in terms of a set of basis function, called wavelets, which are localized both in location and in scale. Up to now, the finite difference method is the primary numerical algorithm for Perona-Malik model, which can bring artifact into the images due to the nonsmoothness of the basis function of the finite difference method [15, 16] as has been said before. The multilevel wavelet numerical method for the nonlinear PDEs has been proposed over ten years, which can take full advantage of the adaptability of the wavelet analysis [17]. The artifacts in image can be eliminated with the wavelet numerical algorithm instead of the finite difference method, as wavelet basis function possesses many excellent properties such as smoothness and compact support. But the support range of wavelet function is much wider than the basis function in the finite difference method [18, 19]. This leads to a lower computational efficiency of wavelet transform in solving 2D nonlinear PDEs. Besides, most of the wavelet algorithms for solving partial differential equations can handle periodic boundary conditions easily. The treatment of general boundary conditions is still an open question especially in solving the nonlinear problems. Construction of the wavelet defined in the interval (interval wavelet) is another good choice to handle the boundary conditions [20, 21]. Compared to the interpolation wavelet, a linear mapping between the external collocation points and the interval ones was supplied in the interval wavelet. The choice of the external collocation points depends on the smoothness and the gradient near each collocation point of the solution of the PDEs. Besides, the condition number of the system of equations obtained by the wavelet collocation method should be taken into account.

To an image with $2^J * 2^J$ pixels ($J \in Z$), the Perona-Malik equation can be discretized into a system of ODEs with 4^J-dimension by the coupling technique of HPM [22–27] and the wavelet collocation method [28, 29]. The corresponding time complexity is about $O(4^{3J})$ with the variational iterative method for the system of ODEs [30]. Obviously, it does not meet the requirement of the larger image processing. Partitioning technique is the effective measure to improve the efficiency of this problem. In other words, the image should be divided into several blocks before denoising to the images. In each of image blocks, the multiple programs can be executed simultaneously. This is similar to the finite element method to some extent. Obviously, if the size of the image blocks is adaptive to whole image, the algorithm efficiency can be improved furthermore. Our research focuses on the general frame of sparse grids and the dynamic choice scheme of the external grid points, which can be used to decrease the boundary effect of each image block, and so, we just talk about the even partitioning in this paper for simplification.

The sparse representation of functions via a linear combination of a small number of basic functions has recently received a lot of attention in several mathematical fields such as approximation theory as well as signal and image processing. The advantage of the sparse grid approach is that it can be extended to nonsmooth solutions by adaptive refinement methods; that is, it can capture the steep waves that appeared in the solution of the PDEs. The main objective of the paper is to present a dynamic choice scheme of the external grid points and a general sparse grid operator for solving the Perona-Malik equation. In other words, the dynamic sparse grid approach provides an adaptive choice scheme on both of the external and the internal grid points. In the presentation of the method, we try to be as general as possible, giving only the main philosophy of the method and leaving some freedom for further exploration of its applications. Both the boundary condition and the condition number are addressed in this work. The first is how to incorporate the dynamic choice scheme on external grid points with the interpolation wavelet basis to construct an effective algorithm of solving partial differential equation. The second is how to construct a stable, accurate, and efficient numerical algorithm for the image denoising model.

2. Construction of Dynamic Sparse Grid Operator

There are many ways to eliminate the boundary effect from the multiscale basis. A simple solution is the even 2-periodical extension $\tilde{f}$ of function $f : [0, 1] \to \mathbb{R}$, which is usually used in image analysis. Unfortunately, this extension generally produces discontinuities at the integers that are indicated by the large transform coefficients near the endpoints 0 and 1. Thus the constructed multiscale basis cannot exactly analyze the boundary behavior of a given function. To solve this problem, the popular method is using special boundary and interior scaling functions such as the interval wavelet to reduce the numerical problem at the boundaries. To the interpolation basis function, the common approach is to define the interpolation basis in the interval with the Lagrange multiplier. In fact, the Lagrange multiplier can be viewed as a map operator, which maps the external collocation points into the definition domain in the multiscale interpolation method. The choice of the amount of the external points relates to the smoothness and gradient near the boundary of the approximated function. In addition, another factor that we should take into account is the condition number of the system of ODEs obtained by the multiscale numerical method.

Obviously, the amount of the external collocation points should be different to different boundary conditions such as the smoothness, gradient near the boundary, and the condition number. In the partition technique about the image processing, the boundary conditions of the different image blocks are obviously different as the randomness of the image. In the representation, we try to give a dynamic choice scheme about the external collocation points to meet the requirement of the image partition technique, in which all above 3 factors are taken into account.

In the presentation of the method, we try to be as general as possible, giving only the main philosophy of the method and leaving some freedom for further exploration of its applications. We illustrate the method using two classical interpolation wavelets: Shannon wavelet and the autocorrelation function of Daubechies scaling functions. But we do not try to predict what wavelet is the best for our algorithm (it is simply impossible, due to the fact that some wavelets work better for some problems and worse for others).

2.1. Basis Functions with Interpolation Property. There are many wavelet functions which possess the interpolation property. The familiar interpolation wavelets family includes Shannon wavelet, Haar wavelet, and Faber-Schauder. Furthermore, it is easy to understand that the autocorrelation function of the orthogonal wavelet function also has the interpolation property. So, the autocorrelation function of the Daubechies scaling function is often employed to construct the wavelet collocation method.

The representation of Shannon wavelet [31, 32] is based upon approximating the Dirac delta function as a band-limited function and is given by

$$\phi(x) = \frac{\sin(\pi x)}{\pi x}. \tag{1}$$

The Shannon wavelet possesses many excellent numerical properties such as interpolating, relative sparse, and orthogonal properties. A perceived disadvantage of (1) is that it tends to zero quite slowly as $|x| \to \infty$. A direct consequence of this is that there are a large number of grid points will contribute to the derivatives calculation of approximated function. For this reason Hoffman et al. [33] have suggested using the Shannon-Gabor wavelet as follows:

$$w(x) = \frac{\sin(\pi x)}{\pi x} \exp\left(-\frac{x^2}{2\sigma^2}\right), \quad \sigma > 0, \tag{2}$$

where σ is the width parameter (or called window size). It has been proofed that (2) can improve the localized and asymptotic behavior of the Shannon scaling function. A consequence of this is that it ensures that derivatives at any one point are more dependent on the neighboring nodal values than on the nodal values further away from the point considered. However, the presence of the Gaussian window destroys the orthogonal properties possessed by the Shannon wavelet, effectively worsening the approximation to a Dirac delta function. In the following, the Shannon wavelet representation of the Dirac delta function is adopted, and it is shown that this representation ensures that the approach is identical to the weighted residual approach.

The autocorrelation functions of compactly supported scaling functions were first studied in the context of the Lagrange iterative interpolation scheme in [34]. Let $\phi(x)$ be the autocorrelation function:

$$\phi(x) = \int_{-\infty}^{\infty} \varphi(y)\varphi(y-x)\,dy, \tag{3}$$

where $\varphi(x)$ is the scaling function which appears in the construction of compactly supported wavelet. The function $\phi(x)$ is exactly the "fundamental function" of the symmetric iterative interpolation scheme introduced in [35]. Thus, there is a simple one-to-one correspondence between iterative interpolation schemes and compactly supported wavelet. In particular, the scaling function corresponding to Daubechies's wavelet with two vanishing moments yields the scheme in [36]. In general, the scaling functions corresponding to Daubechies's wavelets with M vanishing moments lead to the iterative interpolation schemes which use the Lagrange polynomials of degree $2M$. Additional variants of iterative interpolation schemes may be obtained using compactly supported wavelets described in [37].

2.2. Construction of Dynamic Interpolation Wavelet in Interval. According to the definition of the interval wavelet, the interval interpolation basis functions can be expressed as

$$w_{jk}(x) = \begin{cases} \phi\left(2^j x - k\right) + \sum\limits_{n=-L+1}^{-1} a_{nk}\phi\left(2^j x - n\right), \\ \quad k = 0, \ldots, L \\ \phi\left(2^j x - k\right), \\ \quad k = L+1, \ldots, 2^j - L - 1 \\ \phi\left(2^j x - k\right) + \sum\limits_{n=2^j+1}^{2^j+L-1} b_{nk}\phi\left(2^j x - n\right), \\ \quad k = 2^j - L, \ldots, 2^j, \end{cases} \tag{4}$$

where

$$a_{nk} = \prod_{\substack{i=L-1 \\ i \neq k}}^{-1} \frac{x_{j,n} - x_{j,i}}{x_{j,k} - x_{j,i}}, \qquad b_{nk} = \prod_{\substack{i=2^j+1 \\ i \neq k}}^{2^j+1+L} \frac{x_{j,n} - x_{j,i}}{x_{j,k} - x_{j,i}}$$
$$x_{j,k} = k\frac{x_{\max} - x_{\min}}{2^j}, \quad k \in \mathbb{Z}, \tag{5}$$

where L is the amount of the external collocation points; the amount of discrete points in the definition domain is $2^j + 1$ ($j \in \mathbb{Z}$); and $[x_{\min}, x_{\max}]$ is the definition domain of the approximated function. Equations (4) and (5) illustrate that the interval wavelet is derived from the domain extension. The supplementary discrete points in the extended domain are called external points. The value of the approximated function at the external points can be obtained by Lagrange extrapolation method. Using the interval wavelet to approximate a function, the boundary effect can be left in the supplementary domain; that is, the boundary effect is eliminated in the definition domain.

According to (4) and (5), the interval wavelet approximant of the function $f(x)\ \ x \in [x_{\min}, x_{\max}]$ can be expressed as

$$f_j(x) = \sum f_j(x_n)\, w_j(2^j x - n), \qquad x_n = x_{\min} + n\frac{x_{\max} - x_{\min}}{2^j}, \tag{6}$$

where $f_j(x_n)$ is the given value at the discrete point x_n. At the external points, $f_j(x_n)$ can be obtained by extrapolation; that is,

$$f_j(x_n) = \begin{cases} \displaystyle\sum_{k=0}^{L-1}\left(f_j(x_k)\prod_{\substack{i=0\\ i\neq k}}^{L-1}\frac{x_n - x_i}{x_k - x_i}\right), & n = -1, \ldots, -L \\ \displaystyle\sum_{k=2^j-L+1}^{2^j}\left(f_j(x_k)\prod_{\substack{i=2^j-L+1\\ k\neq i}}^{2^j}\frac{x_n - x_i}{x_k - x_i}\right), & n = 2^j + 1, \ldots, 2^j + L. \end{cases} \tag{7}$$

So, the interval wavelet approximant of $f(x)$ can be rewritten as

$$\begin{aligned} f_j(x) = &\sum_{n=-L}^{-1}\left(\sum_{k=0}^{L-1} f_j(x_k)\prod_{i=0}^{L-1}\frac{x_n - x_i}{x_k - x_i}\right)\omega(2^j x - n) \\ &+ \sum_{n=0}^{2^j} f_j(x_k)\,\omega(2^j x - n) \\ &+ \sum_{n=2^j+1}^{2^j+L}\left(\sum_{k=2^j-L}^{2^j} f_j(x_k)\prod_{i=2^j-L}^{2^j}\frac{x_n - x_i}{x_k - x_i}\right)\omega(2^j x - n). \end{aligned} \tag{8}$$

Let

$$LS_L(x_n) = \sum_{k=0}^{L-1} f_j(x_k)\prod_{i=0}^{L-1}\frac{x_n - x_i}{x_k - x_i}, \qquad LE_L(x_n) = \sum_{k=2^j-L}^{2^j} f_j(x_k)\prod_{i=2^j-L}^{2^j}\frac{x_n - x_i}{x_k - x_i}. \tag{9}$$

Then,

$$\begin{aligned} f_j(x) = &\sum_{n=-L}^{-1} LS_L(x_n)\,\omega(2^j x - n) + \sum_{n=0}^{2^j} f_j(x_k)\,\omega(2^j x - n) \\ &+ \sum_{n=2^j+1}^{2^j+L} LE_L(x_n)\,\omega(2^j x - n), \end{aligned} \tag{10}$$

where $LS_L(x_n)$ and $LE_L(x_n)$ correspond to the left and the right external points, respectively. They are obtained by Lagrange extrapolation using the internal collocation points near the boundary. So, the interval wavelet's influence on the boundary effect can be attributed to Lagrange extrapolation. It should be pointed out that we did not care about the reliability of the extrapolation. The only function of the extrapolation is enlarging the definition domain of the given function which can avoid the boundary effect that occurred in the domain. Therefore, we can discuss the choice of L by means of Lagrange inner- and extrapolation error polynomial as follows:

$$R_L(x) = \frac{f^{(L+1)}(\xi)}{(L+1)!}\prod_{i=0}^{L}(x - x_i), \quad \text{for some } \xi \text{ between } x, x_0, \ldots, x_L. \tag{11}$$

Equation (11) indicates that the approximation error is related to both the smoothness and the gradient of the original function near the boundary. Setting different L can satisfy the error tolerance.

2.3. Adaptive Interval Interpolation Wavelet. The interval interpolation wavelet is often used to solve the diffusion PDEs with Neumann boundary conditions. The smoothness and gradient of the PDE's solution usually vary with the time parameter. If the parameter L is a constant, we have to take a bigger value in order to obtain result with higher calculation precision. But the bigger L usually introduces the famous Gibbs phenomenon into the numerical solution, which usually makes the algorithm become invalid. In addition, the bigger L will bring much more calculation. To keep higher numerical precision and save calculation, the best way is to design a procedure that L can vary with the curve's smoothness and gradient dynamically.

In this dynamic procedure, the error estimation equation (11) can be taken as the criterion about L. But in most cases, we cannot know the smoothness and the derivative's order of the original function. This can be solved by substituting the difference coefficient for the derivative. This is coincident with the Newton interpolation equation which is equivalent with Lagrange interpolation equation. In addition, the Lagrange interpolation algorithm has no inheritance which is the key feature of Newton interpolation. So, the basis function has to be calculated repeatedly as interpolation points are added into the calculation, which increases the computation complexity greatly. In contrast to the Lagrange method, the advantage of Newton interpolation method is that the basis function need not be recalculated as one point is added except only one more term which is needed to be added, which reduces the number of computed operations, especially the multiplication. So, it is convenient using the Newton interpolation method to construct the dynamic procedure.

2.3.1. Newton Interpolation. The expression of Newton interpolation can be written as

$$\begin{aligned} N_n(x) = &f(x_0) + (x - x_0) f(x_0, x_1) \\ &+ (x - x_0)(x - x_1) f(x_0, x_1, x_2) + \cdots \end{aligned}$$

$$+\left(x-x_0\right)\left(x-x_1\right)\cdots\left(x-x_{n-1}\right)$$
$$\times f\left(x_0,x_1,\ldots,x_n\right). \tag{12}$$

Substitute the Newton interpolation instead of the Lagrange interpolation into (29), which can be rewritten as

$$\begin{aligned} f_j(x) = {} & \sum_{n=-L}^{-1}\left(NS_L\left(x_n\right)\right)\omega\left(2^jx-n\right) \\ & + \sum_{n=0}^{2^j} f_j\left(x_n\right)\omega\left(2^jx-n\right) \\ & + \sum_{n=2^j+1}^{2^j+L}\left(NE_L\left(x_n\right)\right)\omega\left(2^jx-n\right), \end{aligned} \tag{13}$$

where

$$\begin{aligned} NS_L\left(x_n\right) = {} & f\left(x_0\right)+\left(x_n-x_0\right)f\left(x_0,x_1\right) \\ & +\left(x_n-x_0\right)\left(x_n-x_1\right)f\left(x_0,x_1,x_2\right)+\cdots \\ & +\left(x_n-x_0\right)\left(x_n-x_1\right)\cdots\left(x_n-x_{L-1}\right) \\ & \times f\left(x_0,x_1,\ldots,x_L\right), \\ NS_R\left(x_n\right) = {} & f\left(x_{2^j}\right)+\left(x_n-x_{2^j}\right)f\left(x_{2^j},x_{2^j-1}\right) \\ & +\left(x_n-x_{2^j}\right)\left(x_n-x_{2^j-1}\right)f\left(x_{2^j},x_{2^j-1},x_{2^j-2}\right) \\ & +\cdots+\left(x_n-x_{2^j}\right) \\ & \times\left(x_n-x_{2^j-1}\right)\cdots\left(x_n-x_{2^j-L}\right) \\ & \times f\left(x_{2^j},x_{2^j-1},\ldots,x_{2^j-L}\right). \end{aligned} \tag{14}$$

2.3.2. Relation between the Newton Interpolation Error and the Choice of L. It is well known that the Newton interpolation is equivalent to the Lagrange interpolation. The corresponding error estimation can be expressed as

$$R_n(x)=\left(x-x_0\right)\left(x-x_1\right)\cdots\left(x-x_n\right)f\left(x,x_0,\ldots,x_n\right). \tag{15}$$

And the simplest criterion to terminate the dynamic choice on L is $|R_n(x)| \le T_a$ (T_a is the absolute error tolerance). Obviously, it is difficult to define T_a which should meet the precision requirement of all approximated curves. In fact, the difference coefficient $f(x,x_0,\ldots,x_n)$ can be used directly as the criterion; that is,

$$\left|f\left(x,x_0,\ldots,x_n\right)\right| < \varepsilon. \tag{16}$$

As mentioned above, once the curves with lower order smoothness are approximated by higher order polynomial expression, the errors will become bigger on the contrary. In fact, even if the L is infinite, the computational precision cannot be satisfied except increasing computational complexity. To avoid this, we design the termination procedure of dynamic choice about L as follows:

if $f(x_0,x_1) < T_a$, then $L=1$,

else, if $f(x_0,x_1,x_2) < T_a$ or $f(x_0,x_1,x_2) < f(x_0,x_1)$, then $L=2$,

else, if $f(x_0,x_1,x_2,x_3) < T_a$ or $f(x_0,x_1,x_2,x_3) < f(x_0,x_1,x_2)$, then $L=3$,

2.3.3. L and the Condition Number of the System of Algebraic Equations. In the field of numerical analysis, the condition number of a function with respect to an argument measures how much the output value of the function can change for a small change in the input argument. This is used to measure how sensitive a function is to changes or errors in the input and how many errors in the output result from an error in the input. There is no doubt that the choice of L can change the condition number of the system of algebraic equations discretized by the wavelet interpolation operator or the finite difference method. Therefore, the choice of L should take the condition number into account. In fact, if the condition number $\mathrm{cond}(A)=10^k$, then you may lose up to k digits of accuracy on top of what would be lost to the numerical method due to loss of precision from arithmetic methods [34]. According to the general rule of thumb, the choice should follow the rule as follows:

$$\frac{\mathrm{Cond}\left(A_{L+1}\right)}{\mathrm{Cond}\left(A_L\right)} < 10. \tag{17}$$

2.3.4. Relation between L and Computation Complexity. The computational complexity of interpolation calculation is not proportional to the increasing points. The former is mainly up to the computation amount of $(x-x_0)(x-x_1)\cdots(x-x_n)$ and the derivative operations. Obviously, according to (2), the increase in computational complexity is $O(L^3)$ when the number of extension points L increases by 1. But the computational complexity of adaptively increasing collocation points is related to the different wavelet functions. For the wavelet with compact support property such as Daubechies wavelet and Shannon wavelet, the value of L is impossible to be infinite. For Haar wavelet which has no smoothness property, L can be taken as 0 at most since it need not be extended. For Faber-Schauder wavelet, L can be taken as 1 at most. For Daubechies wavelet, L can be taken as different values according to the order of vanishing moments, but it must be finite. For the wavelets without compact support property, L can take value dynamically, such as Shannon wavelet. The computational complexity of increasing points is mainly up to the wavelet function of itself.

3. Construction of the Multilevel Interpolation Operator Based on the Interval Wavelet

Let the definition domain of the image be $(x_{\min},x_{\max})\times(y_{\min},y_{\max})$; the discretization points can be defined as

$(x_{k_1}^j, y_{k_2}^j)$, where j is a scale parameter and k_1 and k_2 are position parameters. So,

$$x_{k_1}^j = x_{\min} + k_1 \frac{x_{\max} - x_{\min}}{2^j}, \quad y_{k_1}^j = y_{\min} + k_2 \frac{y_{\max} - y_{\min}}{2^j}, \quad j, k_1, k_2 \in \mathbb{Z}. \tag{18}$$

In addition, $w_{k_1,k_2}^{j(m,n)}(x, y)$ denotes the multiscale wavelet function and the corresponding mth and nth derivatives with respect to x and y, respectively. The level set function $\phi(x, y, t)$ and the corresponding derivative function can be discretized as follows:

$$\begin{aligned}\phi^{J(m,n)}(x, y, t) &= \sum_{k_{01}=0}^{1} \sum_{k_{02}=0}^{1} \phi\left(x_{k_{01}}^0, y_{k_{02}}^0\right) w_{k_{01},k_{02}}^{0(m,n)}(x, y) \\ &+ \sum_{j=0}^{J-1} \sum_{k_{11}=0}^{2^j-1} \sum_{k_{12}=0}^{2^j-1} \left[\alpha_{j,k_{11},k_{12}}^1(t)\, w_{2k_{11}+1,2k_{12}}^{j+1(m,n)}(x, y) + \alpha_{j,k_{11},k_{12}}^2(t)\, w_{2k_{11},2k_{12}+1}^{j+1(m,n)}(x, y) + \alpha_{j,k_{11},k_{12}}^3(t) \times w_{2k_{11}+1,2k_{12}+1}^{j+1(m,n)}(x, y)\right],\end{aligned} \tag{19}$$

where j and J are constants, which denote the wavelet scale number and the maximum of the scale number, respectively. $\alpha_{j,k_{11},k_{12}}^1$, $\alpha_{j,k_{11},k_{12}}^2$, and $\alpha_{j,k_{11},k_{12}}^3$ are the wavelet coefficients at the points $(x_{k_1}^j, y_{k_2}^j)$. According to the interpolation wavelet transform theory, the wavelet coefficients can be written as

$$\begin{aligned}\alpha_{j,k_1,k_2}^1 &= \phi\left(x_{j+1,2k_1+1}, y_{j+1,2k_2}\right) - I_j\phi\left(x_{j+1,2k_1+1}, y_{j+1,2k_2}\right), \\ \alpha_{j,k_1,k_2}^2 &= \phi\left(x_{j+1,2k_1}, y_{j+1,2k_2+1}\right) - I_j\phi\left(x_{j+1,2k_1}, y_{j+1,2k_2+1}\right), \\ \alpha_{j,k_1,k_2}^3 &= \phi\left(x_{j+1,2k_1+1}, y_{j+1,2k_2+1}\right) - I_j\phi\left(x_{j+1,2k_1+1}, y_{j+1,2k_2+1}\right),\end{aligned} \tag{20}$$

where I_j denotes the multilevel interpolation operator. In order to obtain the multilevel interpolation operator, it is necessary to express the wavelet coefficients $\alpha_{j,k_1,k_2}^1, \alpha_{j,k_1,k_2}^2$, and α_{j,k_1,k_2}^3 as a weighted sum of u in all of the collocation points in the J level. Therefore, we should give the definition of the restriction operator as follows:

$$R_{k_1,k_2,m_1,m_2}^{l,l,j,j} = \begin{cases} 1, & x_{k_1}^l = x_{m_1}^j,\ y_{k_2}^l = y_{m_2}^j \\ 0, & \text{otherwise.} \end{cases} \tag{21}$$

Using the restriction operator, $u(x_{2k_1+1}^{j+1}, y_{2k_2}^{j+1})$, $u(x_{2k_1}^{j+1}, y_{2k_2+1}^{j+1})$, and $u(x_{2k_1+1}^{j+1}, y_{2k_2+1}^{j+1})$ can be rewritten as

$$\begin{aligned}\phi\left(x_{2k_1+1}^{j+1}, y_{2k_2}^{j+1}\right) &= \sum_{n_1=0}^{2^J} \sum_{n_2=0}^{2^J} R_{2k_1+1,2k_2,n_1,n_2}^{j+1,j+1,J,J} \phi\left(x_{n_1}^J, y_{n_2}^J\right), \\ \phi\left(x_{2k_1}^{j+1}, y_{2k_2+1}^{j+1}\right) &= \sum_{n_1=0}^{2^J} \sum_{n_2=0}^{2^J} R_{2k_1,2k_2+1,n_1,n_2}^{j+1,j+1,J,J} \phi\left(x_{n_1}^J, y_{n_2}^J\right), \\ \phi\left(x_{2k_1+1}^{j+1}, y_{2k_2+1}^{j+1}\right) &= \sum_{n_1=0}^{2^J} \sum_{n_2=0}^{2^J} R_{2k_1+1,2k_2+1,n_1,n_2}^{j+1,j+1,J,J} \phi\left(x_{n_1}^J, y_{n_2}^J\right).\end{aligned} \tag{22}$$

Introducing the extension operators $C1$, $C2$, and $C3$, and substituting (22) into (20), the wavelet coefficients can be rewritten as

$$\begin{aligned}\alpha_{j,k_1,k_2}^1 &= \sum_{n_1=0}^{2^J} \sum_{n_2=0}^{2^J} R_{2k_1+1,2k_2,n_1,n_2}^{j+1,j+1,J,J} \phi\left(x_{n_1}^J, y_{n_2}^J\right) \\ &- \left[\sum_{n_1=0}^{2^J} \sum_{n_2=0}^{2^J} \sum_{k_{01}=0}^{2^{j_0}} \sum_{k_{02}=0}^{2^{j_0}} R_{k_{01},k_{02},n_1,n_2}^{j_0,j_0,J,J} \times \phi\left(x_{n_1}^J, y_{n_2}^J\right) w_{k_{01},k_{02}}^{j_0}\left(x_{2k_1+1}^{j+1}, y_{2k_2}^{j+1}\right)\right. \\ &+ \sum_{j_1=j_0}^{j-1} \sum_{n_1=0}^{2^J} \sum_{n_2=0}^{2^J} \sum_{k_{11}=0}^{2^{j_1}} \sum_{k_{12}=0}^{2^{j_1}} \left(C1_{k_{11},k_{12},n_1,n_2}^{j_1,j_1,J,J} w_{2k_{11}+1,2k_{12}}^{j_1+1} \times \left(x_{2k_1+1}^{j+1}, y_{2k_2}^{j+1}\right) \phi\left(x_{n_1}^J, y_{n_2}^J\right)\right. \\ &+ C2_{k_{11},k_{12},n_1,n_2}^{j_1,j_1,J,J} w_{2k_{11},2k_{12}+1}^{j_1+1} \times \left(x_{2k_1+1}^{j+1}, y_{2k_2}^{j+1}\right) u\left(x_{n_1}^J, y_{n_2}^J\right) \\ &+ \left.\left. C3_{k_{11},k_{12},n_1,n_2}^{j_1,j_1,J,J} w_{2k_{11}+1,2k_{12}+1}^{j_1+1} \times \left(x_{2k_1+1}^{j+1}, y_{2k_2}^{j+1}\right) \times \phi\left(x_{n_1}^J, y_{n_2}^J\right)\right)\right] \\ &= \sum_{n_1=0}^{2^J} \sum_{n_2=0}^{2^J} C1_{k_1,k_2,n_1,n_2}^{j,j,J,J} \phi\left(x_{n_1}^J, y_{n_2}^J\right).\end{aligned} \tag{23}$$

α_{j,k_1,k_2}^2 and α_{j,k_1,k_2}^3 are similar with α_{j,k_1,k_2}^1. From above equation, the extension operator can be obtained as

$$C1_{k_1,k_2,n_1,n_2}^{j,j,J,J} = R_{2k_1+1,2k_2,n_1,n_2}^{j+1,j+1,J,J}$$

$$
\begin{aligned}
&-\Bigg[\sum_{k_{01}=0}^{2^{j_0}}\sum_{k_{02}=0}^{2^{j_0}} R_{k_{01},k_{02},n_1,n_2}^{j_0,j_0,J,J}\phi\left(x_{n_1}^J, y_{n_2}^J\right) w_{k_{01},k_{02}}^{j_0}\left(x_{2k_1+1}^{j+1}, y_{2k_2}^{j+1}\right)\\
&\quad+\sum_{j_1=j_0}^{j-1}\sum_{n_2=0}^{2^J}\sum_{k_{11}=0}^{2^{j_1}}\left(C1_{k_{11},k_{12},n_1,n_2}^{j_1,j_1,J,J} w_{2k_{11}+1,2k_{12}}^{j_1+1}\left(x_{2k_1+1}^{j+1}, y_{2k_2}^{j+1}\right)\right.\\
&\qquad\times\phi\left(x_{n_1}^J, y_{n_2}^J\right)\\
&\qquad+C2_{k_{11},k_{12},n_1,n_2}^{j_1,j_1,J,J} w_{2k_{11},2k_{12}+1}^{j_1+1}\\
&\qquad\times\left(x_{2k_1+1}^{j+1}, y_{2k_2}^{j+1}\right)\phi\left(x_{n_1}^J, y_{n_2}^J\right)\\
&\qquad+C3_{k_{11},k_{12},n_1,n_2}^{j_1,j_1,J,J} w_{2k_{11}+1,2k_{12}+1}^{j_1+1}\\
&\qquad\left.\times\left(x_{2k_1+1}^{j+1}, y_{2k_2}^{j+1}\right)\ \phi\left(x_{n_1}^J, y_{n_2}^J\right)\right)\Bigg].
\end{aligned}
\tag{24}
$$

$C2$ and $C3$ can be obtained with the same method. Therefore, the calculation time complexity of the wavelet transform coefficients $\alpha_{j,k_{11},k_{12}}^1$, $\alpha_{j,k_{11},k_{12}}^2$, and $\alpha_{j,k_{11},k_{12}}^3$ is $O((1/3)4^{2J-1})$.

Substituting $\alpha_{j,k_{11},k_{12}}^1$, $\alpha_{j,k_{11},k_{12}}^2$, and $\alpha_{j,k_{11},k_{12}}^3$ and $C1$, $C2$, and $C3$ into (2), the multilevel wavelet interpolation operator can be obtained as

$$
\begin{aligned}
&I_{n_1,n_2}(x,y)\\
&=\sum_{k_{01}=0}^{2^{j_0}}\sum_{k_{02}=0}^{2^{j_0}} R_{k_{01},k_{02},n_1,n_2}^{j_0,j_0,J,J} w_{k_{01},k_{02}}^{j_0}(x,y)\\
&\quad+\sum_{j=j_0}^{J-1}\sum_{k_1=0}^{2^j}\sum_{k_2=0}^{2^j}\left(C1_{k_1,k_2,n_1,n_2}^{j,j,J,J} w_{2k_1+1,2k_2}^{j+1}(x,y)\,\phi\left(x_{n_1}^J, y_{n_2}^J\right)\right.\\
&\qquad+C2_{k_1,k_2,n_1,n_2}^{j,j,J,J} w_{2k_1,2k_2+1}^{j+1}\\
&\qquad\times(x,y)\,\phi\left(x_{n_1}^J, y_{n_2}^J\right)\\
&\qquad+C3_{k_1,k_2,n_1,n_2}^{j,j,J,J} w_{2k_1+1,2k_2+1}^{j+1}\\
&\qquad\left.\times(x,y)\,\phi\left(x_{n_1}^J, y_{n_2}^J\right)\right).
\end{aligned}
\tag{25}
$$

Then, (10) can be rewritten as

$$
\phi^{J(m,n)}(x,y,t)=\sum_{n_1}^{2^J}\sum_{n_2}^{2^J} I_{n_1,n_2}(x,y)\,\phi\left(x_{n_1}^J, y_{n_2}^J\right). \tag{26}
$$

Substituting (26) into (13), the multilevel wavelet discretization scheme of Perona-Malik model can be obtained.

The purpose of constructing the multilevel sparse grid approach is to decrease the amount of the collocation points and then improve the efficiency of the algorithm. But the efficiency will be eliminated if the computation complexity of the multilevel wavelet interpolation operator is too high. It is easy to understand that the interpolation wavelet coefficient is the error between the interpolation result and the exact result at the same collocation point. And so, the wavelet coefficient must be the function of the parameter t. In other words, the wavelet coefficient should vary with the time parameter t. Then, the interpolation operator can be viewed as a nonlinear problem. HPM is an efficient and effective tool to solve nonlinear problem. Aiming to improve the efficiency of the multilevel wavelet interpolation operators, HPM would be employed to construct a novel interpolation operator in this section.

For convenience, ϕ and its derivative in (5) should be rewritten as

$$
\frac{\partial\phi}{\partial t}=F\left(t,x,y,\phi,\frac{\partial\phi}{\partial x},\frac{\partial\phi}{\partial y},\frac{\partial^2\phi}{\partial x^2},\frac{\partial^2\phi}{\partial x\partial y},\frac{\partial^2\phi}{\partial y^2}\right)\quad(t>0) \tag{27}
$$

$$
\begin{aligned}
&\phi(x,y,0)=\phi_0\ (x,y),\\
&\frac{d\phi^J(x,y,t)}{dt}\\
&\quad=F\left[t,x,y,\phi^J(x,y,t),\right.\\
&\qquad\phi^{J(1,0)}(x,y,t),\phi^{J(0,1)}(x,y,t),\\
&\qquad\left.\phi^{J(2,0)}(x,y,t),\phi^{J(1,1)}(x,y,t),\phi^{J(0,2)}(x,y,t)\right],
\end{aligned}
\tag{28}
$$

respectively, where

$$
\begin{aligned}
&\phi^J(x,y,t)\\
&\quad=\sum_{k_{01}=0}^{1}\sum_{k_{02}=0}^{1}\phi\left(x_{k_{01}}^0, y_{k_{02}}^0\right) w_{k_{01},k_{02}}^0(x,y)\\
&\qquad+\sum_{j=0}^{J-1}\sum_{k_{11}=0}^{2^j-1}\sum_{k_{12}=0}^{2^j-1}\left[\alpha_{j,k_{11},k_{12}}^1 w_{2k_{11}+1,2k_{12}}^{j+1}(x,y)\right.\\
&\qquad\qquad+\alpha_{j,k_{11},k_{12}}^2 w_{2k_{11},2k_{12}+1}^{j+1}(x,y)\\
&\qquad\qquad\left.+\ \alpha_{j,k_{11},k_{12}}^3 w_{2k_{11}+1,2k_{12}+1}^{j+1}(x,y)\right].
\end{aligned}
\tag{29}
$$

The value of $\phi^J(x,y,t_n)$ at t_n is denoted by ϕ_n, and

$$
\begin{aligned}
&F\left[t_n,x,y,\phi^J(x,y,t_n),\phi^{J(1,0)}(x,y,t_n),\phi^{J(0,1)}(x,y,t_n),\right.\\
&\qquad\left.\phi^{J(2,0)}(x,y,t_n),\phi^{J(1,1)}(x,y,t_n),\phi^{J(0,2)}(x,y,t_n)\right]
\end{aligned}
\tag{30}
$$

is denoted by F_n. And then, a linear homotopy function can be constructed as

$$
\phi^J(x,y,t)=(1-\varepsilon)F_n+\varepsilon F_{n+1}. \tag{31}
$$

It is easy to identify the homotopy parameter as

$$\varepsilon(t) = \frac{t - t_n}{t_{n+1} - t_n} \quad t \in [t_n, t_{n+1}] \;\therefore \varepsilon \in [0,1]. \tag{32}$$

According to the perturbation theory, the solution of (31) can be expressed as the power series expansion of ε:

$$\phi^J = \phi_0^J + \varepsilon\phi_1^J + \varepsilon^2\phi_2^J + \cdots. \tag{33}$$

Substituting (29) into (27) and rearranging based on powers of ε-terms, we have

$$\begin{aligned}
&\varepsilon^0:\ \phi_0^J = F_n\\
&\varepsilon^1:\ \phi_1^J = F_{n+1} - F_n\\
&\vdots
\end{aligned} \tag{34}$$

According to HPM, we obtain the wavelet coefficients $\alpha^1_{j,k_1,k_2}(t_{n+1})$, $\alpha^2_{j,k_1,k_2}(t_{n+1})$, and $\alpha^3_{j,k_1,k_2}(t_{n+1})$ at t_n as follows:

$$\begin{aligned}
\alpha^1_{j,k_1,k_2} &= \phi\left(x^{j+1}_{2k_1+1}, y^{j+1}_{2k_2}\right) - I_j\phi\left(x^{j+1}_{2k_1+1}, y^{j+1}_{2k_2}\right)\\
&= \phi\left(x^{j+1}_{2k_1+1}, y^{j+1}_{2k_2}\right)\\
&\quad - \Bigg[\sum_{k_{01}=0}^{1}\sum_{k_{02}=0}^{1}\phi\left(x^0_{k_{01}}, y^0_{k_{02}}\right)w^0_{k_{01},k_{02}}\left(x^{j+1}_{2k_1+1}, y^{j+1}_{2k_2}\right)\\
&\qquad + \sum_{j_1=0}^{j-1}\sum_{k_{11}=0}^{2^{j_1}}\sum_{k_{12}=0}^{2^{j_1}}\Big(\alpha^1_{j_1,k_{11},k_{12}}w^{j_1+1}_{2k_{11}+1,2k_{12}}\\
&\qquad\qquad \times\left(x^{j+1}_{2k_1+1}, y^{j+1}_{2k_2}\right)\\
&\qquad\qquad + \alpha^2_{j_1,k_{11},k_{12}}w^{j_1+1}_{2k_{11},2k_{12}+1}\\
&\qquad\qquad \times\left(x^{j+1}_{2k_1+1}, y^{j+1}_{2k_2}\right)\\
&\qquad\qquad + \alpha^3_{j_1,k_{11},k_{12}}w^{j_1+1}_{2k_{11}+1,2k_{12}+1}\\
&\qquad\qquad \times\left(x^{j+1}_{2k_1+1}, y^{j+1}_{2k_2}\right)\Big)\Bigg],\\
\alpha^2_{j,k_1,k_2} &= \phi\left(x^{j+1}_{2k_1}, y^{j+1}_{2k_2+1}\right) - I_j\phi\left(x^{j+1}_{2k_1}, y^{j+1}_{2k_2+1}\right)\\
&= \phi\left(x^{j+1}_{2k_1}, y^{j+1}_{2k_2+1}\right)\\
&\quad - \Bigg[\sum_{k_{01}=0}^{1}\sum_{k_{02}=0}^{1}\phi\left(x^0_{k_{01}}, y^0_{k_{02}}\right)w^0_{k_{01},k_{02}}\left(x^{j+1}_{2k_1}, y^{j+1}_{2k_2+1}\right)\\
&\qquad + \sum_{j_1=0}^{j-1}\sum_{k_{11}=0}^{2^{j_1}}\sum_{k_{12}=0}^{2^{j_1}}\Big(\alpha^1_{j_1,k_{11},k_{12}}w^{j_1+1}_{2k_{11}+1,2k_{12}}\\
&\qquad\qquad \times\left(x^{j+1}_{2k_1}, y^{j+1}_{2k_2+1}\right)\\
&\qquad\qquad + \alpha^2_{j_1,k_{11},k_{12}}w^{j_1+1}_{2k_{11},2k_{12}+1}\\
&\qquad\qquad \times\left(x^{j+1}_{2k_1}, y^{j+1}_{2k_2+1}\right)\\
&\qquad\qquad + \alpha^3_{j_1,k_{11},k_{12}}w^{j_1+1}_{2k_{11}+1,2k_{12}+1}\\
&\qquad\qquad \times\left(x^{j+1}_{2k_1}, y^{j+1}_{2k_2+1}\right)\Big)\Bigg],\\
\alpha^3_{j,k_1,k_2} &= \phi\left(x^{j+1}_{2k_1+1}, y^{j+1}_{2k_2+1}\right) - I_j\phi\left(x^{j+1}_{2k_1+1}, y^{j+1}_{2k_2+1}\right)\\
&= \phi\left(x^{j+1}_{2k_1+1}, y^{j+1}_{2k_2+1}\right)\\
&\quad - \Bigg[\sum_{k_{01}=0}^{1}\sum_{k_{02}=0}^{1}\phi\left(x^0_{k_{01}}, y^0_{k_{02}}\right)w^0_{k_{01},k_{02}}\left(x^{j+1}_{2k_1+1}, y^{j+1}_{2k_2+1}\right)\\
&\qquad + \sum_{j_1=0}^{j-1}\sum_{k_{11}=0}^{2^{j_1}}\sum_{k_{12}=0}^{2^{j_1}}\Big(\alpha^1_{j_1,k_{11},k_{12}}w^{j_1+1}_{2k_{11}+1,2k_{12}}\\
&\qquad\qquad \times\left(x^{j+1}_{2k_1+1}, y^{j+1}_{2k_2+1}\right)\\
&\qquad\qquad + \alpha^2_{j_1,k_{11},k_{12}}w^{j_1+1}_{2k_{11},2k_{12}+1}\\
&\qquad\qquad \times\left(x^{j+1}_{2k_1+1}, y^{j+1}_{2k_2+1}\right)\\
&\qquad\qquad + \alpha^3_{j_1,k_{11},k_{12}}w^{j_1+1}_{2k_{11}+1,2k_{12}+1}\\
&\qquad\qquad \times\left(x^{j+1}_{2k_1+1}, y^{j+1}_{2k_2+1}\right)\Big)\Bigg].
\end{aligned} \tag{35}$$

Obviously, the calculation time complexity of the wavelet transform coefficients α^1_{j,k_1,k_2}, α^2_{j,k_1,k_2}, and α^3_{j,k_1,k_2} is $O(4^J)$, which is decreased greatly than in (11) which is $O((1/3)4^{2J-1})$.

Substituting the wavelet transform coefficient (35) into (29), we obtain

$$\begin{aligned}
\phi^J&(x, y, t_{n+1})\\
&= \phi^J(x, y, t_n)\\
&\quad + \frac{\Delta t}{2}\Big[F\left(t_n, x, y, \phi^J(x, y, t_n),\right.\\
&\qquad\qquad \phi^{J(1,0)}(x, y, t_n), \phi^{J(0,1)}(x, y, t_n),\\
&\qquad\qquad \phi^{J(2,0)}(x, y, t_n), \phi^{J(1,1)}(x, y, t_n),\\
&\qquad\qquad \left.\phi^{J(0,2)}(x, y, t_n)\right)\\
&\qquad + F\left(t_{n+1}, x, y, \phi_0^J(x, y, t_{n+1}),\right.\\
&\qquad\qquad \phi_0^{J(1,0)}(x, y, t_{n+1}), \phi_0^{J(0,1)}(x, y, t_{n+1}),
\end{aligned}$$

$$\phi_0^{J(2,0)}(x,y,t_{n+1}),\phi_0^{J(1,1)}(x,y,t_{n+1}),$$
$$\left.\phi_0^{J(0,2)}(x,y,t_{n+1}))\right]. \quad (36)$$

And the derivative function

$$\begin{aligned}
&\phi^{J(m,n)}(x,y) \\
&= \sum_{k_{01}=0}^{1}\sum_{k_{02}=0}^{1}\phi\left(x_{k_{01}}^{0},y_{k_{02}}^{0}\right)w_{k_{01},k_{02}}^{0(m,n)}(x,y) \\
&\quad + \sum_{j=0}^{J-1}\sum_{k_{11}=0}^{2^j-1}\sum_{k_{12}=0}^{2^j-1}\left[\alpha_{j,k_{11},k_{12}}^{1}w_{2k_{11}+1,2k_{12}}^{j+1(m,n)}(x,y)\right. \\
&\qquad + \alpha_{j,k_{11},k_{12}}^{2}w_{2k_{11},2k_{12}+1}^{j+1(m,n)}(x,y) \\
&\qquad \left. + \alpha_{j,k_{11},k_{12}}^{3}w_{2k_{11}+1,2k_{12}+1}^{j+1(m,n)}(x,y)\right].
\end{aligned} \quad (37)$$

Obviously, the computation complexity is decreased greatly comparing with (26).

4. Numerical Experiences and Discussion

In this section, we take some images as examples to illustrate the efficiency of the dynamic interval wavelet interpolation operator based on HPM in partitioning technique on the image processing. In fact, the partitioning technique is a scheme to divide the image into several subimages in the multiscale wavelet numerical method to improve the efficiency. The dynamic interval wavelet provides an adaptive choice scheme for the external collocation points to eliminate the boundary effect of the subimages. Perona-Malik equation is employed as the denoising model, which is an anisotropic diffusion image denoising model that was proposed by Perona and Malik. It has been widely used in various image processing fields. It can be represented as the nonlinear partial differential equations:

$$\begin{aligned}
\frac{\partial u(x,y,t)}{\partial t} &= \operatorname{div}(c(|\nabla u|)\nabla u), \\
u(x,y,0) &= f(x,y),
\end{aligned} \quad (38)$$

where (x,y) denotes pixel position, t is the time parameter, $f(x,y)$ is the 2D image being processed, $u(x,y,t)$ is the image after diffusion processing, and $u(x,y,0)$ is the initial value. div denotes the divergence operator, ∇u denotes the gradient operator, and $c(|\nabla u|)$ denotes the diffusion coefficient, which is nonnegative decreasing function of the image gradient modulus. It is usually taken as

$$c(|\nabla u|) = \frac{1}{1+(\nabla u/k)^2} \quad (39)$$

or

$$c(|\nabla u|) = \exp\left[-\left(\frac{\nabla u}{k}\right)^2\right], \quad (40)$$

where k is a constant.

Two different medical images are taken as examples to test the characteristic of different interpolation wavelets, which is showed in Figure 1. One is the human brain (Figure 1(a)), which has so clear contour that that image cannot be represented as a continuous function near the contour. The Gibbs phenomenon is possible to be introduced into the image near the boundary. So, this can be used to test the advantages of the multiscale wavelet approximation comparing with the difference operator. Another one is the image of the locust coelom, which has many microgrooves without clear boundary. This image is used to test the characteristic of different interpolation wavelets, which is showed in Figure 1(b).

4.1. Comparison between the Sparse Grid Approach and the Finite Different Method. It has been mentioned above that the brain image is used to test the difference between the sparse grid approach and the finite difference method and the difference between different wavelet functions which are taken as the basis functions in the sparse grid approach. In this experiment, all the results are obtained by solving the Perona-Malik equation with different methods, which have been showed in Figure 2.

Two interpolation wavelet scaling functions are employed to test the dynamic sparse grid approach for image denoising proposed in this paper. The Shannon wavelet possesses the smoothness and or the orthogonality but has no compact support property. Daubechies scaling function possess almost all the excellent properties in numerical algorithm such as smoothness, orthogonality, and compact support property. But what we utilized in this research is the autocorrelative function of the Daubechies scaling function, which keeps the better edge preserving property although it loses the orthogonality. It can be easily observed from Figure 2(c) that the evident artifacts appeared in the denoised image obtained by the Shannon sparse grid approach. That is, the Gibbs phenomenon has appeared in the Shannon scaling function representation of the image near the boundary. In contrast to the Shannon wavelet, the denoised image (Figure 2(b)) obtained by the Daubechies wavelet sparse grid approach has clear boundary. It is easy to understand that the compact support property of the wavelet scaling function is helpful to eliminate the Gibbs phenomenon and so to improve the numerical performances of the wavelet numerical methods.

Comparing with the sparse grid approaches, the finite difference method utilizes the difference operator to approximate the derivative in Perona-Malik equation, which decreases the value of the derivative to some extent. Therefore, the edge of the brain contour is smoothed in denoised images; this is showed in Figure 2(d). It should be noticed that the edge of the denoised image obtained by the Shannon wavelet sparse grid approach is more clear than that obtained by the finite difference method, in despite of the appearing artifacts.

4.2. Comparison between the Dynamic Interval Wavelet and the Static Interval Wavelet. For convenience of comparison, we call the interval interpolation wavelet constructed by the

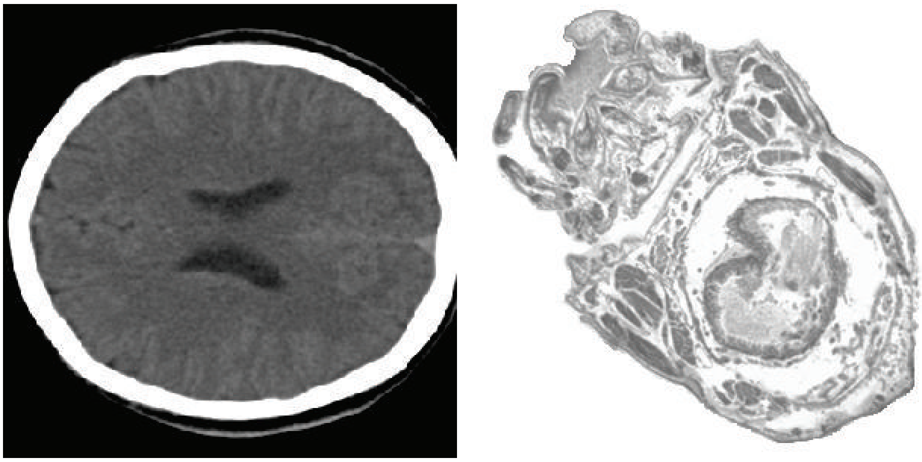

(a) Image of human brain (b) Image of locust coelom

Figure 1: Original images.

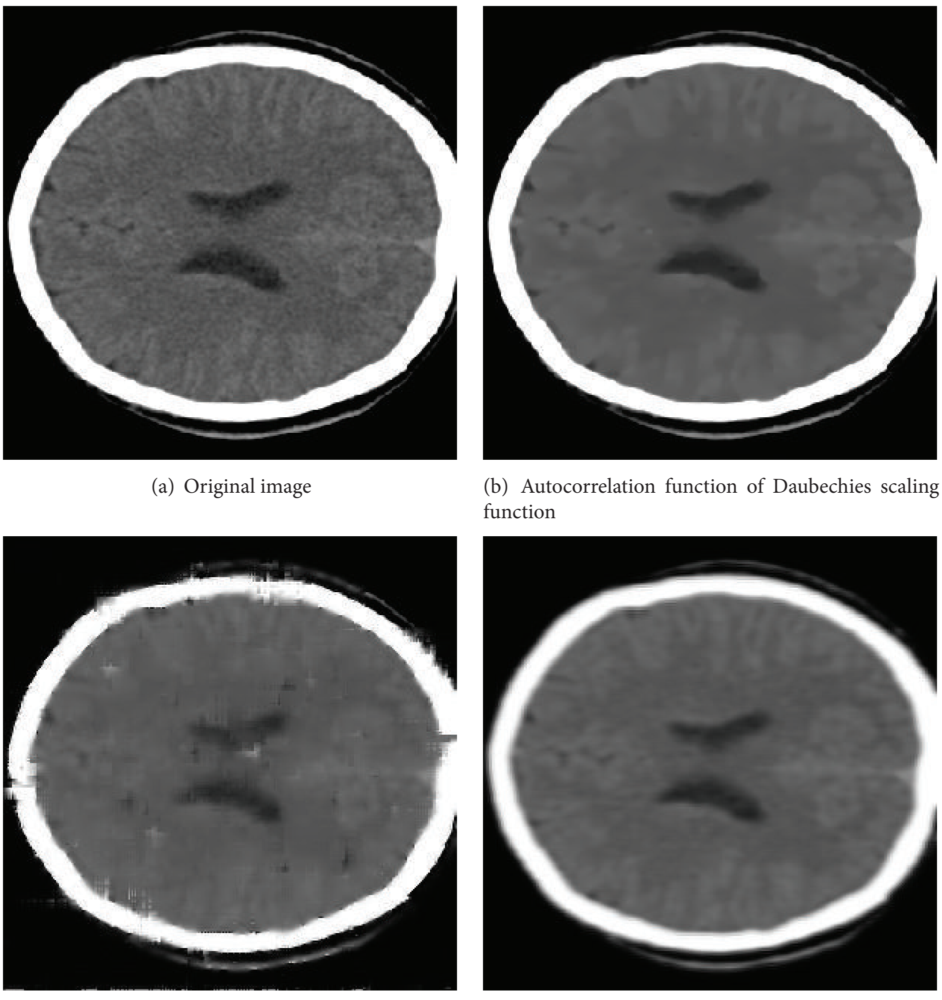

(a) Original image (b) Autocorrelation function of Daubechies scaling function

(c) Shannon scaling function (d) Finite difference method

Figure 2: Comparison between different numerical methods for image denoising (time step $\tau = 0.00001$, terminal time $t = 0.00005$).

Table 1: Condition number of each image block at different times.

Block number	Condition number				
	$t = 0.00001$	$t = 0.00002$	$t = 0.00003$	$t = 0.00004$	$t = 0.00005$
1	9.6829	7.7193	6.7935	6.8257	5.9730
2	13.7539	12.8756	11.8760	11.8703	11.3319
3	9.2841	8.8832	8.1376	7.8737	6.8713
4	9.6829	7.7193	6.7935	6.8257	5.9730
5	1.6816	1.6931	1.7153	1.7378	1.8923
6	13.9357	12.9657	11.8891	11.8757	10.3356
7	13.7543	12.8757	11.8765	10.8701	9.3318
8	13.7556	12.8781	11.8776	11.8734	11.3329
9	43.9354	32.9663	31.8882	28.8749	21.3346
10	3.2389	2.9137	2.2917	1.9365	1.2919
11	8.5692	6.9416	6.6971	5.2875	4.3907
12	31.9823	29.3266	28.8330	25.6736	20.1976
13	15.1617	14.7818	13.8967	12.5738	12.3428
14	12.9614	12.1973	10.9887	10.1725	9.3189
15	4.6593	3.7938	2.5476	2.3789	1.9916
16	14.6835	13.9864	13.1838	12.8897	11.3156
17	12.8113	12.1031	10.1763	9.5627	8.2474
18	14.9834	13.6523	12.7719	12.1658	11.7829
19	13.6689	12.1791	11.1782	10.5977	8.9664
20	125.4782	110.3379	98.9073	89.7761	80.2749
21	1.6816	1.6931	1.7153	1.7378	1.8923
22	2.4589	2.6623	3.7662	3.8955	4.5811
23	43.2983	39.6744	36.7943	32.1079	28.6179
24	211.5877	198.7219	180.7089	86.9125	81.8510
25	185.7428	170.5897	160.0987	52.1757	83.0421

Lagrange interpolator as static interval wavelet and the interval interpolation wavelet based on the Newton interpolator as the dynamic interval wavelet. The difference between two interval wavelets above is the choice of the parameter L. The value of L is constant to the static interval wavelet, and it varies with both of the boundary condition and the condition number of the system ODEs obtained from the sparse grid approach.

The purpose of constructing of the interval wavelet is to eliminate the boundary effect in the partitioning technique on the image denoising process. In this section, the image of locust coelom ($300 * 300$ pixels) is taken as example to compare the difference between the dynamic and static interval wavelets. According to the partitioning technique, the image is divided evenly into 25 parts for simplification. So, the size of each image block is $60 * 60$ pixels (Figure 3). According to the sparse grid approach based on HPM, the calculation amount decreases from $(300 * 300)^3$ to $25 * (60 * 60)^3$. It has been mentioned that there are many ways to eliminate the boundary effect such as the extension method and the interval wavelet method. There is no doubt that the interval wavelet method is more efficient than the extension method. According to the interval interpolation wavelet based on the Lagrange interpolator, the amount of the external collocation points L is a constant. With increase of L, the calculation amount will increase correspondingly.

L is taken as 1, 2, and 3, respectively, in the experiments. It is easy to be observed from Figures 3(a)–3(c) that there are more collocation points near the boundary of each of block images in all 3 cases. In fact, the adaptive increase of the collocation points can also eliminate the boundary effect. Therefore, there are no artifacts appearing in the denoised images in the first two cases. But the increase of the collocation points can increase the calculation amount greatly. According to the definition of the interval interpolation wavelet based on the Lagrange operator, the increase of L can improve the smoothness and the precision of the approximated function near the boundary. This is helpful to decrease the boundary effect in theory. In contrast to the theory, the collocation points in the whole image domain increased so much that the artifacts appeared in the denoised subimages when $L = 3$ comparing to other two cases (Figure 3(c)). As a matter of fact, this is caused by the increase of the condition number of the system of ODEs obtained by the sparse grid approach. That is, the increase of the value of L can induce the condition number change greatly; this is showed in Table 1. It has been pointed out in Section 2 that if the condition number $\mathrm{cond}(A) = 10^k$, then you may lose up to k digits of accuracy on top of what would be lost to the numerical method due to loss of precision from arithmetic methods. This also illustrates that the condition number must be taken into account in the dynamic interval wavelet. Figure 3(d) is the result obtained by the dynamic interval sparse grid approach. The distribution of the collocation points in Figure 3(d) is just correlative with the image content itself and is not correlative with the partitioning scheme of the

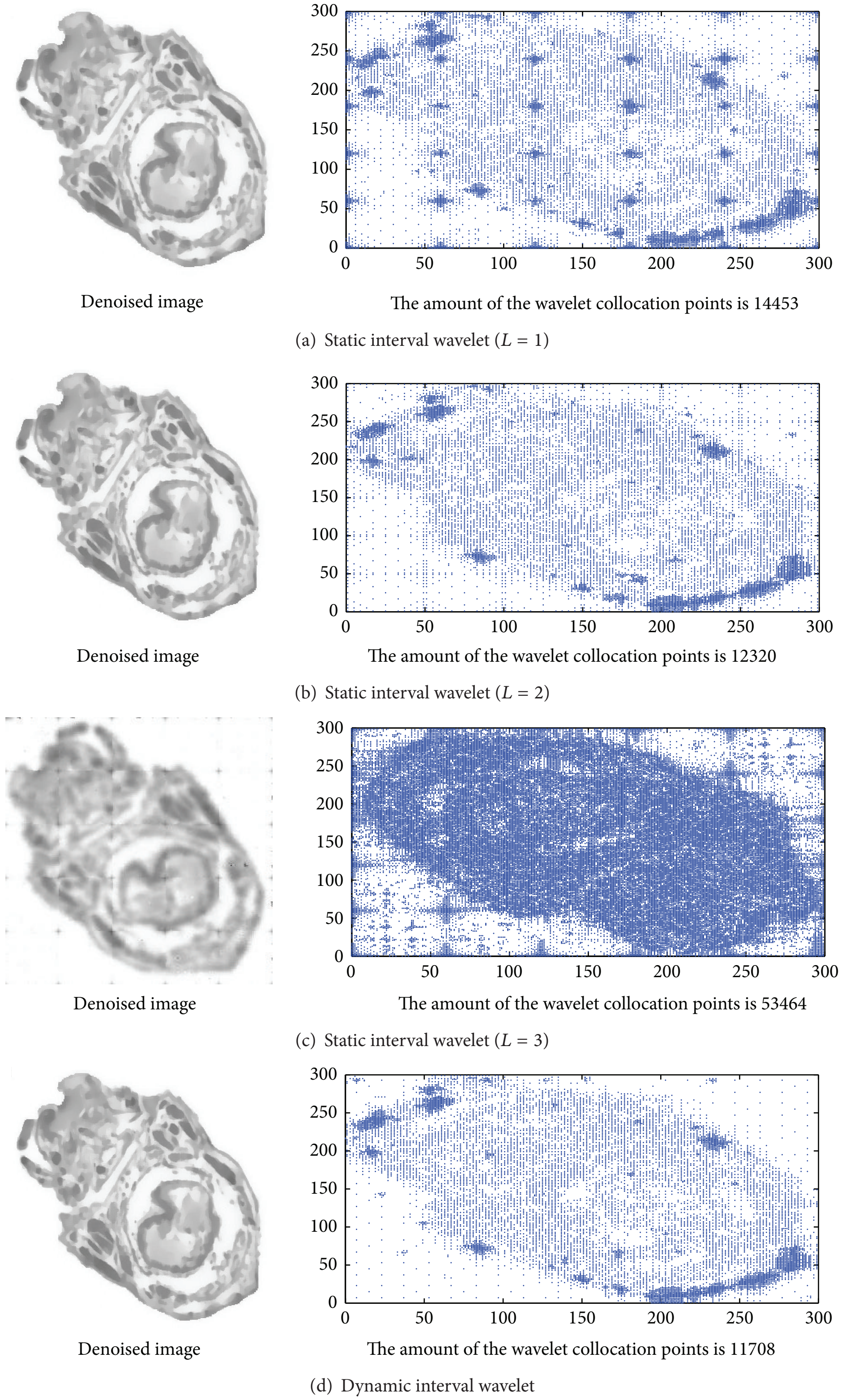

Figure 3: Comparison between the dynamic interval wavelet and the static interval wavelet.

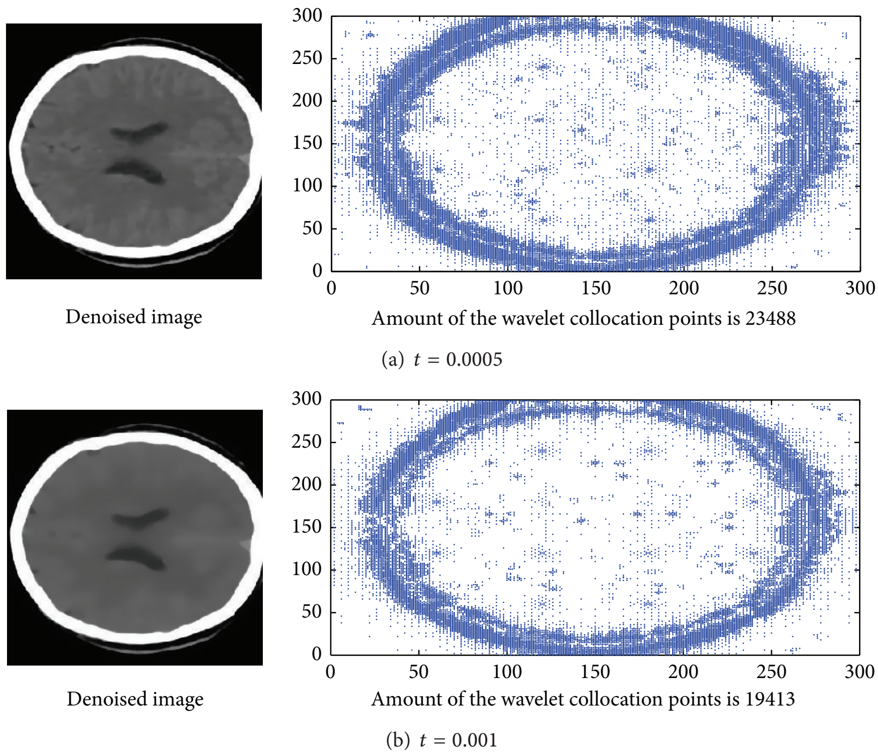

Figure 4: Adaptability of the multiscale sparse grid approach in image denoising (time step $\tau = 0.00001$).

image anymore. The amount of the wavelet collocation points also decreased accordingly.

4.3. Adaptability of the Wavelet Collocation Points. In this research, the dynamic interpolation operator was viewed as a nonlinear problem, and so HPM is employed in construction of the dynamic interpolation wavelet defined in interval. This is helpful to improve the efficiency of the multilevel wavelet interpolation operators. In this section, the autocorrelation function of the Daubechies scaling function is employed to construct the dynamic interval wavelet. The brain image is taken as example to test the precision and efficiency of the HPM-based dynamic interval wavelet proposed in this research. The experiment results were showed in Figure 4. It is easy to be observed that the noise pixels of the brain images were smoothed completely and the edges of the brain contour were preserved perfectly. With the increase of the iteration times, more and more trivial objects such as the noise pixels are being smoothed, and more areas in the brain image are becoming smoother. Accordingly, the amount of the wavelet collocation points should be smaller and smaller. This has been illustrated in Figures 4(a) and 4(b). In this experiment, the time step $\tau = 0.00001$; the definition domain of the parameter t is $[0, 0.001]$. The experiment results show that the amount of the wavelet collocation points decreases from 23488 to 19413 with the parameter t increasing from 0.0005 to 0.001. According to the finite difference method, the amount of the collocation points should be 90000, which is greater than the sparse grid approach, evidently. This illustrates that the dynamic interval sparse grid approach proposed in this paper is more efficient than the finite difference method.

5. Conclusions

The dynamic interval wavelet and the corresponding numerical method proposed in this paper are intrinsically an adaptive choice scheme on the external collocation points. In partitioning technique about the image processing, the dynamic sparse grid approach can be used to eliminate the boundary effect and improve the algorithm efficiency. In this method, the wavelet interpolation operator is constructed based on the homotopy perturbation method, which can decrease the calculation amount greatly. In addition, comparing with the finite difference method, the dynamic interval sparse grid approach can preserve the object edge more clear, especially in the case that the edge is sharper. For simplification, the image is divided evenly into several parts according to the partitioning scheme in the experiments. It is obvious that the partitioning scheme can be adaptive, which can improve the efficiency furthermore.

Conflict of Interests

The authors declare that there is no conflict of interests regarding the publication of this paper.

Acknowledgments

This work is supported by the National Natural Science Foundation of China (no. 41171337) and the National Key Technology R&D Program of China (no. 2012BAD35B02).

References

[1] H.-H. Yan, "Adaptive wavelet precise integration method for nonlinear Black-Scholes model based on variational iteration method," *Abstract and Applied Analysis*, vol. 2013, Article ID 735919, 6 pages, 2013.

[2] L.-W. Liu, "Interval wavelet numerical method on fokker-planck equations for nonlinear random system," *Advances in Mathematical Physics*, vol. 2013, Article ID 651357, 7 pages, 2013.

[3] R.-Y. Xing, "Wavelet-based homotopy analysis method for nonlinear matrix system and its application in burgers equation," *Mathematical Problems in Engineering*, vol. 2013, Article ID 982810, 7 pages, 2013.

[4] P. Perona and J. Malik, "Scale-space and edge detection using anisotropic diffusion," *IEEE Transactions on Pattern Analysis and Machine Intelligence*, vol. 12, no. 7, pp. 629–639, 1990.

[5] A.-M. Wazwaz, "The tanh-coth method for solitons and kink solutions for nonlinear parabolic equations," *Applied Mathematics and Computation*, vol. 188, no. 2, pp. 1467–1475, 2007.

[6] A.-M. Wazwaz, "The tan h method: solitons and periodic solutions for the Dodd-Bullough-Mikhailov and the Tzitzeica-Dodd-Bullough equations," *Chaos, Solitons & Fractals*, vol. 25, no. 1, pp. 55–63, 2005.

[7] A.-M. Wazwaz, "The sine-cosine method for obtaining solutions with compact and noncompact structures," *Applied Mathematics and Computation*, vol. 159, no. 2, pp. 559–576, 2004.

[8] H. Jafari, H. Tajadodi, and D. Baleanu, "A modified variational iteration method for solving fractional Riccati differential equation by Adomian polynomials," *Fractional Calculus and Applied Analysis*, vol. 16, no. 1, pp. 109–122, 2013.

[9] H. Jafari, M. Saeidy, and D. Baleanu, "The variational iteration method for solving n-th order fuzzy differential equations," *Central European Journal of Physics*, vol. 10, no. 1, pp. 76–85, 2012.

[10] H. Jafari, M. Alipour, and H. Tajadodi, "Convergence of homotopy perturbation method for solving integral equations," *Thai Journal of Mathematics*, vol. 8, no. 3, pp. 511–520, 2010.

[11] H. Jafari, C. Chun, S. Seifi, and M. Saeidy, "Analytical solution for nonlinear gas dynamic equation by homotopy analysis method," *Applications and Applied Mathematics*, vol. 4, no. 1, pp. 149–154, 2009.

[12] H. Jafari, N. Kadkhoda, and C. M. Khalique, "Exact solutions of ϕ equation using lie symmetry approach along with the simplest equation and Exp-function methods," *Abstract and Applied Analysis*, vol. 2012, Article ID 350287, 7 pages, 2012.

[13] O. V. Vasilyev and S. Paolucci, "A dynamically adaptive multilevel wavelet collocation method for solving partial differential equations in a finite domain," *Journal of Computational Physics*, vol. 125, no. 2, pp. 498–512, 1996.

[14] H. Schaeffer, R. Caflisch, C. D. Hauck, and S. Osher, "Sparse dynamics for partial differential equations," *Proceedings of the National Academy of Sciences of the United States of America*, vol. 110, no. 17, pp. 6634–6639, 2013.

[15] C. Lopez-Molina, B. de Baets, J. Cerron, M. Galar, and H. Bustince, "A generalization of the Perona-Malik anisotropic diffusion method using restricted dissimilarity functions," *International Journal of Computational Intelligence Systems*, vol. 6, no. 1, pp. 14–28, 2013.

[16] I. Daubechies and G. Teschke, "Variational image restoration by means of wavelets: simultaneous decomposition, deblurring, and denoising," *Applied and Computational Harmonic Analysis*, vol. 19, no. 1, pp. 1–16, 2005.

[17] I. Daubechies and G. Teschke, "Wavelet based image decomposition by variational functionals," in *Wavelet Applications in Industrial Processing*, vol. 5266 of *Proceedings of SPIE*, pp. 94–105, The International Society for Optical Engineering, Providence, RI, USA, February 2004.

[18] C. Cattani, "Shannon wavelets theory," *Mathematical Problems in Engineering*, vol. 2008, Article ID 164808, 24 pages, 2008.

[19] C. Cattani, "Harmonic wavelets towards the solution of nonlinear PDE," *Computers and Mathematics with Applications*, vol. 50, no. 8-9, pp. 1191–1210, 2005.

[20] S.-L. Mei, H.-L. Lv, and Q. Ma, "Construction of interval wavelet based on restricted variational principle and its application for solving differential equations," *Mathematical Problems in Engineering*, vol. 2008, Article ID 629253, 14 pages, 2008.

[21] S.-L. Mei, Q.-S. Lu, S.-W. Zhang, and L. Jin, "Adaptive interval wavelet precise integration method for partial differential equations," *Applied Mathematics and Mechanics*, vol. 26, no. 3, pp. 364–371, 2005.

[22] J.-H. He, "Asymptotic methods for solitary solutions and compactons," *Abstract and Applied Analysis*, vol. 2012, Article ID 916793, 130 pages, 2012.

[23] J.-H. He, "New interpretation of homotopy perturbation method," *International Journal of Modern Physics B*, vol. 20, no. 18, pp. 2561–2568, 2006.

[24] A. A. Elbeleze, A. Kiliçman, and B. M. Taib, "Homotopy perturbation method for fractional black-scholes european option pricing equations using sumudu transform," *Mathematical Problems in Engineering*, vol. 2013, Article ID 524852, 7 pages, 2013.

[25] A. R. Ghotbi, H. Bararnia, G. Domairry, and A. Barari, "Investigation of a powerful analytical method into natural convection boundary layer flow," *Communications in Nonlinear Science and Numerical Simulation*, vol. 14, no. 5, pp. 2222–2228, 2009.

[26] S. H. Hosein Nia, A. N. Ranjbar, D. D. Ganji, H. Soltani, and J. Ghasemi, "Maintaining the stability of nonlinear differential equations by the enhancement of HPM," *Physics Letters A*, vol. 372, no. 16, pp. 2855–2861, 2008.

[27] M. Esmaeilpour and D. D. Ganji, "Application of He's homotopy perturbation method to boundary layer flow and convection heat transfer over a flat plate," *Physics Letters A*, vol. 372, no. 1, pp. 33–38, 2007.

[28] S.-L. Pang, "Wavelet numerical method for nonlinear random system," *Transactions of the Chinese Society of Agricultural Machinery*, vol. 38, no. 3, pp. 168–170, 2007.

[29] E. Quak and N. Weyrich, "Decomposition and reconstruction algorithms for spline wavelets on a bounded interval," *Applied and Computational Harmonic Analysis*, vol. 1, no. 3, pp. 217–231, 1994.

[30] S.-L. Mei and S.-W. Zhang, "Coupling technique of variational iteration and homotopy perturbation methods for nonlinear matrix differential equations," *Computers and Mathematics with Applications*, vol. 54, no. 7-8, pp. 1092–1100, 2007.

[31] C. Cattani, "Connection coefficients of Shannon wavelets," *Mathematical Modelling and Analysis*, vol. 11, no. 2, pp. 117–132, 2006.

[32] C. Cattani, "Shannon wavelets for the solution of integrodifferential equations," *Mathematical Problems in Engineering*, vol. 2010, Article ID 408418, 22 pages, 2010.

[33] D. K. Hoffman, G. W. Wei, D. S. Zhang, and D. J. Kouri, "Shannon-Gabor wavelet distributed approximating functional," *Chemical Physics Letters*, vol. 287, no. 1-2, pp. 119–124, 1998.

[34] S. Dubuc, "Interpolation through an iterative scheme," *Journal of Mathematical Analysis and Applications*, vol. 114, no. 1, pp. 185–204, 1986.

[35] G. Deslauriers and S. Dubuc, "Symmetric iterative interpolation processes," *Constructive Approximation*, vol. 5, no. 1, pp. 49–68, 1989.

[36] I. Daubechies, "Orthonormal bases of compactly supported wavelets," *Communications on Pure and Applied Mathematics*, vol. 41, no. 7, pp. 909–996, 1988.

[37] E. Ward Cheney and D. R. Kincaid, *Numerical Mathematics and Computing*, Thomson Higher Education, Belmont, Calif, USA, 6th edition, 2008.

Hindawi Publishing Corporation
The Scientific World Journal
Volume 2014, Article ID 721865, 6 pages
http://dx.doi.org/10.1155/2014/721865

Research Article

Approximate Analytical Solutions of the Regularized Long Wave Equation Using the Optimal Homotopy Perturbation Method

Constantin Bota and Bogdan Căruntu

Department of Mathematics, Politehnica University of Timişoara, P-ta Victoriei 2, 300006 Timişoara, Romania

Correspondence should be addressed to Constantin Bota; constantin.bota@mat.upt.ro

Received 31 January 2014; Accepted 23 February 2014; Published 3 June 2014

Academic Editors: D. Baleanu, H. Jafari, and C. M. Khalique

The paper presents the optimal homotopy perturbation method, which is a new method to find approximate analytical solutions for nonlinear partial differential equations. Based on the well-known homotopy perturbation method, the optimal homotopy perturbation method presents an accelerated convergence compared to the regular homotopy perturbation method. The applications presented emphasize the high accuracy of the method by means of a comparison with previous results.

1. Introduction

A significant part of the natural technological processes and phenomena are usually modelled by means of partial differential equations. Thus it is very important to find solutions of these equations. However, as in many cases the computation of exact solutions is not possible; numerical or approximate solutions must be computed.

In the present paper we present a new approximation method named optimal homotopy perturbation method (OHPM). As the name suggests, the method is based on the homotopy perturbation method [1, 2] and its main feature is an accelerated convergence compared to the regular homotopy perturbation method.

The applications presented show that the approximate solutions obtained by using OHPM requires less iterations in comparison with other iterative methods for approximate solutions of partial differential equations.

2. The Optimal Homotopy Perturbation Method

We consider the following problem:

$$\mathfrak{L}(u(x,t)) + \mathfrak{N}(u(x,t)) - f(x,t) = 0, \qquad B(u) = 0. \tag{1}$$

Here $\mathfrak{L}$ is a linear operator, $u(x,t)$ is the unknown function, $\mathfrak{N}$ is a nonlinear operator, $f(x,t)$ is a known, given function, and B is a boundary operator.

If $\tilde{u}$ is an approximate solution of (1), we evaluate the error obtained by replacing the exact solution u with the approximate one $\tilde{u}$ as the remainder:

$$R(x,t,\tilde{u}) = \mathfrak{L}(\tilde{u}(x,t)) + \mathfrak{N}(\tilde{u}(x,t)) - f(x,t). \tag{2}$$

The first step in applying OHPM is to attach to the problem (1) the family of equations (see [1, 2]):

$$(1-p)\left[\mathfrak{L}(\Phi(x,t,p)) - f(x,t)\right] + p\left[\mathfrak{L}(\Phi(x,t,p)) + \mathfrak{N}(\Phi(x,t,p)) - f(x,t)\right] = 0, \tag{3}$$

where $p \in [0,1]$ is an embedding parameter and $\Phi(x,t,p)$ is an unknown function.

When $p = 0$, $\Phi(x,t,0) = u_0(x,t)$ and when $p = 1$, $\Phi(x,t,1) = u(x,t)$. Thus, as p increases from 0 to 1, the solution $\Phi(x,t,p)$ varies from $u_0(x,t)$ to the solution $u(x,t)$, where $u_0(x,t)$ is obtained from the following:

$$\mathfrak{L}(u_0(x,t)) - f(x,t) = 0, \qquad B(u_0) = 0. \tag{4}$$

We consider the following expansion of $\Phi(x,t,p)$:

$$\Phi(x,t,p) = u_0(x,t) + \sum_{m\geq 1} u_m(x,t)\, p^m. \tag{5}$$

Substituting the relation (5) into (3), collecting the same powers of p, and equating each coefficient of the powers of p with zero we obtain

$$\mathfrak{L}\left(u_m(x,t)\right) = -\mathfrak{N}_{m-1}\left(u_0(x,t), u_1(x,t), \ldots, u_{m-1}(x,t)\right)$$
$$m \geq 1, \ldots, B\left(u_m\right) = 0, \tag{6}$$

where $\mathfrak{N}_i$, $i \geq 0$ are the coefficients of p^i in the nonlinear operator $\mathfrak{N}$:

$$\begin{aligned}\mathfrak{N}(u(x,t)) &= \mathfrak{N}_0\left(u_0(x,t)\right) + p\mathfrak{N}_1\left(u_0(x,t), u_1(x,t)\right)\\ &\quad + p^2\mathfrak{N}_2\left(u_0(x,t), u_1(x,t), u_2(x,t)\right) + \cdots .\end{aligned} \tag{7}$$

We remark that u_m, $m \geq 1$ are obtained from the linear equations (6), which are easily solved together with the boundary conditions.

We denote $f_m = u_0 + u_1 + \cdots + u_m$.

We consider the set S_m $(m = 0, 1, 2, \ldots)$ containing the functions $\varphi_{m0}, \varphi_{m1}, \varphi_{m2}, \ldots, \varphi_{mn_m}$, chosen as linearly independent functions in the vector space of the continuous functions on the real domain Ω such that $S_{m-1} \subseteq S_m$ and $u_0+u_1+\cdots+u_m$ is a real linear combination of these functions.

We remark that such a construction is always possible. For example we can choose $S_m = \{u_0, u_1, \ldots, u_m\}$, $m = 0, 1, 2, \ldots$. In this case $\varphi_{m0} = u_0$, $\varphi_{m1} = u_1$, $\varphi_{m2} = u_2, \ldots, \varphi_{mn_m} = u_m$.

Definition 1. We call an HP-sequence of the problem (1) a sequence of functions $\{s_m(x,t)\}_{m\in\mathbb{N}}$ of the form $s_m(x,t) = \sum_{k=0}^{n_m} \alpha_m^k \varphi_{mk}$, where $m \in \mathbb{N}$, $\alpha_m^k \in \mathbb{R}$.

A function of the sequence is called an HP-function of the problem (1).

We call the HP-sequence $\{s_m(x,t)\}_{m\in\mathbb{N}}$, convergent to the solution of the problem (1) if $\lim_{m\to\infty} R(x,t,s_m(x,t)) = 0$.

Definition 2. We call an *ϵ-approximate* HP-solution of the problem (1) on the real domain Ω an HP-function $\tilde{u}$ which satisfies the following condition:

$$\left|R(x,t,\tilde{u})\right| < \epsilon \tag{8}$$

together with the boundary conditions from (1).

Definition 3. We call a *weak δ-approximate HP-solution* of the problem (1) on the real domain Ω an HP-function $\tilde{u}$ satisfying the relation $\int_\Omega R^2(x,t,\tilde{u})\,dx\,dt \leq \delta$, together with the boundary conditions from (1).

We will find a weak ϵ-approximate HP-solution of the type $\tilde{u} = \sum_{k=0}^{n_m} c_m^k \varphi_{mk}$ where $m \geq 0$ and the constants c_m^k are calculated using the following steps.

(i) We substitute the approximate solution $\tilde{u}$ in (1) and obtain the following expression:

$$\mathfrak{R}\left(x,t,c_m^k\right) = R(x,t,\tilde{u}). \tag{9}$$

(ii) We attach to the problem (1) the following real functional:

$$J\left(c_m^k\right) = \int_\Omega \mathfrak{R}^2\left(x,t,c_m^k\right) dx\,dt, \tag{10}$$

where, by imposing the boundary conditions we can determine $l \in N$, $l \leq m$ such that $c_0^m, c_1^m, \ldots, c_l^m$ are computed as functions of $c_{l+1}^m, c_{l+2}^m, \ldots, c_n^m$.

(iii) We compute the values of $\tilde{c}_{l+1}^m, \tilde{c}_{l+2}^m, \ldots, \tilde{c}_n^m$ as the values which give the minimum of the functional (10) and the values of $\tilde{c}_0^m, \tilde{c}_1^m, \ldots, \tilde{c}_l^m$ again as functions of $\tilde{c}_{l+1}^m, \tilde{c}_{l+2}^m, \ldots, \tilde{c}_n^m$ by using the boundary conditions.

(iv) Using the constants $\tilde{c}_0^m, \ldots, \tilde{c}_n^m$ thus determined, we consider the HP-sequence

$$s_m(x,t) = \sum_{k=0}^{n_m} \tilde{c}_m^k \varphi_{mk}. \tag{11}$$

The following convergence theorem holds.

Theorem 4. *The HP-sequence $s_m(x,t)$ from* (11) *satisfies the following property:*

$$\lim_{m\to\infty} \int_\Omega R^2\left(x,t,s_m(x,t)\right) dx\,dt = 0. \tag{12}$$

Moreover, $\forall\epsilon > 0$, $\exists m_0 \in \mathbb{N}$ such that $\forall m \in \mathbb{N}$, $m > m_0$ it follows that $s_m(t)$ is a weak ϵ-approximate HP-solution of the problem (1).

Proof. Based on the way the HP-function $s_m(x,t)$ is computed, the following inequality holds:

$$\begin{aligned}0 &\leq \int_\Omega R^2\left(x,t,s_m(x,t)\right) dx\,dt\\ &\leq \int_\Omega R^2\left(t,f_m(x,t)\right) dx\,dt, \quad \forall m \in \mathbb{N}.\end{aligned} \tag{13}$$

It follows that

$$\begin{aligned}0 &\leq \lim_{m\to\infty} \int_\Omega R^2\left(x,t,s_m(x,t)\right) dx\,dt\\ &\leq \lim_{m\to\infty} \int_\Omega R^2\left(x,t,f_m(x,t)\right) dx\,dt = 0, \quad \forall m \in \mathbb{N}.\end{aligned} \tag{14}$$

We obtain

$$\lim_{m\to\infty} \int_\Omega R^2\left(x,t,s_m(x,t)\right) dx\,dt = 0. \tag{15}$$

From this limit we obtain that $\forall\epsilon > 0$, $\exists m_0 \in \mathbb{N}$ such that $\forall m \in \mathbb{N}$, $m > m_0$ it follows that $s_m(x,t)$ is a weak ϵ-approximate HP-solution of the problem (1). □

Remark 5. Any ϵ-approximate HP-solution of the problem (1) is also a weak approximate HP-solution, but the opposite is not always true. It follows that the set of weak approximate HP-solutions of the problem (1) also contains the approximate HP-solutions of the problem.

Taking into account the above remark, in order to find ϵ-approximate HP-solutions of the problem (1) by the OHPM method we will first determine weak approximate HP-solutions, $\tilde{u}$. If $|R(x,t,\tilde{u})| < \epsilon$ then $\tilde{u}$ is also an ϵ-approximate HP-solution of the problem.

3. Applications

In this section we apply OHPM to find approximate analytical solutions for the regularized long wave (RLW) equation.

The RLW equation is a nonlinear evolution equation. These kind of equations are frequently used to model a variety of physical phenomena such as ion-acoustic waves in plasma, magnetohydrodynamics waves in plasma, longitudinal dispersive waves in elastic rods, pressure waves in liquid gas bubble mixtures, and rotating flow down a tube.

The RLW equation was introduced in [3] where it was used to describe the behaviour of the undular bore.

For some restricted initial and boundary conditions, exact analytical solutions for the RLW equation were computed (see, e.g., [4]). However, in most cases it is not possible to find such exact analytical solutions and usually numerical methods are used. Among the numerical methods recently employed for RLW-type equations we mention finite difference methods [5–8], multistep mixed finite element methods [9], the method of lines [10], and meshless finite-point methods [11].

Taking into account the usefulness of analytical solutions versus numerical ones, various approximation methods were also employed to find approximate analytical solutions for various RLW-type equations, such as the homotopy perturbation method [12], the variational iteration method [12], the homotopy asymptotic method [13, 14], and the Riccati expansion method [15].

In the following, for two test problems presented in [12], we compare solutions obtained by using OHPM with previous results obtained by using the homotopy perturbation method and the variational iteration method.

3.1. Application 1. Our first application is the following RLW problem [12]:

$$u_t - u_{xxt} + \left(\frac{u^2}{2}\right)_x = 0, \qquad u(x,0) = x. \tag{16}$$

In [12] approximate solutions of (16) are computed using the homotopy perturbation method (HPM) and the variational iteration method (VIM).

The exact solution of this problem is $u_e(x,t) = x/(t+1)$.

The fifth order solution computed in [12] by using the variational iteration method is

$$\begin{aligned} u_{\mathrm{VIM}}(x,t) &= x\cdot\left(-\frac{t^{31}}{109876902975}+\frac{t^{30}}{3544416225}-\frac{t^{29}}{236294415}\right.\\ &\quad+\frac{13t^{28}}{315059220}-\frac{2t^{27}}{6751269}+\frac{t^{26}}{595350}-\frac{5309t^{25}}{675126900}\\ &\quad+\frac{16927t^{24}}{540101520}-\frac{2447t^{23}}{22504230}+\frac{557t^{22}}{1666980}\\ &\quad-\frac{207509t^{21}}{225042300}+\frac{16511t^{20}}{7144200}-\frac{162179t^{19}}{30541455}+\frac{2588t^{18}}{229635}\\ &\quad-\frac{1080013t^{17}}{48580560}+\frac{43363t^{16}}{1058400}-\frac{63283t^{15}}{893025}+\frac{1019t^{14}}{8820}\\ &\quad-\frac{13141t^{13}}{73710}+\frac{17779t^{12}}{68040}-\frac{1477t^{11}}{4050}+\frac{27523t^{10}}{56700}\\ &\quad-\frac{3497t^{9}}{5670}+\frac{943t^{8}}{1260}-\frac{13t^{7}}{15}+\frac{43t^{6}}{45}\\ &\quad\left.-t^5+t^4-t^3+t^2-t+1\right). \end{aligned} \tag{17}$$

The fifth order solution computed in [12] by using the homotopy perturbation method is of the form (5)

$$\begin{aligned} u_{\mathrm{HPM}}(x,t) &= x\cdot\left(-\frac{1382t^{11}}{155925}-\frac{1382t^{10}}{14175}-\frac{326t^{9}}{567}\right.\\ &\quad-\frac{626t^{8}}{315}-\frac{1303t^{7}}{315}-\frac{199t^{6}}{45}\\ &\quad\left.-t^5+t^4-t^3+t^2-t+1\right). \end{aligned} \tag{18}$$

Using OHPM, the following steps are performed.

(i) Choosing the same homotopy (3) as used in [12] we obtain the same solutions:

$$\begin{aligned} u_0(x,t) &= x\cdot(t+1)\\ u_1(x,t) &= -x\cdot t\cdot(2+t+t^2/3)\\ u_2(x,t) &= 2\cdot x\cdot t^2\cdot(15+15\cdot t+5\cdot t^2+t^3)/15. \end{aligned}$$

It follows that we obtain the sets $S_0 = \{x, x\cdot t\}$, $S_1 = \{x\cdot t, x\cdot t^2, x\cdot t^3\}$, $S_2 = \{x\cdot t^2, x\cdot t^3, x\cdot t^4, x\cdot t^5\}$.

We will compute a second order approximate solution, by taking into account the terms from S_0, S_1, and S_2 and we will compare this solution with the fifth order solutions from [12]. Our second order approximate solution will have the expression $u_{\mathrm{OHPM}}(x,t) = c_0\cdot x + c_1\cdot x\cdot t + c_2\cdot x\cdot t^2 + c_3\cdot x\cdot t^3 + c_4\cdot x\cdot t^4 + c_5\cdot x\cdot t^5$.

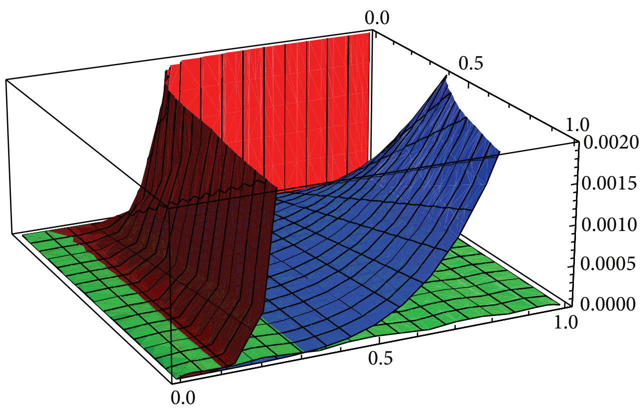

Figure 1: The absolute differences corresponding to the HPM solution (red surface), VIM solution (blue surface), and OHPM solution (green surface) for problem (16).

(ii) Imposing the boundary condition $u_{\mathrm{OHPM}}(x,0) = x$ we obtain $c_0 = 1$.

Replacing this expression of c_0 in the expression of u_{OHPM} we obtain the following:

$u_{\mathrm{OHPM}}(x,t) = x + c_1 \cdot x \cdot t + c_2 \cdot x \cdot t^2 + c_3 \cdot x \cdot t^3 + c_4 \cdot x \cdot t^4 + c_5 \cdot x \cdot t^5$.

We introduce u_{OHPM} in the remainder $\mathfrak{R}$ given by (2) and (9) and we compute the functional $J(c_1, c_2, c_3, c_4, c_5)$ of (10).

We remark that while the expression of the functional is too long to be included here, the computation is simple and straightforward using a dedicated mathematical software (we used the Wolfram Mathematica 9 software).

(iii) We compute the minimum of the functional J and, by replacing the corresponding values of the parameters c_1, c_2, c_3, c_4, c_5, we obtain the following second order approximation:

$\tilde{u}_{\mathrm{OHPM}}(x,t) = -0.109895t^5x + 0.434798t^4x - 0.789112t^3x + 0.961938t^2x - 0.997729tx + x$.

Figure 1 presents the comparison of the absolute errors (computed as the absolute values of the differences between the exact solutions and the approximate solutions) corresponding to the fifth order approximation obtained by using HPM (red surface), to the fifth order approximation obtained by using VIM (blue surface) and to the second order approximation obtained by OHPM (green surface).

Table 1 presents the same comparison for several values of x and t.

It is easy to see that, overall, the approximations obtained by using OHPM are much more accurate than the ones previously computed by using HPM and VIM. Moreover, our approximate solutions are not only more accurate but also, at the same time, present a much simpler expression since they are second order approximate solutions while the previous ones are fifth order approximate solutions.

Table 1: The absolute differences corresponding to the HPM solution (red surface), VIM solution (blue surface), and OHPM solution (green surface) for problem (16).

	HPM	VIM	OHPM
$x = t = 0$	0	0	0
$x = t = 0.2$	$7.894\,10^{-5}$	$3.256\,10^{-7}$	$1.081\,10^{-5}$
$x = t = 0.4$	$1.171\,10^{-2}$	$2.555\,10^{-5}$	$1.398\,10^{-5}$
$x = t = 0.6$	$2.346\,10^{-1}$	$2.819\,10^{-4}$	$9.787\,10^{-6}$
$x = t = 0.8$	2.075	$1.420\,10^{-3}$	$3.280\,10^{-5}$
$x = t = 1$	$1.172\,10^{1}$	$4.700\,10^{-3}$	$2.408\,10^{-7}$

3.2. Application 2. Our second application is the RLW problem (also from [12]):

$$u_t - u_{xxxx} = 0,\qquad u(x,0) = \sin(x). \tag{19}$$

Again in [12] approximate solutions of (16) are computed using the homotopy perturbation method (HPM) and the variational iteration method (VIM).

The exact solution of this problem is $u_e(x,t) = e^{-t}\sin(x)$.

The fourth order solution computed in [12] by using the variational iteration method is $u_{\mathrm{VIM}}(x,t) = (1/24)(t^4 - 4t^3 + 12t^2 - 24t + 24)\sin(x)$.

The third order solution computed in [12] by using the homotopy perturbation method is of the form (5) $u_{\mathrm{HPM}}(x,t) = -(1/24)(t^4 + 4t^3 - 12t^2 + 24t - 24)\sin(x)$.

Using OHPM, the following steps are performed.

(i) Choosing the same homotopy (3) as used in [12] we obtain the same solutions:

$$u_0(x,t) = (t+1)\cdot\sin(x)$$
$$u_1(x,t) = (1/2)\cdot t\cdot(t+4)\cdot(-\sin(x))$$
$$u_2(x,t) = (1/6)\cdot t^2\cdot(t+6)\cdot\sin(x).$$

It follows that we obtain the sets $S_0 = \{\sin(x), \sin(x)\cdot t\}$, $S_1 = \{\sin(x)\cdot t, \sin(x)\cdot t^2\}$, $S_2 = \{\sin(x)\cdot t^2, \sin(x)\cdot t^3\}$.

Hence we will compute a second order approximate solution of the following form:

$u_{\mathrm{OHPM}}(x,t) = c_0\cdot\sin(x) + c_1\cdot\sin(x)\cdot t + c_2\cdot\sin(x)\cdot t^2 + c_3\cdot\sin(x)\cdot t^3$.

(ii) Imposing the boundary condition $u_{\mathrm{OHPM}}(x,0) = x$ we obtain $c_0 = 1$.

Replacing this expression of c_0 in the expression of u_{OHPM} we obtain the following:

$u_{\mathrm{OHPM}}(x,t) = \sin(x) + c_1\cdot\sin(x)\cdot t + c_2\cdot\sin(x)\cdot t^2 + c_3\cdot\sin(x)\cdot t^3$.

We introduce u_{OHPM} in the remainder $\mathfrak{R}$ given by (2) and (9) and we compute the functional $J(c_1, c_2, c_3)$ of (10).

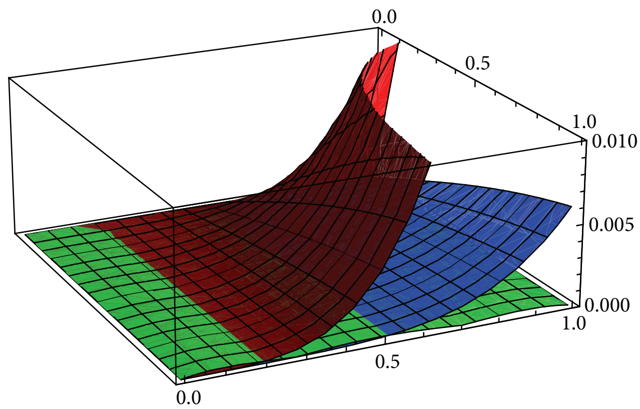

Figure 2: The absolute differences corresponding to the HPM solution (red surface), VIM solution (blue surface), and OHPM solution (green surface) for problem (19).

Table 2: The absolute differences corresponding to the HPM solution (red surface), VIM solution (blue surface), and OHPM solution (green surface) for problem (19).

	HPM	VIM	OHPM
$x = t = 0$	0	0	0
$x = t = 0.2$	$2.598\,10^{-5}$	$5.126\,10^{-7}$	$3.268\,10^{-5}$
$x = t = 0.4$	$7.996\,10^{-4}$	$3.113\,10^{-5}$	$9.737\,10^{-5}$
$x = t = 0.6$	$5.766\,10^{-3}$	$3.322\,10^{-4}$	$1.279\,10^{-4}$
$x = t = 0.8$	$2.276\,10^{-2}$	$1.725\,10^{-3}$	$1.233\,10^{-4}$
$x = t = 1$	$6.413\,10^{2}$	$5.992\,10^{-3}$	$9.511\,10^{-7}$

(iii) We compute the minimum of the functional J and, by replacing the corresponding values of the parameters c_1, c_2, c_3, we obtain the following second order approximation:

$\tilde{u}_{\mathrm{OHPM}}(x,t) = -0.102902t^3\sin(x) + 0.465235t^2\sin(x) - 0.994455t\sin(x) + \sin(x)$.

Figure 2 presents the comparison of the absolute errors corresponding to the third order approximation obtained by using HPM (red surface), to the fourth order approximation obtained by using VIM (blue surface), and to the second order approximation obtained by OHPM (green surface).

Table 2 presents the same comparison for several values of x and t.

Again, overall, the approximations obtained by using OHPM are more accurate than the ones previously computed by using HPM and VIM while, at the same time, they present a much simpler expression.

4. Conclusions

In the present paper the new optimal homotopy perturbation method is introduced as a straightforward and efficient method to compute approximate solutions for nonlinear partial differential equations.

The optimal homotopy perturbation method has an accelerated convergence compared to the regular homotopy perturbation method, fact proved by the included applications. The method is a powerful one since not only were we capable to find more accurate approximations, but also the approximations computed consist of fewer terms than the previous solutions.

Conflict of Interests

The authors declare that there is no conflict of interests regarding the publication of this paper.

References

[1] J.-H. He, "A coupling method of a homotopy technique and a perturbation technique for non-linear problems," *International Journal of Non-Linear Mechanics*, vol. 35, no. 1, pp. 37–43, 2000.

[2] J. H. He and J.-H. He, "Recent development of the homotopy perturbation method," *Topological Methods in Nonlinear Analysis*, vol. 31, no. 2, pp. 205–209, 2008.

[3] D. H. Peregrine, "Calculations of the development of an undular bore," *Journal of Fluid Mechanics*, vol. 25, no. 2, pp. 321–330, 1966.

[4] T. B. Benjamin, J. L. Bona, and J. J. Mahony, "Model equations for long waves in non-linear dispersive systems," *Philosophical Transactions of the Royal Society A*, vol. 272, pp. 47–48, 1972.

[5] S. Kutluay and A. Esen, "A finite difference solution of the regularized long-wave equation," *Mathematical Problems in Engineering*, vol. 2006, Article ID 85743, 14 pages, 2006.

[6] J. Hu, B. Hu, and Y. Xu, "C-N difference schemes for dissipative symmetric regularized long wave equations with damping term," *Mathematical Problems in Engineering*, vol. 2011, Article ID 651642, 16 pages, 2011.

[7] X. Pan and L. Zhang, "Numerical simulation for general Rosenau-RLW equation: an average linearized conservative scheme," *Mathematical Problems in Engineering*, vol. 2012, Article ID 517818, 15 pages, 2012.

[8] J. Hu and Y. Wang, "A high-accuracy linear conservative difference scheme for Rosenau-RLW equation," *Mathematical Problems in Engineering*, vol. 2013, Article ID 870291, 8 pages, 2013.

[9] Y. Liu, H. Li, Y. Du, and J. Wang, "Explicit multistep mixed finite element method for RLW equation," *Abstract and Applied Analysis*, vol. 2013, Article ID 768976, 12 pages, 2013.

[10] H. O. Bakodah and M. A. Banaja, "The method of lines solution of the regularized long-wave equation using Runge-Kutta time discretization method," *Mathematical Problems in Engineering*, vol. 2013, Article ID 804317, 8 pages, 2013.

[11] L. Pérez Pozo, R. Meneses, C. Spa, and O. Durán, "A meshless finite-point approximation for solving the RLW equation," *Mathematical Problems in Engineering*, vol. 2012, Article ID 802414, 22 pages, 2012.

[12] D. D. Ganji, H. Tari, and M. B. Jooybari, "Variational iteration method and homotopy perturbation method for nonlinear evolution equations," *Computers and Mathematics with Applications*, vol. 54, no. 7-8, pp. 1018–1027, 2007.

[13] R. Nawaz, S. Islam, I. A. Shah, M. Idrees, and H. Ullah, "Optimal homotopy asymptotic method to nonlinear damped generalized regularized long-wave equation," *Mathematical Problems in Engineering*, vol. 2013, Article ID 503137, 13 pages, 2013.

[14] H. Jafari, K. Sayevand, H. Tajadodi, and D. Baleanu, "Homotopy analysis method for solving Abel differential equation of fractional order," *Central European Journal of Physics*, vol. 11, no. 10, pp. 1523–1527, 2013.

[15] E. A.-B. Abde-Salam and E. A. Yousif, "Solution of nonlinear space-time fractional differential equations using the fractional Riccati expansion method," *Mathematical Problems in Engineering*, vol. 2013, Article ID 846283, 6 pages, 2013.

Hindawi Publishing Corporation
The Scientific World Journal
Volume 2014, Article ID 454865, 8 pages
http://dx.doi.org/10.1155/2014/454865

Research Article

Solution of Some Types of Differential Equations: Operational Calculus and Inverse Differential Operators

K. Zhukovsky

Faculty of Physics, M. V. Lomonosov Moscow State University, Leninskie Gory, Moscow 119899, Russia

Correspondence should be addressed to K. Zhukovsky; zhukovsky@physics.msu.ru

Received 23 January 2014; Accepted 23 February 2014; Published 30 April 2014

Academic Editors: D. Baleanu and H. Jafari

We present a general method of operational nature to analyze and obtain solutions for a variety of equations of mathematical physics and related mathematical problems. We construct inverse differential operators and produce operational identities, involving inverse derivatives and families of generalised orthogonal polynomials, such as Hermite and Laguerre polynomial families. We develop the methodology of inverse and exponential operators, employing them for the study of partial differential equations. Advantages of the operational technique, combined with the use of integral transforms, generating functions with exponentials and their integrals, for solving a wide class of partial derivative equations, related to heat, wave, and transport problems, are demonstrated.

1. Introduction

Most of physical systems can be described by appropriate sets of differential equations, which are well suited as models for systems. Hence, understanding of differential equations and finding its solutions are of primary importance for pure mathematics as for physics. With rapidly developing computer methods for the solutions of equations, the question of understanding of the obtained solutions and their application to real physical situations remains opened for analytical study. There are few types of differential equations, allowing explicit and straightforward analytical solutions. It is common knowledge that expansion into series of Hermite, Laguerre, and other relevant polynomials [1] is useful when solving many physical problems (see, e.g., [2, 3]). Generalised forms of these polynomials exist with many variables and indices [4, 5]. In what follows, we develop an analytical method to obtain solutions for various types of partial differential equations on the base of operational identities, employing expansions in series of Hermite, Laguerre polynomials, and their modified forms [1, 6]. The key for building these solutions will be an operational approach and development of the formalism of inverse functions and inverse differential operators, already touched in [7, 8]. We will demonstrate in what follows that when used properly and combined, in particular, with integral transforms, such an approach leads to elegant analytical solutions with transparent physical meaning without particularly cumbersome calculations.

2. Inverse Derivative

For a common differential operator $D = d/dx$ we can define an inverse derivative, such that upon the action on a function $f(x)$ it gives another function $F(x)$:

$$D^{-1} f(x) = F(x), \tag{1}$$

whose derivative is $F'(x) = f(x)$. Evidently, the inverse derivative D^{-1} is executed by an integral operator being the inverse of differential operator, acting on $f(x)$, and its general form is $\int f(x) = F(x) + C$, where C is the constant of integration. The action of its nth order

$$D_x^{-n} f(x) = \frac{1}{(n-1)!} \int_0^x (x-\xi)^{n-1} f(\xi)\, d\xi, \quad (n \in N = \{1, 2, 3, \ldots\}) \tag{2}$$

can be complemented with the definition of the action of zero order derivative as follows:

$$D_x^0 f(x) = f(x), \tag{3}$$

so that evidently

$$D_x^{-n}\mathbf{1} = \frac{x^n}{n!}, \quad (n \in N_0 = N \cup \{0\}). \tag{4}$$

In what follows we will appeal to various modifications of the following equation:

$$(\beta^2 - D^2)^\nu F(x) = f(x). \tag{5}$$

Thus, it is important to construct the particular integral $F(x)$ with the help of the following operational identity (see, e.g., [6]):

$$\begin{gathered}\hat{q}^{-\nu} = \frac{1}{\Gamma(\nu)}\int_0^\infty \exp(-\hat{q}t)\, t^{\nu-1}\,dt, \\ \min\{\operatorname{Re}(q), \operatorname{Re}(\nu)\} > 0.\end{gathered} \tag{6}$$

For the operator $\hat{q} = \beta^2 - D^2$ we have

$$\begin{aligned}&(\beta^2 - D^2)^{-\nu} f(x) \\ &\quad = \frac{1}{\Gamma(\nu)}\int_0^\infty \exp(-\beta^2 t)\, t^{\nu-1} \exp(tD^2)\, f(x)\,dt.\end{aligned} \tag{7}$$

We will also make explicit use of the generalized form of the Glaisher operational rule [9]; action of the operator $\hat{S} = \exp(tD_x^2)$ on the function $f(x) = \exp(-x^2)$ yields

$$\begin{aligned}\hat{S} f(x) &= \exp\left(y\frac{\partial^2}{\partial x^2}\right)\exp(-x^2) \\ &= \frac{1}{\sqrt{1+4y}}\exp\left(-\frac{x^2}{1+4y}\right).\end{aligned} \tag{8}$$

Exponential operator mentioned above is closely related to Hermite orthogonal polynomials:

$$H_n(x, y) = n!\sum_{r=0}^{[n/2]} \frac{x^{n-2r} y^r}{(n-2r)!r!}, \tag{9}$$

as demonstrated in [4, 5, 10] by operational relations:

$$H_n(x, y) = \exp\left(y\frac{\partial^2}{\partial x^2}\right) x^n. \tag{10}$$

Moreover, the following generating function for Hermite polynomials exists:

$$\exp(xt + yt^2) = \sum_{n=0}^\infty \frac{t^n}{n!} H_n(x, y). \tag{11}$$

Note also an easy to prove and useful relation [11]:

$$z^n H_n(x, y) = H_n(xz, yz^2). \tag{12}$$

Laguerre polynomials of two variables [4]

$$L_n(x, y) = \exp\left(-y\frac{\partial}{\partial x}x\frac{\partial}{\partial x}\right)\frac{(-x)^n}{n!} = n!\sum_{r=0}^{n}\frac{(-1)^r y^{n-r} x^r}{(n-r)!(r!)^2} \tag{13}$$

are related to the following operator $\partial_x x \partial_x$ [10]:

$${}_L D_x = \frac{\partial}{\partial x}x\frac{\partial}{\partial x} = \frac{\partial}{\partial D_x^{-1}}, \tag{14}$$

sometimes called Laguerre derivative ${}_L D_x$. Note their noncommutative relation with the inverse derivative operator:

$$\left[{}_L D_x, D_x^{-1}\right] = -1, \qquad ([A, B] = AB - BA). \tag{15}$$

They represent solutions of the following partial differential equation with proper initial conditions:

$$\partial_y L_n(x, y) = -(\partial_x x \partial_x) L_n(x, y), \tag{16}$$

where

$$L_n(x, y) = n!\sum_{r=0}^{n}\frac{(-1)^r y^{n-r} x^r}{(n-r)!(r!)^2}, \tag{17}$$

with proper initial conditions:

$$L_n(x, 0) = \frac{(-x)^n}{n!}. \tag{18}$$

In the following sections, we will investigate the possibilities to solve some partial differential equations, involving the differential operators studied above. Now we just note how the technique of inverse operator, applied for derivatives of various orders and their combinations and combined with integral transforms, allows for easy and straightforward solutions of various types of differential equations.

3. Diffusion Type, Heat Propagation Type Problems, and Inverse Derivatives

Heat propagation and diffusion type problems play a key role in the theory of partial differential equations. Combination of exponential operator technique and inverse derivative together with the operational identities of the previous section is useful for the solution of a broad spectrum of partial differential equations, related to heat and diffusion processes. Some of them have been already studied by operational method (see, e.g., [10, 12]). Below we will focus on the generalities of the solution of the following problem:

$$\frac{\partial}{\partial y}F(x, y) = (\hat{P} + \hat{M})\{F(x, y)\}, \tag{19}$$

with initial conditions

$$F(x, 0) = q(x). \tag{20}$$

We will employ operational approach, combined with integral transforms and exponential operator technique. Formal solution for our generic formulation reads as follows:

$$F(x,y)=\exp\left(y\left(\widehat{M}+\widehat{P}\right)\right)q(x). \tag{21}$$

We would like to underline that operators $\widehat{P}$ and $\widehat{M}$ may not commute, so, dependently on the value of their commutator, we will obtain different sequences of operators in (23), disentangling $\widehat{P}$ and $\widehat{M}$ [13, 14]. In the simplest case, when operators $\widehat{M}$ and $\widehat{P}$ are multiplication and differentiation operators, respectively, they can be easily disentangled in the exponent with account for

$$\left[\widehat{P},\widehat{M}\right]=1, \tag{22}$$

which yields

$$\begin{aligned}F(x,y)&=\exp\left(y\left(\widehat{M}+\widehat{P}\right)\right)q(x)\\&=\exp\left(-\frac{y^2}{2}\right)\exp\left(y\widehat{P}\right)\exp\left(y\widehat{M}\right)q(x).\end{aligned} \tag{23}$$

Explicit expressions for the action of these operators on the initial condition function $g(x)$ can be obtained by integral transforms, series expansions, and operational technique to be evaluated in every special case. This formulation, simple in its essence, nevertheless has wide application and allows us to frame either some of integrodifferential equations in this scheme. An elegant and interesting example is given by the following equation:

$$\begin{gathered}\frac{\partial}{\partial t}F(x,t)=-\frac{\partial}{\partial x}x\frac{\partial}{\partial x}F(x,t)+\int_0^x F(\xi,t)\,d\xi,\\F(x,0)=g(x).\end{gathered} \tag{24}$$

Its formal solution reads

$$F(x,t)=\exp\left(\widehat{A}+\widehat{B}\right)g(x), \tag{25}$$

where operators

$$\widehat{A}=-t_L D_x=-t\frac{\partial}{\partial D_x^{-1}},\qquad \widehat{B}=tD_x^{-1} \tag{26}$$

do not commute:

$$\left[\widehat{A},\widehat{B}\right]=-t^2. \tag{27}$$

Evidently, operators in the exponential disentangle:

$$\begin{aligned}F(x,t)&=\exp\left(\widehat{A}+\widehat{B}\right)q(x)\\&=\exp\left(\frac{t^2}{2}\right)\exp\left(tD_x^{-1}\right)\exp\left(-t\frac{\partial}{\partial D_x^{-1}}\right)g(x).\end{aligned} \tag{28}$$

Thus, we have obtained the solution of the integrodifferential equation (24) as a sequence of exponential operators, transforming the initial condition $g(x)$. Our further steps depend on the explicit form of this function. In the most general case of $g(x)$ we may take advantage of the inverse derivative technique. First, consider the action of the operator $\exp(-\partial/(\partial D_x^{-1}))$ on $g(x)$:

$$f(x,t)=\exp\left(-t\frac{\partial}{\partial D_x^{-1}}\right)g(x), \tag{29}$$

where D_x^{-1} is defined in (2). Equation (29) represents, in fact, the diffusion process and it is the solution of the following initial value problem:

$$\frac{\partial}{\partial t}f(x,t)=-\frac{\partial}{\partial x}x\frac{\partial}{\partial x}f(x,t),\quad f(x,0)=g(x). \tag{30}$$

Relevant studies were performed in [10, 12]. The initial condition function $f(x,0)=g(x)$ can be written as follows:

$$g(x)=\varphi\left(D_x^{-1}\right)\mathbf{1}, \tag{31}$$

and the image $\varphi(x)$ is explicitly given by the following integral:

$$\varphi(x)=\int_0^\infty \exp(-\zeta)\,g(x\zeta)\,d\zeta, \tag{32}$$

which is supposed to converge. Then the result of the Laguerre diffusion (29) appears in the form of the translation of the image function φ:

$$f(x,y)=\varphi\left(D_x^{-1}-t\right)\mathbf{1}. \tag{33}$$

Consequently, we have to apply the exponential operator $\exp(tD_x^{-1})$, which can be expanded in series:

$$F(x,t)=\exp\left(\frac{t^2}{2}\right)\sum_{n=0}^\infty\frac{t^n D_x^{-n}}{n!}f(x,t). \tag{34}$$

The simplest example of the initial function $g(x)=\exp(-x)$ demonstrates the technique sketched above, resulting in

$$\varphi(x)=\frac{1}{(1+x)}\quad\text{when }|x|<1, \tag{35}$$

and the Laguerre diffusion contribution (29) produces the following function:

$$f(x,t)=\frac{1}{1-t}\exp\left(-\frac{1}{1-t}x\right). \tag{36}$$

The inverse derivative action on the exponent reads $D_x^{-n}\exp(\alpha x)=\exp(\alpha x)/\alpha^n$ and eventually we obtain

$$\begin{aligned}F(x,t)&=\exp\left(\frac{t^2}{2}\right)\frac{1}{1-t}\sum_{n=0}^\infty\frac{t^n D_x^{-n}}{n!}\exp\left(-\frac{1}{1-t}x\right)\\&=\frac{1}{1-t}\exp\left(-\frac{x}{1-t}\right)\exp\left(-t(1-t)+\frac{t^2}{2}\right).\end{aligned} \tag{37}$$

In conclusion of the present chapter we consider the example of the solution of a heat propagation type equation by operational method, involving the inverse derivative operator and exponential operator technique. We recall that the common heat equation with initial condition problem

$$\frac{\partial}{\partial t} f(x,t) = \partial_x^2 f(x,t), \qquad f(x,0) = g(x) \tag{38}$$

can be solved by Gauss transforms:

$$f(x,t) = \frac{1}{2\sqrt{\pi t}} \int_{-\infty}^{\infty} \exp\left(-\frac{(x-\xi)^2}{4t}\right) g(\xi)\, d\xi. \tag{39}$$

In complete analogy with the above statements, we can solve the heat-type equation with differential operator ${}_L D_x$ (14) with, for example, the following initial condition:

$$\frac{\partial}{\partial t} f(x,t) = {}_L D_x^2 f(x,t), \qquad f(x,0) = g(x). \tag{40}$$

The Laguerre heat-type propagation problem (40) possesses the following solution (see the Appendix):

$$f(x,t) = \frac{1}{2\sqrt{\pi t}} \int_{-\infty}^{\infty} e^{-\xi^2/4t}\, {}_H C_0\left(\frac{-\xi x}{2t}, -\frac{x^2}{4t}\right) \varphi(\xi)\, d\xi. \tag{41}$$

4. Operational Approach and Other Types of Differential Equations

Operational approach to solution of partial differential equations, demonstrated on the examples of diffusion-like and heat-like equations with $\partial_x x \partial_x$ derivatives, can be further extended to other equation types. Consider the following example of a rather complicated differential equation:

$$\begin{aligned} \frac{1}{\rho}\frac{\partial}{\partial t} A(x,t) = x^2 \frac{\partial^2}{\partial x^2} A(x,t) + \lambda x \frac{\partial}{\partial x} A(x,t) \\ - \mu A(x,t), \quad g(x) = A(x,0), \end{aligned} \tag{42}$$

where ρ, λ, and μ are some arbitrary constant coefficients and function $g(x) = A(x, t = 0)$ is the initial condition. By introducing operator $\overline{D} = x\partial_x$ and distinguishing the perfect square, we rewrite (42):

$$\frac{1}{\rho}\frac{\partial}{\partial\, t} A(x,t) = \left(\left(\overline{D} + \frac{\lambda}{2}\right)^2 - \varepsilon\right) A(x,t), \tag{43}$$

where

$$\varepsilon = \mu + \left(\frac{\lambda}{2}\right)^2. \tag{44}$$

Thus, the following exponential solution for (42) appears:

$$A(x,t) = \exp\left\{\rho t \left(\left(\overline{D} + \frac{\lambda}{2}\right)^2 - \varepsilon\right)\right\} g(x). \tag{45}$$

Now making use of the operational identity

$$\exp\left(\hat{p}^2\right) = \frac{1}{\sqrt{\pi}} \int_{-\infty}^{\infty} \exp\left(-\xi^2 + 2\xi\hat{p}\right) d\xi \tag{46}$$

and applying $\exp(a\overline{D})$ according to

$$\exp\left(ax\partial_x\right) f(x) = f\left(e^a x\right), \tag{47}$$

we obtain the following compact expression for $A(x,t)$:

$$\begin{aligned} A(x,t) = \frac{\exp(-\rho\varepsilon t)}{\sqrt{\pi}} \\ \times \int_{-\infty}^{\infty} \exp\left[-\sigma^2 + \sigma\alpha\frac{\lambda}{2\rho}\right] g\left(x \exp(\sigma\alpha)\right) d\sigma, \end{aligned} \tag{48}$$

where

$$\alpha = \alpha(t) = 2\sqrt{\rho t}. \tag{49}$$

Consider two simple examples of initial condition functions. The first one is

$$g(x) = x^n. \tag{50}$$

Then we immediately obtain the solution of (42) as follows:

$$A(x,t) = x^n \exp\left\{\rho t\left(n^2 + \lambda n - \mu\right)\right\}. \tag{51}$$

The second example is given by the following initial condition function:

$$g(x) = \ln x. \tag{52}$$

Trivial computations yield the following solution:

$$A(x,t) = \left(\ln x + \rho t \lambda\right) \exp\left(-\rho t \mu\right). \tag{53}$$

Thus, operational technique, combined with integral transforms, operational identities, and extended forms of orthogonal polynomials, represents powerful tool for finding solutions of various classes of differential equations and initial value problems. Note that within the framework of inverse differential operators, developed and described above, the usage of the evolution operator method opens new possibilities, which we will elucidate in what follows.

Let us consider the following generalization of the heat equation:

$$\partial_t F(x,t) = \alpha \partial_x^2 F(x,t) + \beta x F(x,t), \tag{54}$$

with the initial condition:

$$F(x,0) = f(x). \tag{55}$$

The evolution type equation (54) contains linear coordinate term in addition to the second order derivative. Its formal solution can be written via the evolution operator $\widehat{U}$:

$$F(x,t) = \widehat{U} f(x), \tag{56}$$

where

$$\widehat{U} = \exp\left(\widehat{A} + \widehat{B}\right), \quad \widehat{A} = \alpha t \partial_x^2, \quad \widehat{B} = \beta t x. \tag{57}$$

The exponential of the evolution operator $\widehat{U}$ in (56) is the sum of two noncommuting operators and it can be written as the ordered product of two exponential operators. Indeed, the commutator of $\widehat{A}$ and $\widehat{B}$ has the following nonzero value:

$$\left[\widehat{A}, \widehat{B}\right] = m\widehat{A}^{1/2} = 2\alpha\beta t^2 \partial_x, \quad m = 2\beta t^{3/2}\alpha^{1/2}. \tag{58}$$

Then we can apply the disentanglement operational identity:

$$e^{\widehat{A}+\widehat{B}} = e^{(m^2/12)-(m/2)\widehat{A}^{1/2}+\widehat{A}} e^{\widehat{B}}, \tag{59}$$

and the following chain rule:

$$e^{p\partial_x^2} e^{qx} g(x) = e^{pq^2} e^{qx} e^{2pq\partial_x} e^{p\partial_x^2} g(x), \tag{60}$$

where p, q are constant parameters. With their help, we obtain the evolution operator $\widehat{U}$ for (54):

$$\widehat{U} = e^{\Phi(x,t;\beta)} \widehat{\Theta}\widehat{S}. \tag{61}$$

Note that we have factorized two commuting operators: the operator of translation in space

$$\widehat{\Theta} = e^{\alpha\beta t^2 \partial_x} \tag{62}$$

and operator

$$\widehat{S} = e^{\alpha t \partial_x^2}, \tag{63}$$

which is, in fact, operator $\widehat{S} = \exp(tD_x^2)$. The phase in $\widehat{U}$ is written as follows:

$$\Phi(x, t; \alpha, \beta) = \frac{1}{3}\alpha\beta^2 t^3 + \beta t x. \tag{64}$$

The action of $\widehat{U}$ on the initial condition function $f(x)$ yields the following solution for our problem:

$$F(x,t) = e^{\Phi(x,t;\alpha,\beta)} \widehat{\Theta}\widehat{S} f(x). \tag{65}$$

Thus, we conclude from the form of (65) that the problem (54) with the initial condition (55) can be solved by the consequent application of commuting operators $\widehat{\Theta}$ (62) and $\widehat{S}$ (63) to $f(x)$, apart from the factor $e^{\Phi(x,t;\alpha,\beta)}$. Now the explicit form of the solution (65) can be obtained by recalling that $\widehat{\Theta}$ acts as a translation operator

$$e^{s\partial_x} g(x) = g(x+s) \tag{66}$$

and that the action of $\widehat{S}$ on the function $g(x)$ yields the solution of the ordinary heat equation, through Gauss-Weierstrass transform (A.1). Accordingly, we denote

$$f(x,t) \equiv \widehat{S} f(x) \equiv e^{\alpha t \partial_x^2} f(x), \tag{67}$$

and we write

$$\widehat{\Theta} f(x,t) = f\left(x + \alpha\beta t^2, t\right). \tag{68}$$

Thus, (54) with initial condition (55) has the following explicit solution:

$$F(x,t) = e^{\Phi(x,t;\alpha,\beta)} \frac{1}{2\sqrt{\pi\alpha t}} \int_{-\infty}^{\infty} e^{-(x+\alpha\beta t^2-\xi)^2/4t\alpha} f(\xi)\, d\xi, \tag{69}$$

provided that the integral converges. Summarizing the above outlined procedure, we conclude that a solution for (54) consists in finding a Gauss transformed function f with a shifted argument:

$$F(x,t) = e^{\Phi(x,t;\alpha,\beta)} f\left(x + \alpha\beta t^2, t\right). \tag{70}$$

Moreover, this is a general observation for this type of equation, valid for any function $f(x)$ (provided the integral converges). In other words, we have obtained the solution of Fokker plank equation as a consequent action of operator $\widehat{S}$ of heat diffusion and operator $\widehat{\Theta}$ of translation on the initial condition function. Note that $f(x,t)$ is the solution of the heat equation, representing a natural propagation phenomenon.

The effect, produced by the translation operator $\widehat{\Theta}$ and the operator $\widehat{S}$, is best illustrated with the example of Gaussian $f(x) = \exp(-x^2)$ evolution, when (69) becomes

$$F(x,t)|_{f(x)=\exp(-x^2)} = \frac{\exp(\Phi(x,t))}{\sqrt{1+4t}} \exp\left(-\frac{\left(x+\beta t^2\right)^2}{1+4t}\right), \quad t \geq 0. \tag{71}$$

The above result is exactly the generalization of Gleisher rule (8), considered earlier in the context of the heat equation. Thus, (71) is the solution of the ordinary heat equation with $\beta = 0$, when the initial function is Gaussian.

Another interesting example of solving (54) appears when the initial function $f(x)$ allows the expansion in the following series:

$$f(x) = \sum_k c_k x^k e^{\gamma x}. \tag{72}$$

In this case, we refer to the identity

$$\exp\left(yD_x^2\right) x^k e^{\gamma\, x} = e^{(\gamma\, x+\gamma^2 y)} H_k(x + 2\gamma y, y), \tag{73}$$

which arises from

$$\exp\left(y\frac{\partial^m}{\partial x^m}\right) f(x) = f\left(x + my\frac{\partial^{m-1}}{\partial x^{m-1}}\right)\mathbf{1} \tag{74}$$

with account for the generating function of Hermite polynomials (11). Then the action (67) of operator $\widehat{S}$ on the initial function (72) produces

$$f(x,t) = \sum_k c_k f_k(x,t).$$
$$f_k(x,t) = e^{\gamma(x+\gamma a)} H_k(x + 2\gamma a, a), \quad a = \alpha t. \tag{75}$$

In addition, the translation, operated by $\widehat{\Theta}$, shifts the argument: $f(x,t) \rightarrow f(x+ab,t)$, $b=\beta t$. Thus, we obtain the solution in a form of Hermite polynomial as follows:

$$F(x,t) = \sum_k c_k e^{\Phi+\Phi_1} H_k\left(x + \frac{\alpha\gamma^2}{\beta}\left(2t\frac{\beta}{\gamma} + t^2\frac{\beta^2}{\gamma^2}\right), \alpha t\right), \tag{76}$$

where Φ is defined by (64) and

$$\Phi_1 = \gamma\left(x + \frac{\alpha\gamma^2}{\beta}\left(t\frac{\beta}{\gamma} + \left(t\frac{\beta}{\gamma}\right)^2\right)\right). \tag{77}$$

It is now evident that, for a short time, when $t \ll \gamma/\beta$, the solution will be spanning in space off the initial function, modulated by $H_k(x,\alpha t)$ and exponentially depending on time:

$$\begin{gathered} F(x,t)|_{t\ll\gamma/\beta} \approx \sum_k c_k \exp\left(\alpha\gamma^2 t + \gamma x\right) H_k(x,\alpha t), \\ F(x,t)|_{t\ll\gamma/\beta, t\ll 1} \approx \sum_k c_k e^{\alpha\gamma^2 t} e^{\gamma x} x^k. \end{gathered} \tag{78}$$

Note that for extended times $t \gg \gamma/\beta$ we have dominance of time variable: $\Phi \gg \Phi_1$, and the solution asymptotically behaves as $\exp(\beta t x)$, while x plays minor role in $H_k(x+2\gamma\alpha t+\alpha\beta t^2, \alpha t)$.

The same operational technique as employed for the treatise of (54) can be easily adopted for the solution of the Schrödinger equation:

$$\begin{gathered} i\hbar\partial_t\Psi(x,t) = -\frac{\hbar^2}{2m}\partial_x^2\Psi(x,t) + Fx\Psi(x,t), \\ \Psi(x,0) = f(x), \end{gathered} \tag{79}$$

where F is constant (F has the dimension of force). Indeed, rescaling variables in (79), we obtain the form of equation, similar to (54):

$$i\partial_\tau\Psi(x,\tau) = -\partial_x^2\Psi(x,\tau) + bx\Psi(x,\tau), \tag{80}$$

where

$$\tau = \frac{\hbar t}{2m}, \qquad b = \frac{2Fm}{\hbar^2}. \tag{81}$$

Following the operational methodology, developed for (54), we write the following solution of (80) in the form (56):

$$\Psi(x,\tau) = \widehat{\widehat{U}} f(x), \tag{82}$$

where

$$\widehat{\widehat{U}} = \exp\left(i\tau\widehat{H}\right), \quad \widehat{H} = \partial_x^2 - bx. \tag{83}$$

Then, on account of the substitution $t \rightarrow i\tau, \beta \rightarrow -b$, operators

$$\widehat{\widehat{\Theta}} = \exp\left(b\tau^2\partial_x\right), \qquad \widehat{\widehat{\Theta}} f(x,\tau) = f\left(x + b\tau^2, \tau\right), \tag{84}$$

$$\widehat{\widehat{S}} = \exp\left(i\tau\partial_x^2\right), \qquad \widehat{\widehat{S}} f(x) = f(x, i\tau) \tag{85}$$

arise. Thus, the solution of the Schrödinger equation is a result of consequent action of the operator $\widehat{\widehat{S}}$ and further action of $\widehat{\widehat{\Theta}}$ on the initial condition function:

$$\Psi(x,t) = \exp(-i\Phi(x,\tau;b))\,\widehat{\widehat{\Theta}}\,\widehat{\widehat{S}} f(x), \tag{86}$$

where Φ is defined by (64). The integral form of the solution then is written as follows:

$$\begin{aligned} \Psi(x,t) = {} & \exp(-i\Phi(x,\tau;b))\frac{1}{2\sqrt{i\pi\tau}} \\ & \times \int_{-\infty}^{\infty} \exp\left(-\frac{\left(x+b\tau^2-\xi\right)^2}{4i\tau}\right) f(\xi)\, d\xi. \end{aligned} \tag{87}$$

Again, as well as in (70), without any assumption on the nature of the initial condition function $f(x)$ of the Schrödinger equation, its solution

$$\Psi(x,\tau) = \exp(-i\Phi(x,\tau;b))\, f\left(x + b\tau^2, i\tau\right), \tag{88}$$

where $f(x,t)$ is given by (85) and is expressed in terms of the function of two variables, obtained by the consequent application of the heat propagation and translation operators (85) and (84) to $f(x)$. So far we have demonstrated as Gauss-Weierstrass transform (A.1) describe the action of $\widehat{\widehat{S}}$ on the initial probability amplitude and how the shift (84) finally yields the explicit form of the solution of Schrödinger equation. It means that the result of the action of evolution operator (83) on $f(x)$ is the product of combined action of translation operator $\widehat{\widehat{\Theta}}$ and heat propagation operator $\widehat{\widehat{S}}$, representing the evolution operator of the free particle.

Now let us consider another Fokker-Plank type equation, that is, the following example:

$$\partial_t F(x,t) = \alpha\partial_x^2 F(x,t) + \beta x\partial_x F(x,t), \tag{89}$$

with initial condition (55). Proceeding along the above outlined scheme of the solution of (54), we write the solution of (89) in general form (56):

$$F(x,t) = \widehat{U} f(x), \qquad \widehat{U} = \exp\left(\widehat{A} + \widehat{B}\right), \tag{90}$$

where operators $\widehat{A}$ and $\widehat{B}$ are defined as follows:

$$\widehat{A} = t\alpha\partial_x^2, \qquad \widehat{B} = t\beta x\partial_x. \tag{91}$$

Quantities $\widehat{A}$ and $\widehat{B}$ evidently do not commute:

$$\left[\widehat{A}, \widehat{B}\right] = 2\alpha\beta t^2\partial_x^2 = m\widehat{A}, \qquad m = 2t\beta. \tag{92}$$

It allows disentanglement of the operators in the exponential according to the following rule:

$$\exp\left(\widehat{A} + \widehat{B}\right) = \exp\left(\frac{1-\exp(-m)}{m}\widehat{A}\right)\exp\left(\widehat{B}\right). \tag{93}$$

Thus, the evolution operator $\widehat{U}$ action on $f(x)$, given below:

$$\widehat{U} f(x) = \exp\left(\sigma \partial_x^2\right) \exp\left(\beta t x \partial_x\right) f(x) = \exp\left(\sigma \partial_x^2\right) f\left(e^{\beta t} x\right), \tag{94}$$

simply reduces to a Gauss transforms, where the parameter $\sigma = \sigma(t)$ reads as follows:

$$\sigma(t) = \frac{(1 - \exp(-2\beta t))\alpha}{\beta}. \tag{95}$$

Upon the trivial change of variables, we obtain

$$\widehat{U} f(x) = \widehat{S} f(y), \quad y = x \exp(b), \quad \widehat{S} = \exp\left(\frac{\rho}{2}\partial_y^2\right), \tag{96}$$

where

$$\rho(t) = \frac{\alpha}{\beta}\left(e^{2\beta t} - 1\right) \tag{97}$$

and, eventually, we end up with the following simple solution of (89):

$$F(x,t) = \frac{1}{\sqrt{2\pi\rho}} \int_{-\infty}^{\infty} e^{-(\exp(\beta t)x - \xi)^2/2\rho} f(\xi)\, d\xi. \tag{98}$$

The same example of the initial Gaussian function $f(x) = \exp(-x^2)$ as in the case of (54) yields (compare with (71))

$$F(x,t)\big|_{f(x)=\exp(-x^2)} = \frac{1}{\sqrt{1+2\rho(t)}} \exp\left(-\frac{e^{2\beta t} x^2}{1+2\rho(t)}\right), \tag{99}$$

where ρ is defined in (97). Note that we can meet the following modified form of Fokker-Plank type equation (89):

$$\partial_t F(x,t) = \alpha \partial_x^2 F(x,t) + \beta \partial_x x F(x,t), \tag{100}$$

in problems, related to propagation of electron beams in accelerators. Its solution arises from (99) immediately and differs from it just by a factor $\exp(\beta t)$, as written below for a Gaussian $f(x)$:

$$\begin{aligned} F(x,t)\big|_{f(x)=\exp(-x^2)} &= \frac{e^{\beta t}}{\sqrt{1+2\rho(t)}} \exp\left(-\frac{e^{2\beta t} x^2}{1+2\rho(t)}\right) \\ &= \frac{1}{\sqrt{\eta(t)}} \exp\left(-\frac{x^2}{\eta(t)}\right), \\ \eta(t) &= 2\frac{\alpha}{\beta}\left(1 - e^{-2\beta t} + \frac{\beta}{2\alpha} e^{-2\beta t}\right). \end{aligned} \tag{101}$$

However, differently from the solution of (54), where we had consequent transforms of the initial condition function $f(x)$ by operators of translation and heat diffusion $\widehat{S}$ (63) (see also [15]), here we have just the action of $\widehat{S}$ alone with much more complicated dependence of the solution on time.

5. Conclusions

Operational method is fast and universal mathematical tool for obtaining solutions of differential equations. Combination of operational method, integral transforms, and theory of special functions together with orthogonal polynomials closely related to them provides a powerful analytical instrument for solving a wide spectrum of differential equations and relevant physical problems. The technique of inverse operator, applied for derivatives of various orders and combined with integral transforms, allows for easy and straightforward solutions of various types of differential equations. With operational approach, we developed the methodology of inverse differential operators and derived a number of operational identities with them. We have demonstrated that using the technique of inverse derivatives and inverse differential operators, combined with exponential operator, integral transforms, and special functions, we can make significant progress in solution of various mathematical problems and relevant physical applications, described by differential equations.

Appendix

In complete analogy with the heat equation solution by Gauss-Weierstrass transform [16]:

$$\exp\left(b\partial_x^2\right) g(x) = \frac{1}{2\sqrt{\pi b}} \int_{-\infty}^{\infty} \exp\left(-\frac{(x-\xi)^2}{4b}\right) g(\xi)\, d\xi, \tag{A.1}$$

accounting for noncommutative relation for operators of inverse derivative D_x^{-1} and ${}_L D_x$, defined through the operational relation (14) and accounting for (31) and (32), we write the solution of (40) in the following form:

$$f(x,t) = \frac{1}{2\sqrt{\pi t}} \int_{-\infty}^{\infty} \exp\left(-\frac{\left(\widehat{D}_x^{-1} - \xi\right)^2}{4t}\right) \mathbf{1} \varphi(\xi)\, d\xi, \tag{A.2}$$

where φ is the image (32) of the initial condition function g. The kernel of the integral in the above formula can be expanded into series of two-variable Hermite polynomials $H_n(x,y)$:

$$\begin{aligned} &\exp\left(-\frac{\left(\widehat{D}_x^{-1} - \xi\right)^2}{4t}\right)\mathbf{1} \\ &= e^{-\xi^2/4t} \sum_{n=0}^{\infty} \frac{\widehat{D}_x^{-n}}{n!} H_n\left(\frac{\xi}{2t}, -\frac{1}{4t}\right) \\ &= e^{-\xi^2/4t} \sum_{n=0}^{\infty} \frac{x^n}{(n!)^2} H_n\left(\frac{\xi}{2t}, -\frac{1}{4t}\right). \end{aligned} \tag{A.3}$$

Taking into account formula (12) for $x^n H_n(\xi/2t, -1/4t)$ in the operational identity above, which can be viewed as a generating function in terms of inverse derivative for

$H_n(x, y)$, we obtain the following expansion for the kernel of the integral:

$$\exp\left(-\frac{\left(\widehat{D}_x^{-1}-\xi\right)}{4t}\right)\mathbf{1}=e^{-\xi^2/4t}\sum_{n=0}^{\infty}\frac{1}{(n!)^2}H_n\left(\frac{x\xi}{2t},-\frac{x^2}{4t}\right), \tag{A.4}$$

where the series of Hermite polynomials of two arguments $H_n(x, y)$ can be expressed in terms of Hermite-Bessel-Tricomi functions ${}_HC_n(x, y)$—generalization of Bessel-Tricomi functions—and related to Bessel-Wright functions and to common Bessel functions [17]:

$${}_HC_n(x, y)=\sum_{m=0}^{\infty}\frac{H_m(-x, y)}{r!\,(n+m)!}, \quad n\in N_0. \tag{A.5}$$

In particular, for $n = 0$, we immediately find our series:

$${}_HC_0(x, y)=\sum_{m=0}^{\infty}\frac{H_m(-x, y)}{(m!)^2}, \tag{A.6}$$

which obviously leads to the solution of the heat-type propagation problem (40) by the following appropriate Gauss transform:

$$f(x, t)=\frac{1}{2\sqrt{\pi t}}\int_{-\infty}^{\infty}e^{-\xi^2/4t}\,{}_HC_0\left(\frac{-\xi x}{2t},-\frac{x^2}{4t}\right)\varphi(\xi)\,d\xi. \tag{A.7}$$

Conflict of Interests

The author declares that there is no conflict of interests regarding the publication of this paper.

References

[1] A. Appèl and J. Kampé de Fériet, *Fonctions Hypergéométriques et Hypersphériques: Polynômes d'Hermite*, Gauthier-Villars, Paris, France, 1926.

[2] D. T. Haimo and C. Markett, "A representation theory for solutions of a higher order heat equation, I," *Journal of Mathematical Analysis and Applications*, vol. 168, no. 1, pp. 89–107, 1992.

[3] D. T. Haimo and C. Markett, "A representation theory for solutions of a higher order heat equation, II," *Journal of Mathematical Analysis and Applications*, vol. 168, no. 2, pp. 289–305, 1992.

[4] G. Dattoli, "Generalized polynomials, operational identities and their applications," *Journal of Computational and Applied Mathematics*, vol. 118, no. 1-2, pp. 111–123, 2000.

[5] G. Dattoli, H. M. Srivastava, and K. Zhukovsky, "Orthogonality properties of the Hermite and related polynomials," *Journal of Computational and Applied Mathematics*, vol. 182, no. 1, pp. 165–172, 2005.

[6] A. Erdélyi, W. Magnus, F. Oberhettinger, and F. G. Tricomi, *Higher Transcendental Functions*, vol. 2, McGraw-Hill Book Company, New York, NY, USA, 1953.

[7] G. Dattoli, B. Germano, M. R. Martinelli, and P. E. Ricci, "Negative derivatives and special functions," *Applied Mathematics and Computation*, vol. 217, no. 8, pp. 3924–3928, 2010.

[8] G. Dattoli, M. Migliorati, and S. Khan, "Solutions of integro-differential equations and operational methods," *Applied Mathematics and Computation*, vol. 186, no. 1, pp. 302–308, 2007.

[9] H. M. Srivastava and H. L. Manocha, *A Treatise on Generating Functions*, Mathematics and its Applications (Ellis Horwood Ltd), Halsted Press, John Wiley and Sons, Chichester, UK, 1984.

[10] G. Dattoli, H. M. Srivastava, and K. Zhukovsky, "A new family of integral transforms and their applications," *Integral Transforms and Special Functions*, vol. 17, no. 1, pp. 31–37, 2006.

[11] H. W. Gould and A. T. Hopper, "Operational formulas connected with two generalizations of Hermite polynomials," *Duke Mathematical Journal*, vol. 29, no. 1, pp. 1–174, 1962.

[12] G. Dattoli, H. M. Srivastava, and K. Zhukovsky, "Operational methods and differential equations with applications to initial-value problems," *Applied Mathematics and Computation*, vol. 184, no. 2, pp. 979–1001, 2007.

[13] G. Dattoli and K. V. Zhukovsky, "Appèl polynomial series expansion," *International Mathematical Forum*, vol. 5, no. 14, pp. 649–6662, 2010.

[14] G. Dattoli, M. Migliorati, and K. Zhukovsky, "Summation formulae and stirling numbers," *International Mathematical Forum*, vol. 4, no. 41, pp. 2017–22040, 2009.

[15] J. E. Avron and I. W. Herbst, "Spectral and scattering theory of Schrödinger operators related to the stark effect," *Communications in Mathematical Physics*, vol. 52, no. 3, pp. 239–254, 1977.

[16] K. B. Wolf, *Integral Transforms in Science and Engineering*, Plenum Press, New York, NY, USA, 1979.

[17] G. N. Watson, *A Treatise on the Theory of Bessel Functions*, Cambridge University Press, Cambridge, UK, 2nd edition, 1944.

Hindawi Publishing Corporation
The Scientific World Journal
Volume 2014, Article ID 716740, 10 pages
http://dx.doi.org/10.1155/2014/716740

Research Article

Global Existence and Energy Decay Rates for a Kirchhoff-Type Wave Equation with Nonlinear Dissipation

Daewook Kim,[1] Dojin Kim,[2] Keum-Shik Hong,[3] and Il Hyo Jung[1]

[1] *Department of Mathematics, Pusan National University, 30 Jangjeon-dong, Geumjeong-gu, Busan 609-735, Republic of Korea*
[2] *Department of Mathematics, Oregon State University, Corvallis, OR 97331, USA*
[3] *Department of Cogno-Mechatronics Engineering and School of Mechanical Engineering, Pusan National University, Busan 609-735, Republic of Korea*

Correspondence should be addressed to Il Hyo Jung; ilhjung@pusan.ac.kr

Received 23 January 2014; Accepted 23 February 2014; Published 7 April 2014

Academic Editors: D. Baleanu and H. Jafari

The first objective of this paper is to prove the existence and uniqueness of global solutions for a Kirchhoff-type wave equation with nonlinear dissipation of the form $Ku'' + M(|A^{1/2}u|^2)Au + g(u') = 0$ under suitable assumptions on K, A, $M(\cdot)$, and $g(\cdot)$. Next, we derive decay estimates of the energy under some growth conditions on the nonlinear dissipation g. Lastly, numerical simulations in order to verify the analytical results are given.

1. Introduction

A mathematical model for the transverse deflection of an elastic string of length $L > 0$ whose ends are held a fixed distance apart is written in the form of the hyperbolic equation

$$\frac{\partial^2 u(x,t)}{\partial t^2} - \left(\alpha + \beta \int_0^L \left|\frac{\partial u(x,t)}{\partial x}\right|^2 dx\right) \frac{\partial^2 u(x,t)}{\partial x^2} = 0, \quad (1)$$

which was proposed by Kirchhoff [1], where $u(x,t)$ is the deflection of the point x of the string at the time t and $\alpha > 0$, β are constants. Kirchhoff first introduced (1) in the study of the oscillations of stretched strings and plates, so that (1) is called the wave equation of Kirchhoff type. The Kirchhoff-type model also appeared in scientific research for beam or plate [2–5]. Such nonlinear Kirchhoff model gives one way to describe the dynamics of an axially moving string. In recent years, axially moving string-like continua such as wires, belts, chains, and band saws have been the subject of study of researchers [6–14].

The mathematical aspects of the natural generalization of the model (1) in $\Omega \subset \mathbb{R}^n$:

$$u'' - M\left(\int_\Omega |\nabla u|^2 dx\right)\Delta u + g(u') = 0, \quad (2)$$

$$u(0) = u_0, \qquad u'(0) = u_1, \quad (3)$$

under some assumptions on $M(\cdot)$, $g(\cdot)$, have been studied, using different methods, by many authors [6, 8, 15–22].

When $g(\cdot) = 0$ and $n = 1$, the problem (2)-(3) was studied by Dickey [16] and Bernstein [15] who considered analytic functions as the initial data (see also Yamada [21] and Ebihara et al. [17]). In case when $g(\cdot) = 0$ and $n \geq 1$, Pohožaev [22] obtained the existence and uniqueness of global solutions for the problem (2)-(3). Lions [20] also formulated Pohožaev's results in an abstract context and obtained better results.

Equation (2) with linear dissipative term, that is, $g(u') = \delta u'$ ($\delta > 0$), was investigated by Mizumachi [23], Nishihara and Yamada [24], Park et al. [25], and Jung and Choi [26]. In fact, they studied the existence, uniqueness, and the energy decay rates of solutions for the problem (2)-(3). On the other hand, related works to a Kirchhoff-type equation with Ku'' instead of u'' can be found in Levine [19]. Jung and Lee [27] got the result for a Kirchhoff-type equation with strong dissipative term. But they studied a simple form with the coefficient $M(\cdot) \equiv 1$. In case of the equation concerning nonlinear Kirchhoff-type coefficient, recently, Kim et al. [8], Ghisi and Gobbino [28], and Aassila and Kaya [29] have studied existence and energy decay rates of global (or local) solutions for the equation. By giving some suitable smallness conditions on the sizes of the initial data, they assured global existence and energy decay rates for the solutions.

In this paper, we study the existence, uniqueness, and the decay estimates of the energy for a class of Kirchhoff-type wave equations in a Hilbert space H:

$$\begin{gathered} Ku'' + M\left(\left|A^{1/2}u\right|^2\right)Au + g\left(u'\right) = 0 \quad \text{in } H, \\ u(0) = u_0, \quad \left(Ku'\right)(0) = K^{1/2}u_1, \end{gathered} \tag{4}$$

where K and A are linear operators in H and $M(\cdot) \in C^1[0,\infty)$. For global existence of this problem, we give some suitable smallness conditions. So, the main contribution of these results is to consider a general model which contains the concrete model (2)-(3) and to improve the results of Kouémou-Patcheu [30] and Jung and Choi [26]. Moreover, as an application, we give some simulation results about solution's shapes and the algebraic decay rate for a Kirchhoff-type wave equation with nonlinear dissipation.

The method applied in this paper is based on the multipliers technique [31], Galerkin's approximate method, and some integral inequalities due to Haraux [32].

This paper is organized as follows. In Section 2, we recall the notation, hypotheses, and some necessary preliminaries and prove the existence and uniqueness of global solutions for the system (4) by employing Feado-Galerkin's techniques under suitable smallness condition. In Section 3, we derive the energy decay rates by using the multiplier technique under suitable growth conditions on g. Finally, in Section 4, we give an example and its numerical simulations to illustrate our results.

2. Preliminaries and Existence

Let Ω be a bounded open domain in $\mathbb{R}^n$ having a smooth boundary Γ and $H = L^2(\Omega)$ with inner product and norm denoted by $(\cdot,\cdot)$ and $|\cdot|$, respectively. Let K be a linear, positive, and self-adjoint operator on H; that is, there is a constant $c > 0$ such that

$$(Ku, u) \geq c|u|^2, \quad \forall u \in H. \tag{5}$$

Let A be a linear, self-adjoint, and positive operator in H, with domain $V := D(A)$ dense in H, $KA = AK$ on $D(A) \cap D(K)$, and the graph norm denoted by $\|\cdot\|$. We assume that the imbedding $V \subset H$ is compact. Identifying H and its dual H', it follows that $V \subset H \subset V'$, where V' is the dual of V. Let $\langle\cdot,\cdot\rangle_{V',V}$ denote the duality pairing between V' and V and $W := D(A^{1/2})$.

Throughout the paper we will make the following assumptions.

(M) $M(s)$ is a $C^1[0,\infty)$ real function and $M'(s) \geq 0$. Furthermore, there exist some positive constants β and γ_0 such that $M(s) \geq \beta > 0$ for all $s \geq 0$ and $|M'(s)s|/M(s) \leq \gamma_0$.

(G) $g : \mathbb{R} \to \mathbb{R}$ is a nondecreasing continuous function such that $g(0) = 0$ and there is a constant $k > 0$ and $q \geq 1$ such that

$$\left|g(x)\right| \leq k\left(1 + |x|^q\right) \quad \forall x \in \mathbb{R}. \tag{6}$$

And $(g(u), Au) \geq 0$ for all $u \in D(A) \cap D(A^{1/2})$. Note that the last assumption of (G) makes sense. In fact, when $A = -\Delta$ and $g(u) = |u|^\alpha u$, $\alpha \geq 1$, we can easily show that $(g(u), Au) \geq 0$ for all $u \in D(A) \cap D(A^{1/2})$.

(H) $M'(s) > M(s)|g(x)|$, $s \in [0,\infty)$, $x \in \mathbb{R}$.

(S) $V \subset L^{q+1}(\Omega)$ for some $q \geq 1$.

Let $\overline{M}(t)$ and $E(t)$ be defined as follows:

$$\overline{M}(t) = \int_0^t M(s)\,ds \tag{7}$$

$$E(t) = \frac{1}{2}\left[\left|K^{1/2}u'\right|^2 + \overline{M}\left(\left|A^{1/2}u\right|^2\right)\right]. \tag{8}$$

And also let us consider the functions

$$\begin{gathered} P(t) := \frac{\left|K^{1/2}u'(t)\right|^2}{M\left(\left|A^{1/2}u\right|^2\right)} + \left|A^{1/2}u(t)\right|^2, \\ Q(t) := \frac{\left|K^{1/2}A^{1/2}u'(t)\right|^2}{M\left(\left|A^{1/2}u\right|^2\right)} + |Au(t)|^2, \\ G(t) := \frac{\left|K^{1/2}u'(t)\right|}{M\left(\left|A^{1/2}u\right|^2\right)}. \end{gathered} \tag{9}$$

Theorem 1. *Let the initial conditions $(u_0, u_1) \in W \times L^{2q}(\Omega)$ satisfy the smallness assumption*

$$\left\|M'\right\|_{L^\infty([0,P(0)])} B(u_0,u_1)\sqrt{Q(0)} < \frac{1}{4}, \tag{10}$$

where $B(u_0,u_1) = \max\{|K^{1/2}u_1|/M(|A^{1/2}u_0|^2), M(|A^{1/2}u_0|^2)/((M(|A^{1/2}u_0|^2))' - g(u_1)M(|A^{1/2}u_0|^2)))\sqrt{Q(0)}\}$. Then there is a unique function $u \in L^\infty(0,T;W) \cap W^{1,\infty}(0,T;V) \cap W^{2,\infty}(0,T;H)$ such that, for any $T > 0$,

$$\begin{gathered} Ku'' + M\left(\left|A^{1/2}u\right|^2\right)Au + g\left(u'\right) = 0 \\ \text{in } L^{(q+1)/q}\left(0,T;V'\right), \end{gathered} \tag{11}$$

$$u(0) = u_0, \qquad \left(Ku'\right)(0) = K^{1/2}u_1. \tag{12}$$

Proof. Assume that, for simplicity, V is separable; then there is a sequence $(e^j)_{j\geq1}$ consisting of eigenfunctions of the operator A corresponding to positive real eigenvalues μ_j tending to $+\infty$ so that $Ae^j = \mu_j e^j$, $j \geq 1$.

Let us denote by V_m the linear hull of $e^1, e^2, \ldots, e^m$. Note that $(e^j)_{j\geq1}$ is a basis of H, V, and W and hence it is dense in H, V, and W. □

Approximate Solutions. We search for a function $u_m(t) = \sum_{j=1}^{m} g_{jm}(t)e^j$ such that, for any $v \in V_m$, $u_m(t)$ satisfies the approximate equation

$$\left(Ku_m''(t) + M\left(\left|A^{1/2}u_m\right|^2\right)Au_m + g\left(u_m'\right), v\right) = 0 \tag{13}$$

and the initial conditions as the projections of u_0 and u_1 over V_m satisfy

$$u_m(0) = u_{0m} = \sum_{j=1}^{m}\left(u_0, e^j\right)e^j \longrightarrow u_0 \quad \text{in } W \tag{14}$$

$$\begin{aligned}\left(Ku_m'\right)(0) &= K^{1/2}u_{1m}\\ &= \sum_{j=1}^{m}\left(u_1, e^j\right)e^j \longrightarrow K^{1/2}u_1 \quad \text{in } L^{2q}(\Omega).\end{aligned} \tag{15}$$

For $v = e^j$, $j = 1, 2, \ldots m$, the system (13)–(15) of ordinary differential equations of variable t has a solution $u_m(t)$ in an interval $[0, t_m)$.

Now we obtain a priori estimates for the solution $u_m(t)$ and it can also be extended to $[0, T)$ for all $T > 0$.

A Priori Estimate I. Let us consider $v = u_m'$ in (13). Using (7), we have

$$\begin{aligned}&\frac{d}{dt}\left(\left|K^{1/2}u_m'(t)\right|^2 + \overline{M}\left(\left|A^{1/2}u_m(t)\right|^2\right)\right)\\ &\quad + 2\left(g\left(u_m'(t)\right), u_m'(t)\right) = 0.\end{aligned} \tag{16}$$

Integrating (16) over $(0, t)$, $t \le t_m$, and using (8), we have

$$\begin{aligned}2E(0) = &\left[\left|K^{1/2}u_m'(t)\right|^2 + \overline{M}\left(\left|A^{1/2}u_m(t)\right|^2\right)\right]\\ &+2\int_0^t\left(g\left(u_m'(s)\right), u_m'(s)\right)ds.\end{aligned} \tag{17}$$

Using (5) and (7), we deduce that

$$\begin{aligned}2E(0) \ge &\left|K^{1/2}u_m'(t)\right|^2 + \beta\left|A^{1/2}u_m(t)\right|^2\\ &+ 2\int_0^t\int_\Omega u_m'(s)\, g\left(u_m'(s)\right)dx\,ds,\end{aligned} \tag{18}$$

where the left-hand side is constant independent of m and t. Thus estimation (18) yields, for any $0 < T < \infty$,

$$u_m' \text{ bounded in } L^\infty(0, T; H), \tag{19}$$

$$K^{1/2}u_m' \text{ bounded in } L^\infty(0, T; H), \tag{20}$$

$$A^{1/2}u_m \text{ bounded in } L^\infty(0, T; H), \tag{21}$$

$$u_m' g\left(u_m'\right) \text{ bounded in } L^1([0, T]\times\Omega). \tag{22}$$

Now we show that $u_m(t)$ can be extended to $[0, \infty)$. We need the following smallness assumption:

$$\begin{aligned}&\left\|M'\right\|_{L^\infty([0,P(0)])}\\ &\times \max\left\{\frac{\left|K^{1/2}u_{m1}\right|}{M\left(\left|A^{1/2}u_{m0}\right|^2\right)}, \left(M\left(\left|A^{1/2}u_{m0}\right|^2\right)\right)\right.\\ &\qquad\times\left(\left(M\left(\left|A^{1/2}u_{m0}\right|^2\right)\right)' - g\left(u_{m1}\right)\right.\\ &\qquad\qquad\left.\times M\left(\left|A^{1/2}u_{m0}\right|^2\right)\right)^{-1}\left.\sqrt{Q(0)}\right\}\\ &\times\sqrt{Q(0)} < \frac{1}{4},\end{aligned} \tag{23}$$

where $P(0) = (|K^{1/2}u_{m1}|^2/M(|A^{1/2}u_{m0}|^2)) + |A^{1/2}u_{m0}|^2$, $Q(0) = (|K^{1/2}A^{1/2}u_{m1}|^2/M(|A^{1/2}u_{m0}|^2)) + |Au_{m0}|^2$.

Let $[0, T^*)$ be the maximal interval where the solution exists. Set $Z(t) := M(|A^{1/2}u_m(t)|^2)$ and

$$T := \sup\left\{\tau \in [0, T^*) \mid \left|\frac{Z'(t)}{Z(t)}\right| \le \frac{1}{2},\ Z(t) > 0,\ \forall t \in [0, \tau)\right\}. \tag{24}$$

With simple computations it follows that

$$\begin{aligned}P'(t) &= -\frac{1}{Z(t)}\left(2\left(g\left(u_m'(t)\right), u_m'(t)\right) + \frac{Z'(t)}{Z(t)}\left|u_m'(t)\right|^2\right)\\ &\le 0,\end{aligned} \tag{25}$$

$$\begin{aligned}&Q'(t)\\ &= -\frac{1}{Z(t)}\left(2\left(g\left(u_m'(t)\right), Au_m'(t)\right) + \frac{Z'(t)}{Z(t)}\left|A^{1/2}u_m'(t)\right|^2\right)\\ &\le 0,\end{aligned} \tag{26}$$

$$\begin{aligned}&\left(G^2\right)'(t)\\ &\le -G(t)\left\{2\left(\frac{Z'(t)}{Z(t)} - \left|g\left(u_m'(t)\right)\right|\right)G(t) - 2\left|Au_m(t)\right|\right\},\end{aligned} \tag{27}$$

for all $t \in [0, T)$.

Next, we show that $T = T^*$. Let us assume by contradiction that $T < T^*$. Since $|Z'(t)| \le (1/2)Z(t)$ in $[0, T)$, we have that

$$0 < Z(0)e^{-T/2} \le Z(T) \le Z(0)e^{T/2}. \tag{28}$$

Since $Z(t)$ and $Z'(t)$ are continuous functions, by the maximality of T we have that necessarily

$$\left|\frac{Z'(t)}{Z(t)}\right| = \frac{1}{2}. \tag{29}$$

From (88) and (89) it follows that P and Q are nonincreasing functions; hence

$$\begin{gathered}\left|A^{1/2}u_m(t)\right|^2 \leq P(t) \leq P(0),\\ \left|Au_m(t)\right|^2 \leq Q(t) \leq Q(0).\end{gathered} \tag{30}$$

Moreover by Lemma 3.1 in [28] we have that

$$G(t) \leq \max\left\{G(0), \frac{Z(0)}{Z'(0) - g(u_{m1})Z(0)}\sqrt{Q(0)}\right\}, \quad \forall t \in [0,T]. \tag{31}$$

By (91)–(31), and the smallness assumption (23), we have that

$$\begin{aligned}\left|\frac{Z'(T)}{Z(T)}\right| &= \left|\frac{2M'\left(\left|A^{1/2}u_m(t)\right|^2\right)\left(u_m'(T), Au_m(T)\right)}{Z(T)}\right|\\ &\leq 2\max_{0\leq r\leq P(0)}\left|M'(r)\right|\frac{\left|u_m'(T)\right|}{Z(T)}\left|Au_m(T)\right|\\ &\leq 2\max_{0\leq r\leq P(0)}\left|M'(r)\right|\\ &\quad\times\max\left\{G(0), \frac{Z(0)}{Z'(0)-g(u_{m1})Z(0)}\sqrt{Q(0)}\right\}\\ &\quad\times\sqrt{Q(0)}\\ &< \frac{1}{2}.\end{aligned} \tag{32}$$

This contradicts (29). Therefore it follows that $u_m(t)$ can be extended to $[0,T)$ for any $T \in (0,\infty)$.

Furthermore, putting $v = Au_m'$ in (13), we get

$$\frac{\left(Ku_m'', Au_m'\right)}{M\left(\left|A^{1/2}u_m\right|^2\right)} + \left(Au_m, Au_m'\right) + \frac{\left(g\left(u_m'\right), Au_m'\right)}{M\left(\left|A^{1/2}u_m\right|^2\right)} = 0. \tag{33}$$

From this we obtain

$$\begin{aligned}&\frac{1}{2}\frac{d}{dt}\left(\frac{\left(Ku_m', Au_m'\right)}{M\left(\left|A^{1/2}u_m\right|^2\right)} + \left|Au_m\right|^2\right) + \frac{\left(g\left(u_m'\right), Au_m'\right)}{M\left(\left|A^{1/2}u_m\right|^2\right)}\\ &\quad = -\frac{\left(Ku_m', Au_m'\right)M'\left(\left|A^{1/2}u_m\right|^2\right)\left(A^{1/2}u_m', A^{1/2}u_m\right)}{\left\{M\left(\left|A^{1/2}u_m\right|^2\right)\right\}^2}.\end{aligned} \tag{34}$$

Integrating (34) over $(0,t)$ and taking into account assumptions (M) and (G), and applying Gronwall's inequality, we obtain

$$Au_m \text{ bounded in } L^\infty(0,T;H). \tag{35}$$

From (6) and (22), it follows that

$$g\left(u_m'\right) \text{ bounded in } L^{(q+1)/q}([0,T]\times\Omega). \tag{36}$$

A Priori Estimate II. Taking $v = u_m''(t)$ in (13) and choosing $t = 0$, we obtain

$$\begin{aligned}&\left|K^{1/2}u_m''(0)\right|^2 + \left(M\left(\left|A^{1/2}u_{0m}\right|^2\right)Au_{0m} + g(u_{1m}), u_m''(0)\right)\\ &\quad = 0.\end{aligned} \tag{37}$$

Thus we have

$$\begin{aligned}\left|K^{1/2}u_m''(0)\right|^2 &\leq \left(\left|g(u_{1m})\right| + \left|M\left(\left|A^{1/2}u_{0m}\right|^2\right)Au_{0m}\right|\right)\left|u_m''(0)\right|\\ &\leq \left(\left|g(u_{1m})\right| + \left|M\left(\left|A^{1/2}u_0\right|^2\right)Au_0\right|\right)\\ &\quad\times\left|K^{1/2}u_m''(0)\right|.\end{aligned} \tag{38}$$

Thanks to the assumption (6), we deduce from (15) that

$$\left(g(u_{1m})\right) \text{ is bounded in } L^2(\Omega). \tag{39}$$

Therefore we conclude that the right-hand side is bounded; that is,

$$K^{1/2}u_m''(0) \text{ bounded in } H. \tag{40}$$

A Priori Estimate III. For $t < T$, we apply (13) at points t and $t+\zeta$ such that $0 < \zeta < T - t$. By taking the difference $v = u_m'(t+\zeta) - u_m'(t)$ in (13) and the assumption (G), we obtain

$$\begin{aligned}0 \geq{} &\left(Ku_m''(t+\zeta) - Ku_m''(t), u_m'(t+\zeta) - u_m'(t)\right)\\ &+\left(M\left(\left|A^{1/2}u_m(t+\zeta)\right|^2\right)Au_m(t+\zeta)\right.\\ &\left.-M\left(\left|A^{1/2}u_m(t)\right|^2\right)Au_m(t), u_m'(t+\zeta) - u_m'(t)\right).\end{aligned} \tag{41}$$

Thus we have

$$\begin{aligned}0 \geq{} &\frac{1}{2}\frac{d}{dt}\left[\left|K^{1/2}\left(u_m'(t+\zeta) - u_m'(t)\right)\right|^2\right]\\ &+ M\left(\left|A^{1/2}u_m(t+\zeta)\right|^2\right)\\ &\times\left(Au_m(t+\zeta) - Au_m(t), u_m'(t+\zeta) - u_m'(t)\right)\\ &+\left[M\left(\left|A^{1/2}u_m(t+\zeta)\right|^2\right) - M\left(\left|A^{1/2}u_m(t)\right|^2\right)\right]\\ &\times\left(Au_m(t), u_m'(t+\zeta) - u_m'(t)\right).\end{aligned} \tag{42}$$

Set

$$\Phi_{\zeta m}(t) = \left|K^{1/2}\left(u_m'(t+\zeta) - u_m'(t)\right)\right|^2. \tag{43}$$

By using (42), Young's inequality, the assumption (M), and the fact that K is positive self-adjoint operator, we see that $\mathbf{\Phi}'_{\zeta m}(t) \le c\mathbf{\Phi}_{\zeta m}(t)$. Therefore we deduce

$$\mathbf{\Phi}_{\zeta m}(t) \le \mathbf{\Phi}_{\zeta m}(0)\exp(cT) \quad \forall t \in [0,T]. \tag{44}$$

Dividing the two sides of (44) by ζ^2, letting $\zeta \to 0$, and using (43), we deduce

$$c\left|u''_m\right|^2 \le \left|K^{1/2}u''_m(0)\right|^2. \tag{45}$$

From (40), it follows that $|u''_m|^2 \le C$.

Since $u_m \in C^2[0,T]$, the previous inequality is verified for all $t \in [0,T]$. Therefore we conclude that

$$u''_m \text{ bounded in } L^\infty(0,T;H). \tag{46}$$

Moreover, using (19) and (46), it follows that

$$\begin{gathered} u'_m \text{ bounded in } L^2(0,T;H), \\ u''_m \text{ bounded in } L^2(0,T;H). \end{gathered} \tag{47}$$

Applying a compactness theorem given in [33], we obtain

$$u'_m \text{ precompact in } L^2(0,T;H). \tag{48}$$

Passage to the Limit. Applying the Dunford-Pettis theorem, we conclude from (19), (21), (36), and (46)-(48), replacing the sequence u_m with a subsequence if needed, that

$$u_m \longrightarrow u \text{ weak-star in } L^\infty(0,T;V), \tag{49}$$
$$u'_m \longrightarrow u' \text{ weak-star in } L^\infty(0,T;H), \tag{50}$$
$$u''_m \longrightarrow u'' \text{ weak-star in } L^\infty(0,T;H), \tag{51}$$
$$u'_m \longrightarrow u' \text{ a.e in } \Omega\times[0,T], \tag{52}$$
$$g\left(u'_m\right) \longrightarrow \psi \text{ weak-starin } L^{(q+1)/q}(0,T;H), \tag{53}$$
$$M\left(\left|A^{1/2}u_m\right|^2\right)Au_m \longrightarrow \chi \text{ weak-star in } L^\infty(0,T;H) \tag{54}$$

for suitable functions $u \in L^\infty(0,T;V)$, $\chi \in L^\infty(0,T;H)$, and $\psi \in L^{(q+1)/q}(\mathbf{\Omega}\times[0,T])$.

Now we are going to show that u is a solution of the problem (11)-(12). Indeed, from (49) to (51), we have

$$\begin{gathered} \int_\Omega u_m(0)e^j dx \longrightarrow \int_\Omega u(0)e^j dx, \\ \int_\Omega u'_m(0)e^j dx \longrightarrow \int_\Omega u'(0)e^j dx \end{gathered} \tag{55}$$

for each fixed $j \ge 1$. So we conclude that, for any $j \ge 1$,

$$\int_{\mathbf{\Omega}}(u_m(0)-u_0)e^j dx = \int_{\mathbf{\Omega}}\left(u'(0)-u_1\right)e^j dx = 0 \quad \text{as } m \longrightarrow \infty, \tag{56}$$

which shows that (12) holds.

We will prove that, in fact, $\chi = M(|A^{1/2}u|^2)Au$; that is,

$$M\left(\left|A^{1/2}u_m\right|^2\right)Au_m \longrightarrow M\left(\left|A^{1/2}u\right|^2\right)Au \quad \text{weak-star in } L^\infty(0,\infty;H). \tag{57}$$

For $v \in L^2(0,T;H)$, we have

$$\begin{aligned} &\int_0^T\left(\chi - M\left(\left|A^{1/2}u\right|^2\right)Au, v\right)dt \\ &\quad= \int_0^T\left(\chi - M\left(\left|A^{1/2}u_m\right|^2\right)Au_m, v\right)dt \\ &\qquad+ \int_0^T M\left(\left|A^{1/2}u\right|^2\right)(Au_m - Au, v)\,dt \\ &\qquad+ \int_0^T\left(M\left(\left|A^{1/2}u_m\right|^2\right) - M\left(\left|A^{1/2}u\right|^2\right)\right) \\ &\qquad\qquad\times(Au_m, v)\,dt. \end{aligned} \tag{58}$$

We deduce from (49) and (54) that the first and second terms in (58) tend to zero as $m \to \infty$. For the last term, using the fact that M is C^1 and (21), we can derive (with some positive constants c_1, c_2)

$$\begin{aligned} &\int_0^T\left(M\left(\left|A^{1/2}u_m\right|^2\right) - M\left(\left|A^{1/2}u\right|^2\right)\right)(Au_m, v)\,dt \\ &\quad\le c_1\int_0^T\left|A(u_m+u), u_m - u\right|dt \\ &\quad\le c_2\left(\int_0^T|u_m-u|^2dt\right)^{1/2}. \end{aligned} \tag{59}$$

Since u_m is bounded in $L^\infty(0,T;V)$ and the injection of V in H is compact, we have

$$u_m \longrightarrow u \text{ strongly in } L^2(0,T;H). \tag{60}$$

From (58) to (60), we deduce (57). It follows from (49), (51), and (57) that, for each fixed $v \in L^{q+1}(0,T;V)$,

$$\begin{aligned} &\int_0^T\left(Ku''_m + M\left(\left|A^{1/2}u_m\right|^2\right)Au_m, v\right)dt \\ &\quad\longrightarrow \int_0^T\left(Ku'' + M\left(\left|A^{1/2}u\right|^2\right)Au, v\right)dt \end{aligned} \tag{61}$$

as $m \to +\infty$.

For the nonlinear term, $g(u')$, it remains to show that, for any fixed $v \in L^{q+1}(0,T;V)$,

$$\int_0^T\int_\Omega vg\left(u'_m\right)dx\,dt \longrightarrow \int_0^T\int_\Omega vg\left(u'\right)dx\,dt \tag{62}$$

as $m \to \infty$.

At this moment we use the following lemma due to Jung and Choi (see [26, page 12]).

Lemma 2. *Suppose that $\Omega \times [0,T]$ is a bounded open domain of $\mathbb{R}^n \times \mathbb{R}$; g_m and g are in $L^q(\Omega\times[0,T])$, $1 < q < \infty$, such that $g_m \to g$ a.e., in $\Omega \times [0,T]$. Then $g_m \to g$ weakly in $L^q(\Omega \times [0,T])$.*

From (53), $g(u_m') \to g(u')$ a.e. in $\Omega \times [0,T]$. By (36), we can use the above lemma and so we have $\psi = g(u')$; that is,

$$g(u_m) \longrightarrow g(u) \quad \text{weak in } L^{(q+1)/q}(\Omega \times (0,T)), \tag{63}$$

which implies (62). Therefore we obtain

$$\int_0^T \left(Ku'' + M\left(\left|A^{1/2}u\right|^2\right)Au + g\left(u'\right), v\right)dt = 0, \quad \forall v \in L^{q+1}(0,T;V). \tag{64}$$

The uniqueness is obtained by a standard method, so we omit the proof here.

3. Energy Estimates

In this section we study the energy estimate under suitable growth conditions on g.

Let us assume that there exist a number $p \geq 1$ and positive constants c_1, $i = 1, 2$, such that

$$c_1 \min\left\{\left|K^{1/2}x\right|, \left|K^{1/2}x\right|^p\right\} \leq |g(x)| \leq c_2 \max\left\{\left|K^{1/2}x\right|, \left|K^{1/2}x\right|^{1/p}\right\} \tag{65}$$

for all $x \in \mathbb{R}$.

Theorem 3. *Assume that (65) holds. Then one obtains the following energy decay:*

$$E(t) \leq \begin{cases} c_0 E(0)e^{-wt} \ \forall t \geq 0, & \text{if } p = 1, \\ \tilde{c}_0(1+t)^{-2/(p-1)} \ \forall t \geq 0, & \text{if } p > 1, \end{cases} \tag{66}$$

where c_0, w, and $\tilde{c}_0$ are some positive constants.

Proof. Let $T > 0$ be arbitrary and fixed and let $u \in L^\infty(0,T;V) \cap W^{2,\infty}(0,T;H)$ be a solution of (11) and (12). Multiplying (11) by u' and integrating by parts in $\Omega\times(s,T)$ $(0 \leq s < T)$, we obtain that

$$E(T) - E(s) = -\int_s^T \left(g\left(u'(t)\right), u'(t)\right)dt. \tag{67}$$

By $(g(u'(t)), u'(t)) \geq 0$ and being the primitive of an integrable function, it follows that the energy E is nonincreasing, locally absolutely continuous and

$$E'(t) = -\left(g\left(u'(t)\right), u'(t)\right) \quad \text{a.e. in } [0,\infty). \tag{68}$$

Here and in what follows we will denote by c diverse positive constants. We are going to show that the energy of this solution satisfies

$$\int_s^T E(t)^{(p+1)/2} \leq cE(s) \quad \forall 0 \leq s \leq T < \infty. \tag{69}$$

Once (69) is satisfied, the integral inequalities given in Komornik [31] and Haraux [32] will establish (66).

Now, multiplying (11) by $E(t)^{(p-1)/2}u$ and integrating by parts, we have

$$\begin{aligned} 0 &= \int_s^T E(t)^{(p-1)/2}\left(Ku'' + M\left(\left|A^{1/2}u\right|^2\right)Au + g\left(u'\right), u\right)dt \\ &= \left[E(t)^{(p-1)/2}\left(Ku', u\right)\right]_s^T \\ &\quad - \frac{p-1}{2}\int_s^T E(t)^{(p-3)/2}E'(t)\left(Ku', u\right)dt \\ &\quad - \int_s^T E(t)^{(p-1)/2}\left|K^{1/2}u'\right|^2 dt \\ &\quad + \int_s^T E(t)^{(p-1)/2}\left(M\left(\left|A^{1/2}u\right|^2\right)\left|A^{1/2}u\right|^2, u\right)dt \\ &\quad + \int_s^T E(t)^{(p-1)/2}\left(g\left(u'\right), u\right)dt. \end{aligned} \tag{70}$$

Note that by the assumption (M) and (21), we can choose some positive number

$$\alpha = \max_{s\in[0,|A^{1/2}u|^2]}\{M(s)\} < \infty \tag{71}$$

so that $2E(t) \leq |K^{1/2}u'|^2 + \alpha|A^{1/2}u|^2$. Thus we deduce that

$$\begin{aligned} &\frac{2\beta}{\alpha}\int_s^T E(t)^{(p+1)/2}dt \\ &\quad \leq -\left[E(t)^{(p-1)/2}\left(Ku', u\right)\right]_s^T \\ &\qquad + \frac{p-1}{2}\int_s^T E(t)^{(p-3)/2}E'(t)\left(Ku', u\right)dt \\ &\qquad + \int_s^T E(t)^{(p-1)/2}\left(\left(1+\alpha^{-1}\right)\left|K^{1/2}u'\right|^2 - \left(g\left(u'\right), u\right)\right)dt \\ &\quad \equiv I_1 + I_2 + I_3. \end{aligned} \tag{72}$$

Using the continuity of the imbedding $V \subset H$, the Cauchy-Schwarz and the Young inequalities, we obtain

$$\left|\left(Ku', u\right)\right| \leq c\left|Ku'\right|\|u\| \leq cE(t). \tag{73}$$

Hence, since $E(t)$ is nonincreasing, we obtain

$$\begin{aligned} I_1 &\leq cE^{(p-1)/2}(0)E(s), \\ I_2 &\leq \frac{(p-1)}{2}\int_s^T cE(t)^{(p-1)/2}E'(t)\,dt \\ &\leq cE^{(p-1)/2}(0)E(s). \end{aligned} \tag{74}$$

In order to estimate the last term I_3 of (72), we set

$$\begin{aligned} \Omega_1 &= \left\{x \in \Omega : \left|K^{1/2}u'(t,x)\right| \leq 1\right\}, \\ \Omega_2 &= \left\{x \in \Omega : \left|K^{1/2}u'(t,x)\right| > 1\right\}. \end{aligned} \tag{75}$$

Then we have

$$\int_\Omega \left|K^{1/2}u'(t,x)\right|^2 dx = \int_{\Omega_1} \left|K^{1/2}u'(t,x)\right|^2 dx + \int_{\Omega_2} \left|K^{1/2}u'(t,x)\right|^2 dx. \tag{76}$$

The Hölder inequality yields

$$\begin{aligned}\int_\Omega \left|K^{1/2}u'(t,x)\right|^2 dx &\le c\left(\int_{\Omega_1} \left|K^{1/2}u'(t,x)\right|^{p+1} dx\right)^{2/(p+1)} + \int_{\Omega_2} \left|K^{1/2}u'(t,x)\right|^2 dx \\ &\equiv J_1 + J_2.\end{aligned} \tag{77}$$

Using (65) and (68), we deduce that

$$\begin{aligned}J_1 &\le c\left(\int_{\Omega_1} u'g(u')\,dx\right)^{2/(p+1)} \le c\left|E'(t)\right|^{2/(p+1)}, \\ J_2 &\le c\int_{\Omega_2} \left|u'g(u')\right| dx \le c\left(-E'(t)\right).\end{aligned} \tag{78}$$

Combining these two inequalities with (77), we obtain

$$\int_\Omega \left|K^{1/2}u'(t,x)\right|^2 dx \le c\left(-E'(t)\right)^{2/(p+1)} + c\left(-E'(t)\right). \tag{79}$$

Applying Young's inequality, it follows that, for any $\epsilon > 0$,

$$\begin{aligned}&\int_s^T E(t)^{(p-1)/2}\left|K^{1/2}u'\right|^2 dt \\ &\quad\le \epsilon c\int_s^T E(t)^{(p+1)/2} dt + c\left(\epsilon^{(1-p)/2} + E^{(p-1)/2}(0)\right)E(s).\end{aligned} \tag{80}$$

It remains to estimate the second term of I_3. Using (88) we have

$$\begin{aligned}&\left|\int_{\Omega_1} ug(u')\,dx\right| \\ &\quad\le c\|u\|_{L^{(p+1)/p}(\Omega_1)}\left\|g(u')\right\|_{L^{p+1}(\Omega_1)} \\ &\quad\le c\|u\|_{L^{(p+1)/p}(\Omega_1)}\left(\int_{\Omega_1} u'g(u')\,dx\right)^{1/(p+1)} \\ &\quad\le cE(t)^{1/2}\left(-E'(t)\right)^{1/(p+1)}.\end{aligned} \tag{81}$$

Similarly, using (6), we obtain

$$\begin{aligned}\left|\int_{\Omega_2} ug(u')\,dx\right| &\le c\|u\|_{L^2(\Omega_2)}\left\|g(u')\right\|_{L^2(\Omega_2)} \\ &\le c\|u\|_{L^2(\Omega_2)}\left\|u'g(u')\right\|_{L^1(\Omega_2)}^{1/2} \\ &\le cE(t)^{1/2}\left(-E'(t)\right)^{1/2}.\end{aligned} \tag{82}$$

From (81) and (82), we deduce

$$\left|\int_\Omega ug(u')\,dx\right| \le cE(t)^{1/2}\left(-E'(t)\right)^{1/(p+1)} + cE(t)^{1/2}\left(-E'(t)\right)^{1/2}. \tag{83}$$

Using Young's inequality and

$$E(t)^{p/2}\left(-E'(t)\right)^{1/2} = E(t)^{(p+1)/4}\left(E(t)^{(p-1)/4}\left(-E'(t)\right)^{1/2}\right), \tag{84}$$

it follows from (82) that, for any $\epsilon > 0$,

$$\begin{aligned}&-\int_s^T E(t)^{(p-1)/2}\left(g(u'),u\right)dt \\ &\quad= -\int_s^T E(t)^{(p-1)/2}\int_\Omega ug(u')\,dx\,dt \\ &\quad\le c\int_s^T E(t)^{p/2}\left(-E'(t)\right)^{1/(p+1)} dt + c\int_s^T E(t)^{p/2}\left(-E'(t)\right)^{1/2} dt \\ &\quad\le 2\epsilon c\int_s^T E(t)^{(p+1)/2} dt + c\left(\epsilon^{-p} + \epsilon^{-1}E(0)^{(p-1)/2}\right) \times \int_s^T \left(-E'(t)\right)dt \\ &\quad\le 2\epsilon c\int_s^T E(t)^{(p+1)/2} dt + c\left(\epsilon^{-p} + \epsilon^{-1}E(0)^{(p-1)/2}\right)E(s).\end{aligned} \tag{85}$$

Combining (80) with (85) and setting $\tilde{\alpha} = 1 + \alpha^{-1}$, we obtain

$$\begin{aligned}I_3 &\le \int_s^T E(t)^{(p-1)/2} 2\left|K^{1/2}u'\right|^2 dt + \int_s^T E(t)^{(p-1)/2}\int_\Omega ug(u')\,dx\,dt \\ &\le (\tilde{\alpha}+2)\,\epsilon c\int_s^T E(t)^{(p+1)/2} dt + c\left(\tilde{\alpha}\epsilon^{(1-p)/2} + \epsilon^{-p} + \left(\tilde{\alpha} + \epsilon^{-1}\right)E(0)^{(p-1)/2}\right)E(s).\end{aligned} \tag{86}$$

Therefore we conclude that

$$\begin{aligned}&\left(\frac{2\beta}{\alpha} - (\tilde{\alpha}+2)\,\epsilon c\right)\int_s^T E^{(p+1)/2} \\ &\quad\le c\left(\tilde{\alpha}\epsilon^{(1-p)/2} + \epsilon^{-p} + \left(\tilde{\alpha} + \epsilon^{-1}\right)E(0)^{(p-1)/2}\right)E(s).\end{aligned} \tag{87}$$

Now we choose ϵ as $\epsilon \in (0, 2\beta/(3\alpha+1)c)$; then (69) follows. □

Table 1: Simulation parameters which are satisfied by theoretical conditions.

Symbols	Definition	Values	Reference
$A(x)$	Cross-sectional area	$0.7853\,(10^{-4}\sin(2^{10}\pi x)+1)\,\mathrm{cm}^2$	[34]
ρ	Mass density of the unit length	$7.850\,\mathrm{g/cm}^2$	[34]

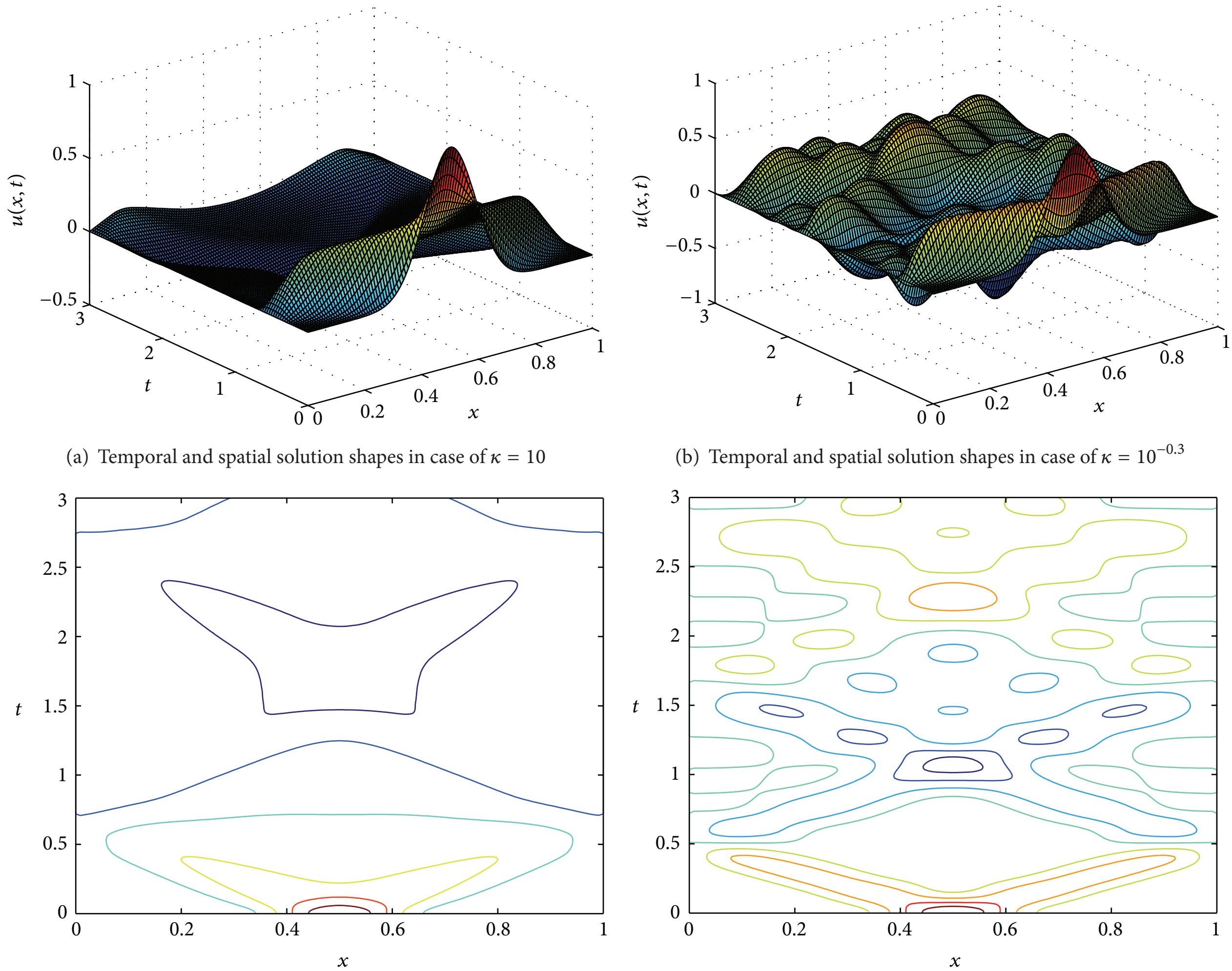

(a) Temporal and spatial solution shapes in case of $\kappa = 10$

(b) Temporal and spatial solution shapes in case of $\kappa = 10^{-0.3}$

(c) Temporal and spatial solution contour line in case of $\kappa = 10$

(d) Temporal and spatial solution contour line in case of $\kappa = 10^{-0.3}$

Figure 1: Solution shapes and contour lines with respect to $\kappa = 10$ and $\kappa = 10^{-0.3}$.

4. Numerical Result

In this section, we consider a Kirchhoff-type equation with heterogeneous string as an application:

$$\begin{aligned}(A(x)\rho)\,u''(x,t) - \left(1+\int_0^1 |\nabla u(x,t)|^2 dx\right)\Delta u(x,t)& \\ +\kappa\left|u'(x,t)\right|^2 u'(x,t) = 0,&\end{aligned} \tag{88}$$

$$\text{in } (x,t) \in (0,1)\times(0,3), \tag{89}$$

$$u(0,t) = u(1,t) = 0 \quad \text{on } (0,3), \tag{90}$$

$$u_0 = u(x,0) = \exp\left(-64\left(x-\frac{1}{2}\right)^2\right) \quad \text{in } (0,1), \tag{91}$$

$$u_1 = u_t(x,0) = 0 \quad \text{in } (0,1), \tag{92}$$

where κ is a positive constant and $A(x)$, ρ are given in Table 1.

Then, the operators $K = A(x)\rho I(I : H \to H$; identity operator), $A = -\Delta$, and the functions $M(s) = s + 1$ and $g(x) = \kappa|x|^2 x$ so that we can easily check that the hypotheses (M), (G), (H), and (S) in Preliminaries are satisfied. The smallness condition satisfies $(\|\nabla u_0\|^2 + 1)\|\Delta u_0\|^2 \approx 0.213 \le 1/4$. Therefore, by Theorem 1, we can deduce the following results.

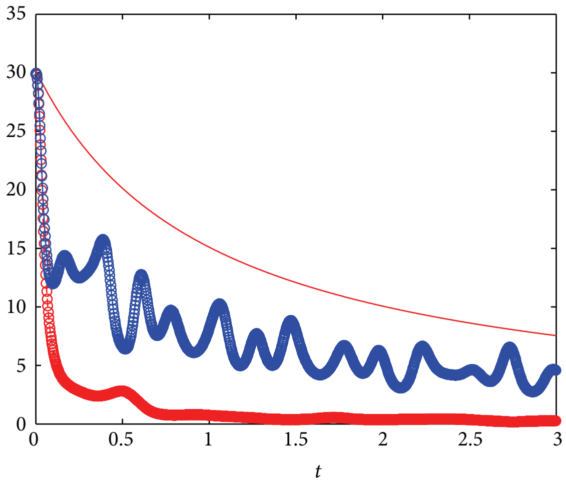

FIGURE 2: Algebraic decay rates of the energy in case of $\kappa = 10$ and $\kappa = 10^{-0.3}$.

Theorem 4. *For any $T > 0$, there is a unique solution $u \in L^{\infty}(0,T;H^2(0,1)) \cap W^{1,\infty}(0,T;H_0^1(0,1)) \cap W^{2,\infty}(0,T;L^2(0,1))$ to the system* (88)–(92).

The energy for the system (88)–(92) is given by

$$E(t) = \frac{1}{2}\left[\int_0^1 \left|\sqrt{A(x)}\rho u'(x,t)\right|^2 dx + \int_0^1 |\nabla u(x,t)|^2 dx + \frac{1}{2}\left(\int_0^1 |\nabla u(x,t)|^2 dx\right)^2\right]. \quad (93)$$

Next, in order to get the energy decay of (88)–(92), we need the value of the parameter p in (65). We can easily check that $p = 3$ when $g(x) = \kappa|x|^2 x$.

Therefore, by Theorem 3, we get the energy decay rates for the energy $E(t)$ as follows.

Theorem 5. *We obtain the following energy decay:*

$$E(t) \le c_1(1+t)^{-1} \quad \forall t \ge 0, \quad (94)$$

where c_1 is a positive constant.

For the numerical simulation, we use the finite difference methods (FDM) which are the implicit multistep methods in time and second-order central difference methods for the space derivative in space in numerical algorithms (see [8, 9, 11]).

Figures 1(a)–1(d) show displacements of solutions to the system (88)–(92) with $\kappa = 10$ and $\kappa = 10^{-0.3}$, respectively.

In case of $\kappa = 10$ and $\kappa = 10^{-0.3}$, we deduce the algebraic decay rate for the energy as shown in Figure 2, respectively. The blue line and red dotted circled line (or blue circled line) show $c_1(t+1)^1$ and $E(t)$ per the two values, respectively, where the parameter value $c_1 = 30.2$ in (94). This result shows that the energy decay rates for solutions are algebraic in case that the system (88)–(92) with the nonlinear damping term $\kappa|u_t|^2 u_t$.

Conflict of Interests

The authors declare that there is no conflict of interests regarding the publication of this paper.

Acknowledgments

The first author's research was supported by Basic Research Program through the National Research Foundation of Korea (NRF) funded by the Ministry of Education, Science and Technology (Grant no. NRF-2013R1A1A2010704). The corresponding author's research was supported by Basic Research Program through the National Research Foundation of Korea (NRF) funded by the Ministry of Education, Science and Technology (Grant no. NRF-2012R1A1B3000599).

References

[1] G. Kirchhoff, *Vorlesungen Über Mechanik*, Teubner, Leipzig, Germany, 1883.

[2] Q. C. Nguyen and K. -S. Hong, "Transverse vibration control of axially moving membranes by regulation of axial velocity," *IEEE Transactions on Control Systems Technology*, vol. 20, no. 4, pp. 1124–1131, 2012.

[3] G. P. Menzala, A. F. Pazoto, and E. Zuazua, "Stabilization of Berger-Timoshenko's equation as limit of the uniform stabilization of the von Kármán system of beams and plates," *Mathematical Modelling and Numerical Analysis*, vol. 36, no. 4, pp. 657–691, 2002.

[4] J. G. Eisley, "Nonlinear vibration of beams and rectangular plates," *Zeitschrift für Angewandte Mathematik und Physik*, vol. 15, no. 2, pp. 167–175, 1964.

[5] S. Woinowsky-Krieger, "The effect of an axial force on the vibration of hinged bars," *Journal of Applied Mechanics*, vol. 17, pp. 35–36, 1950.

[6] L. Chen, C. W. Lim, and H. Ding, "Energetics and conserved quantity of an axially moving string undergoing three-dimensional nonlinear vibration," *Acta Mechanica Sinica*, vol. 24, no. 2, pp. 215–221, 2008.

[7] K.-S. Hong, "Asymptotic behavior analysis of a coupled time-varying system: application to adaptive systems," *IEEE Transactions on Automatic Control*, vol. 42, no. 12, pp. 1693–1697, 1997.

[8] D. Kim, S. Kim, and I. H. Jung, "Stabilization for the Kirchhoff type equation from an axially moving heterogeneous string modeling with boundary feedback control," *Nonlinear Analysis. Theory, Methods and Applications*, vol. 75, no. 8, pp. 3598–3617, 2012.

[9] D. Kim and I. H. Jung, "Asymptotic behavior of a nonlinear Kirchhoff type equation with spring boundary conditions," *Computers and Mathematics with Applications*, vol. 62, no. 8, pp. 3004–3014, 2011.

[10] D. Kim, Y. H. Kang, M. J. Lee, and I. H. Jung, “Energy decay rate for a quasi-linear wave equation with localized strong dissipation,” *Computers and Mathematics with Applications*, vol. 62, no. 1, pp. 164–172, 2011.

[11] D. Kim, Y. H. Kang, J. B. Lee, G. R. Ko, and I. H. Jung, “Stabilization for a nonlinear Kirchhoff equation by boundary feedback control,” *Journal of Engineering Mathematics*, vol. 77, pp. 197–209, 2012.

[12] I.-S. Liu and M. A. Rincon, “Effect of moving boundaries on the vibrating elastic string,” *Applied Numerical Mathematics*, vol. 47, no. 2, pp. 159–172, 2003.

[13] F. Pellicano and F. Vestroni, “Complex dynamics of high-speed axially moving systems,” *Journal of Sound and Vibration*, vol. 258, no. 1, pp. 31–44, 2002.

[14] S. M. Shahruz and S. A. Parasurama, “Suppression of vibration in the axially moving Kirchhoff string by boundary control,” *Journal of Sound and Vibration*, vol. 214, no. 3, pp. 567–575, 1998.

[15] S. Bernstein, “Sur une classe d’équations fonctionelles aux dérivées partielles,” *Izvestiya Akademii Nauk SSSR. Seriya Matematicheskaya*, vol. 4, pp. 17–26, 1940.

[16] R. W. Dickey, “The initial value problem for a nonlinear semi-infinite string,” *Proceedings of the Royal Society of Edinburgh*, vol. 82, pp. 19–26, 1978.

[17] Y. Ebihara, L. A. Medeiros, and M. Milla Miranda, “Local solutions for a nonlinear degenerate Hyperbolic equation,” *Nonlinear Analysis. Theory, Methods and Applications*, vol. 10, no. 1, pp. 27–40, 1986.

[18] T. G. Ha, D. Kim, and I. H. Jung, “Grobal existence and uniform decay rates for the semi-linear wave equation with damping and source terms,” *Computers and Mathematics with Applications*, vol. 67, pp. 692–707, 2014.

[19] H. A. Levine, “Instability and nonexistence of global solutions to nonlinear equations of the form $Pu_{tt} = -Au + \mathscr{F}(u)$,” *Transactions of the American Mathematical Society*, vol. 192, pp. 1–21, 1974.

[20] J. E. Lions, “On some questions in boundary value problems of mathematical physics,” in *Proceedings of the International Symposium on Continuum Mechanics and Partial Differential Equations*, North Holland, Amsterdam, The Netherlands, 1978.

[21] Y. Yamada, “Some nonlinear degenerate wave equations,” *Nonlinear Analysis*, vol. 11, no. 10, pp. 1155–1168, 1987.

[22] S. I. Pohožaev, “On a class of quasilinear hyperbolic equations,” *Matematicheskii Sbornik*, vol. 25, pp. 145–158, 1975.

[23] T. Mizumachi, “Time decay of solutions to degenerate Kirchhoff type equation,” *Nonlinear Analysis. Theory, Methods and Applications*, vol. 33, no. 3, pp. 235–252, 1998.

[24] K. Nishihara and Y. Yamada, “On global solutions of some degenerate quasilinear hyperbolic equations with dissipative terms,” *Funkcialaj Ekvacioj*, vol. 33, pp. 151–159, 1990.

[25] J. Y. Park, I. H. Jung, and Y. H. Kang, “Generalized quasilinear hyperbolic equations and Yosida approximations,” *Journal of the Australian Mathematical Society*, vol. 74, no. 1, pp. 69–86, 2003.

[26] I. H. Jung and J. Choi, “Energy decay estimates for a Kirchhoff model with viscosity,” *Bulletin of the Korean Mathematical Society*, vol. 43, no. 2, pp. 245–252, 2006.

[27] I. H. Jung and Y.-H. Lee, “Exponential decay for the solutions of wave equations of kirchhoff type with strong damping,” *Acta Mathematica Hungarica*, vol. 92, no. 1-2, pp. 163–170, 2001.

[28] M. Ghisi and M. Gobbino, “Global existence and asymptotic behaviour for a mildly degenerate dissipative hyperbolic equation of Kirchhoff type,” *Asymptotic Analysis*, vol. 40, no. 1, pp. 25–36, 2004.

[29] M. Aassila and D. Kaya, “On local solutions of a mildly degenerate hyperbolic equation,” *Journal of Mathematical Analysis and Applications*, vol. 238, no. 2, pp. 418–428, 1999.

[30] S. Kouémou-Patcheu, “Global existence and exponential decay estimates for a damped quasilinear equation,” *Communications in Partial Differential Equations*, vol. 22, no. 11-12, pp. 2007–2024, 1997.

[31] V. Komornik, *Exact Controllability and Stabilizaion—The Multiplier Method*, John Wiley, New York, NY, USA, 1994.

[32] A. Haraux, “Oscillations forcées pour certains systèmes dissipatifs nonlinéaires,” Publications du Laboratoire d’Analyse Numérique, No. 78010 Université Pierre et Marie Curie, Paris, France, 1978.

[33] J. L. Lions, *Quelques Méthodesde Résolution des Prolèmes aux Limites Non Linéarires*, Dunod Gauthiers-Villars, Paris, France, 1968.

[34] Q. C. Nguyen and K. -S. Hong, “Simultaneous control of longitudinal and transverse vibrations of an axially moving string with velocity tracking,” *Journal of Sound and Vibration*, vol. 331, no. 13, pp. 3006–3019, 2012.

Hindawi Publishing Corporation
The Scientific World Journal
Volume 2014, Article ID 287256, 11 pages
http://dx.doi.org/10.1155/2014/287256

Research Article

Limit of Riemann Solutions to the Nonsymmetric System of Keyfitz-Kranzer Type

Lihui Guo and Gan Yin

College of Mathematics and System Sciences, Xinjiang University, Urumqi 830046, China

Correspondence should be addressed to Gan Yin; ganyin1980@gmail.com

Received 18 January 2014; Accepted 2 March 2014; Published 3 April 2014

Academic Editors: D. Baleanu and H. Jafari

The limit of Riemann solutions to the nonsymmetric system of Keyfitz-Kranzer type with a scaled pressure is considered for both polytropic gas and generalized Chaplygin gas. In the former case, the delta shock wave can be obtained as the limit of shock wave and contact discontinuity when $u_- > u_+$ and the parameter ϵ tends to zero. The point is, the delta shock wave is not the one of transport equations, which is obviously different from cases of some other systems such as Euler equations or relativistic Euler equations. For the generalized Chaplygin gas, unlike the polytropic or isothermal gas, there exists a certain critical value ϵ_2 depending only on the Riemann initial data, such that when ϵ drops to ϵ_2, the delta shock wave appears as $u_- > u_+$, which is actually a delta solution of the same system in one critical case. Then as ϵ becomes smaller and goes to zero at last, the delta shock wave solution is the exact one of transport equations. Furthermore, the vacuum states and contact discontinuities can be obtained as the limit of Riemann solutions when $u_- < u_+$ and $u_- = u_+$, respectively.

1. Introduction

The nonsymmetric system of Keyfitz-Kranzer type can be written as

$$\begin{aligned} &\rho_t + (\rho\phi(\rho, u_1, u_2, \dots, u_n))_x = 0, \\ &(\rho u_i)_t + (\rho u_i \phi(\rho, u_1, u_2, \dots, u_n))_x, \quad i = 1, 2, \dots, n, \end{aligned} \tag{1}$$

where

$$\phi(\rho, u) = \phi(u) - p(\rho) \tag{2}$$

is a nonlinear function. A more general form of system (1) was first derived as a model for the elastic string by Keyfitz and Kranzer [1].

When $n = 1$, $\phi(\rho, u) = u - p$, and $p = p(\rho)$, system (1) can be read as

$$\begin{aligned} &\rho_t + (\rho(u - p))_x = 0, \\ &(\rho u)_t + (\rho u(u - p))_x = 0. \end{aligned} \tag{3}$$

Let $u = v + p$; system (3) can be rewritten as the Aw-Rascle model [2]:

$$\begin{aligned} &\rho_t + (\rho v)_x = 0, \\ &(\rho(v + p))_t + (\rho v(v + p))_x = 0, \end{aligned} \tag{4}$$

where ρ, v represent the density and the velocity of cars on the roadway, respectively; the state equation $p(\rho) = \rho^\gamma$, $\gamma > 0$ is smooth and strictly increasing with

$$2p'(\rho) + \rho p''(\rho) > 0 \quad \text{for } \rho > 0. \tag{5}$$

The Aw-Rascle model (4) resolves all the obvious inconsistencies and explains instabilities in car traffic flow, especially near the vacuum, that is, for light traffic with few slow drivers. In 2008, Berthelin et al. [3] studied the limit behavior which was investigated by changing p into ϵp and taking $p(\rho) = (1/\rho - 1/\rho^*)$, $\rho \le \rho^*$, where ρ^* is the maximal density which corresponds to a total traffic jam and is assumed to be a fixed constant although it should depend on the velocity in practice. Then, Shen and Sun [4] studied the limit behavior without the constraint of the maximal density, in which the delta shock and vacuum state were obtained through perturbing the pressure $p(\rho)$ suitably.

For the nonsymmetric system of Keyfitz-Kranzer type (3), under the following two assumptions on $p(\rho)$,

$$\begin{gathered} p(0)=0, \qquad \lim_{\rho\to 0}\rho p'(\rho)=0, \\ \rho p''(\rho)+2p'(\rho)>0 \quad \text{for } \rho>0, \\ \lim_{\rho\to 0}\rho p(\rho)=0, \qquad \lim_{\rho\to\infty}\rho p'(\rho)\ge A, \\ \rho p''(\rho)+2p'(\rho)>0 \quad \text{for } \rho>0, \end{gathered} \tag{6}$$

Lu [5] established the existence of global bounded weak solutions of the Cauchy problem by using the compensated compactness method. Recently, Lu [6] studied the existence of global entropy solutions to general system of Keyfitz-Kranzer type (3). In 2013, Cheng [7] considered the Riemann problem and two kinds of interactions of elementary waves for system (3) with the state equation for Chaplygin gas:

$$p(\rho)=-\frac{1}{\rho}. \tag{7}$$

In this paper, our main purpose is to study the limit behavior of Riemann solutions to the nonsymmetric system of Keyfitz-Kranzer type (3) as the parameter ϵ goes to zero. In 2001, Li [8] was concerned with the limits of Riemann solutions to the compressed Euler equations for isothermal gas by letting the temperature go to zero. Then Chen and Liu [9, 10] presented the results of the compressible Euler equations as pressure vanishes. There are many results on the vanishing pressure limits of Riemann solutions; we refer readers to [4, 11–13] and the references cited therein for more details.

As the pressure vanishes, system (3) formally transforms into the so-called pressureless gas dynamics model or transport equations:

$$\rho_t+(\rho u)_x=0, \qquad (\rho u)_t+(\rho u^2)_x=0, \tag{8}$$

where ρ and u stand for the density and the velocity of the gas, respectively. System (8) is also called zero-pressure gas dynamics. It can be derived from zero-pressure isentropic gas dynamics [14]. System (8) is referred to as the adhesion particle dynamics system to describe the motion process of free particles sticking under collision in the low temperature and the information of large-scale structure in the universe [15, 16]. It is easy to see that the delta shock and vacuum do occur in the Riemann solutions of (8); see [17]. We also refer readers to [4, 18–23] and the references cited therein for some results on delta shock waves.

By letting p be ϵp, system (3) can be changed to

$$\begin{gathered} \rho_t+(\rho(u-\epsilon p))_x=0, \\ (\rho u)_t+(\rho u(u-\epsilon p))_x=0. \end{gathered} \tag{9}$$

In the present paper, we focus on system (9) with equation of state for both polytropic gas and generalized Chaplygin gas. Firstly, we study limit of Riemann solutions to system (9) with the state equation

$$p(\rho)=\rho^{\gamma}, \quad \gamma>0, \tag{10}$$

as ϵ tends to zero. If $u_- > u_+$, we found that the Riemann solution tends to a delta shock wave solution when $\epsilon \to 0$. However, the propagating speed and the strength of the delta shock wave in the limit situation are different from the classical results of transport equations (8) with the same Riemann initial data. If $u_- < u_+$, the Riemann solution tends to a two-contact discontinuity solution to the transport equations (8) as $\epsilon \to 0$. The intermediate state between the two-contact discontinuities is a vacuum state. When $u_- = u_+$, the Riemann solutions converge to one-contact discontinuity solutions of system (8). Then, we investigate system (9) for generalized Chaplygin gas:

$$p(\rho)=-\rho^{-\alpha}, \quad 0<\alpha\le 1, \tag{11}$$

where $\alpha = 1$ is for Chaplygin gas. We find that, as ϵ arrives at a certain critical value ϵ_2 depending only on the given Riemann initial data $(u_\pm, \rho_\pm)$, the solution involving one shock and one contact discontinuity converges to a delta shock solution of system (9) and (11). Eventually, when ϵ tends to zero, the delta shock wave solution is exactly the solution of transport equations (8). Thus we can see that the process of delta shock wave formation is obviously different from those in [4, 8–13] and so forth.

The paper is organized as follows. In Section 2, we give some preliminary knowledge for system (8). In Section 3, we present the Riemann solutions to system (9). In Section 4, we display the limit of Riemann solutions to the nonsymmetric system of Keyfitz-Kranzer type (9).

2. The Riemann Solutions of System (8)

In this section, we briefly review the Riemann solutions of (8) with initial data:

$$(u(x,0), \rho(x,0))=(u_\pm, \rho_\pm), \quad \pm x>0, \tag{12}$$

where $\rho_\pm > 0$, the detailed study of which can be founded in [17].

Transport equations (8) have a double eigenvalue $\lambda = u$ with only one corresponding right eigenvector $r = (1, 0)^\top$. By simple calculation, we obtain $\nabla\lambda \cdot r = 0$, which means that system (8) is linearly degenerate.

Given any two constant states $(u_\pm, \rho_\pm)$, we can constructively obtain the Riemann solutions of (8) and (12) containing contact discontinuities, vacuum, or delta shock wave.

For the case $u_- < u_+$, the solution containing two contact discontinuities and a vacuum state can be expressed as

$$(u,\rho)(x,t)=\begin{cases}(u_-,\rho_-), & x\le u_-t,\\ (\xi,0), & u_-t\le x\le u_+t,\\ (u_+,\rho_+), & x\ge u_+t.\end{cases} \tag{13}$$

For the case $u_- = u_+$, we connect the constant states $(u_\pm, \rho_\pm)$ by one contact discontinuity.

For the case $u_- > u_+$, a solution containing a weighted δ-measure supported on a line will be constructed to connect the constant $(u_\pm, \rho_\pm)$. So we define the solution in the sense of distributions as follows.

Definition 1. A pair (u, ρ) constitutes a solution of (8) in the sense of distributions if it satisfies

$$\int_0^{+\infty}\int_{-\infty}^{+\infty}\left(\rho\phi_t + (\rho u)\phi_x\right)\mathrm{d}x\ \mathrm{d}t = 0,$$
$$\int_0^{+\infty}\int_{-\infty}^{+\infty}\left((\rho u)\phi_t + \left(\rho u^2\right)\phi_x\right)\mathrm{d}x\ \mathrm{d}t = 0, \tag{14}$$

for any test function $\phi \in C_0^{\infty}(R^+ \times R)$.

Moreover, we define a two-dimensional weighted delta functions as follows.

Definition 2. A two-dimensional weighted delta function $w(s)\delta_l$ supported on a smooth curve L parameterized as $t = t(s)$, $x = x(s)$ $(c \le s \le d)$ is defined by

$$\langle w(s)\delta_l, \phi\rangle = \int_c^d w(s)\phi(t(s), x(s))\,\mathrm{d}s, \tag{15}$$

for all test functions $\phi \in C_0^{\infty}(R^+ \times R)$.

With these definitions, one can construct a δ-measure solution as

$$(u,\rho)(t,x) = \begin{cases}(u_-, \rho_-), & x < u_\delta t,\\ (u_\delta, \omega(t)\delta(x - u_\delta t)), & x = u_\delta t,\\ (u_+, \rho_+), & x > u_\delta t,\end{cases} \tag{16}$$

where $\omega(t)$ and u_δ are weight and velocity of the delta shock wave, respectively, satisfying the generalized Rankine-Hugoniot condition:

$$\frac{\mathrm{d}x(t)}{\mathrm{d}t} = u_\delta,$$
$$\frac{\mathrm{d}\omega(t)}{\mathrm{d}t} = u_\delta[\rho] - [\rho u], \tag{17}$$
$$\frac{\mathrm{d}\omega(t)u_\delta}{\mathrm{d}t} = u_\delta[\rho u] - \left[\rho u^2\right],$$

with initial data $\omega(0) = 0$, where $[\rho] = \rho_+ - \rho_-$. By simple calculation, we obtain

$$u_\delta = \frac{\sqrt{\rho_+}u_+ + \sqrt{\rho_-}u_-}{\sqrt{\rho_+} + \sqrt{\rho_-}},$$
$$\omega(t) = \sqrt{\rho_-\rho_+}\left(u_- - u_+\right)t, \tag{18}$$

for $\rho_- \ne \rho_+$, and

$$u_\delta = \frac{u_+ - u_-}{2},$$
$$\omega(t) = \rho_+\left(u_- - u_+\right)t, \tag{19}$$

for $\rho_- = \rho_+$.

We can also justify that the delta shock wave satisfies the entropy condition:

$$u_+ < u_\delta < u_-, \tag{20}$$

which means that all the characteristics on both sides of the delta shock are incoming.

3. The Riemann Solutions for System (9)

In this section, we analyze some basic properties and solve the Riemann problem for (9).

3.1. The Riemann Solutions for System (9) *and* (10). System (9) and (10) have two eigenvalues

$$\lambda_1 = u - \epsilon(\gamma+1)\rho^{\gamma}, \qquad \lambda_2 = u - \epsilon\rho^{\gamma}, \tag{21}$$

with corresponding right eigenvectors

$$r_1 = (1,0)^T, \qquad r_2 = \left(\rho, \epsilon\gamma\rho^{\gamma}\right)^T, \tag{22}$$

satisfying

$$\nabla\lambda_1 \cdot r_1 = -\epsilon\gamma(\gamma+1)\rho^{\gamma-1} \ne 0, \qquad \nabla\lambda_2 \cdot r_2 = 0. \tag{23}$$

So the 1-characteristic field is genuinely nonlinear, and the 2-characteristic field is always linearly degenerate.

Since (9)-(10) and (12) remain invariant under a uniform expansion of coordinates $t \to \beta t$ and $x \to \beta x$, $\beta > 0$, the solution is only connected with $\xi = x/t$. Thus we should seek the self-similar solution

$$(u,\rho)(x,t) = (u,\rho)(\xi), \quad \xi = \frac{x}{t}. \tag{24}$$

Then, the Riemann problem (9)-(10) and (12) can be reduced to

$$-\xi\rho_\xi + \left(\rho\left(u - \epsilon\rho^{\gamma}\right)\right)_\xi = 0,$$
$$-\xi(\rho u)_\xi + \left(\rho u\left(u - \epsilon\rho^{\gamma}\right)\right)_\xi = 0, \tag{25}$$

with $(u,\rho)(\pm\infty) = (u_\pm, \rho_\pm)$.

For smooth solutions, system (25) can be rewritten as

$$\begin{pmatrix} u - \epsilon(\gamma+1)\rho^{\gamma} - \xi & \rho \\ 0 & u - \epsilon\rho^{\gamma} - \xi\end{pmatrix}\begin{pmatrix}\mathrm{d}\rho \\ \mathrm{d}u\end{pmatrix} = 0, \tag{26}$$

which provides either the general solutions (constant states),

$$(u,\rho)(\xi) = \text{const}, \quad (\rho > 0), \tag{27}$$

or rarefaction wave, which is wave of the first characteristic family,

$$R: \begin{cases}\xi = u - \epsilon(\gamma+1)\rho^{\gamma},\\ u = u_-, \qquad \rho < \rho_-,\end{cases} \tag{28}$$

or contact discontinuity, which is of the second characteristic family,

$$J\colon \begin{cases}\xi = u - \epsilon\rho^{\gamma},\\ u = u_- + \epsilon\left(\rho^{\gamma} - \rho_-^{\gamma}\right).\end{cases} \tag{29}$$

For a bounded discontinuity at $\xi = \sigma_\epsilon$, the Rankine-Hugoniot condition

$$-\sigma_\epsilon[\rho] + \left[\rho\left(u - \epsilon\rho^{\gamma}\right)\right] = 0,$$
$$-\sigma_\epsilon[\rho u] + \left[\rho u\left(u - \epsilon\rho^{\gamma}\right)\right] = 0, \tag{30}$$

holds, where $[\rho] = \rho - \rho_-$ and σ_ϵ is the velocity of the discontinuity. From (30), we obtain either shock wave, which is wave of the first characteristic family,

$$S: \begin{cases} \sigma_\epsilon = u - \dfrac{\epsilon\left(\rho^{\gamma+1} - \rho_-^{\gamma+1}\right)}{\rho - \rho_-}, \\ u = u_-, \qquad \rho > \rho_-, \end{cases} \tag{31}$$

or contact discontinuity, which is of the second characteristic family,

$$J: \begin{cases} \sigma_\epsilon = u - \epsilon\rho^\gamma, \\ u = u_- + \epsilon\left(\rho^\gamma - \rho_-^\gamma\right). \end{cases} \tag{32}$$

Here we notice that the shock wave curve and the rarefaction wave curve passing through the same point (u_-, ρ_-) coincid in the phase plane; that is, (9)-(10) belong to "Temple class" [24].

Through the point (u_-, ρ_-), we draw the curve $u = u_-$ for $\rho > 0$ in the phase plane, which is parallel to the ρ-axis. We denote it by R when $\rho < \rho_-$ and S when $\rho > \rho_-$. Through the point (u_-, ρ_-), we draw the curve (29) which intersects the u-axis at the point $(u_- - \epsilon\rho_-^\gamma, 0)$, denoted by J. Then the phase plane is divided into four regions (see Figure 1). Thus we can construct the Riemann solutions of system (9)-(10) as follows:

(1) when $(u_+, \rho_+) \in \mathrm{I}(u_-, \rho_-)$, that is, $u_+ > u_-$ and $u_+ < u_- + \epsilon(\rho^\gamma - \rho_-^\gamma)$, the solution is $S + J$;

(2) when $(u_+, \rho_+) \in \mathrm{II}(u_-, \rho_-)$, that is, $u_+ > u_-$ and $u_+ > u_- + \epsilon(\rho^\gamma - \rho_-^\gamma)$, the solution is $R + J$;

(3) when $(u_+, \rho_+) \in \mathrm{III}(u_-, \rho_-)$, that is, $u_+ < u_-$ and $u_+ > u_- + \epsilon(\rho^\gamma - \rho_-^\gamma)$, the solution is $R + J$;

(4) when $(u_+, \rho_+) \in \mathrm{IV}(u_-, \rho_-)$, that is, $u_+ < u_-$ and $u_+ < u_- + \epsilon(\rho^\gamma - \rho_-^\gamma)$, the solution is $S + J$.

3.2. The Riemann Solutions of System (9) *and* (11). Systems (9) and (11) have two eigenvalues:

$$\lambda_1 = u + \epsilon(1-\alpha)\rho^{-\alpha}, \qquad \lambda_2 = u + \epsilon\rho^{-\alpha}, \tag{33}$$

with corresponding right eigenvectors:

$$r_1 = (1, 0)^T, \qquad r_2 = \left(\rho, \epsilon\alpha\rho^{-\alpha}\right)^T, \tag{34}$$

satisfying

$$\nabla\lambda_1 \cdot r_1 = -\epsilon\alpha(1-\alpha)\rho^{-\alpha-1}, \qquad \nabla\lambda_2 \cdot r_2 = 0. \tag{35}$$

Thus the 1-characteristic field is genuinely nonlinear and 2-characteristic field is always linearly degenerate as $0 < \alpha < 1$, while both the two characteristic fields are fully linearly degenerate as $\alpha = 1$.

When $0 < \alpha < 1$, we get rarefaction wave and shock wave which can be expressed by

$$\begin{gathered} R: \begin{cases} \xi = u + \epsilon(1-\alpha)\rho^{-\alpha}, \\ u = u_-, \qquad \rho < \rho_-, \end{cases} \\ S: \begin{cases} \sigma_\epsilon = u + \dfrac{\epsilon\left(\rho^{1-\alpha} - \rho_-^{1-\alpha}\right)}{\rho - \rho_-}, \\ u = u_-, \qquad \rho > \rho_-, \end{cases} \end{gathered} \tag{36}$$

or contact discontinuity which can be expressed by

$$J: \begin{cases} \tau_\epsilon = u + \epsilon\rho^{-\alpha}, \\ u = u_- + \epsilon\left(\rho_-^{-\alpha} - \rho^{-\alpha}\right). \end{cases} \tag{37}$$

When $0 < \alpha < 1$, through the point (u_-, ρ_-), we draw the curve $u = u_-$ for $\rho > 0$ in the phase plane, denoted by R when $\rho < \rho_-$ and S when $\rho > \rho_-$. Through the point (u_-, ρ_-), we draw the curve (37) which has two asymptotes $u = u_- + \epsilon\rho_-^{-\alpha}$ and $\rho = 0$, denoted by J. Through the point $(u_- - \epsilon/\rho_-^\alpha, \rho_-)$, we draw the curve (37), which has two asymptotic lines $u = u_-$ and $\rho = 0$, denoted by S_δ. Then the phase plane is divided into five regions; see Figure 2.

For any given (u_-, ρ_-), the Riemann solution is showed as follows:

(1) when $(u_+, \rho_+) \in \mathrm{I}(u_-, \rho_-)$, that is, $u_+ > u_-$ and $u_+ < u_- + \epsilon(\rho_-^{-\alpha} - \rho^{-\alpha})$, the solution is $S + J$;

(2) when $(u_+, \rho_+) \in \mathrm{II}(u_-, \rho_-)$, that is, $u_+ > u_-$ and $u_+ > u_- + \epsilon(\rho_-^{-\alpha} - \rho^{-\alpha})$, the solution is $R + J$;

(3) when $(u_+, \rho_+) \in \mathrm{III}(u_-, \rho_-)$, that is, $u_+ < u_-$ and $u_+ > u_- + \epsilon(\rho_-^{-\alpha} - \rho^{-\alpha})$, the solution is $R + J$;

(4) when $(u_+, \rho_+) \in \mathrm{IV}(u_-, \rho_-)$, that is, $u_+ < u_-$ and $u_+ < u_- + \epsilon(\rho_-^{-\alpha} - \rho^{-\alpha})$, the solution is $S + J$.

The nonvacuum intermediate constant state (u_*, ρ_*) is given by

$$(u_*, \rho_*) = \left(u_-, \sqrt[\alpha]{\frac{\epsilon}{u_+ - u_- + \epsilon\rho_+^{-\alpha}}}\right). \tag{38}$$

When $(u_+, \rho_+) \in \mathrm{V}(u_-, \rho_-)$, we introduce a definition of δ-measure solution, in which we introduce a definition of a generalized solution [19, 20, 22, 25] for system (9) and (11).

Suppose that $\Gamma = \{\gamma_i \mid i \in I\}$ is a graph in the closed upper half-plane $\{(x,t) \mid x \in \mathbb{R}, t \in [0, +\infty)\} \subset \mathbb{R}^2$ containing smooth arcs $\gamma_i, i \in I$, and I is a finite set. I_0 is subset of I such that an arc γ_k for $k \in I_0$ starts from the point of the x-axis; $\Gamma_0 = \{x_k^0 \mid k \in I_0\}$ is the set of initial points of arc $\gamma_k, k \in I_0$.

Consider the δ-shock wave type initial data $(u^0(x), \rho^0(x))$, where

$$\rho^0(x) = \rho_0(x) + w^0\delta(\Gamma_0), \tag{39}$$

$u^0, \rho_0 \in L^\infty(\mathbb{R}; \mathbb{R})$, $w^0\delta(\Gamma_0) = \sum_{k\in I_0} w_k^0 \delta(x - x_k^0)$, and w_k^0 are constants for $k \in I_0$. Furthermore, the pressure $p = -\rho^{-\alpha}$ in (11) is a nonlinear term with respect to ρ defined by $p^0(x,t) = -\rho_0^{-\alpha}$.

Definition 3. A pair of distributions $(u(x,t), \rho(x,t))$ and a graph Γ, where $\rho(x,t)$ and $p(x,t)$ have the form

$$\rho(x,t) = \overline{\rho}(x,t) + w(x,t)\delta(\Gamma), \qquad p(x,t) = -\rho(x,t)^{-\alpha}, \tag{40}$$

$u, \overline{\rho} \in L^\infty(\mathbb{R} \times \mathbb{R}_+; \mathbb{R})$, $w(x,t)\delta(\Gamma) = \sum_{i\in I} w_i(x,t)\delta(\gamma_i)$, $w_i(x,t) \in C(\Gamma)$ for $i \in I$ is called a generalized δ-shock wave

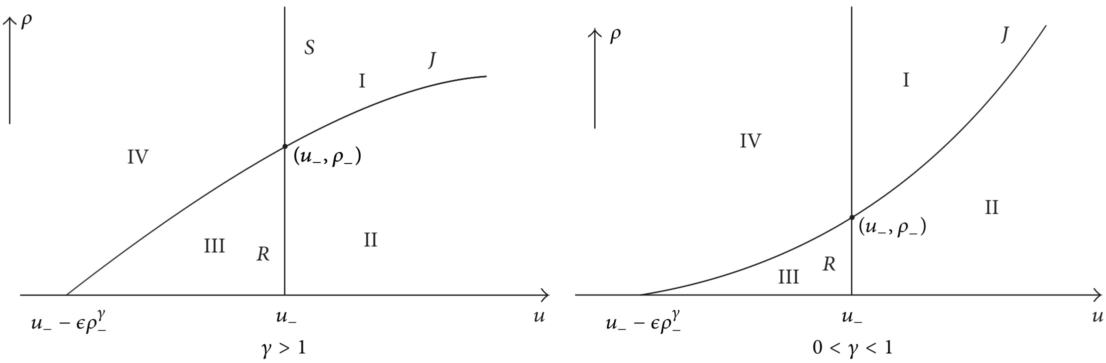

Figure 1: The upper half (u, ρ) plane with $p = \rho^{\gamma}$ is divided into 4 regions for both cases $\gamma > 1$ and $0 < \gamma < 1$.

type solution of system (9) with the initial data $(u^0(x), \rho^0(x))$ if the integral identities

$$\begin{gathered}\int_0^{+\infty}\int_{-\infty}^{+\infty}\left(\overline{\rho}\phi_t + \overline{\rho}\left(u - \epsilon p\right)\phi_x\right)dx\,dt \\ + \sum_{i\in I}\int_{\gamma_i}\omega_i\left(x,t\right)\frac{\partial\phi}{\partial l}dl \\ + \int_{-\infty}^{+\infty}\rho_0\left(x\right)\phi\left(x,0\right)dx + \sum_{k\in I_0} w_k^0\phi\left(x_k^0, 0\right) = 0, \\ \int_0^{+\infty}\int_{-\infty}^{+\infty}\left(\overline{\rho}u\phi_t + \overline{\rho}u\left(u - \epsilon p\right)\phi_x\right)dx\,dt \\ + \sum_{i\in I}\int_{\gamma_i} w_i\left(x,t\right)u_\delta\left(x,t\right)\frac{\partial\phi}{\partial l}dl \\ + \int_{-\infty}^{+\infty}\rho_0\left(x\right)u_0\left(x\right)\phi\left(x,0\right)dx \\ + \sum_{k\in I_0} w_k^0 u_\delta^0\left(x_k^0\right)\phi\left(x_k^0, 0\right) = 0\end{gathered} \tag{41}$$

hold for any test functions $\phi(x,t) \in \mathscr{D}(\mathbb{R}\times\mathbb{R}_+)$, where $\partial\phi/\partial l$ is the tangential derivative on the graph Γ, $\int_{\gamma_i} dl$ is a line integral along the arc γ_i, $u_\delta(x,t)$ is the velocity of the δ-shock wave, and $u_\delta^0(x_k^0) = u_\delta(x_k^0, 0), k \in I_0$.

Theorem 4. *When $(u_+, \rho_+) \in V$, for the Riemann problem* (9)*,* (11)*, and* (12)*, there is a δ-shock wave solution $(u(x,t), \rho(x,t))$ with form*

$$\begin{aligned}u\left(x,t\right) &= u_- + [u]\,H\left(x - x\left(t\right)\right), \\ \rho\left(x,t\right) &= \rho_- + [\rho]\,H\left(x - x\left(t\right)\right) + w\left(t\right)\delta\left(x - x\left(t\right)\right),\end{aligned} \tag{42}$$

which satisfies the integral identities (41) *in the sense of Definition 3, where $\Gamma = \{(x,t) \mid x = x(t) = \sigma t, t \geq 0\}$, $\overline{\rho}(x,t) = \rho_- + [\rho]H(x - x(t))$,*

$$\int_\Gamma w\left(x,t\right)\frac{\partial\phi\left(x,t\right)}{\partial l} = \int_0^\infty w\left(x,t\right)\frac{d\phi\left(x,t\right)}{dt}, \tag{43}$$

and $H(x)$ is the Heaviside function $H(x) = 0(1)$, $x < (>)0$.

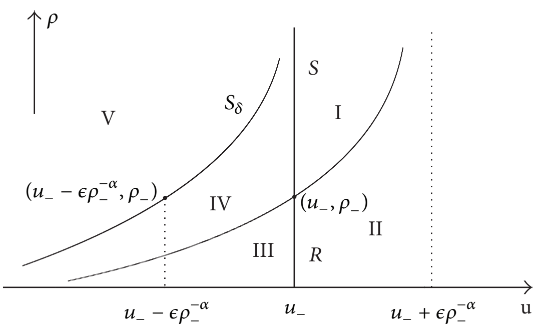

Figure 2: The upper half (u, ρ) plane with $p = \rho^{\alpha}$ $(0 < \alpha < 1)$ is divided into 5 regions.

Suppose that $\Omega \subset \mathbb{R}\times\mathbb{R}_+$ is a region cut by a smooth curve $\Gamma = \{(x,t) \mid x = x(t)\}$ into left and right hand parts $\Omega_\pm = \{(x,t) \mid \pm(x - x(t)) > 0\}$; $(u(x,t), \rho(x,t))$ is a generalized δ-shock wave solution of system (9) and (11); functions $\overline{\rho}(x,t)$ and $u(x,t)$ are smooth in $\Omega_\pm$ and have one-side limits $\overline{\rho}_\pm, u_\pm$ on the curve Γ. Then the generalized Rankine-Hugoniot conditions for δ-shock wave are

$$\begin{aligned}\frac{\mathrm{d}x\left(t\right)}{\mathrm{d}t} &= u_\delta, \\ \frac{\mathrm{d}\omega\left(t\right)}{\mathrm{d}t} &= u_\delta\left[\rho\right] - \left[\rho\left(u + \epsilon\rho^{-\alpha}\right)\right], \\ \frac{\mathrm{d}\left(\omega\left(t\right)u_\delta\right)}{\mathrm{d}t} &= u_\delta\left[\rho u\right] - \left[\rho u\left(u + \epsilon\rho^{-\alpha}\right)\right],\end{aligned} \tag{44}$$

with initial data $\omega(0) = 0$, where $[\rho] = \rho_+ - \rho_-$, $0 < \alpha < 1$.

From (44), we obtain

$$\begin{aligned}u_\delta = &\Big(\left[2\rho u + \epsilon\rho^{1-\alpha}\right] \\ &+ \sqrt{\left[2\rho u + \epsilon\rho^{1-\alpha}\right]^2 - 4\left[\rho\right]\left[\rho u\left(u + \epsilon\rho^{-\alpha}\right)\right]}\Big) \\ &\times\left(2\left[\rho\right]\right)^{-1},\end{aligned}$$

$$\omega(t) = \left(\left(-\left[\epsilon\rho^{1-\alpha}\right] + \sqrt{\left[2\rho u + \epsilon\rho^{1-\alpha}\right]^2 - 4\left[\rho\right]\left[\rho u\left(u + \epsilon\rho^{-\alpha}\right)\right]}\right) \times (2)^{-1}\right) t, \tag{45}$$

as $\rho_- \neq \rho_+$, and

$$\begin{aligned} u_\delta &= \frac{u_+ - u_- + \epsilon\rho_+^{-\alpha}}{2}, \\ \omega(t) &= \rho_+ (u_- - u_+) t, \end{aligned} \tag{46}$$

as $\rho_- = \rho_+$.

We also can justify that the delta shock wave satisfies the entropy condition:

$$\lambda_2(u_+, \rho_+) \leq u_\delta \leq \lambda_1(u_-, \rho_-), \tag{47}$$

which means that all the characteristics on both sides of the delta shock are not outcoming.

When $\alpha = 1$, the detailed study can be found in [7]; we omit it.

Thus, we have obtained the solutions of the Riemann problem for (9).

4. Limit of Riemann Solutions to the Keyfitz-Kranzer Type System

In this section, our main purpose is to consider the limits of the Riemann solutions of (9) and compare them with the corresponding Riemann solutions to transport equations (8). Our discussion depends on the order of u_- and u_+.

4.1. The Limits of Riemann Solutions of (9)-(10). Firstly, we display the limit of Riemann solution to (9)-(10) for $u_- < u_+$.

Lemma 5. *In the case $u_- < u_+$, when $\rho_- \geq \rho_+$, $(u_+, \rho_+) \in \mathrm{II}(u_-, \rho_-)$ for arbitrary ϵ; when $\rho_- < \rho_+$, there exists $\epsilon_0 = (u_+ - u_-)/(\rho_+^\gamma - \rho_-^\gamma) > 0$, such that $(u_+, \rho_+) \in \mathrm{II}(u_-, \rho_-)$ when $0 < \epsilon < \epsilon_0$.*

This lemma shows that the curve J becomes steeper as ϵ is much small. As $u_- < u_+$, from Lemma 5, we know that $(u_+, \rho_+) \in \mathrm{II}(u_-, \rho_-)$ when $0 < \epsilon < \epsilon_0$. Then the Riemann solutions of (9)-(10) consist of the rarefaction wave R and the contact discontinuity J with the intermediate constant state (u_*, ρ_*) besides the two constant states $(u_\pm, \rho_\pm)$ as this form:

$$(u^\epsilon, \rho^\epsilon)(\xi) = \begin{cases} (u_-, \rho_-), & -\infty < \xi \leq \lambda_1(u_-, \rho_-), \\ R, & \lambda_1(u_-, \rho_-) \leq \xi \leq \lambda_1(u_*, \rho_*), \\ (u_*, \rho_*), & \lambda_1(u_*, \rho_*) \leq \xi < \tau_\epsilon \\ (u_+, \rho_+), & \tau_\epsilon < \xi < +\infty, \end{cases} \tag{48}$$

where λ_1 is determined by (21),

$$\tau_\epsilon = u_+ - \epsilon\rho_+^\gamma, \tag{49}$$

$$(u_*, \rho_*) = \left(u_-, \sqrt[\gamma]{\frac{u_- - u_+}{\epsilon} + \rho_+^\gamma}\right). \tag{50}$$

When $u_- < u_+$, from (50), and when ϵ is small enough to satisfy $0 < \epsilon \leq (u_+ - u_-)/\rho_+^\gamma$, we know that a vacuum state appears in the Riemann solutions of (9)-(10). By (21), (49), and (50), it is easy to get that

$$\begin{aligned} &\lim_{\epsilon\to 0}\lambda_1(u_-, \rho_-) = \lim_{\epsilon\to 0}\left(u_- - \epsilon(\gamma+1)\rho_-^\gamma\right) = u_-, \\ &\lim_{\epsilon\to 0}\lambda_1(u_*, \rho_*) = \lim_{\epsilon\to 0}\left(u_* - \epsilon(\gamma+1)\rho_*^\gamma\right) = u_-, \\ &\lim_{\epsilon\to 0}\tau_\epsilon = \lim_{\epsilon\to 0}\left(u_+ - \epsilon\rho_+^\gamma\right) = u_+, \end{aligned} \tag{51}$$

which mean that the rarefaction wave R and the contact discontinuity J: $u_* - \epsilon\rho_*^\gamma = u_+ - \epsilon\rho_+^\gamma$ become the contact discontinuities J_1: $u = u_-$ and J_2: $u = u_+$, respectively, as $\epsilon \to 0$. Meanwhile the vacuum state will fill up the region between the two contact discontinuities, which is exactly identical with the corresponding Riemann solutions of system (8).

Secondly, when $u_+ = u_-$, the Riemann solution contains a shock wave S with the propagating speed σ_ϵ besides the states $(u_\pm, \rho_\pm)$ for $\rho_+ > \rho_-$, or a rarefaction wave R with the speed $\lambda_1(u, \rho)$ ($\rho_- \geq \rho \geq \rho_+$) for $\rho_+ < \rho_-$; see Figure 1. From (31) and (50), we obtain

$$\lim_{\epsilon\to 0}\sigma_\epsilon = \lim_{\epsilon\to 0}\left(u - \frac{\epsilon\left(\rho^{\gamma+1} - \rho_-^{\gamma+1}\right)}{\rho - \rho_-}\right) = u_-, \tag{52}$$

or from (21) and (50), we have

$$\begin{aligned} \lim_{\epsilon\to 0}\lambda_1(u_-, \rho_-) &= \lim_{\epsilon\to 0}\left(u_- - \epsilon(\gamma+1)\rho_-^\gamma\right) = \lim_{\epsilon\to 0}\lambda_1(u_+, \rho_+) \\ &= \lim_{\epsilon\to 0}\left(u_+ - \epsilon(\gamma+1)\rho_+^\gamma\right) = u_-. \end{aligned} \tag{53}$$

We conclude that, when $u_- = u_+$, the Riemann solution of system (9)-(10) containing one shock wave or one rarefaction wave converges to the contact discontinuity solution of the transport equations (8) as $\epsilon \to 0$.

Finally, we display the limit of Riemann solutions to (9)-(10) for $u_- > u_+$.

Lemma 6. *In the case $u_- > u_+$, when $\rho_- \leq \rho_+$, $(u_+, \rho_+) \in \mathrm{IV}(u_-, \rho_-)$ for arbitrary ϵ; when $\rho_- > \rho_+$, there exists $\epsilon_1 = (u_- - u_+)/(\rho_-^\gamma - \rho_+^\gamma) > 0$, such that $(u_+, \rho_+) \in \mathrm{IV}(u_-, \rho_-)$ when $0 < \epsilon < \epsilon_1$.*

From this lemma we know that the contact discontinuity J becomes steeper and steeper when ϵ decreases; that is, $(u_+, \rho_+) \in \mathrm{IV}(u_-, \rho_-)$ for small ϵ. In this case, the Riemann solution of (9)-(10) consists of a shock wave S and a contact discontinuity J with the intermediate constant state (u_*, ρ_*) as

$$(u^\epsilon, \rho^\epsilon) = \begin{cases} (u_-, \rho_-), & -\infty < \xi < \sigma_\epsilon, \\ (u_*, \rho_*), & \sigma_\epsilon < \xi < \tau_\epsilon, \\ (u_+, \rho_+), & \tau_\epsilon < \xi < +\infty, \end{cases} \tag{54}$$

where (u_*, ρ_*) is given by (50) and

$$\sigma_\epsilon = u_- - \frac{\epsilon \left(\rho_*^{\gamma+1} - \rho_-^{\gamma+1}\right)}{\rho_* - \rho_-}. \tag{55}$$

When $u_- > u_+$, from (50), it is easy to see that

$$\lim_{\epsilon \to 0} \rho_* = \lim_{\epsilon \to 0} \sqrt[\gamma]{\frac{u_- - u_+}{\epsilon} + \rho_+^\gamma} = \infty. \tag{56}$$

By (55), we obtain

$$\lim_{\epsilon \to 0} \sigma_\epsilon = \lim_{\epsilon \to 0} \left(u_- - \frac{\epsilon \left(\rho_*^{\gamma+1} - \rho_-^{\gamma+1}\right)}{\rho_* - \rho_-} \right) = u_+. \tag{57}$$

From (56)-(57) and

$$\lim_{\epsilon \to 0} \tau_\epsilon = \lim_{\epsilon \to 0} \left(u_+ - \epsilon \rho_+^\gamma\right) = u_+, \tag{58}$$

we know that S and J coincide with a new type of nonlinear hyperbolic wave which is called the delta shock wave in [23]. Compared with the corresponding Riemann solutions of (8), it is clear to see that the propagation speed of the delta shock wave here is $u_\delta = u_+$ which is different from that of (8).

From (30), we have

$$\begin{aligned} \sigma_\epsilon (\rho_* - \rho_-) &= \rho_* \left(u_* - \epsilon \rho_*^\gamma\right) - \rho_- \left(u_- - \epsilon \rho_-^\gamma\right), \\ \tau_\epsilon (\rho_+ - \rho_*) &= \rho_+ \left(u_+ - \epsilon \rho_+^\gamma\right) - \rho_* \left(u_* - \epsilon \rho_*^\gamma\right), \end{aligned} \tag{59}$$

which mean that

$$\lim_{\epsilon \to 0} (\sigma_\epsilon - \tau_\epsilon) \rho_* = u_+ [\rho] - [\rho u] = \rho_- (u_- - u_+). \tag{60}$$

It is obvious that

$$\omega(t) = \lim_{\epsilon \to 0} \int_{\sigma_\epsilon t}^{\tau_\epsilon t} \rho_* dx = \lim_{\epsilon \to 0} (\sigma_\epsilon - \tau_\epsilon) \rho_* t = \rho_- (u_- - u_+) t. \tag{61}$$

From (61), we obtain that the strength of the delta shock wave is also different from transport equations (8), which may be due to the different propagation speed of the delta shock wave. For the limit situation of (9)-(10), the characteristics on the left side of the delta shock wave will come into the delta shock wave line $x = u_+ t$ while the characteristics on the right side of it will be parallel to it. For transport equations (8), the characteristics on the two sides will come into the delta shock wave curve $x = u_\delta t$. So, the Riemann solution of (9)-(10) does not converge to solution of (8) as $\epsilon \to 0$ when $u_- > u_+$.

4.2. The Limit of Riemann Solutions of System (9) *and* (11). In this subsection, we deal with the limit behavior of Riemann solutions to system (9) and (11).

Firstly, we display the limit of Riemann solutions to (9) and (11) for $u_- < u_+$.

Lemma 7. *For the case $u_- < u_+$, when $\rho_- \geq \rho_+$, $(u_+, \rho_+) \in \mathrm{II}(u_-, \rho_-)$ for arbitrary ϵ; when $\rho_- < \rho_+$, then there exists $\epsilon_0 = (u_+ - u_-)/(\rho_-^{-\alpha} - \rho_+^{-\alpha}) > 0$ such that $(u_+, \rho_+) \in \mathrm{II}(u_-, \rho_-)$ as $0 < \epsilon < \epsilon_0$.*

From Lemma 7, we know that the contact discontinuity J becomes steeper as ϵ becomes smaller and smaller; that is, $(u_+, \rho_+) \in \mathrm{II}(u_-, \rho_-)$ for small ϵ. Then the Riemann solution of (9) and (11) consists of a rarefaction wave R and a contact discontinuity J with the intermediate constant state (u_*, ρ_*) besides the two constant states $(u_\pm, \rho_\pm)$, which has this form:

$$(u^\epsilon, \rho^\epsilon) = \begin{cases} (u_-, \rho_-), & -\infty < \xi < \lambda_1 (u_-, \rho_-), \\ R, & \lambda_1 (u_-, \rho_-) \leq \xi \leq \lambda_1 (u_*, \rho_*), \\ (u_*, \rho_*), & \lambda_1 (u_*, \rho_*) < \xi < \tau_\epsilon, \\ (u_+, \rho_+), & \tau_\epsilon < \xi < +\infty, \end{cases} \tag{62}$$

where λ_1, (u_*, ρ_*) are determined by (33) and (38), respectively, and

$$\tau_\epsilon = u_+ + \epsilon \rho_+^{-\alpha}. \tag{63}$$

From (38), we obtain

$$\lim_{\epsilon \to 0} \rho_* = \lim_{\epsilon \to 0} \sqrt[\alpha]{\frac{\epsilon}{u_+ - u_- + \epsilon \rho_+^{-\alpha}}} = 0, \tag{64}$$

and then a vacuum state appears in the Riemann solution of (9)–(11).

By (33), (38), and (63), we get

$$\begin{gathered} \lim_{\epsilon \to 0} \lambda_1 (u_-, \rho_-) = \lim_{\epsilon \to 0} \lambda_1 (u_*, \rho_*) = u_-, \\ \lim_{\epsilon \to 0} \tau_\epsilon = u_+, \end{gathered} \tag{65}$$

which mean that the rarefaction wave R and the contact discontinuity J become the contact discontinuities J_1: $u = u_-$ and J_2: $u = u_+$, respectively, as $\epsilon \to 0$. Meanwhile the vacuum state will fill up the region between the two contact discontinuities, which is exactly identical with the corresponding Riemann solution of system (8).

Secondly, when $u_+ = u_-$, as done in Section 4.1, it is easy to see that the Riemann solution of (9) and (11) converges to the contact discontinuity of system (8); we omit it.

Finally, we discuss the limit of Riemann solutions of (9) and (11) when $u_- > u_+$.

Lemma 8. *If $u_- > u_+$, then there exist $\epsilon_1, \epsilon_2 > 0$ such that $(u_+, \rho_+) \in \mathrm{IV}(u_-, \rho_-)$ when $\epsilon_2 < \epsilon < \epsilon_1$; $(u_+, \rho_+) \in \mathrm{V}(u_-, \rho_-)$ when $0 < \epsilon < \epsilon_2$.*

Proof. When $\rho_- \leq \rho_+$, it is easy to find that $(u_+, \rho_+) \in \mathrm{IV} \cup \mathrm{V}(u_-, \rho_-)$ for arbitrary ϵ directly from Figure 2. On the other hand, when $\rho_- > \rho_+$ and $(u_+, \rho_+) \in \mathrm{IV} \cup \mathrm{V}(u_-, \rho_-)$, see Figure 2 together with (37), we can get that ϵ should satisfy $u_+ + \epsilon\rho_+^{-\alpha} < u_- + \epsilon\rho_-^{-\alpha}$, which gives $\epsilon < (u_- - u_+)/(\rho_+^{-\alpha} - \rho_-^{-\alpha})$. In one word, $(u_+, \rho_+) \in \mathrm{IV} \cup \mathrm{V}(u_-, \rho_-)$ for small ϵ.

If $(u_+, \rho_+) \in \mathrm{IV}(u_-, \rho_-)$, (u_+, ρ_+) should satisfy $u_+ < u_-$, $u_+ + \epsilon\rho_+^{-\alpha} < u_- + \epsilon\rho_-^{-\alpha}$, and $u_+ > u_- - \epsilon\rho_+^{-\alpha}$. From the above inequalities, we obtain $(u_+, \rho_+) \in \mathrm{IV}(u_-, \rho_-)$ when $\epsilon_2 < \epsilon < \epsilon_1$, and $(u_+, \rho_+) \in \mathrm{V}(u_-, \rho_-)$ when $0 < \epsilon < \epsilon_2$, where

$$\epsilon_1 = \frac{u_- - u_+}{\rho_+^{-\alpha} - \rho_-^{-\alpha}}, \qquad \epsilon_2 = (u_- - u_+)\,\rho_+^{\alpha}. \tag{66}$$

The results have been obtained. □

When $u_- > u_+$ and $\epsilon_2 < \epsilon < \epsilon_1$, the Riemann solution of (9) and (11) consists of a shock wave S and a contact discontinuity J with the intermediate state (u_*, ρ_*) besides the two constant states $(u_\pm, \rho_\pm)$, which is as this form:

$$(u^\epsilon, \rho^\epsilon) = \begin{cases} (u_-, \rho_-), & -\infty < \xi < \sigma_\epsilon, \\ (u_*, \rho_*), & \sigma_\epsilon < \xi < \tau_\epsilon, \\ (u_+, \rho_+), & \tau_\epsilon < \xi < +\infty, \end{cases} \tag{67}$$

where (u_*, ρ_*), τ_ϵ are determined by (38) and (63), respectively, and

$$\sigma_\epsilon = u_- + \frac{\epsilon\left(\rho_*^{1-\alpha} - \rho_-^{1-\alpha}\right)}{\rho_* - \rho_-}. \tag{68}$$

It is easy to see that

$$\epsilon\rho_*^{-\alpha} = u_+ - u_- + \epsilon\rho_+^{-\alpha}. \tag{69}$$

For given $\rho_+ > 0$, letting $\epsilon \to \epsilon_2 = (u_- - u_+)\rho_+^{\alpha}$ in (69) yields

$$\lim_{\epsilon\to\epsilon_2} \epsilon\rho_*^{-\alpha} = \lim_{\epsilon\to\epsilon_2} \left(u_+ - u_- + \epsilon\rho_+^{-\alpha}\right) = 0. \tag{70}$$

Hence, we deduce that

$$\lim_{\epsilon\to\epsilon_2} \rho_* = \infty. \tag{71}$$

Thus we have the following result.

Lemma 9. *Consider*

$$\lim_{\epsilon\to\epsilon_2} u_* = \lim_{\epsilon\to\epsilon_2} \sigma_\epsilon = \lim_{\epsilon\to\epsilon_2} \tau_\epsilon = u_-, \tag{72}$$

where $\sigma_\epsilon, \tau_\epsilon$ is given by (63) *and* (68), *and*

$$\lim_{\epsilon\to\epsilon_2} \int_{\tau_\epsilon t}^{\sigma_\epsilon t} \rho_* dx = \left(u_- [\rho] - [\rho(u - \epsilon p)]\right) t. \tag{73}$$

Proof. Due to (63) and (68), we get

$$\begin{aligned} \lim_{\epsilon\to\epsilon_2} \sigma_\epsilon &= \lim_{\epsilon\to\epsilon_2} \left(u_- + \frac{\epsilon\left(\rho_*^{1-\alpha} - \rho_-^{1-\alpha}\right)}{\rho_* - \rho_-}\right) = u_-, \\ \lim_{\epsilon\to\epsilon_2} \tau_\epsilon &= \lim_{\epsilon\to\epsilon_2} \left(u_+ + \epsilon\rho_+^{-\alpha}\right) = u_-. \end{aligned} \tag{74}$$

Thus it can be seen from (74) that shock wave S and contact discontinuity J will coalesce together when ϵ arrives at ϵ_2.

Using the Rankine-Hugoniot condition for shock S and contact discontinuity J, we have

$$\begin{aligned} \sigma_\epsilon (\rho_* - \rho_-) &= \rho_* \left(u_* + \epsilon\rho_*^{-\alpha}\right) - \rho_- \left(u_- + \epsilon\rho_-^{-\alpha}\right), \\ \tau_\epsilon (\rho_+ - \rho_*) &= \rho_+ \left(u_+ + \epsilon\rho_+^{-\alpha}\right) - \rho_* \left(u_* + \epsilon\rho_*^{-\alpha}\right), \end{aligned} \tag{75}$$

which implies that

$$\lim_{\epsilon\to\epsilon_2} (\sigma_\epsilon - \tau_\epsilon)\,\rho_* = \left(u_- [\rho] - [\rho(u - \epsilon p)]\right). \tag{76}$$

It is obvious that

$$\lim_{\epsilon\to\epsilon_2} \int_{\sigma_\epsilon t}^{\tau_\epsilon t} \rho_* dx = \lim_{\epsilon\to\epsilon_2} (\sigma_\epsilon - \tau_\epsilon)\,\rho_* t = \left(u_- [\rho] - [\rho(u - \epsilon p)]\right) t. \tag{77}$$

The proof is completed. □

From Lemma 5, it can be concluded that the shock wave S and contact discontinuity J will coincide when ϵ tends to ϵ_2. On the other hand, for $\rho_+ \neq \rho_-$, by substituting $\epsilon = \epsilon_2 = (u_- - u_+)\rho_+^{\alpha}$ into (45), we have

$$\begin{aligned} u_\delta &= u_-, \\ \omega(t) &= \left(u_\delta [\rho] - [\rho(u - \epsilon p)]\right) t. \end{aligned} \tag{78}$$

So, we obtain that the quantities u_δ, $\omega(t)$ and the limits of u_*, σ_ϵ and τ_ϵ are consistent with (45) as proposed for the Riemann solutions of (9) and (11) for $\rho_+ \neq \rho_-$ when we take $\epsilon = \epsilon_2$. Otherwise, the assert is obviously true when $\rho_+ = \rho_-$. Thus, it uniquely determines that the limit of the Riemann solutions to system (9) and (11) when $\epsilon \to \epsilon_2$ in the case $(u_+, \rho_+) \in \mathrm{IV}(u_-, \rho_-)$ is just the delta shock solution of (9) and (11) in the case $(u_+, \rho_+) \in S_\delta$, where the curve S_δ is actually the boundary between the regions $\mathrm{IV}(u_-, \rho_-)$ and $\mathrm{V}(u_-, \rho_-)$.

Theorem 10. *In the case $u_- > u_+$, for each fixed $\epsilon \in (\epsilon_2, \epsilon_1)$, assume that $(u^\epsilon, \rho^\epsilon)$ is a solution containing the shock wave S and contact discontinuity J of* (9) *and* (11) *with Riemann initial data, constructed in Section 3.2. Then, $(u^\epsilon, \rho^\epsilon)$ converges in the sense of distributions, when $\epsilon \to \epsilon_2$, and the limit functions ρ and ρu are the sum of step function and a δ-measure with weights*

$$\left(u_\delta [\rho] - [\rho(u - \epsilon p)]\right) t, \qquad \left(u_\delta [\rho u] - [\rho u(u - \epsilon p)]\right) t, \tag{79}$$

respectively, and then form a delta shock solutions of (9) *and* (11) *when $\epsilon \to \epsilon_2$.*

Proof. When $(u_+, \rho_+) \in \mathrm{IV}(u_-, \rho_-)$, let $\xi = x/t$; then for each fixed $\epsilon > 0$, the Riemann solutions are determined by

$$(u^\epsilon, \rho^\epsilon)(\xi) = \begin{cases} (u_-, \rho_-), & -\infty < \xi < \sigma_\epsilon, \\ (u_*^\epsilon, \rho_*^\epsilon), & \sigma_\epsilon < \xi < \tau_\epsilon, \\ (u_+, \rho_+), & \tau_\epsilon < \xi < \infty, \end{cases} \tag{80}$$

which satisfy

$$\begin{aligned}&\int_{-\infty}^{\infty}(\xi-(u^{\epsilon}(\xi)-\epsilon p(\rho^{\epsilon})))\rho^{\epsilon}(\xi)\phi'(\xi)\,d\xi\\&\quad+\int_{-\infty}^{\infty}\rho^{\epsilon}(\xi)\phi(\xi)\,d\xi=0,\\&\int_{-\infty}^{\infty}(\xi-(u^{\epsilon}(\xi)-\epsilon p(\rho^{\epsilon})))\rho^{\epsilon}(\xi)u^{\epsilon}(\xi)\phi'(\xi)\,d\xi\\&\quad+\int_{-\infty}^{\infty}\rho^{\epsilon}(\xi)u^{\epsilon}(\xi)\phi(\xi)\,d\xi=0,\end{aligned}\tag{81}$$

for any test function $\phi\in C_0^{\infty}(-\infty,\infty)$.

The first integral in (81) can be decomposed into

$$\left\{\int_{-\infty}^{\sigma_\epsilon}+\int_{\sigma_\epsilon}^{\tau_\epsilon}+\int_{\tau_\epsilon}^{\infty}\right\}(\xi-(u^{\epsilon}(\xi)-\epsilon p(\rho^{\epsilon})))\rho^{\epsilon}(\xi)\phi'(\xi)\,d\xi.\tag{82}$$

The sum of the first and the last terms in (82) is

$$\begin{aligned}&\int_{-\infty}^{\sigma_\epsilon}(\xi-(u_- -\epsilon p_-))\rho_-\phi'(\xi)\,d\xi\\&\quad+\int_{\tau_\epsilon}^{\infty}(\xi-(u_+ -\epsilon p_+))\rho_+\phi'(\xi)\,d\xi\\&=-\rho_-(u_- -\epsilon p_-)\phi(\sigma_\epsilon)+\rho_+(u_+ -\epsilon p_+)\phi(\tau_\epsilon)\\&\quad+\rho_-\sigma_\epsilon\phi(\sigma_\epsilon)-\rho_+\tau_\epsilon\phi(\tau_\epsilon)\\&\quad-\rho_-\int_{-\infty}^{\sigma_\epsilon}\phi(\xi)\,d\xi-\rho_+\int_{\tau_\epsilon}^{\infty}\phi(\xi)\,d\xi.\end{aligned}\tag{83}$$

Letting $\epsilon\to\epsilon_2$ in (83), we have

$$\begin{aligned}&\lim_{\epsilon\to\epsilon_2}\left(\int_{-\infty}^{\sigma_\epsilon}+\int_{\tau_\epsilon}^{\infty}\right)(\xi-(u^{\epsilon}(\xi)-\epsilon p(\rho^{\epsilon})))\rho^{\epsilon}(\xi)\phi'(\xi)\,d\xi\\&\quad=([\rho(u-\epsilon p)]-u_\delta[\rho])\phi(u_\delta)\\&\qquad-\int_{-\infty}^{\infty}\rho_0(\xi-u_\delta)\phi(\xi)\,d\xi,\end{aligned}\tag{84}$$

where $\rho_0(\xi)=\rho_-+[\rho]H(\xi-\sigma)$ and H is the Heaviside function.

The second term in (82) can be calculated by

$$\begin{aligned}&\int_{\sigma_\epsilon}^{\tau_\epsilon}(\xi-(u^{\epsilon}(\xi)-\epsilon p(\rho^{\epsilon})))\rho^{\epsilon}(\xi)\phi'(\xi)\,d\xi\\&\quad=-\rho_*^{\epsilon}(u_*^{\epsilon}-\epsilon p(\rho_*^{\epsilon}))(\phi(\sigma_\epsilon)-\phi(\tau_\epsilon))\\&\qquad-\rho_*^{\epsilon}\int_{\sigma_\epsilon}^{\tau_\epsilon}\phi\xi\,d\xi+\rho_*^{\epsilon}(\tau_\epsilon\phi\tau_\epsilon-\sigma_\epsilon\phi(\sigma_\epsilon)).\end{aligned}\tag{85}$$

By $\lim_{\epsilon\to\epsilon_2}u_*^{\epsilon}=\lim_{\epsilon\to\epsilon_2}\sigma_\epsilon=\lim_{\epsilon\to\epsilon_2}\tau_\epsilon=u_\delta=u_-$, we obtain

$$\lim_{\epsilon\to\epsilon_2}\int_{\sigma_\epsilon}^{\tau_\epsilon}(\xi-(u^{\epsilon}(\xi)-\epsilon p(\rho^{\epsilon})))\rho^{\epsilon}(\xi)\phi'(\xi)\,d\xi=0.\tag{86}$$

Then, from $(81)_1$, (84), and (86), we get that

$$\begin{aligned}&\lim_{\epsilon\to\epsilon_2}\int_{-\infty}^{\infty}(\rho^{\epsilon}(\xi)-\rho_0(\xi-u_\delta))\phi(\xi)\,d\xi\\&\quad=(u_\delta[\rho]-[\rho(u-\epsilon p)])\phi(u_\delta)\end{aligned}\tag{87}$$

holds for any test function $\phi\in C_0^{\infty}(-\infty,\infty)$.

With the same reason as above, we have

$$\begin{aligned}&\lim_{\epsilon\to\epsilon_2}\int_{-\infty}^{\infty}(\rho^{\epsilon}(\xi)u^{\epsilon}(\xi)-\rho_0u_0(\xi-u_\delta))\phi(\xi)\,d\xi\\&\quad=(u_\delta[\rho u]-[\rho u(u-\epsilon p)])\phi(u_\delta).\end{aligned}\tag{88}$$

Finally, we study the limits of ρ^{ϵ} and $\rho^{\epsilon}u^{\epsilon}$ as $\epsilon\to\epsilon_2$, by tracing the time-dependence of weights of the δ-measure.

Let $\varphi(x,t)\in C_0^{\infty}((-\infty,\infty)\times[0,\infty))$ and set $\widetilde{\varphi}(\xi,t):=\varphi(\xi t,t))$; then we obtain

$$\begin{aligned}&\lim_{\epsilon\to\epsilon_2}\int_0^{\infty}\int_{-\infty}^{\infty}\rho^{\epsilon}\left(\frac{x}{t}\right)\varphi(x,t)\,dx\,dt\\&\quad=\lim_{\epsilon\to\epsilon_2}\int_0^{\infty}t\left(\int_{-\infty}^{\infty}\rho^{\epsilon}(\xi)\widetilde{\varphi}(\xi,t)\,d\xi\right)dt.\end{aligned}\tag{89}$$

On the other hand,

$$\begin{aligned}&\lim_{\epsilon\to\epsilon_2}\int_{-\infty}^{\infty}\rho^{\epsilon}(\xi)\widetilde{\varphi}(\xi,t)\,d\xi\\&\quad=\int_{-\infty}^{\infty}\rho_0(\xi-u_\delta)\widetilde{\varphi}(\xi,t)\,d\xi\\&\qquad+(u_\delta[\rho]-[\rho(u-\epsilon p)])\widetilde{\varphi}(\xi,t)\\&\quad=t^{-1}\int_{-\infty}^{\infty}\rho_0(x-u_\delta t)\varphi(x,t)\,dx\\&\qquad+(u_\delta[\rho]-[\rho(u-\epsilon p)])\varphi(u_\delta t,t).\end{aligned}\tag{90}$$

By (89) and (90), we get

$$\begin{aligned}&\lim_{\epsilon\to\epsilon_2}\int_0^{\infty}\int_{-\infty}^{\infty}\rho^{\epsilon}\left(\frac{x}{t}\right)\varphi(x,t)\,dx\,dt\\&\quad=\int_0^{\infty}\int_{-\infty}^{\infty}\rho_0(x-u_\delta t)\varphi(x,t)\,dx\,dt\\&\qquad+\int_0^{\infty}t(u_\delta[\rho]-[\rho(u-\epsilon p)])\varphi(x,t)\,dt.\end{aligned}\tag{91}$$

With the same reason as before, we obtain

$$\begin{aligned}&\lim_{\epsilon\to\epsilon_2}\int_0^{\infty}\int_{-\infty}^{\infty}\rho^{\epsilon}\left(\frac{x}{t}\right)u^{\epsilon}\left(\frac{x}{t}\right)\varphi(x,t)\,dx\,dt\\&\quad=\int_0^{\infty}\int_{-\infty}^{\infty}\rho_0u_0(x-u_\delta t)\varphi(x,t)\,dx\,dt\\&\qquad+\int_0^{\infty}t(u_\delta[\rho u]-[\rho u(u-\epsilon p)])\varphi(x,t)\,dt.\end{aligned}\tag{92}$$

Thus the result has been obtained. □

When $u_- > u_+$ and $0 < \epsilon < \epsilon_2$, $(u_+, \rho_+) \in \mathrm{V}(u_-, \rho_-)$. So the Riemann solution of (9) and (11) consists of a delta shock wave besides the constant states $(u_\pm, \rho_\pm)$. We want to observe the behavior of strength and propagation speed of the delta shock wave when ϵ decreases and finally tends to zero.

For $\rho_+ \neq \rho_-$, letting $\epsilon \to 0$ in (45), we have

$$\begin{aligned} \lim_{\epsilon \to 0} u_\delta(\epsilon) &= \frac{\sqrt{\rho_+}u_+ + \sqrt{\rho_-}u_-}{\sqrt{\rho_+} + \sqrt{\rho_-}}, \\ \lim_{\epsilon \to 0} \omega(t, \epsilon) &= \sqrt{\rho_- \rho_+}\,(u_- - u_+)\,t. \end{aligned} \tag{93}$$

For the special situation $\rho_+ = \rho_-$, by (46), we can obtain the same result as above.

From the above discussion, we can conclude that the limit of the strength and propagation speed of the delta shock wave in Riemann solution of system (9) and (11) are in accordance with those of transport equations (8) with the same Riemann initial data. That is to say, the delta shock solution to system (9) and (11) converges to the delta shock solution to transport equations (8) as pressure vanishes.

Combining the results of the above, when $(u_+, \rho_+) \in \mathrm{IV}(u_-, \rho_-)$, we conclude that the shock wave and a contact discontinuity coincide as a delta shock wave when $\epsilon \to \epsilon_2$. As ϵ continues to drop and goes to zero eventually, the delta shock solution is nothing but the Riemann solution to transport equations (8).

5. Conclusion

So far, the discussion for limit of Riemann solutions to the nonsymmetric system of Keyfitz-Kranzer type with both the polytropic gas and generalized Chaplygin gas has been completed. From the above analysis, as the pressure vanishes, there appear delta shock wave, vacuum state, and contact discontinuity when $u_- > u_+$, $u_- < u_+$, and $u_- = u_+$, respectively. For the polytropic gas, different from cases of some other systems such as Euler equations or relativistic Euler equations, the delta shock wave is not the one of transport equations as parameter ϵ tends to zero. For the generalized Chaplygin gas, the delta shock wave appears as parameter ϵ tends to ϵ_2, depending only on the Riemann initial data. Then as ϵ becomes smaller and goes to zero at last, the delta shock wave solution is the exact one of transport equations.

Conflict of Interests

The authors declare that there is no conflict of interests regarding the publication of this paper.

Acknowledgment

This paper is supported by the National Natural Science Foundation of China (no. 11101348).

References

[1] B. L. Keyfitz and H. C. Kranzer, "A system of non-strictly hyperbolic conservation laws arising in elasticity theory," *Archive for Rational Mechanics and Analysis*, vol. 72, no. 3, pp. 219–241, 1980.

[2] A. Aw and M. Rascle, "Resurrection of "second order" models of traffic flow," *SIAM Journal on Applied Mathematics*, vol. 60, no. 3, pp. 916–938, 2000.

[3] F. Berthelin, P. Degond, M. Delitala, and M. Rascle, "A model for the formation and evolution of traffic jams," *Archive for Rational Mechanics and Analysis*, vol. 187, no. 2, pp. 185–220, 2008.

[4] C. Shen and M. Sun, "Formation of delta shocks and vacuum states in the vanishing pressure limit of Riemann solutions to the perturbed Aw-Rascle model," *Journal of Differential Equations*, vol. 249, no. 12, pp. 3024–3051, 2010.

[5] Y.-G. Lu, "Existence of global bounded weak solutions to nonsymmetric systems of Keyfitz-Kranzer type," *Journal of Functional Analysis*, vol. 261, no. 10, pp. 2797–2815, 2011.

[6] Y. G. Lu, "Existence of global entropy solutions to general system of Keyfitz-Kranzer type," *Journal of Functional Analysis*, vol. 264, pp. 2457–2468, 2013.

[7] H. J. Cheng, "Delta shock waves for a linearly degenerate hyperbolic system of conservation laws of Keyfitz-Kranzer type," *Advances in Mathematical Physics*, vol. 2013, Article ID 958120, 10 pages, 2013.

[8] J. Q. Li, "Note on the compressible euler equations with zero temperature," *Applied Mathematics Letters*, vol. 14, no. 4, pp. 519–523, 2001.

[9] G.-Q. Chen and H. Liu, "Formation of δ-shocks and vacuum states in the vanishing pressure limit of solutions to the euler equations for isentropic fluids," *SIAM Journal on Mathematical Analysis*, vol. 34, no. 4, pp. 925–938, 2003.

[10] G.-Q. Chen and H. Liu, "Concentration and cavitation in the vanishing pressure limit of solutions to the Euler equations for nonisentropic fluids," *Physica D: Nonlinear Phenomena*, vol. 189, no. 1-2, pp. 141–165, 2004.

[11] D. Mitrović and M. Nedeljkov, "Delta shock waves as a limit of shock waves," *Journal of Hyperbolic Differential Equations*, vol. 4, no. 4, pp. 629–653, 2007.

[12] C. Shen, "The limits of Riemann solutions to the isentropic magnetogasdynamics," *Applied Mathematics Letters*, vol. 24, no. 7, pp. 1124–1129, 2011.

[13] G. Yin and W. Sheng, "Delta shocks and vacuum states in vanishing pressure limits of solutions to the relativistic Euler equations for polytropic gases," *Journal of Mathematical Analysis and Applications*, vol. 355, no. 2, pp. 594–605, 2009.

[14] F. Bouchut, "On zero-pressure gas dynamics," in *Advance in Kinetic Theory and Computing*, vol. 22 of *Series on Advances in Mathematics*, pp. 171–190, World Scientific, River Edge, NJ, USA, 1994.

[15] E. Weinan, Y. G. Rykov, and Y. G. Sinai, "Generalized variational principles, global weak solutions and behavior with random initial data for systems of conservation laws arising in adhesion particle dynamics," *Communications in Mathematical Physics*, vol. 177, no. 2, pp. 349–380, 1996.

[16] S. F. Shandarin and Y. B. Zeldovich, "The large-scale structure of the universe: turbulence, intermittency, structures in a self-gravitating medium," *Reviews of Modern Physics*, vol. 61, no. 2, pp. 185–220, 1989.

[17] W. Sheng and T. Zhang, "The Riemann problem for the transportation equations in gas dynamics," *Memoirs of the American Mathematical Society*, vol. 137, no. 654, 1999.

[18] V. G. Danilov and V. M. Shelkovich, "Delta-shock wave type solution of hyperbolic systems of conservation laws," *Quarterly of Applied Mathematics*, vol. 63, no. 3, pp. 401–427, 2005.

[19] V. G. Danilov and V. M. Shelkovich, "Dynamics of propagation and interaction of δ-shock waves in conservation law systems," *Journal of Differential Equations*, vol. 211, no. 2, pp. 333–381, 2005.

[20] M. Nedeljkov, "Delta and singular delta locus for one-dimensional systems of conservation laws," *Mathematical Methods in the Applied Sciences*, vol. 27, no. 8, pp. 931–955, 2004.

[21] M. Nedeljkov and M. Oberguggenberger, "Interactions of delta shock waves in a strictly hyperbolic system of conservation laws," *Journal of Mathematical Analysis and Applications*, vol. 344, no. 2, pp. 1143–1157, 2008.

[22] V. M. Shelkovich, "δ- and δ'-Shock wave types of singular solutions of systems of conservation laws and transport and concentration processes," *Russian Mathematical Surveys*, vol. 63, no. 3, pp. 473–546, 2008.

[23] D. C. Tan, T. Zhang, T. Chang, and Y. X. Zheng, "Delta-shock waves as limits of vanishing ciscosity for hyperbolic systems of conservation laws," *Journal of Differential Equations*, vol. 112, no. 1, pp. 1–32, 1994.

[24] B. Temple, "System of conservation laws with invariant submanifolds," *Transactions of the American Mathematical Society*, vol. 280, pp. 781–795, 1983.

[25] E. Y. Panov and V. M. Shelkovich, "δ'-Shock waves as a new type of solutions to systems of conservation laws," *Journal of Differential Equations*, vol. 228, no. 1, pp. 49–86, 2006.

Hindawi Publishing Corporation
The Scientific World Journal
Volume 2014, Article ID 780269, 13 pages
http://dx.doi.org/10.1155/2014/780269

Research Article

Two Different Methods for Numerical Solution of the Modified Burgers' Equation

Seydi Battal Gazi Karakoç,[1] Ali Başhan,[2] and Turabi Geyikli[2]

[1] *Department of Mathematics, Faculty of Science and Art, Nevsehir Haci Bektas Veli University, 50300 Nevsehir, Turkey*
[2] *Department of Mathematics, Faculty of Science and Art, Inonu University, 44280 Malatya, Turkey*

Correspondence should be addressed to Seydi Battal Gazi Karakoç; sbgkarakoc@nevsehir.edu.tr

Received 23 January 2014; Accepted 23 February 2014; Published 3 April 2014

Academic Editors: D. Baleanu and H. Jafari

A numerical solution of the modified Burgers' equation (MBE) is obtained by using quartic B-spline subdomain finite element method (SFEM) over which the nonlinear term is locally linearized and using quartic B-spline differential quadrature (QBDQM) method. The accuracy and efficiency of the methods are discussed by computing L_2 and L_∞ error norms. Comparisons are made with those of some earlier papers. The obtained numerical results show that the methods are effective numerical schemes to solve the MBE. A linear stability analysis, based on the von Neumann scheme, shows the SFEM is unconditionally stable. A rate of convergence analysis is also given for the DQM.

1. Introduction

The one-dimensional Burgers' equation first suggested by Bateman [1] and later treated by Burgers' [2] has the form

$$U_t + UU_x - \nu U_{xx} = 0, \tag{1}$$

where ν is a positive parameter and the subscripts x and t denote space and time derivatives, respectively. Burgers' model of turbulence is very important in fluid dynamics model and study of this model and the theory of shock waves has been considered by many authors for both conceptual understanding of a class of physical flows and for testing various numerical methods [3]. Relationship between (1) and both turbulence theory and shock wave theory was presented by Cole [4]. He also obtained an exact solution of the equation. Analytical solutions of the equation were found for restricted values of ν which represent the kinematics viscosity of the fluid motion. So the numerical solution of Burgers' equation has been subject of many papers. Various numerical methods have been studied based on finite difference [5, 6], Runge-Kutta-Chebyshev method [7, 8], group-theoretic methods [9], and finite element methods including Galerkin, Petrov-Galerkin, least squares, and collocation [10–13].

The modified Burgers' equation (MBE) which we discuss in this paper is based upon Burgers' equation (BE) of the form

$$U_t + U^2U_x - \nu U_{xx} = 0. \tag{2}$$

The equation has the strong nonlinear aspects and has been used in many practical transport problems, for instance, nonlinear waves in a medium with low-frequency pumping or absorption, turbulence transport, wave processes in thermoelastic medium, transport and dispersion of pollutants in rivers and sediment transport, and ion reflection at quasi-perpendicular shocks. Recently, some numerical studies of the equation have been presented: Ramadan and El-Danaf [14] obtained the numerical solutions of the MBE using quintic B-spline collocation finite element method. A special lattice Boltzmann model is developed by Duan et al. [15]. Dağ et al. [16] have developed a Galerkin finite element solution of the equation using quintic B-splines and time-split technique. A solution based on sextic B-spline collocation method is proposed by Irk [17]. Roshan and Bhamra [18] applied a Petrov-Galerkin method using a linear hat function as the trial function and a cubic B-spline function as the test function. A discontinuous Galerkin method is presented by Zhang et al. [19]. Bratsos [20] has used a finite difference scheme based on fourth-order rational approximants to the matrix-exponential term in a two-time level recurrence relation for calculating the numerical solution of the equation.

Recently, DQM has become a very efficient and effective method to obtain the numerical solutions of various types of partial differential equations. In 1972, Bellman et al. [21] first introduced differential quadrature method (DQM) for solving partial differential equations. The main idea behind the method is to find out the weighting coefficients of the functional values at nodal points by using base functions of which derivatives are already known at the same nodal points over the entire region. Various researchers have developed different types of DQMs by utilizing various test functions; Bellman et al. [22] have used Legendre polynomials and spline functions in order to get weighting coefficients. Quan and Chang [23, 24] have presented an explicit formulation for determining the weighting coefficients using Lagrange interpolation polynomials. Zhong [25], Guo and Zhong [26], and Zhong and Lan [27] have introduced another efficient DQM as spline based DQM and applied it to different problems. Shu and Wu [28] have considered some of the implicit formulations of weighting coefficients with the help of radial basis functions. Nonlinear Burgers' equation is solved using polynomial based differential quadrature method by Korkmaz and Dağ [29]. The DQM has many advantages over the classical techniques; mainly, it prevents linearization and perturbation in order to find better solutions of given nonlinear equations. Since QBDQM do not need transforming for solving the equation, the method has been preferred.

In the present work, we have applied a subdomain finite element method and a quartic B-spline differential quadrature method to the MBE. To show the performance and accuracy of the methods and make comparisons of numerical solutions, we have taken different values of v.

2. Numerical Methods

To implement the numerical schemes, the interval $[a,b]$ is splitted up into uniformly sized intervals by the nodes x_m, $m = 1,2,\dots,N$, such that $a = x_0 < x_1 \cdots < x_N = b$, where $h = (x_{m+1} - x_m)$.

2.1. Subdomain Finite Element Method (SFEM). We will consider (2) with the boundary conditions chosen from

$$\begin{aligned} U(a,t) &= \beta_1, \qquad U(b,t) = \beta_2, \\ U_x(a,t) &= 0, \qquad U_x(b,t) = 0, \\ U_{xx}(a,t) &= 0, \qquad U_{xx}(b,t) = 0, \quad t > 0, \end{aligned} \tag{3}$$

with the initial condition

$$U(x,0) = f(x), \quad a \le x \le b, \tag{4}$$

where β_1 and β_2 are constants. The quartic B-splines $\phi_m(x)$ $(m = -2(1)\ N+1)$ at the knots x_m which form a basis over the interval $[a,b]$ are defined by the relationships [30]

$$\phi_m(x) = \frac{1}{h^4}\begin{cases} (x-x_{m-2})^4, & x \in [x_{m-2}, x_{m-1}], \\ (x-x_{m-2})^4 - 5(x-x_{m-1})^4, & x \in [x_{m-1}, x_m], \\ (x-x_{m-2})^4 - 5(x-x_{m-1})^4 + 10(x-x_m)^4, & x \in [x_m, x_{m+1}], \\ (x_{m+3}-x)^4 - 5(x_{m+2}-x)^4, & x \in [x_{m+1}, x_{m+2}], \\ (x_{m+3}-x)^4, & x \in [x_{m+2}, x_{m+3}], \\ 0, & \text{otherwise}. \end{cases} \tag{5}$$

Our numerical treatment for solving the MBE using the subdomain finite element method with quartic B-splines is to find a global approximation $U_N(x,t)$ to the exact solution $U(x,t)$ that can be expressed in the following form:

$$U_N(x,t) = \sum_{j=-2}^{N+1} \delta_j(t)\,\phi_j(x), \tag{6}$$

where δ_j are time-dependent parameters to be determined from both boundary and weighted residual conditions. The nodal values U_m, U'_m, U''_m, and U'''_m at the knots x_m can be obtained from (5) and (6) in the following form:

$$\begin{aligned} U_m &= U(x_m) = \delta_{m-2} + 11\delta_{m-1} + 11\delta_m + \delta_{m+1}, \\ U'_m &= U'(x_m) = \frac{4}{h}(-\delta_{m-2} - 3\delta_{m-1} + 3\delta_m + \delta_{m+1}), \\ U''_m &= U''(x_m) = \frac{12}{h^2}(\delta_{m-2} - \delta_{m-1} - \delta_m + \delta_{m+1}), \\ U'''_m &= U'''(x_m) = \frac{24}{h^3}(-\delta_{m-2} + 3\delta_{m-1} - 3\delta_m + \delta_{m+1}). \end{aligned} \tag{7}$$

For each element, using the local coordinate transformation

$$h\xi = x - x_m, \quad 0 \le \xi \le 1, \tag{8}$$

a typical finite interval $[x_m, x_{m+1}]$ is mapped into the interval $[0,1]$. Therefore, the quartic B-spline shape functions over the element $[0,1]$ can be defined as

$$\phi^e = \begin{cases} \phi_{m-2} = 1 - 4\xi + 6\xi^2 - 4\xi^3 + \xi^4, \\ \phi_{m-1} = 11 - 12\xi - 6\xi^2 + 12\xi^3 - \xi^4, \\ \phi_m = 11 + 12\xi - 6\xi^2 - 12\xi^3 + \xi^4, \\ \phi_{m+1} = 1 + 4\xi + 6\xi^2 + 4\xi^3 - \xi^4, \\ \phi_{m+2} = \xi^4. \end{cases} \tag{9}$$

All other splines, apart from $\phi_{m-2}(x)$, $\phi_{m-1}(x)$, $\phi_m(x)$, $\phi_{m+1}(x)$, and $\phi_{m+2}(x)$, are zero over the element $[0,1]$. So, the approximation equation (6) over this element can be written in terms of basis functions given in (9) as

$$U_N(\xi,t)=\sum_{j=m-2}^{m+2}\delta_j(t)\,\phi_j(\xi), \tag{10}$$

where δ_{m-2}, δ_{m-1}, δ_m, δ_{m+1}, and δ_{m+2} act as element parameters and B-splines $\phi_{m-2}(x)$, ϕ_{m-1}, ϕ_m, ϕ_{m+1}, and ϕ_{m+2} as element shape functions. Applying the subdomain approach to (33) with the weight function

$$W_m(x)=\begin{cases}1, & x\in[x_m,x_{m+1}],\\ 0, & \text{otherwise}\end{cases} \tag{11}$$

we obtain the weak form of (2)

$$\int_{x_m}^{x_{m+1}} 1.\left(U_t+U^2U_x-vU_{xx}\right)dx=0. \tag{12}$$

Using the transformation (8) into the weak form (12) and then integrating (12) term by term with some manipulation by parts result in

$$\begin{aligned}&\frac{h}{5}\left(\dot\delta_{m-2}+26\dot\delta_{m-1}+66\dot\delta_m+26\dot\delta_{m+1}+\dot\delta_{m+2}\right)\\&\quad+Z_m\left(-\delta_{m-2}-10\delta_{m-1}+10\delta_{m+1}+\delta_{m+2}\right)\\&\quad-\frac{4v}{h}\left(\delta_{m-2}+2\delta_{m-1}-6\delta_m+2\delta_{m+1}+\delta_{m+2}\right)=0,\end{aligned} \tag{13}$$

where the dot denotes differentiation with respect to t, and

$$Z_m=\left(\delta_{m-2}+11\delta_{m-1}+11\delta_m+\delta_{m+1}\right)^2. \tag{14}$$

In (13) using the Crank-Nicolson formula and its time derivative that is discretized by the forward difference approach, respectively,

$$\delta_m=\frac{\delta_m^n+\delta_m^{n+1}}{2},\qquad \dot\delta_m=\frac{\delta_m^{n+1}-\delta_m^n}{\Delta t} \tag{15}$$

we obtain a recurrence relationship between the two time levels n and $n+1$ relating two unknown parameters δ_i^{n+1} and δ_i^n, for $i=m-2,m-1,\ldots,m+2$,

$$\begin{aligned}&\alpha_{m1}\delta_{m-2}^{n+1}+\alpha_{m2}\delta_{m-1}^{n+1}+\alpha_{m3}\delta_m^{n+1}+\alpha_{m4}\delta_{m+1}^{n+1}\\&\quad+\alpha_{m5}\delta_{m+2}^{n+1}\\&\quad=\alpha_{m6}\delta_{m-2}^n+\alpha_{m7}\delta_{m-1}^n+\alpha_{m8}\delta_m^n+\alpha_{m9}\delta_{m+1}^n\\&\quad+\alpha_{m10}\delta_{m+2}^n,\\&\qquad m=0,1,\ldots,N-1,\end{aligned} \tag{16}$$

where

$$\begin{gathered}\alpha_{m1}=1-EZ_m-M,\qquad \alpha_{m2}=26-10EZ_m-2M,\\ \alpha_{m3}=66+6M,\qquad \alpha_{m4}=26+10EZ_m-2M,\\ \alpha_{m5}=1+EZ_m-M,\qquad \alpha_{m6}=1+EZ_m+M,\\ \alpha_{m7}=26+10EZ_m+2M,\qquad \alpha_{m8}=66-6M,\\ \alpha_{m9}=26-10EZ_m+2M,\qquad \alpha_{m10}=1-EZ_m+M,\\ E=\frac{5\Delta t}{2h},\qquad M=\frac{20v\Delta t}{2h^2}.\end{gathered} \tag{17}$$

Obviously, the system (16) consists of N equations in the $N+4$ unknowns $(\delta_{-2},\delta_{-1},\ldots,\delta_{N+1})$. To get a unique solution of the system, we need four additional constraints. These are obtained from the boundary conditions (3) and can be used to eliminate δ_{-2}, δ_{-1}, δ_N, and δ_{N+1} from the system (16) which then becomes a matrix equation for the N unknowns $d=(\delta_0,\delta_1,\ldots,\delta_{N-1})$ of the form

$$Ad^{n+1}=Bd^n. \tag{18}$$

A lumped value of Z_m is obtained from $(U_m+U_{m+1})^2/4$ as

$$Z_m=\frac{1}{4}\left(\delta_{m-2}+12\delta_{m-1}+22\delta_m+12\delta_{m+1}+\delta_{m+2}\right)^2. \tag{19}$$

The resulting system can be solved with a variant of Thomas algorithm and we need an inner iteration $(\delta^*)^{n+1}=\delta^n+(1/2)(\delta^{n+1}-\delta^n)$ at each time step to cope with the nonlinear term Z_m. A typical member of the matrix system (16) is rewritten in terms of the nodal parameters δ_m^n as

$$\begin{aligned}&\gamma_1\delta_{m-2}^{n+1}+\gamma_2\delta_{m-1}^{n+1}+\gamma_3\delta_m^{n+1}+\gamma_4\delta_{m+1}^{n+1}+\gamma_5\delta_{m+2}^{n+1}\\&\quad=\gamma_6\delta_{m-2}^n+\gamma_7\delta_{m-1}^n+\gamma_8\delta_m^n+\gamma_9\delta_{m+1}^n+\gamma_{10}\delta_{m+2}^n,\end{aligned} \tag{20}$$

where

$$\begin{gathered}\gamma_1=\alpha-\beta-\lambda,\qquad \gamma_2=26\alpha-10\beta-2\lambda,\\ \gamma_3=66\alpha+6\lambda,\qquad \gamma_4=26\alpha+10\beta-2\lambda,\\ \gamma_5=\alpha+\beta-\lambda,\qquad \gamma_6=\alpha+\beta+\lambda,\\ \gamma_7=26\alpha+10\beta+2\lambda,\qquad \gamma_8=66\alpha-6\lambda,\\ \gamma_9=26\alpha-10\beta+2\lambda,\qquad \gamma_{10}=\alpha-\beta+\lambda,\\ \alpha=1,\quad \beta=EZ_m,\quad \lambda=M.\end{gathered} \tag{21}$$

Before the solution process begins iteratively, the initial vector $\delta^0 = (\delta_0, \delta_1, \ldots, \delta_{N-1})$ must be determined by means of the following requirements:

$$\begin{gathered}
U'(a,0) = \frac{4}{h}\left(-\delta_{-2}^0 - 3\delta_{-1}^0 + 3\delta_0^0 + \delta_1^0\right) = 0,\\
U''(a,0) = \frac{12}{h^2}\left(\delta_{-2}^0 - \delta_{-1}^0 - \delta_0^0 + \delta_1^0\right) = 0,\\
U(x_m,0) = \delta_{m-2}^0 + 11\delta_{m-1}^0 + 11\delta_m^0 + \delta_{m+1}^0 = f(x),\\
m = 0,1,\ldots,N-1,\\
U'(b,0) = \frac{4}{h}\left(-\delta_{N-2}^0 - 3\delta_{N-1}^0 + 3\delta_N^0 + \delta_{N+1}^0\right) = 0,\\
U''(b,0) = \frac{12}{h^2}\left(\delta_{N-2}^0 - \delta_{N-1}^0 - \delta_N^0 + \delta_{N+1}^0\right) = 0.
\end{gathered} \tag{22}$$

If we eliminate the parameters δ_{-2}^0, δ_{-1}^0, δ_N^0, and δ_{N+1}^0 from the system (16), we obtain $N \times N$ matrix system of the following form:

$$A\delta^0 = B, \tag{23}$$

where A is

$$A = \begin{bmatrix} 18 & 6 & & & & & & \\ 11.5 & 11.5 & 1 & & & & & \\ 1 & 11 & 11 & 1 & & & & \\ & & & & 1 & 11 & 11 & 1 \\ & & & & & 2 & 14 & 8 \end{bmatrix}, \tag{24}$$

$\delta^0 = [\delta_0^0, \delta_1^0, \ldots, \delta_{N-1}^0]^T$, and $B = [U(x_0,0), U(x_1,0), \ldots, U(x_{N-1},0)]^T$. This system is solved by using a variant of Thomas algorithm.

2.2. Linear Stability Analysis. We have investigated stability of the scheme by using the von Neumann method. In order to apply the stability analysis, the MBE needs to be linearized by assuming that the quantity U in the nonlinear term U^2U_x is locally constant. The growth factor of a typical Fourier mode is defined as

$$\delta_j^n = \xi^n e^{ijkh}, \tag{25}$$

where k is mode number and h is the element size. Substituting (37) into the scheme (20), we have

$$g = \frac{A_1 + ib}{A_2 - ib}, \tag{26}$$

where

$$\begin{gathered}
A_1 = (\alpha - \lambda)\cos(2kh) + (26\alpha - 2\lambda)\cos(kh) + 66 + 6\lambda,\\
A_2 = (\alpha + \lambda)\cos(2kh) + (26\alpha + 2\lambda)\cos(kh) + 66 - 6\lambda,\\
b = \sin(2kh) + 10\sin(kh).
\end{gathered} \tag{27}$$

We can see that $A_1^2 < A_2^2$ and taking the modulus of (38) gives $|g| \le 1$, so we find that the scheme (20) is unconditionally stable.

2.3. Quartic B-Spline Differential Quadrature Method (QBDQM). DQM can be defined as an approximation to a derivative of a given function by using the linear summation of its values at specific discrete nodal points over the solution domain of a problem. Provided that any given function $U(x)$ is enough smooth over the solution domain, its derivatives with respect to x at a nodal point x_i can be approximated by a linear summation of all the functional values in the solution domain, namely,

$$\begin{gathered}
U_x^{(r)}(x_i) = \frac{dU^{(r)}}{dx^{(r)}}\Big|_{x_i} = \sum_{j=1}^{N} w_{ij}^{(r)} U(x_j),\\
i = 1,2,\ldots,N, \quad r = 1,2,\ldots,N-1,
\end{gathered} \tag{28}$$

where r denotes the order of the derivative, $w_{ij}^{(r)}$ represent the weighting coefficients of the rth order derivative approximation, and N denotes the number of nodal points in the solution domain. Here, the index j represents the fact that $w_{ij}^{(r)}$ is the corresponding weighting coefficient of the functional value $U(x_j)$. We need first- and second-order derivative of the function $U(x)$. So, we will find value of (28) for the $r = 1, 2$. If we consider (28), then it is seen that the fundamental process for approximating the derivatives of any given function through DQM is to find out the corresponding weighting coefficients $w_{ij}^{(r)}$. The main idea of the DQM approximation is to find out the corresponding weighting coefficients $w_{ij}^{(r)}$ by means of a set of base functions spanning the problem domain. While determining the corresponding weighting coefficients different basis may be used. Using the quartic B-splines as test functions in the fundamental DQM equation (28) leads to the equation

$$\begin{gathered}
\frac{d^{(r)}Q_m(x_i)}{dx^{(r)}} = \sum_{j=m-1}^{m+2} w_{i,j}^{(r)} Q_m(x_j),\\
m = -1,0,\ldots,N+2, \quad i = 1,2,\ldots,N.
\end{gathered} \tag{29}$$

2.4. First-Order Derivative Approximation. When DQM methodology is applied, the fundamental equality for determining the corresponding weighting coefficients of the first-order derivative approximation is obtained as Korkmaz used [31]

$$\begin{gathered}
\frac{dQ_m(x_i)}{dx} = \sum_{j=m-1}^{m+2} w_{i,j}^{(1)} Q_m(x_j),\\
m = -1,0,\ldots,N+1, \quad i = 1,2,\ldots,N.
\end{gathered} \tag{30}$$

In this process, the initial step for finding out the corresponding weighting coefficients $w_{i,j}^{(1)}$, $j = -2,-1,\ldots,N+3$, of the first nodal point x_1 is to apply the test functions Q_m, $m = -1,0,\ldots,N+1$, at the nodal point x_1. After all the Q_m test functions are applied, we get the following system of algebraic equation system:

$$\begin{bmatrix} 1 & 11 & 11 & 1 & & & & \\ & 1 & 11 & 11 & 1 & & & \\ & & \ddots & \ddots & \ddots & \ddots & & \\ & & & & & & & \\ & & & 1 & 11 & 11 & 1 & \\ & & & & 1 & 11 & 11 & 1 \end{bmatrix} \begin{bmatrix} w_{1,-2}^{(1)} \\ w_{1,-1}^{(1)} \\ w_{1,0}^{(1)} \\ w_{1,1}^{(1)} \\ w_{1,2}^{(1)} \\ \vdots \\ w_{1,N+2}^{(1)} \\ w_{1,N+3}^{(1)} \end{bmatrix} = \begin{bmatrix} -\frac{4}{h} \\ -\frac{12}{h} \\ \frac{12}{h} \\ \frac{4}{h} \\ 0 \\ \vdots \\ 0 \\ 0 \end{bmatrix}. \tag{31}$$

The weighting coefficients $w_{1,j}^{(1)}$ related to the first grid point are determined by solving the system (31). This system consists of $N+6$ unknowns and $N+3$ equations. To have a unique solution, it is required to add three additional equations to the system. These are

$$\begin{aligned} \frac{d^{(2)}Q_{-1}(x_1)}{dx^{(2)}} &= \sum_{j=-2}^{1} w_{1,j}^{(1)} Q'_{-1}(x_j), \\ \frac{d^{(2)}Q_{N+1}(x_1)}{dx^{(2)}} &= \sum_{j=N}^{N+3} w_{1,j}^{(1)} Q'_{N+1}(x_j), \\ \frac{d^{(3)}Q_{N+1}(x_1)}{\partial x^{(3)}} &= \sum_{j=N}^{N+3} w_{1,j}^{(1)} Q''_{N+1}(x_j). \end{aligned} \tag{32}$$

By using these equations which we obtained by derivations, three unknown terms will be eliminated from the system. Consider

$$\begin{bmatrix} 8 & 14 & 2 & & & & \\ 1 & 11 & 11 & 1 & & & \\ & \ddots & \ddots & \ddots & \ddots & & \\ & & & & & & \\ & & & 1 & 11 & 11 & 1 \\ & & & & 2 & 23 & 23 \\ & & & & & 6 & 18 \end{bmatrix} \begin{bmatrix} w_{1,-1}^{(1)} \\ w_{1,0}^{(1)} \\ w_{1,1}^{(1)} \\ w_{1,2}^{(1)} \\ w_{1,3}^{(1)} \\ \vdots \\ w_{1,N}^{(1)} \\ w_{1,N+1}^{(1)} \end{bmatrix} = \begin{bmatrix} -\frac{7}{h} \\ -\frac{12}{h} \\ \frac{12}{h} \\ \frac{4}{h} \\ 0 \\ \vdots \\ 0 \\ 0 \end{bmatrix}. \tag{33}$$

To determine the weighting coefficients, $w_{k,j}^{(1)}$, $j = -1, 0, \ldots, N+1$, at grid points x_k, $2 \le k \le N-1$, we got the following algebraic equation system:

$$\begin{bmatrix} 8 & 14 & 2 & & & & \\ 1 & 11 & 11 & 1 & & & \\ & \ddots & \ddots & \ddots & \ddots & & \\ & & & & & & \\ & & & 1 & 11 & 11 & 1 \\ & & & & 2 & 23 & 23 \\ & & & & & 6 & 18 \end{bmatrix} \begin{bmatrix} w_{k,-1}^{(1)} \\ \vdots \\ w_{k,k-3}^{(1)} \\ w_{k,k-2}^{(1)} \\ w_{k,k-1}^{(1)} \\ w_{k,k}^{(1)} \\ w_{k,k+1}^{(1)} \\ w_{k,k+2}^{(1)} \\ \vdots \\ w_{k,N+1}^{(1)} \end{bmatrix}$$

$$= \begin{bmatrix} 0 \\ \vdots \\ 0 \\ \dfrac{-4}{h} \\ \dfrac{-12}{h} \\ \dfrac{12}{h} \\ \dfrac{4}{h} \\ 0 \\ \vdots \\ 0 \end{bmatrix}. \tag{34}$$

For the last grid point of the domain x_N, determine weighting coefficients, $w_{N,j}^{(1)}$, $j = -1, 0, \ldots, N+1$, we got the following algebraic equation system:

$$\begin{bmatrix} 8 & 14 & 2 & & & & & \\ 1 & 11 & 11 & 1 & & & & \\ & \ddots & \ddots & \ddots & \ddots & & & \\ & & & & 1 & 11 & 11 & 1 \\ & & & & & 2 & 23 & 23 \\ & & & & & & 6 & 18 \end{bmatrix} \begin{bmatrix} w_{N,-1}^{(1)} \\ w_{N,0}^{(1)} \\ \vdots \\ w_{N,N-3}^{(1)} \\ w_{N,N-2}^{(1)} \\ w_{N,N-1}^{(1)} \\ w_{N,N}^{(1)} \\ w_{N,N+1}^{(1)} \end{bmatrix} = \begin{bmatrix} 0 \\ 0 \\ \vdots \\ 0 \\ \dfrac{-4}{h} \\ \dfrac{-12}{h} \\ \dfrac{53}{2h} \\ \dfrac{17}{h} \end{bmatrix}. \tag{35}$$

2.5. Second-Order Derivative Approximation

2.5. Second-Order Derivative Approximation. The general form of DQM approximation to the problem on the solution domain is

$$\frac{d^2 Q_m}{dx^2}(x_i) = \sum_{j=m-1}^{m+2} w_{i,j}^{(2)} Q_m(x_j), \qquad m = -1, 0, \ldots, N+1, \quad i = 1, 2, \ldots, N, \tag{36}$$

Table 1: L_2 and L_∞ error norms for $h = 0.005$, $\Delta t = 0.01$, and $\nu = 0.001$ (SFEM).

Time	$L_2 \times 10^3$	$L_\infty \times 10^3$
2	0.0054945	0.0282049
3	0.0082404	0.0422421
4	0.0109858	0.0562280
5	0.0137296	0.0701566
6	0.0164729	0.0840427
7	0.0192154	0.0978975
8	0.0219573	0.1116934
9	0.0246985	0.1254466
10	0.0274379	0.1391304

where $w_{i,j}^{(2)}$ represents the corresponding weighting coefficients of the second-order derivative approximations. Similarly, for finding out the weighting coefficients of the first grid point x_1 all test functions Q_m, $m = -1, 0, \ldots, N+1$, are used and the following algebraic equations system is obtained:

$$\begin{bmatrix} 1 & 11 & 11 & 1 & & & & & \\ & 1 & 11 & 11 & 1 & & & & \\ & & \ddots & \ddots & \ddots & \ddots & & & \\ & & & & 1 & 11 & 11 & 1 & \\ & & & & & 1 & 11 & 11 & 1 \end{bmatrix} \begin{bmatrix} w_{1,-2}^{(2)} \\ w_{1,-1}^{(2)} \\ w_{1,0}^{(2)} \\ w_{1,1}^{(2)} \\ w_{1,2}^{(2)} \\ \vdots \\ w_{1,N+2}^{(2)} \\ w_{1,N+3}^{(2)} \end{bmatrix} = \begin{bmatrix} \dfrac{12}{h^2} \\ -\dfrac{12}{h^2} \\ -\dfrac{12}{h^2} \\ \dfrac{12}{h^2} \\ 0 \\ \vdots \\ 0 \\ 0 \end{bmatrix}. \tag{37}$$

Here, the system (37) consists of $N+6$ unknowns and $N+3$ equations. To have a unique solution, it is required to add new equations to the system. These are

$$\frac{d^3 Q_{-1}(x_1)}{dx^3} = \sum_{j=-2}^{1} w_{1,j}^{(1)} Q'_{-1}(x_j), \tag{38}$$

$$\frac{d^3 Q_{N+1}(x_1)}{dx^3} = \sum_{j=N}^{N+3} w_{1,j}^{(1)} Q'_{N+1}(x_j). \qquad (39)$$

If we used (38) and (39) we obtain the following equations system:

$$\begin{bmatrix} 8 & 14 & 2 & & & & & \\ 1 & 11 & 11 & 1 & & & & \\ & \ddots & \ddots & \ddots & \ddots & & & \\ & & & & & & & \\ & & & & 1 & 11 & 11 & 1 \\ & & & & & 2 & 14 & 8 \end{bmatrix} \begin{bmatrix} w_{1,-1}^{(2)} \\ w_{1,0}^{(2)} \\ w_{1,1}^{(2)} \\ w_{1,2}^{(2)} \\ w_{1,3}^{(2)} \\ \vdots \\ w_{1,N+1}^{(2)} \\ w_{1,N+2}^{(2)} \end{bmatrix} = \begin{bmatrix} \frac{18}{h^2} \\ -\frac{12}{h^2} \\ -\frac{12}{h^2} \\ \frac{12}{h^2} \\ 0 \\ \vdots \\ 0 \\ 0 \end{bmatrix}. \qquad (40)$$

Quartic B-splines have not got fourth-order derivations at the grid points so we cannot eliminate the unknown term $w_{1,N+2}^{(2)}$ by the one more derivation of (39). We will use first-order weighting coefficients instead of second-order weighting coefficients which are introduced by Shu [32]

$$w_{i,j}^{(2)} = 2w_{i,j}^{(1)} \left(w_{i,i}^{(1)} - \frac{1}{x_i - x_j} \right), \quad i \neq j. \qquad (41)$$

After we use (41),

$$A_1 = w_{1,N+2}^{(2)} = 2w_{1,N+2}^{(1)} \left(w_{1,1}^{(1)} - \frac{1}{x_1 - x_{N+2}} \right),$$

$$\begin{bmatrix} 8 & 14 & 2 & & & \\ 1 & 11 & 11 & 1 & & \\ & \ddots & \ddots & \ddots & \ddots & \\ & & & & & \\ & & & 1 & 11 & 11 \\ & & & & 2 & 14 \end{bmatrix} \begin{bmatrix} w_{1,-1}^{(2)} \\ w_{1,0}^{(2)} \\ w_{1,1}^{(2)} \\ w_{1,2}^{(2)} \\ w_{1,3}^{(2)} \\ \vdots \\ w_{1,N}^{(2)} \\ w_{1,N+1}^{(2)} \end{bmatrix} = \begin{bmatrix} \frac{18}{h^2} \\ -\frac{12}{h^2} \\ -\frac{12}{h^2} \\ \frac{12}{h^2} \\ 0 \\ \vdots \\ -A_1 \\ -8A_1 \end{bmatrix} \qquad (42)$$

system (42) is obtained. To determine the weighting coefficients $w_{k,j}^{(2)}$, $j = -1, 0, \ldots, N+1$, at grid points x_k, $2 \leq k \leq N-1$, we got the following algebraic system:

$$\begin{bmatrix} 8 & 14 & 2 & & & \\ 1 & 11 & 11 & 1 & & \\ & \ddots & \ddots & \ddots & \ddots & \\ & & & & & \\ & & & 1 & 11 & 11 \\ & & & & 2 & 14 \end{bmatrix} \begin{bmatrix} w_{k,-1}^{(2)} \\ \vdots \\ w_{k,k-3}^{(2)} \\ w_{k,k-2}^{(2)} \\ w_{k,k-1}^{(2)} \\ w_{k,k}^{(2)} \\ w_{k,k+1}^{(2)} \\ w_{k,k+2}^{(2)} \\ \vdots \\ w_{k,N-1}^{(2)} \\ w_{k,N}^{(2)} \\ w_{k,N+1}^{(2)} \end{bmatrix}$$

Table 2: L_2 and L_∞ error norms for $h = 0.005$, $\Delta t = 0.001$, and $\nu = 0.005$ (SFEM).

Time	$L_2 \times 10^3$	$L_\infty \times 10^3$
2	0.0246966	0.0845689
3	0.0370384	0.1266222
4	0.0493707	0.1684362
5	0.0616997	0.2101319
6	0.0740253	0.2516392
7	0.0863444	0.2930178
8	0.0986573	0.3341922
9	0.1109636	0.3752457
10	0.1232629	0.4160477

Table 3: L_2 and L_∞ error norms for $h = 0.005$, $\Delta t = 0.01$, and $\nu = 0.01$ (SFEM).

Time	$L_2 \times 10^3$	$L_\infty \times 10^3$
2	0.0978574	0.2806243
3	0.1467089	0.4185981
4	0.1955072	0.5550286
5	0.2442506	0.6898713
6	0.2929396	0.8238629
7	0.3415703	0.9566688
8	0.3901436	1.0881289
9	0.4386580	1.2182231
10	0.4871136	1.3469237

$$= \begin{bmatrix} 0 \\ \vdots \\ \dfrac{12}{h^2} \\ -\dfrac{12}{h^2} \\ -\dfrac{12}{h^2} \\ \dfrac{12}{h^2} \\ 0 \\ \vdots \\ 0 \\ -A_k \\ -8A_k \end{bmatrix}, \tag{43}$$

where A_k equals $A_k = w_{k,N+2}^{(2)} = 2w_{k,N+2}^{(1)}(w_{k,k}^{(1)} - 1/(x_k - x_{N+2}))$.

For the last grid point of the domain x_N with the same idea, determine weighting coefficients $w_{N,j}^{(2)}$, $j = -1, 0, \ldots, N+1$, we got the following algebraic equation system:

Table 4: L_2 and L_∞ error norms for $h = 0.02$, $\Delta t = 0.01$, and $\nu = 0.01$ (SFEM).

Time	$L_2 \times 10^3$	$L_\infty \times 10^3$
2	0.0973818	0.2802526
3	0.1460008	0.4184872
4	0.1945704	0.5554121
5	0.2430873	0.6910062
6	0.2915506	0.8252312
7	0.3399602	0.9580433
8	0.3883156	1.0894413
9	0.4366131	1.2194111
10	0.4848547	1.3479880

$$\begin{bmatrix} 8 & 14 & 2 & & & & \\ 1 & 11 & 11 & 1 & & & \\ & \ddots & \ddots & \ddots & \ddots & & \\ & & & & & & \\ & & & & 1 & 11 & 11 \\ & & & & & 2 & 14 \end{bmatrix} \begin{bmatrix} w_{N,-1}^{(2)} \\ w_{N,0}^{(2)} \\ \vdots \\ w_{N,N-3}^{(2)} \\ w_{N,N-2}^{(2)} \\ w_{N,N-1}^{(2)} \\ w_{N,N}^{(2)} \\ w_{N,N+1}^{(2)} \end{bmatrix} = \begin{bmatrix} 0 \\ 0 \\ \vdots \\ 0 \\ \dfrac{12}{h^2} \\ -\dfrac{12}{h^2} \\ -\dfrac{12}{h^2} - A_N \\ \dfrac{18}{h^2} - 8A_N \end{bmatrix}, \tag{44}$$

where A_N equals $A_N = w_{N,N+2}^{(2)} = 2w_{N,N+2}^{(1)}(w_{N,N}^{(1)} - 1/(x_N - x_{N+2}))$.

3. Test Problem and Experimental Results

In this section, we obtained numerical solutions of the MBE by the subdomain finite element method and differential

TABLE 5: L_2 and L_∞ error norms for $\nu = 0.01$, $\Delta t = 0.01$, and $h = 0.02$.

Time	QBDQM [$h = 0.02$]		Ramadan et al. [13] [$h = 0.02$]	
	$L_2 \times 10^3$	$L_\infty \times 10^3$	$L_2 \times 10^3$	$L_\infty \times 10^3$
2	0.7955855586	1.3795978925	0.7904296620	1.7030921188
3	0.6690533313	1.1943543646	0.6551928290	1.1832698216
4	0.5250528343	0.9764154381	0.5576794264	0.9964523368
5	0.4048512821	0.7849457015	0.5105617536	0.8561342445
6	0.3452210304	0.6374950443	0.5167229575	0.7610530060
7	0.3638648688	0.6705419608	0.5677438614	1.0654548090
8	0.4337013450	0.9863405006	0.6427542266	1.3581113635
9	0.5197862999	1.2551335234	0.7236430257	1.6048306653
10	0.6042925888	1.4747885309	0.8002564201	1.8023938553

TABLE 6: L_2 and L_∞ error norms for $\nu = 0.01$, $\Delta t = 0.01$, and $N = 81$ at $0 \le x \le 1.3$.

Time	QBDQM	
	$L_2 \times 10^3$	$L_\infty \times 10^3$
2	0.7607107169	1.3704182195
3	0.6480181273	1.1854984190
4	0.5604986926	1.0052476452
5	0.4927784148	0.8654032419
6	0.4359075842	0.7531551023
7	0.3885737191	0.6601326512
8	0.3520185942	0.5833334970
9	0.3282544303	0.5201323663
10	0.3187570280	0.4691560472

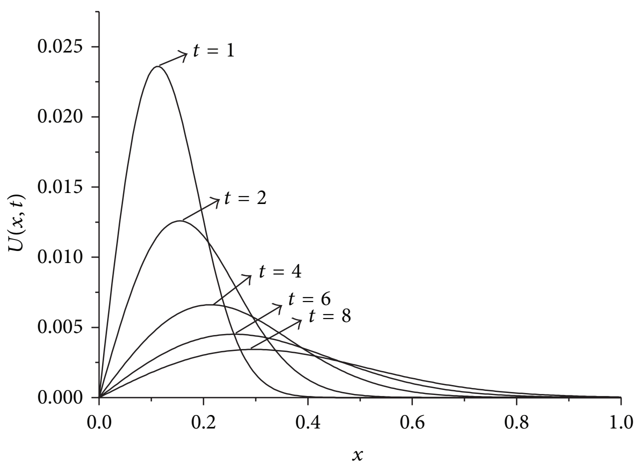

FIGURE 1: Solution behavior of the equation with $h = 0.005$, $t = 0.01$, and $\nu = 0.01$.

quadrature method. The accuracy of the numerical method is checked using the error norms L_2 and L_∞, respectively,

$$L_2 = \left\| U^{\text{exact}} - U_N \right\|_2 \simeq \sqrt{h \sum_{J=1}^{N} \left| U_j^{\text{exact}} - (U_N)_j \right|^2},$$
$$L_\infty = \left\| U^{\text{exact}} - U_N \right\|_\infty \simeq \max_j \left| U_j^{\text{exact}} - (U_N)_j \right|, \quad j = 1, 2, \ldots, N-1. \tag{45}$$

All numerical calculations were computed in double precision arithmetic on a Pentium 4 PC using a Fortran compiler. The analytical solution of modified Burgers' equation is given in [33] as

$$U(x,t) = \frac{(x/t)}{1 + \left(\sqrt{t}/c_0\right) \exp\left(x^2/4\nu t\right)}, \tag{46}$$

where c_0 is a constant and $0 < c_0 < 1$. For our numerical calculation, we take $c_0 = 0.5$. We use the initial condition for (46), evaluating at $t = 1$, and the boundary conditions are taken as $U(0,t) = U_x(0,t) = 0$ and $U(1,t) = U_x(1,t) = 0$.

3.1. Experimental Results for FEM. For the numerical simulation, we have chosen the various viscosity parameters $\nu = 0.01, 0.001, 0.005$, space steps $h = 0.02, 0.005$, and time steps $\Delta t = 0.01, 0.001$ over the interval $0 \le x \le 1$. The computed values of the error norms L_2 and L_∞ are presented at some selected times up to $t = 10$. The obtained results are tabulated in Tables 1, 2, 3, and 4. It is clearly seen that the results obtained by the SFEM are found to be more acceptable. Also, we observe from these tables that if the value of viscosity decreases, the value of the error norms will decrease. When the value of viscosity parameter is smaller we get better results. The behaviors of the numerical solutions for viscosity $\nu = 0.01, 0.005, 0.001$, space steps $h = 0.02, 0.005$, and time steps $\Delta t = 0.01, 0.001$ at times $t = 1, 2, 4, 6$, and 8 are shown in Figures 1, 2, and 3. As seen in the figures, the top curve is at $t = 1$ and the bottom curve is at $t = 8$. Also, we have observed from the figures that as the time increases the curve of the numerical solution decays. With smaller viscosity value, numerical solution decay gets faster.

3.2. Experimental Results for QBDQM. We calculate the numerical rates of convergence (ROC) with the help of the following formula:

$$\text{ROC} \approx \frac{\ln\left(E(N_2)/E(N_1)\right)}{\ln\left(N_1/N_2\right)}. \tag{47}$$

Table 7: L_2 and L_∞ error norms for $\nu = 0.001$, $\Delta t = 0.01$, and $h = 0.005$.

Time	QBDQM		Ramadan et al. [13]	
	$L_2 \times 10^3$	$L_\infty \times 10^3$	$L_2 \times 10^3$	$L_\infty \times 10^3$
2	0.1370706949	0.4453892504	0.1835491190	0.8185211112
3	0.1168507335	0.3842839811	0.1441424335	0.5234833346
4	0.1019761971	0.3258391192	0.1144110783	0.3563537207
5	0.0920706001	0.2816616769	0.0947865272	0.2549790058
6	0.0849484881	0.2484289381	0.0814174677	0.2134847835
7	0.0794570772	0.2225471690	0.0718977757	0.1880048432
8	0.0750035859	0.2019577762	0.0648368942	0.1682601770
9	0.0712618898	0.1851510002	0.0594114970	0.1524074966
10	0.0680382860	0.1711033543	0.0551151456	0.1394312127

Table 8: Error norms and rate of convergence for various numbers of grid points at $t = 10$.

N	$L_2 \times 10^3$	ROC(L_2)	$L_\infty \times 10^3$	ROC(L_∞)
11	0.43	—	0.98	—
21	0.35	0.31	0.88	0.16
31	0.22	1.19	0.52	1.35
41	0.17	0.92	0.39	1.02
51	0.14	0.88	0.30	1.20
81	0.10	0.72	0.19	0.98

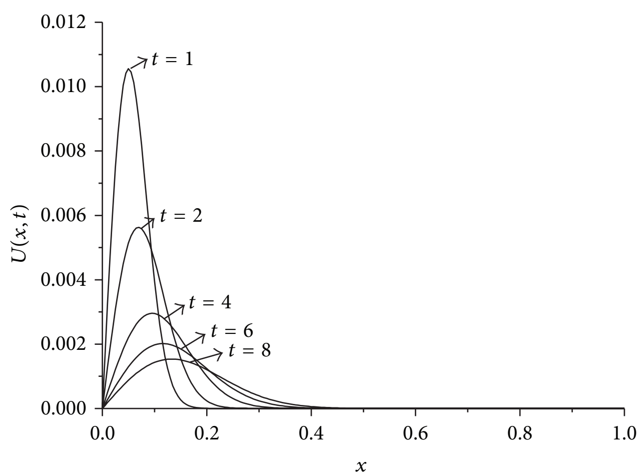

Figure 2: Solution behavior of the equation with $h = 0,005$, $t = 0,01$, and $\nu = 0.001$.

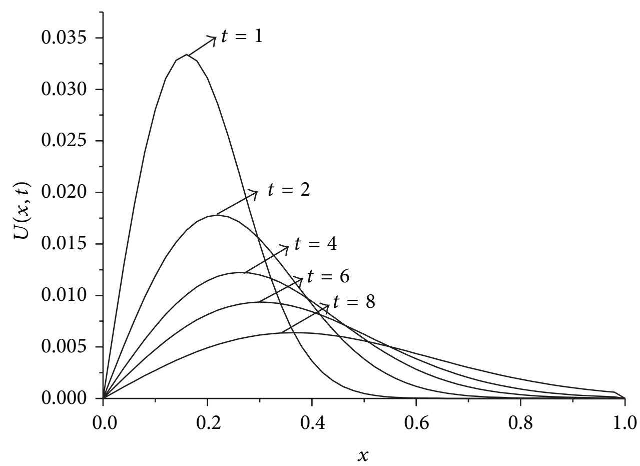

Figure 3: Solution behavior of the equation with $h = 0,02$, $t = 0,01$, and $\nu = 0.01$.

Here $E(N_j)$ denotes either the L_2 error norm or the L_∞ error norm in case of using N_j grid points. Therefore, some further numerical runs for different numbers of space steps have been performed. Ultimately, some computations have been made about the ROC by assuming that these methods are algebraically convergent in space. Namely, we suppose that $E(N) \sim N^p$ for some $p < 0$ when $E(N)$ denotes the L_2 or the L_∞ error norms by using N subintervals.

For the numerical treatment, we have taken the different viscosity parameters $\nu = 0.01, 0.001$ and time step $\Delta t = 0.01$ over the intervals $0 \le x \le 1$ and $0 \le x \le 1.3$. As it is seen from Figure 4 when we select the solution domain $0 \le x \le 1$ the right part of the shock wave cannot be seen clearly. By using the larger domain like $0 \le x \le 1.3$ as seen in Figure 5 solution is got better than narrow domain $0 \le x \le 1$ shown in Figure 4. The computed values of the error norms L_2 and L_∞ are presented at some selected times up to $t = 10$. The obtained results are recorded in Tables 5 and 6. As it is seen from the tables, the error norms L_2 and L_∞ are sufficiently small and satisfactorily acceptable. We obtain better results if the value of viscosity parameter is smaller, as shown in Table 7. The behaviors of the numerical solutions for viscosity $\nu = 0.01$ and 0.001 and time step $\Delta t = 0.01$ at times $t = 1, 3, 5, 7$, and 9 are shown in Figures 4–6. It is observed from the figures that the top curve is at $t = 1$ and the bottom curve is at $t = 9$. It is obviously seen that smaller viscosity value ν in shock wave with smaller amplitude and propagation front becomes smoother. Also, we have seen from the figures that, as the time increases, the curve of the numerical solution decays. With smaller viscosity value, numerical solution decay gets faster. These numerical solutions graphs also agree with published earlier work [13]. Distributions of the error at time $t = 10$ are drawn for solitary waves, Figures 7 and 8, from which maximum error happens

Table 9: Comparison of our results with earlier studies.

Values and methods	$L_2 \times 10^3$ $t = 2$	$L_\infty \times 10^3$ $t = 2$	$L_2 \times 10^3$ $t = 10$	$L_\infty \times 10^3$ $t = 10$
$\nu = 0.005$, $\Delta t = 0.001$, $h = 0.005$				
SFEM	0.02469	0.08456	0.12326	0.41604
[14]	0.25786	0.72264	0.18735	0.30006
[17] SBCM1	0.22890	0.58623	0.14042	0.23019
[17] SBCM2	0.23397	0.58424	0.13747	0.22626
$\nu = 0.001$, $\Delta t = 0.01$, $h = 0.005$				
SFEM	0.00549	0.02820	0.02743	0.13913
QBDQM	0.13707	0.44538	0.06803	0.17110
[13]	0.18354	0.81852	0.05511	0.13943
[14]	0.06703	0.27967	0.05010	0.12129
[17] SBCM1	0.06843	0.26233	0.04080	0.10295
[17] SBCM2	0.07220	0.25975	0.03871	0.09882
[18]	0.06607	0.26186	0.04160	0.10470
$\nu = 0.01$, $\Delta t = 0.01$, and $h = 0.005$				
SFEM	0.09785	0.28062	0.48711	1.34692
[14]	0.52308	1.21698	0.64007	1.28124
[17] SBCM1	0.38489	0.82934	0.54826	1.28127
[17] SBCM2	0.39078	0.82734	0.54612	1.28127
[18]	0.37552	0.81766	0.19391	0.23074
$\nu = 0.01$, $\Delta t = 0.01$, and $h = 0.02$				
SFEM	0.09738	0.28025	0.48485	1.34798
QBDQM	0.79558	1.37959	0.60429	1.47478
[13]	0.79042	1.70309	0.80025	1.80239
[17] SBCM1	0.38474	0.82611	0.55985	1.28127
[17] SBCM2	0.41321	0.81502	0.55095	1.28127

at the right hand boundary when greater value of viscosity $\nu = 0.01$ is used, and with smaller value of viscosity $\nu = 0.001$, maximum error is recorded around the location where shock wave has the highest amplitude. The L_2 and L_∞ error norms and numerical rate of convergence analysis for $\nu = 0.001$ and $\Delta t = 0.01$ and different numbers of grid points are tabulated in Table 8.

Table 9 presents a comparison of the values of the error norms obtained by the present methods with those obtained by other methods [13, 14, 17, 18]. It is clearly seen from the table that the error norm L_2 obtained by the SFEM is smaller than those given in [13, 14, 17, 18] whereas the error norm L_∞ is very close to those given in [14, 17, 18]. The error norm L_∞ is better than the paper [13]. For the QBDQM both L_2 and L_∞ are almost the same as these papers.

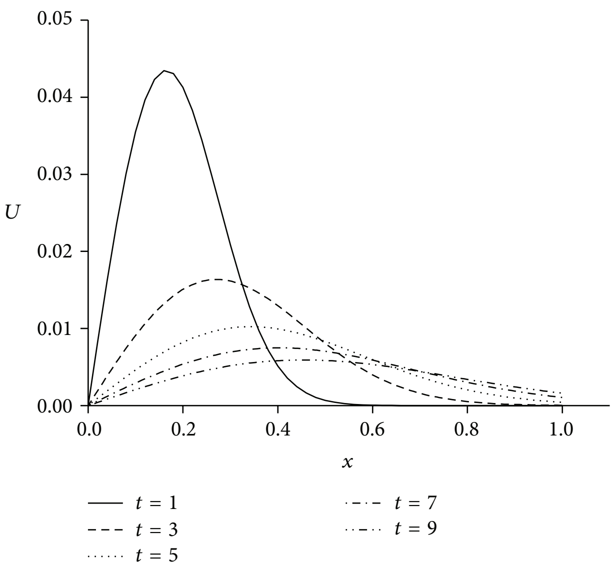

Figure 4: Solutions for $\nu = 0.01$, $h = 0.02$, $\Delta t = 0.01$, and $0 \le x \le 1$.

4. Conclusion

In this paper, SFEM and DQM based on quartic B-splines have been set up to find the numerical solution of the MBE (2). The performance of the schemes has been considered by studying the propagation of a single solitary wave. The efficiency and accuracy of the methods were shown by calculating the error norms L_2 and L_∞. Stability analysis of the approximation obtained by the schemes shows that the methods are unconditionally stable. An obvious conclusion can be drawn from the numerical results that for the SFEM L_2 error norm is found to be better than the methods cited in

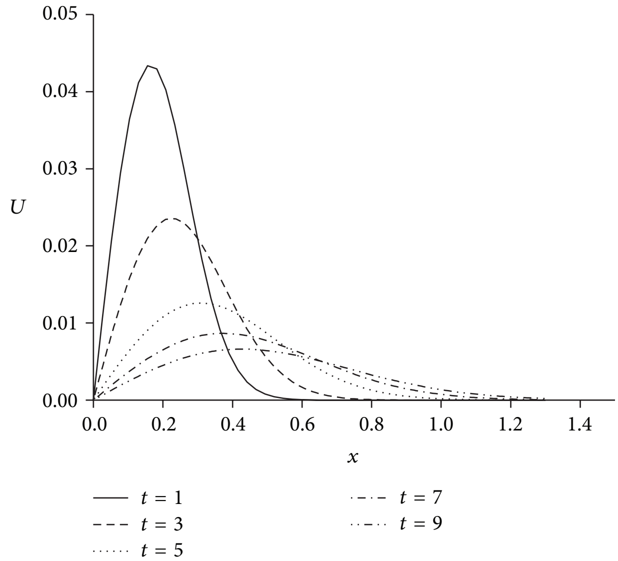

Figure 5: Solutions for $\nu = 0.01$, $h = 0.02$, $\Delta t = 0.01$, and $0 \leq x \leq 1.3$.

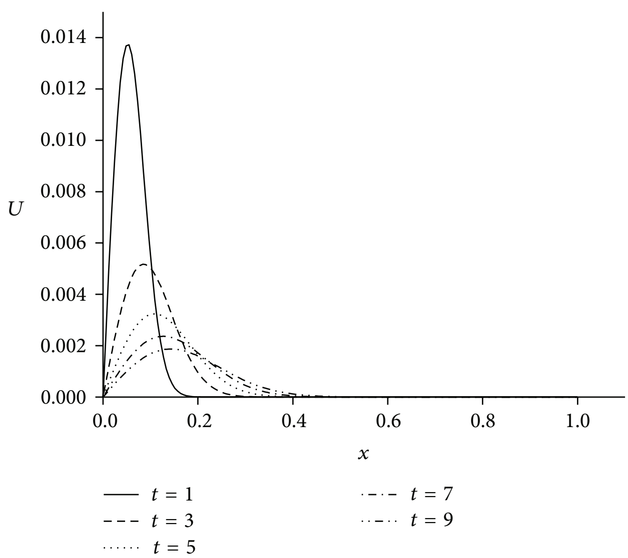

Figure 6: Solutions for $\nu = 0.001$, $\Delta t = 0.01$, $N = 166$, and $0 \leq x \leq 1$.

[13, 14, 17, 18] whereas L_∞ error norm is found to be very close to values given in [13, 14, 17, 18]. The obtained results show that our methods can be used to produce reasonable accurate numerical solutions of modified Burgers' equation. So these methods are reliable for getting the numerical solutions of the physically important nonlinear problems.

Conflict of Interests

The authors declare that there is no conflict of interests regarding the publication of this paper.

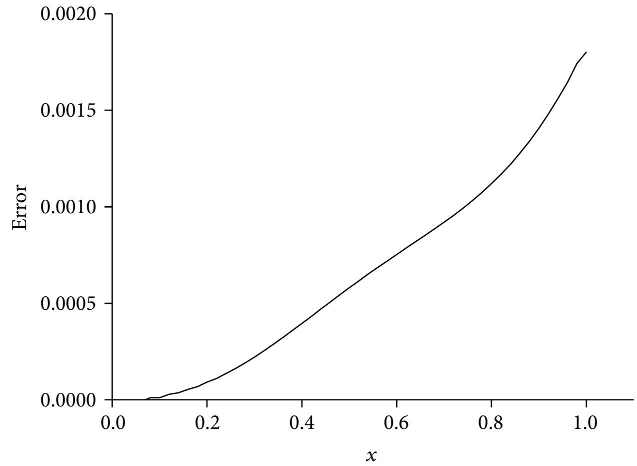

Figure 7: Errors for $\nu = 0.01$, $\Delta t = 0.01$, $h = 0.02$, and $0 \leq x \leq 1$.

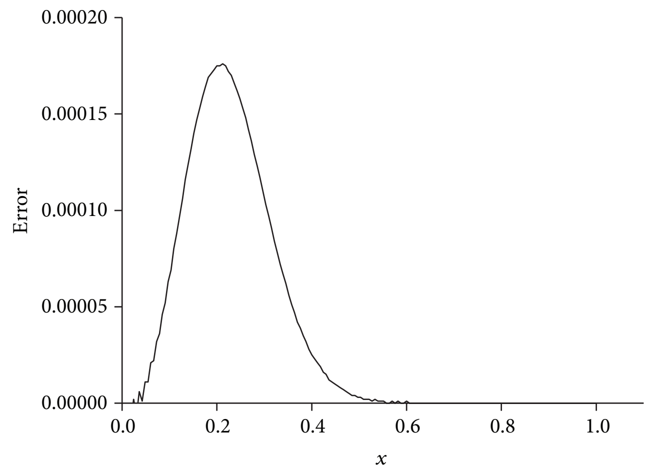

Figure 8: Errors for $\nu = 0.001$, $\Delta t = 0.01$, and $N = 166$, $0 \leq x \leq 1$.

References

[1] H. Bateman, "Some recent researches on the motion of fluids," *Monthly Weather Review*, vol. 43, pp. 163–170, 1915.

[2] J. M. Burgers, "A mathematical model illustrating the theory of turbulance," *Advances in Applied Mechanics*, vol. 1, pp. 171–199, 1948.

[3] E. N. Aksan, A. Özdeş, and T. Öziş, "A numerical solution of Burgers' equation based on least squares approximation," *Applied Mathematics and Computation*, vol. 176, no. 1, pp. 270–279, 2006.

[4] J. D. Cole, "On a quasi-linear parabolic equations occuring in aerodynamics," *Quarterly of Applied Mathematics*, vol. 9, pp. 225–236, 1951.

[5] J. Caldwell and P. Smith, "Solution of Burgers' equation with a large Reynolds number," *Applied Mathematical Modelling*, vol. 6, no. 5, pp. 381–385, 1982.

[6] S. Kutluay, A. R. Bahadir, and A. Özdeş, "Numerical solution of one-dimensional Burgers equation: explicit and exact-explicit finite difference methods," *Journal of Computational and Applied Mathematics*, vol. 103, no. 2, pp. 251–261, 1999.

[7] R. C. Mittal and P. Singhal, "Numerical solution of Burger's equation," *Communications in Numerical Methods in Engineering*, vol. 9, no. 5, pp. 397–406, 1993.

[8] R. C. Mittal and P. Singhal, "Numerical solution of periodic burgers equation," *Indian Journal of Pure and Applied Mathematics*, vol. 27, no. 7, pp. 689–700, 1996.

[9] M. B. Abd-el-Malek and S. M. A. El-Mansi, "Group theoretic methods applied to Burgers' equation," *Journal of Computational and Applied Mathematics*, vol. 115, no. 1-2, pp. 1–12, 2000.

[10] T. Öziş, E. N. Aksan, and A. Özdeş, "A finite element approach for solution of Burgers' equation," *Applied Mathematics and Computation*, vol. 139, no. 2-3, pp. 417–428, 2003.

[11] L. R. T. Gardner, G. A. Gardner, and A. Dogan, "A Petrov-Galerkin finite element scheme for Burgers' equation," *Arabian Journal for Science and Engineering*, vol. 22, no. 2, pp. 99–109, 1997.

[12] S. Kutluay, A. Esen, and I. Dag, "Numerical solutions of the Burgers' equation by the least-squares quadratic B-spline finite element method," *Journal of Computational and Applied Mathematics*, vol. 167, no. 1, pp. 21–33, 2004.

[13] M. A. Ramadan, T. S. El-Danaf, and F. E. I. A. Alaal, "A numerical solution of the Burgers' equation using septic B-splines," *Chaos, Solitons and Fractals*, vol. 26, no. 4, pp. 1249–1258, 2005.

[14] M. A. Ramadan and T. S. El-Danaf, "Numerical treatment for the modified burgers equation," *Mathematics and Computers in Simulation*, vol. 70, no. 2, pp. 90–98, 2005.

[15] Y. Duan, R. Liu, and Y. Jiang, "Lattice Boltzmann model for the modified Burgers' equation," *Applied Mathematics and Computation*, vol. 202, no. 2, pp. 489–497, 2008.

[16] I. Dağ, B. Saka, and D. Irk, "Galerkin method for the numerical solution of the RLW equation using quintic B-splines," *Journal of Computational and Applied Mathematics*, vol. 190, no. 1-2, pp. 532–547, 2006.

[17] D. Irk, "Sextic B-spline collocation method for the modified Burgers' equation," *Kybernetes*, vol. 38, no. 9, pp. 1599–1620, 2009.

[18] T. Roshan and K. S. Bhamra, "Numerical solutions of the modified Burgers' equation by Petrov-Galerkin method," *Applied Mathematics and Computation*, vol. 218, no. 7, pp. 3673–3679, 2011.

[19] R. P. Zhang, X. J. Yu, and G. Z. Zhao, "Modified Burgers' equation by the local discontinuous Galerkin method," *Chinese Physics B*, vol. 22, Article ID 030210, 2013.

[20] A. G. Bratsos, "A fourth-order numerical scheme for solving the modified Burgers equation," *Computers and Mathematics with Applications*, vol. 60, no. 5, pp. 1393–1400, 2010.

[21] R. Bellman, B. G. Kashef, and J. Casti, "Differential quadrature: a technique for the rapid solution of nonlinear partial differential equations," *Journal of Computational Physics*, vol. 10, no. 1, pp. 40–52, 1972.

[22] R. Bellman, B. Kashef, E. S. Lee, and R. Vasudevan, "Differential Quadrature and Splines," in *Computers and Mathematics with Applications*, pp. 371–376, Pergamon, Oxford, UK, 1976.

[23] J. R. Quan and C. T. Chang, "New insights in solving distributed system equations by the quadrature method—I," *Computers and Chemical Engineering*, vol. 13, no. 7, pp. 779–788, 1989.

[24] J. R. Quan and C. T. Chang, "New sightings in involving distributed system equations by the quadrature methods—II," *Computers and Chemical Engineering*, vol. 13, pp. 717–724, 1989.

[25] H. Zhong, "Spline-based differential quadrature for fourth order differential equations and its application to Kirchhoff plates," *Applied Mathematical Modelling*, vol. 28, no. 4, pp. 353–366, 2004.

[26] Q. Guo and H. Zhong, "Non-linear vibration analysis of beams by a spline-based differential quadrature method," *Journal of Sound and Vibration*, vol. 269, no. 1-2, pp. 413–420, 2004.

[27] H. Zhong and M. Lan, "Solution of nonlinear initial-value problems by the spline-based differential quadrature method," *Journal of Sound and Vibration*, vol. 296, no. 4-5, pp. 908–918, 2006.

[28] C. Shu and Y. L. Wu, "Integrated radial basis functions-based differential quadrature method and its performance," *International Journal for Numerical Methods in Fluids*, vol. 53, no. 6, pp. 969–984, 2007.

[29] A. Korkmaz and I. Dağ, "Polynomial based differential quadrature method for numerical solution of nonlinear Burgers equation," *Journal of the Franklin Institute*, vol. 348, no. 10, pp. 2863–2875, 2011.

[30] P. M. Prenter, *Splines and Variational Methods*, John Wiley, New York, NY, USA, 1975.

[31] A. Korkmaz, *Numerical solutions of some one dimensional partial differential equations using B-spline differential quadrature method [Doctoral dissertation]*, Eskisehir Osmangazi University, 2010.

[32] C. Shu, *Differential Quadrature and Its Application in Engineering*, Springer, London, UK, 2000.

[33] S. E. Harris, "Sonic shocks governed by the modified Burgers' equation," *European Journal of Applied Mathematics*, vol. 6, pp. 75–107, 1996.

Hindawi Publishing Corporation
The Scientific World Journal
Volume 2014, Article ID 214821, 11 pages
http://dx.doi.org/10.1155/2014/214821

Review Article

Recent Progress on Nonlinear Schrödinger Systems with Quadratic Interactions

Chunhua Li[1] and Nakao Hayashi[2]

[1] *Department of Mathematics, College of Science, Yanbian University, No.977 Gongyuan Road, Yanji, Jilin 133002, China*
[2] *Department of Mathematics, Graduate School of Science, Osaka University, Toyonaka, Osaka 560-0043, Japan*

Correspondence should be addressed to Chunhua Li; sxlch@ybu.edu.cn

Received 20 January 2014; Accepted 2 March 2014; Published 31 March 2014

Academic Editors: D. Baleanu and C. M. Khalique

The study of nonlinear Schrödinger systems with quadratic interactions has attracted much attention in the recent years. In this paper, we summarize time decay estimates of small solutions to the systems under the mass resonance condition in 2-dimensional space. We show the existence of wave operators and modified wave operators of the systems under some mass conditions in n-dimensional space, where $n \geq 2$. The existence of scattering operators and finite time blow-up of the solutions for the systems in higher space dimensions is also shown.

1. Introduction

In this paper we survey recent progress on asymptotic behavior of solutions to nonlinear Schrödinger system,

$$\begin{aligned} i\partial_t v_j + \frac{1}{2m_j}\Delta v_j &= F_j\left(v_1,\dots,v_l\right) + G_j\left(v_j\right), \\ & \qquad t\in\mathbb{R},\ x\in\mathbb{R}^n, \\ v_j(0,x) &= \phi_j, \quad x\in\mathbb{R}^n, \end{aligned} \tag{1}$$

based on papers [1–9], where $1 \leq j \leq l$, $\overline{v_j}$ is the complex conjugate of v_j, m_j is a mass of particle, and nonlinearities have the form

$$\begin{aligned} F_j\left(v_1,\dots,v_l\right) &= \sum_{1\leq m\leq k\leq 2l} \lambda^j_{m,k} v_m v_k, \\ G_j\left(v_j\right) &= \mu_j \left|v_j\right| v_j \end{aligned} \tag{2}$$

with

$$\begin{aligned} v_m, v_k, v_j \in &\left\{v_1,\dots,v_l,\overline{v_1},\dots,\overline{v_l}\right\} \\ &= \left\{v_1,\dots,v_l,v_{l+1},\dots,v_{2l}\right\}, \quad \lambda^j_{m,k},\ \mu_j\in\mathbb{C}. \end{aligned} \tag{3}$$

Nonlinear Schrödinger systems with quadratic interactions are physically important subjects (see, e.g., [10] and references cited therein). The quadratic nonlinearities of nonlinear Schrödinger systems in two space dimensions are interesting mathematical problems since they are regarded as the borderline between short range and long range interactions. In this case, asymptotic behavior of solutions to nonlinear systems is different from that to linear systems under mass resonance conditions and is the same as that to linear systems under mass nonresonance conditions. Namely, it is impossible to find solutions of nonlinear systems in the neighborhood of those of linear systems under mass resonance conditions.

If $F_j(v_j) \equiv 0$, then we have a single nonlinear Schrödinger equation:

$$i\partial_t v_j + \frac{1}{2m_j}\Delta v_j = \mu_j \left|v_j\right| v_j. \tag{4}$$

There are a lot of works on this subject since the work by Ginibre and Velo [11] which is considered a milestone of the field. We refer the text book by Cazenave [12] concerning the development on studies of (4) for details.

It is interesting to compare (1) with the system of nonlinear Klein-Gordon equations

$$\frac{1}{2c^2 m_j}\partial_t^2 u_j - \frac{1}{2m_j}\Delta u_j + \frac{m_j c^2}{2} u_j = -F_j(u_1,\dots,u_l) - G_j(u_j) \tag{5}$$

in $(t,x) \in \mathbb{R}\times\mathbb{R}^n$ for $1 \le j \le l$, under the gauge invariant condition

$$F_j(v_1,\dots,v_l) = e^{im_j\theta} F_j\left(e^{-im_1\theta}v_1,\dots,e^{-im_l\theta}v_l\right) \tag{6}$$

for any $\theta \in \mathbb{R}$, where c is the speed of light. If we let $u_j = e^{-itm_jc^2}v_j$ in (5), then by the condition (6) we find that v_j satisfies

$$\begin{aligned}\frac{1}{2c^2 m_j}\partial_t^2 v_j - i\partial_t v_j - \frac{1}{2m_j}\Delta v_j &= -e^{im_j\theta}F_j\left(e^{-im_1\theta}v_1,\dots,e^{-im_l\theta}v_l\right) \\ &\quad - e^{im_j\theta}G_j\left(e^{-im_j\theta}v_j\right) \\ &= -F_j(v_1,\dots,v_l) - G_j(v_j)\end{aligned} \tag{7}$$

with $\theta = tc^2$ for $1 \le j \le l$. Therefore nonrelativistic version of (5) can be obtained by letting $c \to \infty$ in (7) formally, which is (1). The first breakthrough on asymptotic behavior of solutions to (5) with $G_j \equiv 0$ was made by Klainerman [13] and Shatah [14] independently when $n = 3$. Their result was improved by a paper [15].

It is natural to require the $\mathbf{L}^2(\mathbb{R}^n)$ conservation law of solutions to (1) from the point of view of quantum mechanics. A sufficient condition is

$$\operatorname{Im}\sum_{j=1}^{l} c_j F_j \overline{v_j} = 0, \tag{8}$$

where $c_j > 0$ for $1 \le j \le l$; then we have $\mathbf{L}^2(\mathbb{R}^n)$ conservation law and as a result global existence in time of solutions to (1) is obtained by combining the conserved identity and the Strichartz estimate for $n \le 4$ (see [16] in which a single equation was considered and the proof used in [16] works for the system).

We now introduce some function spaces to present exact statements of our results. For any $m, s \in \mathbb{R}$ and $1 \le p \le \infty$, weighted Sobolev space $\mathbf{H}_p^{m,s}(\mathbb{R}^n)$ is defined by

$$\mathbf{H}_p^{m,s}(\mathbb{R}^n) = \left\{ f \in \mathbb{S}'(\mathbb{R}^n); \|f\|_{\mathbf{H}_p^{m,s}(\mathbb{R}^n)} < \infty \right\}, \tag{9}$$

where

$$\|f\|_{\mathbf{H}_p^{m,s}(\mathbb{R}^n)} = \left\|(1-\Delta)^{m/2}\left(1+|x|^2\right)^{s/2} f\right\|_{\mathbf{L}^p(\mathbb{R}^n)}. \tag{10}$$

We write $\mathbf{H}_2^{m,s}(\mathbb{R}^n) = \mathbf{H}^{m,s}(\mathbb{R}^n)$ and $\mathbf{H}^{m,0}(\mathbb{R}^n) = \mathbf{H}^m(\mathbb{R}^n)$ for simplicity. $\mathbf{L}^p(\mathbb{R}^n)$ denotes the usual Lebesgue space with the norm

$$\|\phi\|_{\mathbf{L}^p(\mathbb{R}^n)} = \left(\int_{\mathbb{R}^n} |\phi(x)|^p dx\right)^{1/p} \tag{11}$$

if $1 \le p < \infty$ and

$$\|\phi\|_{\mathbf{L}^\infty(\mathbb{R}^n)} = \operatorname{ess}\cdot\sup_{x\in\mathbb{R}^n} |\phi(x)|. \tag{12}$$

By $\dot{\mathbf{B}}_{p,q}^s(\mathbb{R}^n)$ we denote the homogeneous Besov space with the seminorm

$$\|\phi\|_{\dot{\mathbf{B}}_{p,q}^s(\mathbb{R}^n)} = \left(\int_0^\infty \lambda^{-1-\sigma q} \sup_{|y|\le\lambda} \sum_{|\alpha|=[s]} \left\|\partial^\alpha(\phi_y - \phi)\right\|_{\mathbf{L}^p(\mathbb{R}^n)}^q d\lambda\right)^{1/q}, \tag{13}$$

where $s = [s] + \sigma$, $0 < \sigma < 1$, $\phi_y(x) = \phi(x+y)$, $1 \le p$, $q \le \infty$, and $[s]$ is the largest integer less than s. It is known that $\dot{\mathbf{B}}_{2,2}^s(\mathbb{R}^n) = \dot{\mathbf{H}}^{s,0}(\mathbb{R}^n)$ (see [17]). We let $\mathbf{C}(\mathbf{I};\mathbf{E})$ be the space of continuous functions from an interval $\mathbf{I}$ to a Banach space $\mathbf{E}$. Different positive constants might be denoted by the same letter C. The homogeneous Sobolev spaces $\dot{\mathbf{H}}^{m,0}(\mathbb{R}^n)$ and $\dot{\mathbf{H}}^{0,s}(\mathbb{R}^n)$ are defined by

$$\begin{aligned}\dot{\mathbf{H}}^{m,0}(\mathbb{R}^n) &= \left\{ f \in \mathbb{S}'(\mathbb{R}^n); \|f\|_{\dot{\mathbf{H}}^{m,0}(\mathbb{R}^n)} = \left\|(-\Delta)^{m/2} f\right\|_{\mathbf{L}^2(\mathbb{R}^n)} < \infty \right\}, \\ \dot{\mathbf{H}}^{0,s}(\mathbb{R}^n) &= \left\{ f \in \mathbb{S}'(\mathbb{R}^n); \|f\|_{\dot{\mathbf{H}}^{0,s}(\mathbb{R}^n)} = \left\||x|^s f\right\|_{\mathbf{L}^2(\mathbb{R}^n)} < \infty \right\},\end{aligned} \tag{14}$$

respectively. We define the dilation operator by

$$(D_\delta\phi)(x) = \frac{1}{(i\delta)^{n/2}}\phi\left(\frac{x}{\delta}\right) \tag{15}$$

for $x \in \mathbb{R}^n$ and $\delta \ne 0$ and define $E = e^{-(i/2)t|\xi|^2}$ and $M = e^{-(i/2t)|x|^2}$ for $t \ne 0$.

Evolution operator $U_\delta(t)$ is written as

$$(U_\delta(t)\phi)(x) = M^{-1/\delta} D_{\delta t}\left(\mathcal{F} M^{-1/\delta}\phi\right)(x), \tag{16}$$

where $\mathcal{F}$, $\mathcal{F}^{-1}$ are the Fourier transform and the inverse Fourier transform, respectively. We also have

$$U_\delta(-t)\phi(x) = i^n M^{1/\delta}\left(\mathcal{F}^{-1} E^\delta D_{1/\delta t}\phi\right)(x). \tag{17}$$

The operator $J_{1/m_j,k} = x_k + i(t/m_j)\partial_k = U_{1/m_j}(t) x_k U_{1/m_j}(-t)$, where $j \in \{1,\dots,l\}$ and $k \in \{1,\dots,n\}$ is an important tool to study time decay of solutions to nonlinear Schrödinger equations satisfying the gauge invariant condition (6) since it acts as a differential operator. Fractional power of J_{1/m_j} is defined as

$$\left|J_{1/m_j}\right|^a(t) = U_{1/m_j}(t)|x|^a U_{1/m_j}(-t), \quad a > 0, \tag{18}$$

which is also represented as (see [18])

$$\left|J_{1/m_j}\right|^a(t) = M^{-m_j}\left(-\frac{t^2}{m_j^2}\Delta\right)^{a/2} M^{m_j}, \tag{19}$$

for $t \neq 0$. Moreover, for $L_{1/m_j} = i\partial_t + (1/2m_j)\Delta$, we have commutation relations such that

$$\left[L_{1/m_j}, \left|J_{1/m_j}\right|^a\right] = 0. \tag{20}$$

Remark 1. The system (1) includes some important nonlinear Schrödinger systems from the physical point of view. For example, the following system appears in a physical model (see e.g., [10, 19]):

$$\begin{aligned} i\partial_t v_1 + \frac{1}{2m_1}\Delta v_1 &= -\left|v_1\right| v_1 - \overline{v_2} v_3, \\ i\partial_t v_2 + \frac{1}{2m_2}\Delta v_2 &= -\left|v_2\right| v_2 - v_3 \overline{v_1}, \\ i\partial_t v_3 + \frac{1}{2m_3}\Delta v_3 &= -\left|v_3\right| v_3 - v_1 v_2, \end{aligned} \tag{21}$$

in $(t,x) \in \mathbb{R}\times\mathbb{R}^2$, where m_j is a mass of particle for $j = 1, 2, 3$. In [10], the system (21) has been derived as a model describing nonlinear interactions between a laser beam and a plasma. In [19], the stability of solitary waves for the system (21) was investigated.

This paper is organized as follows. Section 2 is devoted to present our recent works and some remarks. From Section 2.1 to Section 2.5, we consider the asymptotic behavior of solutions to nonlinear Schrödinger systems. In Section 2.1, we survey the results on the time decay estimates of solutions to nonlinear Schrödinger systems for $n = 2$ shown in [4–7, 9]. In Section 2.2, wave operators of nonlinear Schrödinger systems are investigated for $n = 2$ based on a paper [1]. Section 2.3 is concerned with the study of modified wave operators for $n = 2$ from a paper [1]. In the last two subsections, we survey the results in [2, 3]. In the last section we consider the related and open problems.

2. Nonlinear Schrödinger Systems

2.1. Time Decay of Solutions to Nonlinear Schrödinger Systems in Two Space Dimensions. To state time decay of solutions to nonlinear Schrödinger systems for $n = 2$, we start with time decay estimates of solutions to linear Schrödinger systems.

For (1), the corresponding linear system is written as

$$\begin{aligned} i\partial_t v_j + \frac{1}{2m_j}\Delta v_j &= 0, \quad t \in \mathbb{R},\ x \in \mathbb{R}^2, \\ v_j(0,x) &= \phi_j, \quad x \in \mathbb{R}^2, \end{aligned} \tag{22}$$

where $1 \le j \le l$.

As we know the solution $v_j(t)$ of (22) is represented as $v_j(t) = U_{1/m_j}(t)\phi_j$. It is known that $v_j(t)$ is decomposed into a main term and a remainder one as

$$U_{1/m_j}(t)\phi_j = e^{(im_j/2t)|x|^2} \frac{m_j}{it} \mathcal{F}\phi_j\left(\frac{m_j x}{t}\right) + R_j \tag{23}$$

for $n = 2$, where R_j decays rapidly in time; indeed we have the estimate

$$\left\|R_j\right\|_{\mathbf{L}^\infty(\mathbb{R}^2)} \le C|t|^{-1-(\gamma/2)} \left\|\phi_j\right\|_{\dot{\mathbf{H}}^{0,1+\gamma}(\mathbb{R}^2)}, \quad 0 \le \gamma \le 1, \tag{24}$$

for $t \neq 0$. By $\|U_{1/m_j}(t)v_j\|_{\mathbf{L}^2(\mathbb{R}^2)} = \|v_j\|_{\mathbf{L}^2(\mathbb{R}^2)}$ and $\mathbf{L}^\infty(\mathbb{R}^2)$ – $\mathbf{L}^1(\mathbb{R}^2)$ time decay estimate

$$\left\|U_{1/m_j}(t)v_j\right\|_{\mathbf{L}^\infty(\mathbb{R}^2)} \le \left(\frac{2\pi}{m_j}|t|\right)^{-1} \left\|v_j\right\|_{\mathbf{L}^1(\mathbb{R}^2)} \tag{25}$$

for $t \neq 0$, we have the following time decay estimates through the interpolation theorem (see [12]).

Theorem 2. *Let $2 \le p \le \infty$, and let p, p' be conjugate indices, $t \neq 0$. Then we have $U_{1/m_j}(t) : \mathbf{L}^{p'}(\mathbb{R}^2) \to \mathbf{L}^p(\mathbb{R}^2)$ which are bounded operators and satisfy*

$$\left\|U_{1/m_j}(t)v_j\right\|_{\mathbf{L}^p(\mathbb{R}^2)} \le \left(\frac{2\pi}{m_j}|t|\right)^{-2((1/2)-(1/p))} \left\|v_j\right\|_{\mathbf{L}^{p'}(\mathbb{R}^2)} \tag{26}$$

for $j = 1, \ldots, l$.

Now we consider a special type of the system (1),

$$\begin{aligned} i\partial_t u_1 + \frac{1}{2m_1}\Delta u_1 &= \lambda \overline{u_1} u_2, \\ i\partial_t u_2 + \frac{1}{2m_2}\Delta u_2 &= \mu u_1^2, \end{aligned} \tag{27}$$

in $(t,x) \in \mathbb{R}\times\mathbb{R}^2$, where m_1 and m_2 are the masses of particles and $\lambda, \mu \in \mathbb{C}$. If we let $u_1 = (1/\sqrt{|\lambda\mu|})v_1$ and $u_2 = (\mu/|\lambda\mu|)v_2$ in the above system, then we obtain the system as below

$$\begin{aligned} i\partial_t v_1 + \frac{1}{2m_1}\Delta v_1 &= \gamma \overline{v_1} v_2, \\ i\partial_t v_2 + \frac{1}{2m_2}\Delta v_2 &= v_1^2, \end{aligned} \tag{28}$$

in $(t,x) \in \mathbb{R} \times \mathbb{R}^2$, where $\gamma = \lambda\mu/|\lambda\mu| \in \mathbb{C}$. Therefore we survey the results on time decay of solutions to the system (28). The first result was obtained in [4].

Theorem 3 (see [4]). *Assume that $2m_1 = m_2$ and $\gamma = 1$. Then there exists $\varepsilon > 0$ such that* (28) *with the initial data*

$$v(0) = (v_1(0), v_2(0)) = (\phi_1, \phi_2) = \phi \tag{29}$$

has a unique global solution

$$v = (v_1, v_2) \in \mathbf{C}\left(\mathbb{R}; \mathbf{H}^2\left(\mathbb{R}^2\right) \cap \mathbf{H}^{0,2}\left(\mathbb{R}^2\right)\right) \tag{30}$$

for any $(\phi_1, \phi_2) \in \mathbf{H}^2(\mathbb{R}^2) \cap \mathbf{H}^{0,2}(\mathbb{R}^2)$ satisfying

$$\|\phi\|_{\mathbf{H}^2(\mathbb{R}^2)\cap\mathbf{H}^{0,2}(\mathbb{R}^2)} = \sum_{j=1}^{2} \left\|\phi_j\right\|_{\mathbf{H}^2(\mathbb{R}^2)\cap\mathbf{H}^{0,2}(\mathbb{R}^2)} \le \varepsilon. \tag{31}$$

Moreover the time decay estimate

$$\|v(t,\cdot)\|_{\mathbf{L}^\infty(\mathbb{R}^2)} = \sum_{j=1}^{2} \left\|v_j(t,\cdot)\right\|_{\mathbf{L}^\infty(\mathbb{R}^2)} \le C(1+|t|)^{-1} \tag{32}$$

is true for all $t \in \mathbb{R}$.

In Theorem 3, the main result is $\mathbf{L}^\infty(\mathbb{R}^2)$ time decay estimates of solutions of (28) and which is the same rate as that of the corresponding free solutions.

When $\gamma = 1$, (28) satisfies the condition (8). Under the condition, $\gamma = 1$, (28) obeys the $\mathbf{L}^2(\mathbb{R}^2)$ conservation law such that

$$\frac{d}{dt}\left(\|v_1\|^2_{\mathbf{L}^2(\mathbb{R}^2)} + \|v_2\|^2_{\mathbf{L}^2(\mathbb{R}^2)}\right) = 0. \tag{33}$$

In the case of the mass resonance condition $2m_1 = m_2$, (28) satisfies the condition (6). Global existence of small solutions for (28) is obtained from the conservation law and the Strichartz estimate. $\mathbf{L}^\infty(\mathbb{R}^2)$ time decay of small solutions for (28) is proved through a priori estimates of local solutions in the norm $\|\mathcal{F}U_{1/m_j}(-t)v_j\|_{\mathbf{L}^\infty(\mathbb{R}^2)}$. The similar idea has been used for construction of $\mathbf{H}^{2,2}(\mathbb{R}^2)$ solutions to a single nonlinear Schrödinger equation by a paper [20]. Theorem 3 extends this idea to (28). The main point in the proof of the result is to derive the ordinary differential equation

$$\begin{aligned} i\partial_t\psi_1 &= \gamma t^{-1}\overline{\psi_1}\psi_2 + O\left(t^{-1-\varepsilon}\right), \\ i\partial_t\psi_2 &= t^{-1}\psi_1^2 + O\left(t^{-1-\varepsilon}\right), \end{aligned} \tag{34}$$

under the condition $2m_1 = m_2$ by using the factorization formulas of Schrödinger evolution group stated in Section 1, where $\psi_j = D_{1/m_j}\mathcal{F}U_{1/m_j}(-t)v_j$ for $j = 1, 2$ and $\varepsilon > 0$. Asymptotic behavior in time of solutions of (28) is determined by that of the ordinary differential equations (34). The main task is to show that remainder terms are estimated from above by $O(t^{-1-\varepsilon})$ which is integrable in time. This is the reason why we use the condition such that the data must be in $\mathbf{H}^{0,\beta}(\mathbb{R}^2)$, $\beta > 1$.

The system (1) is a generalization of (28). For the system (1), we have global existence theorem and time decay estimates as follows.

Theorem 4 (see [5]). *One assumes that* $\phi = (\phi_1, \ldots, \phi_l) \in \mathbf{H}^{2,2}(\mathbb{R}^2)$ *and* F_j *satisfies the conditions* (6) *and* (8) *for each* $j \in \{1, \ldots, l\}$. *Then there exists* $\varepsilon > 0$ *such that* (1) *has a unique global solution*

$$v = (v_1, \ldots, v_l) \in \mathbf{C}\left(\mathbb{R}; \mathbf{H}^{2,2}\left(\mathbb{R}^2\right)\right) \tag{35}$$

for any $\phi = (\phi_1, \ldots, \phi_l) \in \mathbf{H}^{2,2}(\mathbb{R}^2)$ *satisfying*

$$\|\phi\|_{\mathbf{H}^{2,2}(\mathbb{R}^2)} = \sum_{i=1}^{l}\|\phi_i\|_{\mathbf{H}^{2,2}(\mathbb{R}^2)} \le \varepsilon. \tag{36}$$

Moreover the time decay estimate

$$\|v(t,\cdot)\|_{\mathbf{L}^\infty(\mathbb{R}^2)} = \sum_{i=1}^{l}\|v_i(t,\cdot)\|_{\mathbf{L}^\infty(\mathbb{R}^2)} \le C(1+|t|)^{-1} \tag{37}$$

is true for all $t \in \mathbb{R}$.

Theorem 4 was improved in [6] by replacing the condition such that $\phi \in \mathbf{H}^{2,2}(\mathbb{R}^2)$ by $\phi \in \mathbf{H}^{\beta}(\mathbb{R}^2) \cap \mathbf{H}^{0,\beta}(\mathbb{R}^2)$ with $1 < \beta$.

Now we focus on the following system:

$$\begin{aligned} i\partial_t v_1 + \frac{1}{2m_1}\Delta v_1 &= \lambda_1 |v_1| v_1 + \mu_1\overline{v_2}v_3, \\ i\partial_t v_2 + \frac{1}{2m_2}\Delta v_2 &= \lambda_2 |v_2| v_2 + \mu_2\overline{v_1}v_3, \\ i\partial_t v_3 + \frac{1}{2m_3}\Delta v_3 &= \lambda_3 |v_3| v_3 + \mu_3 v_1 v_2, \\ v_j(0,x) &= \phi_j(x), \quad j = 1, 2, 3, \end{aligned} \tag{38}$$

in $(t,x) \in \mathbb{R}\times\mathbb{R}^2$, where m_1, m_2, m_3 are the masses of particles and $\lambda_1, \lambda_2, \lambda_3, \mu_1, \mu_2, \mu_3 \in \mathbb{C} \setminus \{0\}$ are constants.

Time decay problem of solutions to (38) is considered in [7]. By using the similar method as [4, 5], we have global existence in time and time decay estimates of small solutions for (38) as below.

Theorem 5 (see [7]). *Assume that the mass resonance condition* $m_1 + m_2 = m_3$ *is satisfied. One also assumes that* $\operatorname{Im}\lambda_j \le 0$ *for* $j = 1, 2, 3$ *and* $\kappa_1\mu_1 + \kappa_2\mu_2 = \kappa_3\overline{\mu_3}$ *with some* $\kappa_1, \kappa_2, \kappa_3 > 0$. *Then there exists* $\varepsilon > 0$ *such that* (38) *has a unique global solution*

$$v = (v_1, v_2, v_3) \in \mathbf{C}\left(\mathbb{R}; \mathbf{H}^s\left(\mathbb{R}^2\right) \cap \mathbf{H}^{0,s}\left(\mathbb{R}^2\right)\right) \tag{39}$$

for any $\phi = (\phi_1, \phi_2, \phi_3) \in \mathbf{H}^s(\mathbb{R}^2) \cap \mathbf{H}^{0,s}(\mathbb{R}^2)$ *satisfying*

$$\|\phi\|_{\mathbf{H}^s(\mathbb{R}^2)\cap\mathbf{H}^{0,s}(\mathbb{R}^2)} = \sum_{i=1}^{3}\|\phi_i\|_{\mathbf{H}^s(\mathbb{R}^2)\cap\mathbf{H}^{0,s}(\mathbb{R}^2)} \le \varepsilon, \tag{40}$$

where $1 < s < 2$. *Moreover, the time decay estimate*

$$\|v(t,\cdot)\|_{\mathbf{L}^\infty(\mathbb{R}^2)} = \sum_{i=1}^{3}\|v_i(t,\cdot)\|_{\mathbf{L}^\infty(\mathbb{R}^2)} \le C(1+|t|)^{-1} \tag{41}$$

is true for all $t \in \mathbb{R}$.

If

$$\operatorname{Im}\lambda_j < 0 \quad \text{for } j = 1, 2, 3, \tag{42}$$

the nonlinear term $\lambda_j|v_j|v_j$ acts as a dissipation one which requires logarithmic correction in time of solutions and the negative time is not considered. We have the following theorem.

Theorem 6 (see [7]). *Suppose that the assumptions of Theorem 5 are fulfilled. Let* v *be the solution to the system* (38) *constructed in Theorem 5. If*

$$\operatorname{Im}\lambda_j < 0 \quad \text{for } j = 1, 2, 3 \tag{43}$$

is satisfied, then the time decay estimate

$$\|v(t,\cdot)\|_{\mathbf{L}^\infty(\mathbb{R}^2)} \le C(1+t)^{-1}\left(\log(2+t)\right)^{-1} \tag{44}$$

is true for all $t \ge 0$.

This phenomenon was found in [21] for a single equation. We note here that the method presented in [7] is different from the one in [21]. It seems that the proof in [21] does not work for the system.

Define the scaled function by $v_{j,\mu}(t) = \mu^2 v_j(\mu^2 t, \mu x)$; then $v_{j,\mu}(t)$ satisfies the system (1) with the initial data $\phi_{j,\mu}(x) = \mu^2\phi_j(\mu x)$. We have

$$\begin{aligned}\left\|\phi_{j,\mu}\right\|^2_{\dot{\mathbf{H}}^{0,2-(n/2)}(\mathbb{R}^n)} &= \int_{\mathbb{R}^n} \mu^4 |x|^{4-n} \left|\phi_j(\mu x)\right|^2 dx \\ &= \left\|\phi_j\right\|^2_{\dot{\mathbf{H}}^{0,2-(n/2)}(\mathbb{R}^n)},\end{aligned} \tag{45}$$

which implies that $\dot{\mathbf{H}}^{0,2-(n/2)}(\mathbb{R}^n)$ is one of the so-called invariant spaces for the problem (1). Other invariant spaces of (1) are given by $\dot{\mathbf{H}}^{(n/2)-2}(\mathbb{R}^n)$. We consider the large time asymptotics of solutions to the system (1) for $n = 2$ in the function space $\dot{\mathbf{H}}^{0,\alpha}(\mathbb{R}^2) \cap \dot{\mathbf{H}}^{0,\beta}(\mathbb{R}^2)$, where α, β satisfy $0 \le \beta < 1 < \alpha \le 2$ and can be taken to be close to 1. Therefore our function space has relation with the invariant space and the considered data are not necessarily in $\mathbf{L}^2(\mathbb{R}^2)$.

Theorem 7 (see [9]). *Assume that* (6) *and* (8) *hold. One also assumes that $\phi = (\phi_1, \ldots, \phi_l) \in \dot{\mathbf{H}}^{0,\alpha}(\mathbb{R}^2) \cap \dot{\mathbf{H}}^{0,\beta}(\mathbb{R}^2)$, where $0 \le \beta < 1 < \alpha \le 2$. Then there exists $\varepsilon > 0$ such that* (1) *has a unique global solution v such that*

$$\begin{aligned}U_{1/m}(-t)\, v &= \left(U_{1/m_1}(-t)\, v_1, \ldots, U_{1/m_l}(-t)\, v_l\right) \\ &\in \mathbf{C}\left(\mathbb{R}; \dot{\mathbf{H}}^{0,\alpha}\left(\mathbb{R}^2\right) \cap \dot{\mathbf{H}}^{0,\beta}\left(\mathbb{R}^2\right)\right)\end{aligned} \tag{46}$$

for any $\phi = (\phi_1, \ldots, \phi_l)$ satisfying

$$\|\phi\|_{\dot{\mathbf{H}}^{0,\alpha}(\mathbb{R}^2)\cap\dot{\mathbf{H}}^{0,\beta}(\mathbb{R}^2)} = \sum_{i=1}^{l} \|\phi_i\|_{\dot{\mathbf{H}}^{0,\alpha}(\mathbb{R}^2)\cap\dot{\mathbf{H}}^{0,\beta}(\mathbb{R}^2)} \le \varepsilon. \tag{47}$$

Moreover, the time decay estimate

$$\|v(t,\cdot)\|_{\mathbf{L}^\infty(\mathbb{R}^2)} = \sum_{i=1}^{l} \|v_i(t,\cdot)\|_{\mathbf{L}^\infty(\mathbb{R}^2)} \le C|t|^{-1} \tag{48}$$

is true for $t \ne 0$.

We note that in [8] we consider the problem (38) under the initial condition $\phi = (\phi_1, \phi_2, \phi_3) \in \dot{\mathbf{H}}^{0,\alpha}(\mathbb{R}^2) \cap \dot{\mathbf{H}}^{0,\delta}(\mathbb{R}^2)$ and the dissipation condition $\operatorname{Im} \lambda_j < 0$, where $0 \le \delta < 1 < \alpha \le 2$. Then we have the time decay estimate such that

$$\|v(t,\cdot)\|_{\mathbf{L}^\infty(\mathbb{R}^2)} \le t^{-1}(\log t)^{-1} \tag{49}$$

for all $t \ge 1$.

In the final part of this subsection, we will show that the assumption (8) is important for obtaining the time decay estimates of solutions. Let us consider the following system:

$$\begin{aligned}&i\partial_t v_1 + \frac{1}{2m_1}\Delta v_1 = 0, \\ &i\partial_t v_2 + \frac{1}{2m_2}\Delta v_2 = v_1^2, \\ &v_1(0) = \phi_1, \quad v_2(0) = \phi_2,\end{aligned} \tag{50}$$

in $(t,x) \in \mathbb{R}\times\mathbb{R}^2$, where m_1, m_2 are the masses of particles. It is obvious that the nonlinearities of (50) do not satisfy the assumption (8). Since the first equation of this system with the initial condition $v_1(0) = \phi_1$ can be considered the Cauchy problem for the linear Schrödinger equation, we find the value of v_1 explicitly by $v_1 = U_{1/m_1}(t)\phi_1$. Therefore, we have

$$\begin{aligned}i\partial_t v_2 + \frac{1}{2m_2}\Delta v_2 &= \left(U_{1/m_1}(t)\,\phi_1\right)^2, \\ v_2(0) &= \phi_2.\end{aligned} \tag{51}$$

For the system (51), we obtain the following result.

Proposition 8 (see [4]). *Suppose that $\phi_1 \in \mathbf{H}^{0,2}(\mathbb{R}^2)$, $\phi_2 \in \mathbf{L}^2(\mathbb{R}^2)$. Let*

$$v_2 \in \mathbf{C}\left([1,\infty); \mathbf{L}^2\left(\mathbb{R}^2\right)\right) \tag{52}$$

be a global solution of (51). *Then the following estimate is true:*

$$\|v_2(t)\|_{\mathbf{L}^2(\mathbb{R}^2)} \ge m_1 \left\|\widehat{\phi_1}\right\|^2_{\mathbf{L}^4(\mathbb{R}^2)} \log t - C\|\phi_1\|^2_{\mathbf{H}^{0,2}(\mathbb{R}^2)} \tag{53}$$

for $t > 1$.

This fact was pointed first in [22, 23] in the case of Klein-Gordon equations and in Remark 3 of [24] in the case of Schrödinger equations.

2.2. Wave Operators of Nonlinear Schrödinger Systems in Two Space Dimensions. First, we briefly explain the definition of the wave operator (see [25]). For a given function $v_+ = (v_{i+})$, we assume that there exists a unique solution $v = (v_i)$ of the system (1) satisfying the asymptotics

$$\lim_{t\to\infty} \|v(t) - U_{1/m}(t)v_+\|_X = 0, \tag{54}$$

where $U_{1/m}(t)v_+$ is the solution of linear problems with the initial data v_+ and $\|\cdot\|_X$ is the norm of Banach space X. Then we define the map $W_+ : v_+ \mapsto v(t)$ and call it the wave operator. We also call v_+ the final state (or the final value) since it is considered the value of $U_{1/m}(-t)v(t)$ at infinity if $U_{1/m}(t)$ is the unitary operator in X. The same problem can be considered for negative time.

To study existence of wave operators for (28), we consider the following problem for given final data (ϕ_{1+}, ϕ_{2+}) :

$$\begin{aligned}&i\partial_t v_1 + \frac{1}{2m_1}\Delta v_1 = \gamma\overline{v_1}v_2, \\ &i\partial_t v_2 + \frac{1}{2m_2}\Delta v_2 = v_1^2, \\ &\left\|v_1(t) - U_{1/m_1}(t)\,\phi_{1+}\right\|_{\mathbf{L}^2(\mathbb{R}^2)} \longrightarrow 0 \quad \text{as } t \longrightarrow \infty, \\ &\left\|v_2(t) - U_{1/m_2}(t)\,\phi_{2+}\right\|_{\mathbf{L}^2(\mathbb{R}^2)} \longrightarrow 0 \quad \text{as } t \longrightarrow \infty,\end{aligned} \tag{55}$$

in $(t,x) \in \mathbb{R}\times\mathbb{R}^2$. If there exists a nontrivial solution for the above system, then we say that there exists a usual wave operator.

We consider (28) under the mass nonresonance conditions $2m_1 \ne m_2$ and $m_1 \ne m_2$.

Theorem 9 (see [1]). *Let $2m_1 \neq m_2$ and $m_1 \neq m_2$. Then there exists $\varepsilon > 0$ such that, for any*

$$\phi_+ = (\phi_{1+}, \phi_{2+}) \in \left(\mathbf{H}^{0,2}\left(\mathbb{R}^2\right) \cap \dot{\mathbf{H}}^{-2b}\left(\mathbb{R}^2\right)\right) \times \mathbf{H}^{0,2}\left(\mathbb{R}^2\right) \tag{56}$$

with the norm

$$\|\phi_{1+}\|_{\mathbf{H}^{0,2}(\mathbb{R}^2)\cap\dot{\mathbf{H}}^{-2b}(\mathbb{R}^2)} + \|\phi_{2+}\|_{\mathbf{H}^{0,2}(\mathbb{R}^2)} \leq \varepsilon, \tag{57}$$

the system (28) *has a unique global solution*

$$v = (v_1, v_2) \in \mathbf{C}\left([1,\infty); \mathbf{L}^2\left(\mathbb{R}^2\right)\right). \tag{58}$$

Moreover, the following estimate

$$\begin{aligned} &\|v(t) - U_{1/m}(t)\phi_+\|_{\mathbf{L}^2(\mathbb{R}^2)} \\ &= \sum_{j=1}^{2} \left\|v_j(t) - U_{1/m_j}(t)\phi_{j+}\right\|_{\mathbf{L}^2(\mathbb{R}^2)} \leq Ct^{-b} \end{aligned} \tag{59}$$

holds for all $t \geq 1$, where $1/2 < b < 1$.

The mass nonresonance conditions $2m_1 \neq m_2$ and $m_1 \neq m_2$ are used to obtain better time decay of solutions. Oscillating properties of nonlinear terms $\overline{v_{1+}}v_{2+}$ and v_{1+}^2 are different from those of solutions to linear problem which yield an additional time decay from nonlinear terms; namely, nonlinear interactions are not critical. By combining this fact and the Strichartz type estimates, the result of Theorem 9 is obtained.

We next consider (28) under the mass condition $m_1 = m_2$ which is also the mass nonresonance case and the support conditions on the data.

Theorem 10 (see [1]). *Let $m_1 = m_2$. Assume that*

$$\begin{gathered} \phi_+ = (\phi_{1+}, \phi_{2+}) \in \left(\mathbf{H}^{0,2}\left(\mathbb{R}^2\right) \cap \dot{\mathbf{H}}^{-2b,0}\left(\mathbb{R}^2\right)\right) \times \mathbf{H}^{1/2,2}\left(\mathbb{R}^2\right), \\ \operatorname{supp} \widehat{\phi_{1+}} \cap \operatorname{supp} \widehat{\phi_{2+}} \textit{ is empty.} \end{gathered} \tag{60}$$

Then there exists $\varepsilon > 0$ such that, for any $\phi_+ = (\phi_{1+}, \phi_{2+})$ with the norm

$$\|\phi_{1+}\|_{\mathbf{H}^{0,2}(\mathbb{R}^2)\cap\dot{\mathbf{H}}^{-2b,0}(\mathbb{R}^2)} + \|\phi_{2+}\|_{\mathbf{H}^{0,2}(\mathbb{R}^2)} \leq \varepsilon, \tag{61}$$

there exists a unique solution

$$v = (v_1, v_2) \in \mathbf{C}\left([1,\infty); \mathbf{L}^2\left(\mathbb{R}^2\right)\right) \tag{62}$$

for the system (28) *satisfying the estimate*

$$\begin{aligned} &\|v(t) - U_{1/m}(t)\phi_+\|_{\mathbf{L}^2(\mathbb{R}^2)} \\ &= \sum_{j=1}^{2} \left\|v_j(t) - U_{1/m_j}(t)\phi_{j+}\right\|_{\mathbf{L}^2(\mathbb{R}^2)} \leq Ct^{-b} \end{aligned} \tag{63}$$

for all $t \geq 1$, where $1/2 < b < 3/4$.

From the result we have wave operators when the support of the Fourier transform of the Schrödinger data is restricted. Restriction on the support of the Fourier transform of the Schrödinger data was used to obtain an improved time decay estimate of the nonlinear term $\overline{v_{1+}}v_{2+}$.

We turn to investigate existence of wave operators for (1). First, we give a necessary condition of existence of asymptotically free solutions.

Theorem 11 (see [5]). *Let $\phi = (\phi_1, \ldots, \phi_l) \in \mathbf{H}^{2,2}(\mathbb{R}^2)$ and let v be global in time of solutions of* (1) *satisfying a priori estimates*

$$\begin{gathered} \int_1^\infty \frac{1}{s^2}\|U_{1/m}(-s)v\|^2_{\mathbf{H}^{0,2}(\mathbb{R}^2)} ds < \infty, \\ \|\mathscr{F}U_{1/m}(-t)v\|_{\mathbf{L}^\infty(\mathbb{R}^2)} \leq C. \end{gathered} \tag{64}$$

We assume that the gauge condition (6) *holds for each $j \in \{1, \ldots, l\}$. If there exists $\widehat{\psi_+} = (\widehat{\psi_{1+}}, \ldots, \widehat{\psi_{l+}}) \in \mathbf{L}^2(\mathbb{R}^2) \cap \mathbf{L}^\infty(\mathbb{R}^2)$ such that*

$$\lim_{t\to\infty} \|v(t) - U_{1/m}(t)\psi_+\|_{\mathbf{L}^2(\mathbb{R}^2)} = 0, \tag{65}$$

then

$$F_j\left(D_{1/m_1}\widehat{\psi_{1+}}, \ldots, D_{1/m_l}\widehat{\psi_{l+}}\right) = 0 \tag{66}$$

for every $j \in \{1, \ldots, l\}$, where $\widehat{\psi_+} = \mathscr{F}\psi_+$.

If the support condition

$$\bigcap_{j=1}^{l} \operatorname{supp} \widehat{\psi_{j+}}\left(m_j\xi\right) \text{ is empty} \tag{67}$$

is satisfied, we have (66).

We give existence of wave operators of the system (1) for small final states by (66).

Theorem 12 (see [5]). *Let $\widehat{\psi_+} = (\widehat{\psi_{1+}}, \ldots, \widehat{\psi_{l+}}) \in \mathbf{H}^{2,2}(\mathbb{R}^2)$ satisfy the so-called support condition* (66). *Assume that F_j satisfies the gauge condition* (6) *for each $j \in \{1, \ldots, l\}$. Then for some $\varepsilon > 0$ there exists a unique global solution $v = (v_1, \ldots, v_l)$ of the system* (1) *such that*

$$\begin{gathered} v \in \mathbf{C}\left([1,\infty); \mathbf{L}^2\left(\mathbb{R}^2\right)\right), \\ \|v(t) - U_{1/m}(t)\psi_+\|_{\mathbf{L}^2(\mathbb{R}^2)} \leq Ct^{-b}, \quad 1/2 < b < 1 \end{gathered} \tag{68}$$

for large t and any $\widehat{\psi_+}$ satisfying

$$\|\psi_+\|_{\mathbf{H}^{2,2}(\mathbb{R}^2)} \leq \varepsilon. \tag{69}$$

Existence of wave operator for a single nonlinear Schrödinger equation was studied in [26, 27].

2.3. Modified Wave Operators of Nonlinear Schrödinger Systems in Two Space Dimensions. In Section 2.2, we discuss the existence of wave operators of the systems (1) and (28). However, if it is impossible to show existence of the wave operator, we have to modify the setting of the problem. We define the modified wave operator (see [25]) as follows. Let us construct a function $v_+ = (v_{i+})$ from a suitable function space and define a function $f(v_+, t)$ by v_+. Then we try to find a unique solution of nonlinear problems under the asymptotic condition

$$\lim_{t\to\infty} \left\| v(t) - U_{1/m}(t) f(v_+, t) \right\|_X = 0, \tag{70}$$

where $\|\cdot\|_X$ is the norm of Banach space X. Namely, the problem is solved if we can define the function f satisfying the asymptotic condition (70) by taking the structure of nonlinear terms into consideration. If we have a positive answer, we can define the map $MW_+ : v_+ \mapsto v(t)$ instead of the wave operator. We call MW_+ the modified wave operator since we modified the final states.

We consider (28) again which is written as

$$\begin{aligned} i\partial_t v_1 + \frac{1}{2m_1}\Delta v_1 &= \gamma \overline{v_1} v_2, \\ i\partial_t v_2 + \frac{1}{2m_2}\Delta v_2 &= v_1^2, \end{aligned} \tag{71}$$

in $(t, x) \in \mathbb{R} \times \mathbb{R}^2$. In Section 2.1, we stated the time decay estimates of solutions to this system in the case of $2m_1 = m_2$ and $\gamma = 1$. Since the nonlinearity is critical in this case, it is impossible to find a solution in the neighborhood of the free final state $(U_{1/m_1}(t)\phi_{1+}, U_{1/m_2}(t)\phi_{2+})$. Indeed we have the nonexistence of the usual scattering states.

Theorem 13 (see [4]). *Let $2m_1 = m_2$, $\gamma = 1$, and let*

$$v = (v_1, v_2) \in \mathbf{C}\left([0,\infty); \mathbf{H}^2\left(\mathbb{R}^2\right) \cap \mathbf{H}^{0,2}\left(\mathbb{R}^2\right)\right) \tag{72}$$

be a global solution obtained in Theorem 3. Then there does not exist any nontrivial scattering state $\phi_+ = (\phi_{1+}, \phi_{2+}) \in \mathbf{H}^2(\mathbb{R}^2) \cap \mathbf{H}^{0,2}(\mathbb{R}^2)$ such that $\phi_{1+} \neq 0$ and

$$\left\| v(t) - U_{1/m}\phi_+ \right\|_{\mathbf{L}^2(\mathbb{R}^2)} = \sum_{j=1}^{2} \left\| v_j(t) - U_{1/m_j}\phi_{j+} \right\|_{\mathbf{L}^2(\mathbb{R}^2)} \longrightarrow 0 \tag{73}$$

as $t \to \infty$.

From the result, we need to modify the final state with time dependence. We note here that the modified wave operator for nonlinear dispersive equation was first constructed in [28] for the cubic nonlinear Schrödinger equations in one space dimension and then constructed in [29] for the derivative nonlinear Schrödinger equation, by changing it via a suitable transformation (see [30]) to a system of cubic nonlinear Schrödinger equations without derivatives of unknown function; see also [31] for recent developments. Two-dimensional case was studied in [32].

In Section 2.2, from (34), we see that the asymptotic behavior of solutions of (28) under the mass resonance condition $2m_1 = m_2$ is determined by the solutions of the following system:

$$\begin{aligned} i\partial_t \varphi_{1\gamma} &= \gamma t^{-1} \overline{\varphi_{1\gamma}} \varphi_{2\gamma}, \\ i\partial_t \varphi_{2\gamma} &= t^{-1} \varphi_{1\gamma}^2. \end{aligned} \tag{74}$$

By calculation we find that the particular solutions of (74) are

$$\begin{aligned} \varphi_{1\gamma}(t,\xi) &= -\frac{i\omega(\xi) e^{i\theta(\xi)}}{1 + \omega(\xi)\log t}, \\ \varphi_{2\gamma}(t,\xi) &= -\frac{i\omega(\xi) e^{2i\theta(\xi)}}{1 + \omega(\xi)\log t} \end{aligned} \tag{75}$$

in the case of $\gamma = -1$ and the particular solutions of (74) are

$$\begin{aligned} \varphi_{1\gamma}(t,\xi) &= \omega(\xi) e^{i\theta(\xi) + (i/\sqrt{2})\omega(\xi)\log t} \\ \varphi_{2\gamma}(t,\xi) &= -\frac{1}{\sqrt{2}}\omega(\xi) e^{2i\theta(\xi) + i\sqrt{2}\omega(\xi)\log t} \end{aligned} \tag{76}$$

in the case of $\gamma = 1$, where $\omega(\xi) > 0$ and $\theta(\xi)$ is a real valued given function. We also find that

$$\varphi_{1\gamma}(\xi) = 0, \qquad \varphi_{2\gamma}(\xi) = \omega(\xi) e^{i\theta(\xi)} \tag{77}$$

are particular solutions of (74) when $\gamma = \pm 1$.

The following theorem shows existence of the modified wave operators of (28).

Theorem 14 (see [1]). *Let $2m_1 = m_2$ and $\gamma = \pm 1$. Then there exists $\varepsilon > 0$ such that, for any $\omega, \theta \in \mathbf{H}^2(\mathbb{R}^2)$ with norm $\|\omega\|_{\mathbf{H}^2(\mathbb{R}^2)} \le \varepsilon$, (28) has a unique global solution*

$$v = (v_1, v_2) \in \mathbf{C}\left([1,\infty); \mathbf{L}^2\left(\mathbb{R}^2\right)\right). \tag{78}$$

Moreover, the following estimate

$$\begin{aligned} &\left\| v(t) + U_{1/m}(t) \mathscr{F}^{-1} D_m \varphi_\gamma(t) \right\|_{\mathbf{L}^2(\mathbb{R}^2)} \\ &= \sum_{j=1}^{2} \left\| v_j(t) + U_{1/m_j}(t) \mathscr{F}^{-1} D_{m_j} \varphi_{j\gamma}(t) \right\|_{\mathbf{L}^2(\mathbb{R}^2)} \le Ct^{-b} \end{aligned} \tag{79}$$

holds for all $t \ge 1$, where $1/2 < b < 1$.

Using the resonance condition, $2m_1 = m_2$, we get the existence of modified wave operators by the contraction mapping principle. Since the identity $U_{1/m_j}(t) = M^{-m_j} D_{t/m_j} \mathscr{F} M^{-m_j}$ is known for $j = 1, 2$, we have the estimate from the above theorem

$$\left\| v(t) - iM^{-m} D_t \mathscr{F} M^{-1/m} \mathscr{F}^{-1} \varphi_\gamma(t) \right\|_{\mathbf{L}^2(\mathbb{R}^2)} \le Ct^{-b} \tag{80}$$

for all $t \ge 1$, where $1/2 < b < 1$.

Existence of modified wave operator for a single nonlinear Schrödinger equation was studied in [26, 27]. Asymptotic behavior of solutions to nonlinear wave systems was studied in [33]. It was shown that the asymptotic behavior of solutions of them depends on the corresponding ordinary differential equations which are related to (74). In [33], another special solution was presented and the method can be applicable to nonlinear Schrödinger systems with a slight modification.

2.4. Nonlinear Schrödinger Systems in Higher Space Dimensions I. In the case of higher space dimensions, $n \geq 3$, the scattering theory for (28)

$$\begin{aligned} i\partial_t v_1 + \frac{1}{2m_1}\Delta v_1 &= \gamma \overline{v_1} v_2, \\ i\partial_t v_2 + \frac{1}{2m_2}\Delta v_2 &= v_1^2 \end{aligned} \tag{81}$$

was studied in [2].

We will explain the scattering problem (See [25]) briefly. We may assume the existence of wave operator W_+ which maps a Banach space X into itself. Namely, for any given $v_+ \in X$, we assume that there exists a unique solution $v(t) \in \mathbf{C}([0,\infty); X)$ of the nonlinear system such that

$$\lim_{t\to\infty} \left\| U_{1/m}(-t)v(t) - v_+ \right\|_X = 0. \tag{82}$$

We consider the initial value problem with the data $v(0)$ which are determined by the solution $v(t)$ in the time interval $t \in [0,\infty)$. If the initial value problem has a unique global solution $v(t) \in \mathbf{C}((-\infty,0]; X)$ and we can find a unique $v_- \in X$ from the solution $v(t)$ satisfying

$$\lim_{t\to-\infty} \left\| U_{1/m}(-t)v(t) - v_- \right\|_X = 0, \tag{83}$$

then we can define the inverse wave operator $W_-^{-1} : v(0) \in X \mapsto v_- \in X$. From this operator we can define $S = W_-^{-1}W_+ : X \to X$. We call the operator the scattering operator.

In the case, $n \geq 4$, existence of the scattering operator was proved in the space $\mathbf{H}^{(n/2)-2}(\mathbb{R}^n)$ which is close to the invariant space $\dot{\mathbf{H}}^{(n/2)-2}(\mathbb{R}^n)$. In the case of $n = 4$, we have the results in the invariant space $\mathbf{L}^2(\mathbb{R}^4)$. In the case of $n = 3$, existence of the scattering operator was proved in the space $\mathbf{H}^{0,1/2}(\mathbb{R}^3)$, under the mass resonance condition $2m_1 = m_2$, which is close to the invariant space $\dot{\mathbf{H}}^{0,1/2}(\mathbb{R}^3)$. To state the following theorem, we introduce

$$B_\varepsilon = \left\{ \phi = (\phi_1, \phi_2) \in \mathbf{H}^{(n/2)-2}(\mathbb{R}^n); \quad \|\phi\|_{\mathbf{H}^{(n/2)-2}(\mathbb{R}^n)} = \sum_{j=1}^{2} \left\|\phi_j\right\|_{\mathbf{H}^{(n/2)-2}(\mathbb{R}^n)} \leq \varepsilon \right\}. \tag{84}$$

Theorem 15 (see [2]). *Let $n \geq 4$. Then there exist ε_0 and C_0 such that $0 < \varepsilon_0 \leq 1 \leq C_0$ with the following property.*

(1) *For any ε with $0 < \varepsilon \leq \varepsilon_0$ and any $\phi = (\phi_1, \phi_2) \in B_\varepsilon$, (28) has a unique global solution $v = (v_1, v_2) \in \mathbf{C}(\mathbb{R}; \mathbf{H}^{(n/2)-2}(\mathbb{R}^n))$. Moreover, there exist unique $\phi_\pm = (\phi_{1\pm}, \phi_{2\pm}) \in B_{C_0\varepsilon}$ such that*

$$\left\| v(t) - U_{1/m}(t)\phi_\pm \right\|_{\mathbf{H}^{(n/2)-2}(\mathbb{R}^n)} \longrightarrow 0 \tag{85}$$

as $t \to \pm\infty$.

$(2)_+$ *For any ε with $0 < \varepsilon \leq \varepsilon_0$ and any $\phi_+ = (\phi_{1+}, \phi_{2+}) \in B_\varepsilon$, (28) has a unique global solution $v = (v_1, v_2) \in \mathbf{C}(\mathbb{R}; \mathbf{H}^{(n/2)-2}(\mathbb{R}^n))$ such that $v(0) = (v_1(0), v_2(0)) \in B_{C_0\varepsilon}$,*

$$\left\| v(t) - U_{1/m}(t)\phi_+ \right\|_{\mathbf{H}^{(n/2)-2}(\mathbb{R}^n)} \longrightarrow 0, \tag{86}$$

as $t \to +\infty$.

$(2)_-$ *For any ε with $0 < \varepsilon \leq \varepsilon_0$ and any $\phi_- = (\phi_{1-}, \phi_{2-}) \in B_\varepsilon$, (28) has a unique solution $v = (v_1, v_2) \in \mathbf{C}(\mathbb{R}; \mathbf{H}^{(n/2)-2}(\mathbb{R}^n))$ such that $v(0) = (v_1(0), v_2(0)) \in B_{C_0\varepsilon}$,*

$$\left\| v(t) - U_{1/m}(t)\phi_- \right\|_{\mathbf{H}^{(n/2)-2}(\mathbb{R}^n)} \longrightarrow 0 \tag{87}$$

as $t \to -\infty$.

Corollary 16 (see [2]). *The wave operators $W_\pm : \phi_\pm \mapsto v(0)$ are defined as mappings from B_ε to $B_{C_0\varepsilon}$ for any ε with $0 < \varepsilon \leq \varepsilon_0$. The scattering operator $S : \phi_+ \mapsto \phi_-$ is defined as a mapping from $B_{C_0^{-1}\varepsilon}$ to $B_{C_0\varepsilon}$ for any ε with $0 < \varepsilon \leq \varepsilon_0$. To state the following theorem, we introduce*

$$\widetilde{B}_\varepsilon = \left\{ \phi = (\phi_1, \phi_2) \in \mathbf{H}^{0,1/2}(\mathbb{R}^3); \quad \|\phi\|_{\mathbf{H}^{0,1/2}(\mathbb{R}^3)} = \sum_{j=1}^{2} \left\|\phi_j\right\|_{\mathbf{H}^{0,1/2}(\mathbb{R}^3)} \leq \varepsilon \right\}. \tag{88}$$

Theorem 17 (see [2]). *Let $2m_1 = m_2$. Then there exist ε_0 and C_0 such that $0 < \varepsilon_0 \leq 1 \leq C_0$ with the following property.*

(1) *For any ε with $0 < \varepsilon \leq \varepsilon_0$ and any $\phi \in \widetilde{B}_\varepsilon$, (28) has a unique solution v with $U_{1/m}(-t)v \in \mathbf{C}(\mathbb{R}; \mathbf{H}^{0,1/2}(\mathbb{R}^3))$. Moreover, there exist unique $\phi_\pm \in \widetilde{B}_{C_0\varepsilon}$ such that*

$$\left\| U_{1/m}(-t)v(t) - \phi_\pm \right\|_{\mathbf{H}^{0,1/2}(\mathbb{R}^3)} \longrightarrow 0 \tag{89}$$

as $t \to \pm\infty$.

$(2)_+$ *For any ε with $0 < \varepsilon \leq \varepsilon_0$ and any $\phi_+ \in \widetilde{B}_\varepsilon$, (28) has a unique solution v with $U_{1/m}(-t)v \in \mathbf{C}(\mathbb{R}; \mathbf{H}^{0,1/2}(\mathbb{R}^3))$ such that $v(0) \in \widetilde{B}_{C_0\varepsilon}$,*

$$\left\| U_{1/m}(-t)v(t) - \phi_+ \right\|_{\mathbf{H}^{0,1/2}(\mathbb{R}^3)} \longrightarrow 0 \tag{90}$$

as $t \to +\infty$.

$(2)_-$ *For any ε with $0 < \varepsilon \leq \varepsilon_0$ and any $\phi_- \in \widetilde{B}_\varepsilon$, (28) has a unique solution v with $U_{1/m}(-t)v \in \mathbf{C}(\mathbb{R}; \mathbf{H}^{0,1/2}(\mathbb{R}^3))$ such that $v(0) \in \widetilde{B}_{C_0\varepsilon}$,*

$$\left\| U_{1/m}(-t)v(t) - \phi_- \right\|_{\mathbf{H}^{0,1/2}(\mathbb{R}^3)} \longrightarrow 0 \tag{91}$$

as $t \to -\infty$.

Corollary 18 (see [2]). *The wave operators $W_\pm : \phi_\pm \mapsto v(0)$ are defined as mappings from $\widetilde{B}_\varepsilon$ to $\widetilde{B}_{C_0\varepsilon}$ for any ε with $0 < \varepsilon \leq \varepsilon_0$. The scattering operator $S : \phi_+ \mapsto \phi_-$ is defined as a mapping from $\widetilde{B}_{C_0^{-1}\varepsilon}$ to $\widetilde{B}_{C_0\varepsilon}$ for any ε with $0 < \varepsilon \leq \varepsilon_0$.*

2.5. Nonlinear Schrödinger Systems in Higher Space Dimensions II. In [3], the finite time blow-up of the negative energy solutions for the system (28) was discussed in the case of $4 \le n \le 6$ under the mass conditions $2m_1 = m_2$ and $\gamma \in \mathbb{R}$. To state the blow-up result we need local existence in time of solutions to (28).

Theorem 19 (see [3]). *Let $n \le 6$ and $m_2 = 2m_1$. Then, for any*

$$\phi = (\phi_1, \phi_2) \in \mathbf{H}^{0,1}(\mathbb{R}^n) \cap \mathbf{H}^1(\mathbb{R}^n), \tag{92}$$

there exists $T(\phi) > 0$ such that (28) has a unique solution v with

$$\begin{aligned} U_{1/m}(-t)\, v(t) &= \left(U_{1/m_1}(-t)\, v_1(t), U_{1/m_2}(-t)\, v_2(t)\right) \\ &\in \mathbf{C}\left([-T,T]; \mathbf{H}^{0,1}(\mathbb{R}^n) \cap \mathbf{H}^1(\mathbb{R}^n)\right). \end{aligned} \tag{93}$$

From Theorem 19 we have the energy conservation law such that

$$\begin{aligned} &\frac{1}{2m_1}\|\nabla v_1(t)\|^2 + \frac{\gamma}{4m_2}\|\nabla v_2(t)\|^2 + \gamma \operatorname{Re}\left(v_2(t), v_1(t)^2\right) \\ &\quad = \frac{1}{2m_1}\|\nabla \phi_1\|^2 + \frac{\gamma}{4m_2}\|\nabla \phi_2\|^2 + \gamma \operatorname{Re}\left(\phi_2, \phi_1^2\right), \end{aligned} \tag{94}$$

where

$$(f, g) = \int f \cdot \overline{g}\, dx. \tag{95}$$

We need the virial identity to prove the blow-up result.

Theorem 20 (see [3]). *Let $n \le 6$ and $m_2 = 2m_1$. Let $\gamma \in \mathbb{R}$ and let v be the local solution constructed in Theorem 19. Then*

$$\begin{aligned} &\|xv_1(t)\|^2_{\mathbf{L}^2(\mathbb{R}^n)} + \gamma\|xv_2(t)\|^2_{\mathbf{L}^2(\mathbb{R}^n)} \\ &\quad = \|x\phi_1\|^2_{\mathbf{L}^2(\mathbb{R}^n)} + \gamma\|x\phi_2\|^2_{\mathbf{L}^2(\mathbb{R}^n)} + P_0 t + \frac{n}{2m_1}E_0 t^2 \\ &\qquad + \frac{4-n}{m_1}\int_0^t (t-s)\left(\frac{1}{2m_1}\|\nabla v_1(s)\|^2_{\mathbf{L}^2(\mathbb{R}^n)}\right. \\ &\qquad\qquad \left. + \frac{\gamma}{8m_1}\|\nabla v_2(s)\|^2_{\mathbf{L}^2(\mathbb{R}^n)}\right) ds \end{aligned} \tag{96}$$

for all $t \in [-T, T]$, where

$$\begin{aligned} P_0 &= \frac{2}{m_1}\operatorname{Im}(\nabla\phi_1, x\phi_1) + \frac{\gamma}{m_1}\operatorname{Im}(\nabla\phi_2, x\phi_2), \\ E_0 &= \frac{1}{2m_1}\|\nabla\phi_1\|^2_{\mathbf{L}^2(\mathbb{R}^n)} + \frac{\gamma}{8m_1}\|\nabla\phi_2\|^2_{\mathbf{L}^2(\mathbb{R}^n)} + \gamma\operatorname{Re}\left(\phi_2, \phi_1^2\right). \end{aligned} \tag{97}$$

By a standard argument, we have the following result

Theorem 21 (see [3]). *Let $4 \le n \le 6$. Let $m_2 = 2m_1$ and $\gamma > 0$. Let ϕ and v be as in Theorem 20. Then the maximal existence time for v is finite in the following cases:*

$$\begin{gathered} E_0 < 0, \\ E_0 = 0, \quad P_0 < 0, \end{gathered} \tag{98}$$

where E_0 and P_0 are as in Theorem 20.

3. Related and Open Problems

Asymptotic behavior in time of solutions to (28)

$$\begin{aligned} i\partial_t v_1 + \frac{1}{2m_1}\Delta v_1 &= \gamma \overline{v_1} v_2, \\ i\partial_t v_2 + \frac{1}{2m_2}\Delta v_2 &= v_1^2, \end{aligned} \tag{99}$$

is an open problem for one space dimension which is considered the subcritical case. Existence of scattering operator is also an open problem for $n = 1, 2$. We now turn to the relativistic version of (28)

$$\begin{aligned} \partial_t^2 u_1 - c^2\Delta u_1 + m_1^2 c^4 u_1 &= -2\gamma c^2 m_1 u_1 u_2, \\ \partial_t^2 u_2 - c^2\Delta u_2 + m_2^2 c^4 u_2 &= -2c^2 m_2 u_1^2. \end{aligned} \tag{100}$$

We let $c = 1$ in (100); then

$$\begin{aligned} \partial_t^2 u_1 - \Delta u_1 + m_1^2 u_1 &= \lambda_1 u_1 u_2, \\ \partial_t^2 u_2 - \Delta u_2 + m_2^2 u_2 &= \lambda_2 u_1^2, \end{aligned} \tag{101}$$

where $\lambda_1, \lambda_2 \in \mathbb{C}$. Asymptotic behavior of solutions to (101) when $n = 2$ was studied in papers [22, 34, 35] with mass nonresonance condition $2m_1 \ne m_2$. Scattering operator was constructed in a paper [36] if $m_2 < 2m_1$. However existence of scattering operator for (28) is an open problem even if $m_2 < 2m_1$. Global existence and time decay of small solutions were obtained in [37] for the resonance case $2m_1 = m_2$, under some regularity and compactness conditions on the initial data. However the large time asymptotics and existence of modified scattering operators are not known for the case. The asymptotic behavior of solutions to (101) in one space dimension is also an open problem.

Small data blow-up for a system of nonlinear Schrodinger equations was studied in [38] under some conditions on nonlinearities, but it is an open problem for (28).

The asymptotic behavior of solutions to quadratic derivative nonlinear Schrödinger systems has been considered recently in papers [39, 40] under some structural conditions on the nonlinearity. If the structural conditions are not satisfied, the problem is open.

Conflict of Interests

The authors declare that there is no conflict of interests regarding the publication of this paper.

References

[1] N. Hayashi, C. Li, and P. I. Naumkin, "Modified wave operator for a system of nonlinear Schrödinger equations in 2D," *Communications in Partial Differential Equations*, vol. 37, no. 6, pp. 947–968, 2012.

[2] N. Hayashi, C. Li, and T. Ozawa, "Small data scattering for a system of nonlinear Schrödinger equations," *Differential Equations & Applications*, vol. 3, no. 3, pp. 415–426, 2011.

[3] N. Hayashi, T. Ozawa, and K. Tanaka, “On a system of nonlinear Schrödinger equations with quadratic interaction,” *Annales de l’Institut Henri Poincaré. Analyse Non Linéaire*, vol. 30, no. 4, pp. 661–690, 2013.

[4] N. Hayashi, C. Li, and P. I. Naumkin, “On a system of nonlinear Schrödinger equations in 2D,” *Differential and Integral Equations*, vol. 24, no. 5-6, pp. 417–434, 2011.

[5] C. Li, “Decay of solutions for a system of nonlinear Schrödinger equations in 2D,” *Discrete and Continuous Dynamical Systems A*, vol. 32, no. 12, pp. 4265–4285, 2012.

[6] C. Li, “Further decay results on the system of NLS equations in lower order Sobolev spaces,” in *Proceedings of the 4th MSJ-SI Conference on Nonlinear Dynamics in Partial Differential Equations*, Kyushu University, September 2011.

[7] S. Katayama, C. Li, and H. Sunagawa, “A remark on decay rates of solutions for a system of quadratic nonlinear Schrödinger equations in 2D,” *Differential and Integral Equations*, vol. 27, no. 3-4, pp. 301–312, 2014.

[8] C. Li and N. Hayashi, “Critical nonlinear Schrödinger equations with data in homogeneous weighted L^2 spaces,” Preprint.

[9] C. Li, “On a system of quadratic nonlinear Schrödinger equations and scale invariant spaces in 2D,” Preprint.

[10] M. Colin and T. Colin, “On a quasilinear Zakharov system describing laser-plasma interactions,” *Differential and Integral Equations*, vol. 17, no. 3-4, pp. 297–330, 2004.

[11] J. Ginibre and G. Velo, “On a class of nonlinear Schrödinger equations. I. The Cauchy problem, general case ; II Scattering theory, general case,” *Journal of Functional Analysis*, vol. 32, no. 1, pp. 1–71, 1979.

[12] T. Cazenave, *Semilinear Schrödinger Equations*, vol. 10, Courant Institute of Mathematical Sciences, New York, NY, USA; American Mathematical Society, Providence, RI, USA, 2003.

[13] S. Klainerman, “Global existence of small amplitude solutions to nonlinear Klein-Gordon equations in four space-time dimensions,” *Communications on Pure and Applied Mathematics*, vol. 38, no. 5, pp. 631–641, 1985.

[14] J. Shatah, “Normal forms and quadratic nonlinear Klein-Gordon equations,” *Communications on Pure and Applied Mathematics*, vol. 38, no. 5, pp. 685–696, 1985.

[15] N. Hayashi and P. I. Naumkin, “Scattering operator for nonlinear Klein-Gordon equations in higher space dimensions,” *Journal of Differential Equations*, vol. 244, no. 1, pp. 188–199, 2008.

[16] Y. Tsutsumi, “L^2-solutions for nonlinear Schrödinger equations and nonlinear groups,” *Funkcialaj Ekvacioj*, vol. 30, no. 1, pp. 115–125, 1987.

[17] J. Bergh and J. Löfström, *Interpolation Spaces*, Springer, New York, NY, USA, 1976.

[18] N. Hayashi and T. Ozawa, “Scattering theory in the weighted $L^2(\mathbf{R}^n)$ spaces for some Schrödinger equations,” *Annales de l’Institut Henri Poincaré. Physique Théorique*, vol. 48, no. 1, pp. 17–37, 1988.

[19] M. Colin, T. Colin, and M. Ohta, “Stability of solitary waves for a system of nonlinear Schrödinger equations with three wave interaction,” *Annales de l’Institut Henri Poincaré. Analyse Non Linéaire*, vol. 26, no. 6, pp. 2211–2226, 2009.

[20] N. Hayashi and P. I. Naumkin, “Asymptotics in large time of solutions to the nonlinear Schrödinger and Hartree equations,” *American Journal of Mathematics*, vol. 120, no. 2, pp. 369–389, 1998.

[21] A. Shimomura, “Asymptotic behavior of solutions for Schrödinger equations with dissipative nonlinearities,” *Communications in Partial Differential Equations*, vol. 31, no. 9, pp. 1407–1423, 2006.

[22] H. Sunagawa, “A note on the large time asymptotics for a system of Klein-Gordon equations,” *Hokkaido Mathematical Journal*, vol. 33, no. 2, pp. 457–472, 2004.

[23] H. Sunagawa, “Large time asymptotics of solutions to nonlinear Klein-Gordon systems,” *Osaka Journal of Mathematics*, vol. 42, no. 1, pp. 65–83, 2005.

[24] Y. Kawahara and H. Sunagawa, “Remarks on global behavior of solutions to nonlinear Schrödinger equations,” *Proceedings of the Japan Academy A: Mathematical Sciences*, vol. 82, no. 8, pp. 117–122, 2006.

[25] N. Hayashi, “Asymptotics of nonlinear dispersive-type evolution equations,” *American Mathematical Society Translations*, vol. 2, no. 230, pp. 21–43, 2010.

[26] N. Hayashi, P. I. Naumkin, A. Shimomura, and S. Tonegawa, “Modified wave operators for nonlinear Schrödinger equations in one and two dimensions,” *Electronic Journal of Differential Equations*, vol. 2004, no. 62, pp. 1–16, 2004.

[27] N. Hayashi, H. Wang, and P. I. Naumkin, “Modified wave operators for nonlinear Schrödinger equations in lower order Sobolev spaces,” *Journal of Hyperbolic Differential Equations*, vol. 8, no. 4, pp. 759–775, 2011.

[28] T. Ozawa, “Long range scattering for nonlinear Schrödinger equations in one space dimension,” *Communications in Mathematical Physics*, vol. 139, no. 3, pp. 479–493, 1991.

[29] N. Hayashi and T. Ozawa, “Modified wave operators for the derivative nonlinear Schrödinger equation,” *Mathematische Annalen*, vol. 298, no. 1, pp. 557–576, 1994.

[30] N. Hayashi, “The initial value problem for the derivative nonlinear Schrödinger equation in the energy space,” *Nonlinear Analysis: Theory, Methods & Applications*, vol. 20, no. 7, pp. 823–833, 1993.

[31] Z. Guo, N. Hayashi, Y. Lin, and P. I. Naumkin, “Modified scattering operator for the derivative nonlinear Schrödinger equation,” *SIAM Journal on Mathematical Analysis*, vol. 45, no. 6, pp. 3854–3871, 2013.

[32] J. Ginibre and T. Ozawa, “Long range scattering for non-linear Schrödinger and Hartree equations in space dimension $n \geq 2$,” *Communications in Mathematical Physics*, vol. 151, no. 3, pp. 619–645, 1993.

[33] S. Katayama, T. Matoba, and H. Sunagawa, “A semilinear hyperbolic system violating the null condition,” http://arxiv.org/abs/1206.0066.

[34] J.-M. Delort, D. Fang, and R. Xue, “Global existence of small solutions for quadratic quasilinear Klein-Gordon systems in two space dimensions,” *Journal of Functional Analysis*, vol. 211, no. 2, pp. 288–323, 2004.

[35] H. Sunagawa, “On global small amplitude solutions to systems of cubic nonlinear Klein-Gordon equations with different mass terms in one space dimension,” *Journal of Differential Equations*, vol. 192, no. 2, pp. 308–325, 2003.

[36] N. Hayashi and P. I. Naumkin, “A system of quadratic nonlinear Klein-Gordon equations in 2D,” *Journal of Differential Equations*, vol. 254, no. 8, pp. 3615–3646, 2013.

[37] Y. Kawahara and H. Sunagawa, “Global small amplitude solutions for two-dimensional nonlinear Klein-Gordon systems in the presence of mass resonance,” *Journal of Differential Equations*, vol. 251, no. 9, pp. 2549–2567, 2011.

[38] T. Ozawa and H. Sunagawa, “Small data blow-up for a system of nonlinear Schrödinger equations,” *Journal of Mathematical Analysis and Applications*, vol. 399, no. 1, pp. 147–155, 2013.

[39] H. Hirayama, “Well-posedness and scattering for a system of quadratic derivative nonlinear Schrödinger equations with low regularity initial data,” http://arxiv-web3.library.cornell.edu/abs/1311.6102.

[40] M. Ikeda, S. Katayama, and H. Sunagawa, “Null structure in a system of quadratic derivative nonlinear Schrödinger equations,” http://arxiv.org/abs/1305.3662.

Hindawi Publishing Corporation
The Scientific World Journal
Volume 2014, Article ID 580871, 5 pages
http://dx.doi.org/10.1155/2014/580871

Research Article

Blowup Phenomena for the Compressible Euler and Euler-Poisson Equations with Initial Functional Conditions

Sen Wong and Manwai Yuen

Department of Mathematics and Information Technology, The Hong Kong Institute of Education, 10 Lo Ping Road, Tai Po, New Territories, Hong Kong

Correspondence should be addressed to Manwai Yuen; nevetsyuen@hotmail.com

Received 16 January 2014; Accepted 2 March 2014; Published 30 March 2014

Academic Editors: D. Baleanu and C. M. Khalique

We study, in the radial symmetric case, the finite time life span of the compressible Euler or Euler-Poisson equations in R^N. For time $t \geq 0$, we can define a functional $H(t)$ associated with the solution of the equations and some testing function f. When the pressure function P of the governing equations is of the form $P = K\rho^\gamma$, where ρ is the density function, K is a constant, and $\gamma > 1$, we can show that the nontrivial C^1 solutions with nonslip boundary condition will blow up in finite time if $H(0)$ satisfies some initial functional conditions defined by the integrals of f. Examples of the testing functions include $r^{N-1}\ln(r+1)$, $r^{N-1}e^r$, $r^{N-1}(r^3 - 3r^2 + 3r + \varepsilon)$, $r^{N-1}\sin((\pi/2)(r/R))$, and $r^{N-1}\sinh r$. The corresponding blowup result for the 1-dimensional nonradial symmetric case is also given.

1. Introduction

The compressible isentropic Euler ($\delta = 0$) or Euler-Poisson ($\delta = \pm 1$) equations for fluids can be written as

$$\rho_t + \nabla \cdot (\rho u) = 0,$$
$$\rho \left[u_t + (u \cdot \nabla) u \right] + \nabla P = \rho \nabla \Phi, \tag{1}$$
$$\Delta \Phi (t, x) = \delta \alpha (N) \rho,$$

where $\alpha(N)$ is a constant related to the unit ball in R^N. As usual, $\rho = \rho(t, x) \geq 0$ and $u = u(t, x) \in \mathbf{R}^N$ are the density and the velocity, respectively. $P = P(\rho)$ is the pressure function. The γ-law for the pressure term $P(\rho)$ can be expressed as

$$P(\rho) = K\rho^\gamma, \tag{2}$$

for which the constant $\gamma \geq 1$. If $K > 0$, it is a system with pressure. If $K = 0$, it is a pressureless system.

When $\delta = -1$, the system is self-attractive. The system (1) is the Newtonian description of gaseous stars (cf. [1, 2]). When $\delta = 1$, the system comprises the Euler-Poisson equations with repulsive forces and can be applied as a semiconductor model [3]. When $\delta = 0$, the system comprises the compressible Euler equations and can be applied as a classical model in fluid mechanics [4, 5].

The solutions in radial symmetry are expressed by

$$\rho = \rho (t, r), \qquad u = \frac{x}{r} V (t, r) =: \frac{x}{r} V, \tag{3}$$

with the radius $r = \left(\sum_{i=1}^{N} x_i^2\right)^{1/2}$.

The Poisson equation $(1)_3$ becomes

$$\Phi_r (t, r) = \frac{\alpha (N) \delta}{r^{N-1}} \int_0^r \rho (t, s) s^{N-1} ds. \tag{4}$$

The equations in radial symmetry can be expressed in the following form:

$$\rho_t + V\rho_r + \rho V_r + \frac{N-1}{r} \rho V = 0,$$
$$\rho \left(V_t + V V_r\right) + P_r = \rho \Phi_r. \tag{5}$$

The blowup phenomena have attracted the attention of many mathematicians. Regarding the Euler equations

($\delta = 0$), Makino et al. [6] first investigated the blowup of "tame solutions." In 1990, Makino and Perthame further analyzed the corresponding solutions for the equations with gravitational forces ($\delta = -1$) [7]. Subsequently, Perthame [8] studied the blowup results for the 3-dimensional pressureless system with repulsive forces ($\delta = 1$). Additional results of the Euler system can be found in [9–12].

In this paper, we introduce the nonslip boundary condition [13], which is expressed by

$$\rho(t,R) = 0, \qquad V(t,R) = 0, \tag{6}$$

for all $t \geq 0$ and with the constant $R > 0$.

In 2011, Yuen used the integration method to show the C^1 blowup phenomenon with a "radial dependent" initial functional:

$$I_0 = \int_0^R r^n V_0 dr > 0, \tag{7}$$

for $n = 1$ [14] and $n > 0$ [15].

Following the integration method, we observe that the functional (7) could be generalized to have the following result.

Theorem 1. *Define the functional associated with the testing function f by*

$$H(t) = \int_0^R f(r) V(t) dr \tag{8}$$

and denote the initial functional $H(0)$ by H_0. Consider the Euler or Euler-Poisson equations (1) in R^N. For pressureless fluids ($K = 0$) or $\gamma > 1$, and the nontrivial classical C^1 solutions (ρ, V) with radial symmetry and the first boundary condition (6), we have the following results.

(a) For the attractive forces ($\delta = -1$), if H_0 satisfies the following initial functional condition:

$$\frac{H_0^2}{2R\int_0^R f(r)\,dr} - M\int_0^R \frac{f(r)}{r^{N-1}} dr > 0, \tag{9}$$

with a total mass M of the fluid and an arbitrary nonnegative and nonzero $C^1[0,R]$ testing function $f(r)$ satisfying the following properties:

(1) $\lim_{r\to 0}(f(r)/r^{N-1})$ *exists,*

(2) $f(r)/r$ *is increasing,*

then the solutions blow up in finite time.

(b) For the nonattractive forces ($\delta = 0$ or 1), if H_0 satisfies the following initial functional condition:

$$H_0 = \int_0^R f(r) V_0 dr > 0, \tag{10}$$

then the solutions blow up on or before the finite time $T = (2R\int_0^R f(r)dr)/H_0$.

2. The Generalized Integration Method

The key ideas in obtaining the above results are (i) to design the right form of generalized functional and find the right class of testing functions and (ii) to transform the nonlinear partial differential equations into the Riccati inequality.

Proof. The density function $\rho(t, x(t; x))$ conserves its nonnegative nature.

The mass equation $(1)_1$

$$\frac{D\rho}{Dt} + \rho\nabla\cdot u = 0, \tag{11}$$

with the material derivative

$$\frac{D}{Dt} = \frac{\partial}{\partial t} + (u\cdot\nabla), \tag{12}$$

could be integrated as

$$\rho(t,x_0) = \rho_0(x_0(0,x_0))\exp\left(-\int_0^t \nabla\cdot u(t,x_0(t;x_0))\,dt\right) \geq 0 \tag{13}$$

for $\rho_0(x_0(0,x_0)) \geq 0$.

For the nontrivial density initial condition in radial symmetry, $\rho_0(r) \neq 0$, we have

$$\begin{gathered} V_t + VV_r + K\gamma\rho^{\gamma-2}\rho_r = \Phi_r \\ V_t + \frac{\partial}{\partial r}\left(\frac{1}{2}V^2\right) + K\gamma\rho^{\gamma-2}\rho_r = \Phi_r \\ f(r)V_t + f(r)\frac{\partial}{\partial r}\left(\frac{1}{2}V^2\right) + K\gamma f(r)\rho^{\gamma-2}\rho_r = f(r)\Phi_r. \end{gathered} \tag{14}$$

(Here we multiplied the function $f(r)$ on both sides.)

Subsequently, we take integration with respect to r from 0 to R for $\gamma > 1$ or $K = 0$:

$$\int_0^R f(r)V_t dr + \int_0^R f(r)\frac{d}{dr}\left(\frac{1}{2}V^2\right) + \int_0^R K\gamma f(r)\rho^{\gamma-2}\rho_r dr = \int_0^R f(r)\Phi_r dr. \tag{15}$$

(a) For $\delta = -1$, we have

$$\int_0^R f(r)V_t dr + \int_0^R f(r)\frac{d}{dr}\left(\frac{1}{2}V^2\right) + \int_0^R \frac{K\gamma f(r)}{\gamma-1}d\rho^{\gamma-1} = -\int_0^R\left[\frac{\alpha(N)f(r)}{r^{N-1}}\int_0^r \rho(t,s)s^{N-1}ds\right]dr, \tag{16}$$

$$\int_0^R f(r)V_t dr + \int_0^R f(r)\frac{d}{dr}\left(\frac{1}{2}V^2\right) + \int_0^R \frac{K\gamma f(r)}{\gamma-1}d\rho^{\gamma-1} \geq -\int_0^R\left[\frac{f(r)M}{r^{N-1}}\right]dr,$$

with the total mass

$$M=\alpha(N)\int_0^R \rho(t,s)\,s^{N-1}ds. \tag{17}$$

Then we apply the integration by parts to deduce

$$\begin{aligned}&\int_0^R f(r)V_t dr-\frac{1}{2}\int_0^R V^2 df(r)\\&\quad+\frac{1}{2}\left[f(r)V^2(t,r)\right]\Big|_{r=0}^{r=R}-\int_0^R\frac{K\gamma f'(r)}{\gamma-1}\rho^{\gamma-1}dr\\&\quad+\frac{K\gamma}{\gamma-1}\left[f(r)\rho^{\gamma-1}(t,r)\right]\Big|_{r=0}^{r=R}\geq-\int_0^R\left[\frac{f(r)M}{r^{N-1}}\right]dr.\end{aligned} \tag{18}$$

Inequality (18) with the first boundary condition (6) becomes

$$\frac{d}{dt}\int_0^R VdF(r)\geq\frac{1}{2}\int_0^R V^2f'(r)\,dr-\int_0^R\left[\frac{f(r)M}{r^{N-1}}\right]dr, \tag{19}$$

with $dF(r)=f(r)dr$ and $\gamma>1$ or $K=0$.

Note that $f(0)=0$ by property 1 and f is increasing by property 2.

Now, we define the assistant functional:

$$H(t)=\int_0^R f(r)\,Vdr=\int_0^R VdF(r). \tag{20}$$

We then use the Cauchy-Schwarz inequality to obtain

$$\begin{aligned}&\left|\int_0^R V\cdot 1dF(r)\right|\leq\left(\int_0^R V^2dF(r)\right)^{1/2}\left(\int_0^R 1dF(r)\right)^{1/2}\\&\left|\int_0^R V\cdot 1dF(r)\right|\leq\left(\int_0^R V^2f(r)dr\right)^{1/2}\left(\int_0^R f(r)dr\right)^{1/2}\\&0\leq\frac{\left|\int_0^R VdF(r)\right|}{\left(\int_0^R f(r)dr\right)^{1/2}}\leq\left(\int_0^R V^2f(r)dr\right)^{1/2}\end{aligned} \tag{21}$$

for $R>0$,

$$\frac{H^2(t)}{\int_0^R f(r)\,dr}\leq\int_0^R V^2f(r)\,dr, \tag{22}$$

$$\frac{H^2(t)}{2R\int_0^R f(r)\,dr}\leq\frac{1}{2R}\int_0^R V^2f(r)\,dr. \tag{23}$$

In view of (23) and (19), we get

$$\begin{aligned}\frac{d}{dt}H(t)&\geq\frac{1}{2}\int_0^R V^2f'(r)\,dr-M\int_0^R\frac{f(r)}{r^{N-1}}dr\\&\geq\frac{1}{2R}\int_0^R V^2f(r)\,dr-M\int_0^R\frac{f(r)}{r^{N-1}}dr\\&\geq\frac{H(t)^2}{2R\int_0^R f(r)\,dr}-M\int_0^R\frac{f(r)}{r^{N-1}}dr,\end{aligned} \tag{24}$$

$$\frac{d}{dt}H(t)\geq\frac{H(t)^2}{2R\int_0^R f(r)\,dr}-M\int_0^R\frac{f(r)}{r^{N-1}}dr, \tag{25}$$

as $f'(r)\geq(1/r)f(r)$ by property 2.

It is well known that, with the initial condition

$$\frac{H_0^2}{2R\int_0^R f(r)\,dr}-M\int_0^R\frac{f(r)}{r^{N-1}}dr>0, \tag{26}$$

the Riccati inequality (25) will blow up on or before the finite time T.

(b) For $\delta=0$ or 1, by a similar analysis, one can show that

$$\frac{d}{dt}H(t)\geq\frac{H(t)^2}{2R\int_0^R f(r)\,dr}. \tag{27}$$

Finally,

$$H(t)\geq\frac{-H_0}{\left(H_0/\left(2R\int_0^R f(r)\,dr\right)\right)t-1}, \tag{28}$$

if we set the initial condition

$$H_0=\int_0^R f(r)\,V_0dr>0. \tag{29}$$

Thus, the solutions blow up on or before the finite time $T=(2R\int_0^R f(r)dr)/H_0$.

The proof is completed. ☐

Remark 2. For the physical explanation of the functional $H(t)$, readers may refer to Sideris' paper [16].

For the construction of testing functions f with the desired properties as required in Theorem 1, one recalls the class of power series:

$$\sum_{i=0}^{\infty}a_ix^i, \tag{30}$$

with the following properties:

(i) all $a_i\geq 0$ for all i and $a_i=0$ for $i<N-1$,

(ii) the radius of convergence is not less than R.

Actually, power series (or real analytic functions) with the above properties constitute a large class of examples for f. Concrete examples include $r^{N-1}e^r$ and $r^{N-1}\sinh r$. Moreover, there are examples with some $a_i<0$: $r^{N-1}\ln(r+1)$, $r^{N-1}\sin((\pi/2)(r/R))$, and $r^{N-1}(r^3-3r^2+3r+\varepsilon)$, where the constant $\varepsilon>0$ can be arbitrary.

3. The 1-Dimensional Nonradial Symmetric Case

In the 1-dimensional case, we can apply a similar argument to gain the result for the nonradial symmetric fluids.

Theorem 3. *Suppose u and ρ have compact support on $[a,b]$ and vanish at the boundaries:*

$$u(t,a)=u(t,b)=\rho(t,a)=\rho(t,b)=0, \tag{31}$$

for all $t \geq 0$. By considering $u(t, x-a)$ and $\rho(t, x-a)$ instead, one may suppose $a \geq 0$. Let $f(x)$ be a nonnegative and nonzero $C^1[a,b]$ testing function, such that $f(x)/x$ is increasing for $x > a$ and the functional is given by

$$H(t) = \int_a^b f(x)\, u(x,t)\, dx. \tag{32}$$

(a) *For $\delta = 1$ or -1, if the initial functional H_0 satisfies*

$$\frac{H_0^2}{2b\int_a^b f(x)\, dx} - \frac{M}{2}\int_a^b f(x)\, dx > 0, \tag{33}$$

then the solutions blow up in finite time.

(b) *For $\delta = 0$, if $H_0 > 0$, then the solutions blow up on or before the finite time $T = (2b\int_a^b f(x)dx)/H_0$.*

Proof. For the 1-dimensional case, $(1)_2$ becomes

$$u_t + uu_x + K\gamma\rho^{\gamma-2}\rho_x = \Phi_x. \tag{34}$$

For $\gamma \neq 1$, one has

$$u_t + \frac{1}{2}\frac{\partial u^2}{\partial x} + \frac{K\gamma}{\gamma-1}\frac{\partial \rho^{\gamma-1}}{\partial x} = \Phi_x. \tag{35}$$

Then, we multiply the above equation by $f(x)$ on both sides, taking integration with respect to x from a to b and using integration by parts, to yield

$$\begin{aligned}\frac{d}{dt}H(t) &+ \frac{1}{2}(f(x)u^2)\Big|_{x=b}^{x=a} - \frac{1}{2}\int_a^b u^2 f'(x)\, dx \\ &+ \frac{K\gamma}{\gamma-1}\left[\left(f(x)\rho^{\gamma-1}\right)\Big|_{x=b}^{x=a} - \int_a^b \rho^{\gamma-1} f'(x)\, dx\right] \\ &= \int_a^b f(x)\,\Phi_x dx.\end{aligned} \tag{36}$$

As $u(t,a) = u(t,b) = \rho(t,a) = \rho(t,b) = 0$, for all t, we get

$$\begin{aligned}\frac{d}{dt}H(t) &= \frac{1}{2}\int_a^b u^2 f'(x)\, dx \\ &\quad + \frac{K\gamma}{\gamma-1}\int_a^b \rho^{\gamma-1} f'(x)\, dx + \int_a^b f(x)\,\Phi_x dx \\ &\geq \frac{1}{2}\int_a^b u^2 f'(x)\, dx + \int_a^b f(x)\,\Phi_x dx.\end{aligned} \tag{37}$$

Using the properties of $f(x)$ and the Cauchy-Schwarz inequality (as in the proof of Theorem 1), we obtain

$$\frac{d}{dt}H(t) \geq \frac{H^2(t)}{2b\int_a^b f(x)\, dx} + \int_a^b f(x)\,\Phi_x dx. \tag{38}$$

On the other hand, by using the following explicit form of Φ_x:

$$\Phi_x(t,x) = \frac{\delta}{2}\left(\int_a^x \rho(t,x)\, dy - \int_x^b \rho(t,x)\, dy\right) \tag{39}$$

and the following estimate:

$$\Phi_x \geq -\frac{|\delta|}{2}M, \tag{40}$$

we get the following.

(a) For $\delta = 1$ or -1,

$$\frac{d}{dt}H(t) \geq \frac{H^2(t)}{2b\int_a^b f(x)\, dx} - \frac{M}{2}\int_a^b f(x)\, dx. \tag{41}$$

(b) For $\delta = 0$,

$$\frac{d}{dt}H(t) \geq \frac{H^2(t)}{2b\int_a^b f(x)\, dx}. \tag{42}$$

Thus, the result immediately follows. □

Conflict of Interests

The authors declare that there is no conflict of interests regarding the publication of this paper.

Acknowledgment

The work of this paper was partially funded by Dean's Research Grant FLASS/ECR-9 from the Hong Kong Institute of Education.

References

[1] J. Binney and S. Tremaine, *Galactic Dynamics*, Princeton University Press, Princeton, NJ, USA, 1994.

[2] S. Chandrasekhar, *An Introduction to the Study of Stellar Structure*, University of Chicago Press, 1939.

[3] F. F. Chen, *Introduction to Plasma Physics and Controlled Fusion*, Plenum, New York, NY, USA, 1984.

[4] P. L. Lions, *Mathematical Topics in Fluid Mechanics*, vol. 1, Clarendon Press, Oxford, UK, 1998.

[5] P. L. Lions, *MathematicalTopics in Fluid Mechanics*, vol. 2, Clarendon Press, Oxford, UK, 1998.

[6] T. Makino, S. Ukai, and S. Kawashima, "On compactly supported solutions of the compressible Euler equation," in *Recent Topics in Nonlinear PDE, III (Tokyo, 1986)*, vol. 148 of *North-Holland Mathematics Studies*, pp. 173–183, North-Holland, Amsterdam, The Netherlands, 1987.

[7] T. Makino and B. Perthame, "On radially symmetric solutions of the Euler-Poisson equation for the evolution of gaseous stars," *Japan Journal of Applied Mathematics*, vol. 7, pp. 165–170, 1990 (French).

[8] B. Perthame, "Non-existence of global solutions to Euler-Poisson equations for repulsive forces," *Japan Journal of Applied Mathematics*, vol. 7, no. 2, pp. 363–367, 1990.

[9] S. Engelberg, "Formation of singularities in the Euler and Euler-Poisson equations," *Physica D: Nonlinear Phenomena*, vol. 98, no. 1, pp. 67–74, 1996.

[10] S. Engelberg, H. Liu, and E. Tadmor, "Critical thresholds in Euler-Poisson equations," *Indiana University Mathematics Journal*, vol. 50, pp. 109–157, 2001.

[11] D. Chae and E. Tadmor, "On the finite time blow-up of the Euler-Poisson equations in R^N," *Communications in Mathematical Sciences*, vol. 6, no. 3, pp. 785–789, 2008.

[12] D. H. Chae and S. Y. Ha, "On the formation of shochs to the compressible Euler equations," *Communications in Mathematical Sciences*, vol. 7, pp. 627–634, 2009.

[13] M. A. Day, "The no-slip condition of fluid dynamics," *Erkenntnis*, vol. 33, no. 3, pp. 285–296, 1990.

[14] M. Yuen, "Blowup for the Euler and EulerPoisson equations with repulsive forces," *Nonlinear Analysis: Theory, Methods & Applications*, vol. 74, no. 4, pp. 1465–1470, 2011.

[15] M. Yuen, "Blowup for the C^1 solutions of the Euler-Poisson equations of gaseous stars in R^N," *Journal of Mathematical Analysis and Applications*, vol. 383, no. 2, pp. 627–633, 2011.

[16] T. C. Sideris, "Formation of singularities in three-dimensional compressible fluids," *Communications in Mathematical Physics*, vol. 101, no. 4, pp. 475–485, 1985.

Hindawi Publishing Corporation
The Scientific World Journal
Volume 2014, Article ID 853139, 9 pages
http://dx.doi.org/10.1155/2014/853139

Research Article

Upper Semicontinuity of Pullback Attractors for the 3D Nonautonomous Benjamin-Bona-Mahony Equations

Xinguang Yang,[1] Xiaosong Wang,[2] Juntao Li,[1] and Lingrui Zhang[3]

[1] *College of Mathematics and Information Science, Henan Normal University, Xinxiang 453007, China*
[2] *College of Information Science, Henan University of Technology, Zhengzhou 450001, China*
[3] *College of Education and Teacher Development, Henan Normal University, Xinxiang 453007, China*

Correspondence should be addressed to Xinguang Yang; yangxinguang@hotmail.com

Received 14 January 2014; Accepted 2 March 2014; Published 26 March 2014

Academic Editors: D. Baleanu and C. M. Khalique

We will study the upper semicontinuity of pullback attractors for the 3D nonautonomouss Benjamin-Bona-Mahony equations with external force perturbation terms. Under some regular assumptions, we can prove the pullback attractors $\mathscr{A}_\varepsilon(t)$ of equation $u_t - \Delta u_t - \nu\Delta u + \nabla\cdot \vec{F}(u) = \varepsilon g(x,t),\ x \in \Omega$, converge to the global attractor $\mathscr{A}$ of the above-mentioned equation with $\varepsilon = 0$ for any $t \in \mathbb{R}$.

1. Introduction

In this paper, we will consider the upper semicontinuity of pullback attractors for the following 3D Benjamin-Bona-Mahony equation:

$$u_t - \Delta u_t - \nu\Delta u + \nabla\cdot \vec{F}(u) = \varepsilon g(x,t), \quad x \in \Omega, \tag{1}$$

$$u(t,x)|_{\partial\Omega} = 0, \tag{2}$$

$$u(\tau,x) = u_\tau(x), \quad \tau \in \mathbb{R}. \tag{3}$$

Here $\Omega \subset \mathbb{R}^3$ is a bounded domain with sufficiently smooth boundary $\partial\Omega$; $u(t,x) = (u_1(t,x), u_2(t,x), u_3(t,x))$ is the velocity vector field; $\nu > 0$ is the kinematic viscosity; $\vec{F}$ is a nonlinear vector function; $\varepsilon \geq 0$ is a small nonnegative parameter; the external force $g(x,t)$ is locally square integrable in time for $(x,t) \in \Omega\times\mathbb{R}$, that is, for any $t \in \mathbb{R}$, $g(x,t) \in L^2_{\text{loc}}(\mathbb{R}; H)$, where $H = (L^2(\Omega))^3$, $V = (H^1_0(\Omega))^3$, and $(\cdot,\cdot)$ and $\|\cdot\|$ are the inner product and norm of H, respectively.

The Benjamin-Bona-Mahony (BBM) equation is a well-known model in physical applications which incorporates dispersive effects for long waves in shallow water that was introduced by Benjamin et al. [1] as an improvement of the Korteweg-de Vries equation (KdV equation) for modeling long waves of small amplitude in two dimensions. Contrasting with the KdV equation, the BBM equation is unstable in its high wave number components. Further, while the KdV equation has an infinite number of integrals of motion, the BBM equation only has three. Both KdV and BBM equations cover cases of surface waves of long wavelength in liquids, acoustic-gravity waves in compressible fluid, hydromagnetic waves in cold plasma, and acoustic waves in harmonic crystals.

For the well-posedness of global solutions for BBM equation, we can refer to [2–7]. For the long-time behavior, such as the existence of global attractor and its structure and the dimension of the attractors, we will discuss the known results in details.

Biler [8] investigated the long-time behavior of 2D generalized BBM equation

$$u_t - \Delta u_t = (b, \nabla u) + u^p (a, \nabla u) \tag{4}$$

in $\mathbb{R}^2$, $t \in \mathbb{R}$. Here $b \neq 0$, $a \in \mathbb{R}^2$, and $p \geq 3$ is an integer. The author proved the supremum norms of the solutions with small initial data decay to zero like $t^{-2/3}$ as t tends to infinity.

By energy equation and weak continuous method, Wang [9] and Wang and Yang [10] investigated the finite-dimensional behavior of solutions and derived the global weak attractor and the strong attractors for BBM equation:

$$u_t - u_{xxt} - \nu u_{xx} + (f(u))_x = g(x) \tag{5}$$

with period boundary value condition in $H^2_{\mathrm{per}}(\Omega)$ and $H^1_{\mathrm{per}}(\Omega)$, respectively. Moreover, Wang et al. [11] got the existence of global attractor for the above BBM equation defined in a three-dimensional channel; the asymptotic compactness of the solution operator is obtained by the uniform estimates on the tails of solutions.

By the decomposition of the semigroup, Wang [12] studied the regularity of attractors for the BBM equation

$$u_t - u_{xxt} - \nu u_{xx} + u_x + uu_x = g(x). \tag{6}$$

He proved that the global attractor is smooth if the forcing term is smooth. In addition, Wang [13] also obtained the approximate inertial manifolds to the global attractors for the generalized BBM equations.

Wang [14] considered the stochastic BBM equations on unbounded domains

$$du - d(\Delta u) - \nu\Delta u dt + \nabla\cdot \vec{F}(u)\, dt = g dt + h dw \tag{7}$$

and concluded the existence of random attractor in H^1_0 under certain assumptions, here w is the two-sided real-valued Wiener process on a probability space. He also proved the random attractor is invariant and attracts every pulled-back tempered random set under the forward flow. The asymptotic compactness of the random dynamical system is established by a tail-estimates method, which shows that the solutions are uniformly asymptotically small when space and time variables approach infinity.

Stanislavova et al. [15] first provided a sufficient condition to verify the asymptotic compactness of an evolution equation defined in an unbounded domain, which involves the Littlewood-Paley projection operators, then they proved the existence of an attractor for the Benjamin-Bona-Mahony equation in the phase space $H^1(\mathbb{R}^3)$ by showing the solutions are point dissipative and asymptotic compact

$$u_t - \Delta u_t - \nu\Delta u + \operatorname{div}(f(u)) = g \tag{8}$$

for $g \in L^2(\mathbb{R}^3)$ and $f(u) = u + (1/2)u^2$. Stanislavova [16] investigated the existence of global attractors of (8) in two dimension.

By the method of orthogonal decomposition, Zhu [17, 18] obtained the asymptotic attractor, global attractor, and its Hausdorff dimension of the damped BBM equations with periodic boundary conditions in homogeneous periodic space $\dot{H}^1_{\mathrm{per}}(\Omega)$

$$u_t - \delta u_{xxt} - \nu u_{xx} + uu_x = f(x) \tag{9}$$

which overcome difficulty coming from the precision of approximate inertial manifolds. Zhu and Mu [19] deduced the exponential decay estimates of solutions for time-delayed BBM equations.

J. Park and S. Park [20] studied the pullback attractors for the nonautonomous BBM equations in unbounded domains

$$u_t - \Delta u_t - \nu\Delta u + \nabla\cdot\overrightarrow{F(u)} = g(x,t), \tag{10}$$

by weak continuous method and some priori estimates in $H^1_0(\Omega)$. Qin et al. [21] derived the existence of pullback attractor of (10) in $H^2_0(\Omega)$ by weak continuous method. Zhao et al. [22] investigated the convergence of corresponding uniform attractors between averaging BBM and state BBM equations.

Moreover, Çelebi et al. [23] deduced the existence of attractors with a finite fractal dimension and the existence of the exponential attractor for the corresponding asymptotically compact semigroup for the periodic initial-boundary value problem of a generalized BBM equation. Chueshov et al. [24] studied the regularity of global attractor for a generalized BBM equation.

For the upper semicontinuity of corresponding attractors between autonomous and perturb nonautonomous systems, we can refer to Bao [25], Hale and Raugel [26], Carvalho et al. [27], Caraballo and Langa [28], Caraballo et al. [29], Fitzgibbon et al. [30], Kloeden [31], Miyamoto [32], Wang and Qin [33], Younsi [34], Wang [35], and Zhou [36].

To our knowledge, there are less results on the upper semicontinuity of pullback attractors for the 3D nonautonomous BBM equations with the nonautonomous perturbation; we will pay attention to this issue in the sequel.

This paper is organized as following. In Section 2, we will recall some fundamental theory of pullback attractors for nonautonomous dynamical systems and give a method to verify the upper semicontinuity of pullback attractors. In Section 3, the upper semicontinuity of pullback attractors for the problems (1)–(3) will be proved.

2. Pullback Attractors of Nonautonomous Dynamical Systems

In this section, we will consider the relationship between pullback attractors $\mathscr{A}_\varepsilon = \{A_\varepsilon(t)\}_{t\in\mathbb{R}}$ for the perturbed nonautonomous system with $\varepsilon > 0$ and global attractor $\mathscr{A}$ for the unperturbed autonomous system with $\varepsilon = 0$ of the following equation:

$$\frac{\partial u}{\partial t} = \mathbb{A}_f u(x,t) + \varepsilon f(x,t). \tag{11}$$

If the global attractor is unique, then the global attractor is the pullback attractor when $\varepsilon = 0$.

Let X be a Banach space with norm $\|\cdot\|_X$. The Hausdorff semidistance $\operatorname{dist}_X(B_1, B_2)$ in X between $B_1 \subseteq X$ and $B_2 \subseteq X$ is defined by

$$\operatorname{dist}_X(B_1, B_2) = \sup_{x\in B_1}\inf_{y\in B_2} d_X(x,y) \quad \text{for } B_1, B_2 \subset X, \tag{12}$$

where $d_X(x, y)$ denotes the distance between two points x and y.

For an autonomous system, $S(t) : X \to X$ $(t \in \mathbb{R})$ is a C_0-semigroup defined on X. If the global attractor $\mathscr{A}$ for $S(t)$ exists, then it has the following properties: (1) $\mathscr{A}$ is an invariant, compact set; (2) $\mathscr{A}$ attracts every bounded sets in X, that is, $\lim_{t\to+\infty}\mathrm{dist}(S(t)B, \mathscr{A}) = 0$ for all bounded subsets $B \subset X$.

For a nonautonomous system, the two-parameter mapping class $\{U(t,\tau)\}_{t\geq\tau}$ is said to be a process in X if

$$\begin{aligned} &U(t,s)U(s,\tau) = U(t,\tau), \quad \forall t \geq s \geq \tau,\ \tau \in \mathbb{R}, \\ &U(\tau,\tau) = Id, \left(\text{identity operator in } X\right), \quad \forall \tau \in \mathbb{R}. \end{aligned} \tag{13}$$

Moreover, throughout the paper, we always assume that the process $U(\cdot,\cdot)$ is continuous in X.

Now we will recall some definitions and framework on the existence theory of pullback attractors.

Definition 1. A family of compact sets $\mathscr{A} = \{A(t)\}_{t\in\mathbb{R}}$ is said to be a pullback attractor for the continuous process $\{U(\cdot,\cdot)\}$ if it satisfies the following:

(i) $\mathscr{A}$ is invariant for all $t \geq \tau$.

(ii) $\mathscr{A}$ is pullback attracting, that is, $\lim_{\tau\to+\infty}\mathrm{dist}(U(t,t-\tau)B, A(t)) = 0$ for all bounded subsets $B \subset X$.

Definition 2. The family of subsets $\mathscr{B} = \{B(t)\}_{t\in\mathbb{R}}$ is said to be pullback absorbing for the process $U(\cdot,\cdot)$, if for every $t \in \mathbb{R}$ and all bounded subsets $B \subset X$, there exists a time $T(t,B) > 0$, such that

$$U(t,t-\tau)B \subset B(t) \quad \forall \tau \geq T(t,B). \tag{14}$$

Definition 3. Let $\mathscr{B} = \{B(t)\}_{t\in\mathbb{R}}$ be a family of subsets in X. A process $U(\cdot,\cdot)$ is said to be pullback $\mathscr{B}$-asymptotically compact in X if for all $t \in \mathbb{R}$, any sequences $\tau_n \to \infty$ and $x_n \in B(t-\tau_n)$; the sequence $\{U(t,t-\tau_n)x_n\}$ is precompact in X.

Theorem 4. *Let the family of sets $\mathscr{B} = \{B(t)\}_{t\in\mathbb{R}}$ be pullback absorbing set for the process $U(\cdot,\cdot)$ and $U(\cdot,\cdot)$ is pullback $\mathscr{B}$-asymptotically compact in X. Then, the family $\mathscr{A} = \{A(t)\}_{t\in\mathbb{R}}$ that is defined by $A(t) = \Lambda(\mathscr{B},t)$ is a pullback attractor for $U(\cdot,\cdot)$ in X for the process $\{U(\cdot,\cdot)\}$, where*

$$\Lambda(\mathscr{B},t) = \bigcap_{s\geq0}\overline{\bigcup_{\tau\geq s}U(t,t-\tau)B(t-\tau)} \quad \text{for each } t \in \mathbb{R}. \tag{15}$$

In the following, we will characterize the pullback $\mathscr{B}$-asymptotic compactness in terms of the noncompact measure.

Definition 5. Let $B \subset X$, $\mathscr{B} = \{B(t)\}_{t\in\mathbb{R}}$ be a family of sets in X. A process $U(\cdot,\cdot)$ is said to be pullback $\mathscr{B}$-κ contracting, if for any $t \in \mathbb{R}$, $\varepsilon > 0$, there exists a time $T_{\mathscr{B}}(t,\varepsilon) > 0$, such that

$$\kappa(U(t,t-\tau)B(t-\tau)) \leq \varepsilon \quad \forall \tau \geq T_{\mathscr{B}}(t,\varepsilon). \tag{16}$$

Here $\kappa(B)$ is the Kuratowski noncompact measure defined as

$$\begin{aligned} &\kappa(B) \\ &\quad = \inf\{\delta > 0 \mid B \text{ admits a finite cover} \\ &\qquad\qquad \text{by sets of diameter} < \delta\}. \end{aligned} \tag{17}$$

Lemma 6. *Let $\mathscr{B} = \{B(t)\}_{t\in\mathbb{R}}$, $\widehat{\mathscr{B}} = \{\widehat{B}(t)\}_{t\in\mathbb{R}}$ be two families of sets in X and satisfy that for any $t \in \mathbb{R}$, there exists a time $T_{\mathscr{B},\widehat{\mathscr{B}}}(t) > 0$, such that*

$$U(t,t-\tau)B(t-\tau) \subset \widehat{B}(t) \quad \forall \tau \geq T_{\mathscr{B},\widehat{\mathscr{B}}}(t). \tag{18}$$

Then $U(\cdot,\cdot)$ is pullback $\mathscr{B}$-asymptotically compact, if it is pullback $\widehat{\mathscr{B}}$-κ contracting.

Proof. See, for example, Wang and Qin [33]. □

Theorem 7. *Assume that the assumptions in Lemma 6 hold. If the process $U(\cdot,\cdot)$ is pullback $\widehat{\mathscr{B}}$-κ contracting and the family of sets $\mathscr{B} = \{B(t)\}_{t\in\mathbb{R}}$ is pullback absorbing for $U(\cdot,\cdot)$, then the process $U(\cdot,\cdot)$ possesses a pullback attractor.*

Proof. See, for example, Wang and Qin [33]. □

Theorem 8. *Let $\mathscr{B} = \{B(t)\}_{t\in\mathbb{R}}$ be a family of sets in X. Suppose $U(\cdot,\cdot) = U_1(\cdot,\cdot) + U_2(\cdot,\cdot) : \mathbb{R}\times\mathbb{R}\times X \to X$ satisfies*

(i) *for any $t \in \mathbb{R}$,*

$$\left\|U_1(t,t-\tau)x_{t-\tau}\right\|_X \leq \Phi(t,\tau) \quad \forall x_{t-\tau} \in B(t-\tau),\ \tau > 0, \tag{19}$$

where $\Phi(\cdot,\cdot) : \mathbb{R}\times\mathbb{R} \to \mathbb{R}^+$ satisfies $\lim_{\tau\to+\infty}\Phi(t,\tau) = 0$ for each $t \in \mathbb{R}$;

(ii) *for any $t \in \mathbb{R}$ and $T \geq 0$, $\bigcup_{0\leq\tau\leq T}U_2(t,t-\tau)B(t-\tau)$ is bounded and $U_2(t,t-\tau)B(t-\tau)$ is precompact in X for any $\tau > 0$.*

Then the process $U(\cdot,\cdot)$ is pullback $\mathscr{B}$-κ contracting in X.

Proof. See, for example, Wang and Qin [33]. □

We now perturb the nonautonomous term with a small parameter $\varepsilon \in (0,\varepsilon_0]$; thus we obtain a nonautonomous dynamical system driven by the process $U_\varepsilon(\cdot,\cdot)$.

For each $t \in \mathbb{R}$, $\tau \in \mathbb{R}$, and $x \in X$, we have

$$(H_1) \quad \lim_{\varepsilon\to0}d_X\left(U_\varepsilon(t,t-\tau)x, S(t)x\right) = 0, \tag{20}$$

uniformly on bounded sets of X.

Theorem 9 (Caraballo et al. [28, 29]). *Assume that (H_1) holds, and for any $\varepsilon \in (0,\varepsilon_0]$, there exist pullback attractors $\mathscr{A}_\varepsilon = \{A_\varepsilon(t)\}_{t\in\mathbb{R}}$ for all $\varepsilon > 0$. If there exists a compact set $K \subset X$, such that*

$$(H_2) \quad \lim_{\varepsilon\to0}dis_X\left(A_\varepsilon(t), K\right) = 0 \quad \text{for any } t \in \mathbb{R}. \tag{21}$$

Then $\mathscr{A}_\varepsilon$ and $\mathscr{A}$ have the upper semicontinuity, that is,

$$\lim_{\varepsilon\to0}dis_X\left(A_\varepsilon(t), \mathscr{A}\right) = 0 \quad \text{for any } t \in \mathbb{R}. \tag{22}$$

In order to apply Theorem 9 to obtain the upper semicontinuity of pullback attractors $\mathscr{A}_\varepsilon$ and global attractor $\mathscr{A}$, we now present a technique to verify (H_2) for the process generated by the nonautonomous dissipative system.

Lemma 10. *Assume that the family $\mathscr{B} = \{B(t)\}_{t\in\mathbb{R}}$ is pullback absorbing for $U(\cdot,\cdot)$, and for each $\varepsilon \in (0,\varepsilon_0]$, $\mathscr{K}_\varepsilon = \{K_\varepsilon(t)\}_{t\in\mathbb{R}}$ is a family of compact sets in X. Suppose $U_\varepsilon(\cdot,\cdot) = U_{1,\varepsilon}(\cdot,\cdot) + U_{2,\varepsilon}(\cdot,\cdot) : \mathbb{R}\times\mathbb{R}\times X \to X$ satisfies*

(i) *for any $t \in \mathbb{R}$ and any $\varepsilon \in (0,\varepsilon_0]$,*

$$\left\|U_{1,\varepsilon}(t,t-\tau)x_{t-\tau}\right\|_X \le \Phi(t,\tau) \quad \forall x_{t-\tau} \in B(t-\tau),\ \tau > 0, \tag{23}$$

where $\Phi(\cdot,\cdot) : \mathbb{R}\times\mathbb{R} \to \mathbb{R}^+$ satisfies $\lim_{\tau\to+\infty}\Phi(t,\tau) = 0$ for each $t \in \mathbb{R}$;

(ii) *for any $t \in \mathbb{R}$ and any $T \ge 0$, $\cup_{0\le\tau\le T}U_{2,\varepsilon}(t,t-\tau)B(t-\tau)$ is bounded, and for any $t \in \mathbb{R}$, there exists a time $T_{\mathscr{B}}(t) > 0$, which is independent of ε, such that*

$$U_{2,\varepsilon}(t,t-\tau)B(t-\tau) \subset K_\varepsilon(t) \quad \forall\tau \ge T_{\mathscr{B}}(t),\ \varepsilon \in (0,\varepsilon_0] \tag{24}$$

and there exists a compact set $K \subset X$, such that

$$(H_2') \quad \lim_{\varepsilon\to 0} dist_X(K_\varepsilon(t), K) = 0, \quad \text{for any } t \in \mathbb{R}. \tag{25}$$

Then for each $\varepsilon \in (0,\varepsilon_0]$, there exists a pullback attractor $\mathscr{A}_\varepsilon = \{A_\varepsilon(t)\}_{t\in\mathbb{R}}$ and (H_2) holds.

Proof. See, for example, Wang and Qin [33]. □

3. Upper Semicontinuity of Pullback Attractors

In this section, firstly, we recall some notations about the functional spaces which will be used later to discuss the regularity of pullback attracting set.

The operator A is denoted by $A = -\Delta$ with domain $D(A) = H^2(\Omega)\bigcap H_0^1(\Omega)$ and λ is the first eigenvalue of A; we consider the family of Hilbert spaces

$$\mathscr{H}^\alpha = D\left(A^{\alpha/2}\right), \quad \alpha \in \mathbb{R} \tag{26}$$

generated by the Laplacian operator with the Dirichlet boundary value conditions equipped with the standard inner product and norm

$$(\cdot,\cdot)_{\mathscr{H}^\alpha} = \left(A^{\alpha/2}\cdot, A^{\alpha/2}\cdot\right), \qquad \|\cdot\|_{\mathscr{H}^\alpha} = \left\|A^{\alpha/2}\cdot\right\| \tag{27}$$

respectively, then we have $D(A^{s/2}) \hookrightarrow D(A^{r/2})$ for any $s > r$ and the continuous embedding

$$\mathscr{H}^s \equiv D\left(A^{s/2}\right) \hookrightarrow \left(L^{6/(3-2s)}(\Omega)\right)^3 \tag{28}$$

for all $s \in [0,3/2)$, $\mathscr{H}^2 = H^2(\Omega)\bigcap H_0^1(\Omega)$.

Then, applying the Helmholtz-Leray projector $\mathscr{P}$ to the systems (1)–(3), we obtain the following problem which is equivalent to the original problems (1)–(3)

$$\begin{gathered} u_t + \nu Au + Au_t + B(u) = \varepsilon f(x,t), \quad (x,t) \in \Omega\times[\tau,\infty), \\ u(x,t) = 0, \quad (x,t) \in \partial\Omega\times[\tau,\infty), \\ u(\tau,x) = u_\tau(x), \quad x \in \Omega. \end{gathered} \tag{29}$$

Here $A = -\mathscr{P}\Delta$, $B(u) = \mathscr{P}(\nabla\cdot\ \vec{F}\ (u))$, and $f(x,t) = \mathscr{P}g(x,t)$.

Assume that $u_\tau \in H_0^1(\Omega)$, the external force $g \in L^2_{\text{loc}}(\mathbb{R}, H)$. Also we assume that there exist constants $\beta > 0$, $0 \le \alpha < \sigma/2$, and $\sigma = 2\nu/((2/\lambda)+2)$, such that

$$\|g(t)\|^2 \le \beta e^{\alpha|t|}, \tag{30}$$

which implies that

$$\begin{gathered} \int_{-\infty}^t e^{\sigma s}\|g(s)\|^2 ds < +\infty, \quad \forall t \in \mathbb{R}, \\ \int_{-\infty}^\tau \left(\int_{-\infty}^t e^{\sigma s/2}\|g(s)\|^2 ds\right) dt < +\infty, \quad \forall\tau \in \mathbb{R}. \end{gathered} \tag{31}$$

Moreover, we assume that

$$\lim_{k\to\infty}\int_{-\infty}^\tau\int_{|x_3|\ge k} e^{\sigma t}\left|g(x,t)\right|^2 dx\,dt = 0, \quad \forall\tau \in \mathbb{R}. \tag{32}$$

From (31), we can easily derive that the term $f(x,t)$ is locally square integrable in time; that is, $f(x,t) \in L^2_{\text{loc}}(\mathbb{R}, H)$ and satisfies

$$\int_{-\infty}^t e^{\eta s}\|f(x,t)\|_H^2 ds < +\infty \tag{33}$$

for $0 < \eta \le \min\{\lambda\nu, \nu, \nu/((2/\lambda)+2)\}$ and any $t \in \mathbb{R}$.

For the nonlinear vector function $\vec{F}\ (s)\ = (F_1(s), F_2(s), F_3(s))$ $(s \in \mathbb{R})$, we denote

$$f_i(s) = F_i'(s), \qquad \mathscr{F}_i(s) = \int_0^s F_i(r)\,dr, \tag{34}$$

where

$$\begin{gathered} \vec{f}\ (s)\ = (f_1(s), f_2(s), f_3(s)), \\ \vec{\mathscr{F}}\ (s)\ = (\mathscr{F}_1(s), \mathscr{F}_2(s), \mathscr{F}_3(s)). \end{gathered} \tag{35}$$

Assume that F_i $(i = 1,2,3)$ are smooth functions satisfying

$$\begin{gathered} F_i(0) = 0, \qquad \left|F_i(s)\right| \le C_1|s| + C_2|s|^2, \\ C_1\left(1+\sigma^2|s|\right) \le \left|f_i(s)\right| \le C_2\left(1+\sigma^2|s|\right), \\ \left|\mathscr{F}_i(s)\right| \le C_1|s|^2 + C_2|s|^3, \end{gathered} \tag{36}$$

for all $s \in \mathbb{R}$, where C_1, C_2, and σ are positive constants.

At last, we will state the main result and the proof of this paper as the following.

Theorem 11. *Assume that* (30)–(36) *hold, and* $u_\tau \in V$, *then the pullback attractors* $\mathscr{A}_\varepsilon = \{\mathscr{A}_\varepsilon(t)\}_{t\in\mathbb{R}}$ *for* (29) *(which is equivalent to* (1)*) with* $\varepsilon > 0$ *and the global attractor* $\mathscr{A}$ *for* (29) *with* $\varepsilon = 0$ *satisfy*

$$\lim_{\varepsilon\to 0^+} dis_V\left(\mathscr{A}_\varepsilon(t), \mathscr{A}\right) = 0 \quad \text{for any } t \in \mathbb{R}. \tag{37}$$

The Hausdorff semidistance $dist(\cdot,\cdot)$ *is defined on the Banach space* V.

In order to apply Theorem 9 and Lemma 10 to prove Theorem 11, we will introduce the existence of global attractor for autonomous system (1) with $\varepsilon = 0$ and pullback attractors for nonautonomous system (1) with $\varepsilon > 0$ in the following lemmas.

Lemma 12. *Assume that* (34)–(36) *hold, and* $u_\tau \in V$, *then the semigroup* $S(t)$ $(t \in \mathbb{R})$ *generated by problem* (29) *(or problems* (1)–(3)*) with* $\varepsilon = 0$ *possesses a global attractor* $\mathscr{A}$ *in* V.

Proof. Using similar technique as in [9–11, 17, 18], we only need to consider the Dirichlet boundary value condition instead of the periodic boundary value condition in these papers which investigated the existence of global attractors. This means that we can obtain our lemma easily, here we omit the details. □

Lemma 13. *Assume that* (30)–(36) *hold, and* $u_\tau \in V$, *then problem* (29) *possesses a unique global solution* $u^\varepsilon(x,t)$ $(\varepsilon \ge 0)$ *satisfying*

$$\begin{gathered} u^\varepsilon(x,t) \in C([\tau,+\infty), V) \cap L^\infty(0,+\infty; V), \\ u_t \in L^2(0,T;V). \end{gathered} \tag{38}$$

Moreover, the process $\{U_\varepsilon(t,\tau)\}$ *generated by the global solutions possess pullback attractors* $\mathscr{A}_\varepsilon$ *for all* $\varepsilon \ge 0$ *in* V.

Proof. See, for example, [20]. □

Now we decompose the solution $u^\varepsilon(t) = U_\varepsilon(t,\tau)u_\tau$ of (29) with initial data $u_\tau \in V$ as

$$u^\varepsilon = U_\varepsilon(t,\tau)u_\tau = U_{1,\varepsilon}(t,\tau)u_\tau + U_{2,\varepsilon}(t,\tau)u_\tau, \tag{39}$$

where

$$\begin{gathered} U_{1,\varepsilon}(t,\tau)u_\tau = v(t), \\ U_{2,\varepsilon}(t,\tau)u_\tau = w(t) \end{gathered} \tag{40}$$

solve the following problems:

$$\begin{gathered} v_t + Av_t + \nu Av + B(v) = 0, \quad \text{in } (x,t) \in \Omega\times[\tau,\infty), \\ v(x,t) = 0, \quad \text{on } \partial\Omega\times[\tau,\infty), \\ v(\tau,x) = v_\tau(x), \quad x \in \Omega, \end{gathered} \tag{41}$$

$$\begin{gathered} w_t + Aw_t + \nu Aw \\ = -B(u) + B(v) + \varepsilon f(x,t), \quad \text{in } (x,t) \in \Omega\times[\tau,\infty), \\ w(x,t) = 0, \quad \text{on } \partial\Omega\times[\tau,\infty), \\ w(\tau,x) = 0, \quad x \in \Omega, \end{gathered} \tag{42}$$

respectively.

Lemma 14. *Suppose that* (34)–(36) *hold. For any bounded set* $B \subset V$ *and* $t \in \mathbb{R}$, *there exists a time* $T(B,t) > 0$, *such that*

$$\begin{gathered} \left\|U_\varepsilon(t,t-\tau)u_{t-\tau}\right\|^2 \le R_\varepsilon(t) \\ \forall\tau \ge T(B,t), \ \text{all } u_{t-\tau} \in B, \end{gathered} \tag{43}$$

where $R_\varepsilon(t) = C\varepsilon e^{-\eta t}\int_{-\infty}^t e^{\eta s}\|f(s)\|_H^2 ds$, *and* C *is a positive constant independent of* B, t, τ.

Proof. We choose $\sigma = 2\nu/((2/\lambda)+2)$, $R_\sigma = \{r : R \to (0,+\infty) \mid \lim_{t\to-\infty} e^{\sigma t}r^2(t) = 0\}$ and denote by $\mathscr{D}_\sigma$ the class of families $\widehat{D} = \{D(t) : t \in R\} \subset \mathscr{D}(H)$ such that $D(t) \subset \overline{B}(0, r_{\widehat{D}}(t))$ for some $r_{\widehat{D}}$, where $\overline{B}(0, r_{\widehat{D}}(t))$ denotes the closed ball in V centered at zero with radius $r_{\widehat{D}}(t)$.

Let $t \in \mathbb{R}$, $\tau \in \mathbb{R}$, and $u_\tau \in V$ be fixed, and denote

$$\begin{aligned} u(r) &= u(r; t-\tau, u_0) \\ &= U(r-t+\tau, t-\tau, u_0) \quad \text{for } r \ge t-\tau. \end{aligned} \tag{44}$$

Since $u \in C((\tau,T);V)$, then for all $u \in V$, we derive that

$$\begin{aligned} &\frac{d}{dt}\left(e^{\sigma t}\|u(t)\|^2 + e^{\sigma t}\|\nabla u(t)\|^2\right) \\ &\quad + 2\nu e^{\sigma t}\|\nabla u(t)\|^2 \\ &\quad = -2e^{\sigma t}\left(\nabla\ \vec{F}(u), \nabla u\right) \\ &\quad + \sigma\left(e^{\sigma t}\|u(t)\|^2 + e^{\sigma t}\|\nabla u\|^2\right) \\ &\quad + 2e^{\sigma t}\left(\varepsilon f(t), u(t)\right) \\ &\quad = \sigma\left(e^{\sigma t}\|u(t)\|^2 + e^{\sigma t}\|\nabla u\|^2\right) \\ &\quad + 2e^{\sigma t}\left(\varepsilon f(t), u(t)\right) \\ &\quad \le \sigma\left(\frac{1}{\lambda}+1\right)e^{\sigma t}\|\nabla u\|^2 + \frac{\sigma}{\lambda}e^{\sigma t}\|\nabla u\|^2 \\ &\quad + \frac{\varepsilon}{\sigma}e^{\sigma t}\|f(t)\|_H^2 \\ &\quad \le \sigma\left(\frac{2}{\lambda}+1\right)e^{\sigma t}\|\nabla u(t)\|^2 + \frac{\varepsilon}{\sigma}e^{\sigma t}\|f(t)\|_H^2 \\ &\quad \le 2\nu e^{\sigma t}\|\nabla u(t)\|^2 + \frac{\varepsilon}{\sigma}e^{\sigma t}\|f(t)\|_H^2, \end{aligned} \tag{45}$$

that is,

$$\frac{d}{dt}\left(e^{\sigma t}\|u(t)\|^2 + e^{\sigma t}\|\nabla u(t)\|^2\right) \le \frac{\varepsilon}{\sigma}e^{\sigma t}\|f(t)\|_H^2, \tag{46}$$

which gives

$$\|u(t)\|^2 + \|\nabla u(t)\|^2 \le e^{-\sigma(t-\tau)}\left(\|u_\tau\|^2 + \|\nabla u_\tau\|^2\right) + \frac{\varepsilon}{\sigma}\int_\tau^t e^{-\sigma(t-\xi)}\|f(\xi)\|_H^2 d\xi \tag{47}$$

for all $\tau \in \mathbb{R}$.

Let $\widehat{D} \in \mathscr{D}_\sigma$ be given, choosing appropriate parameter σ, we easily get

$$\left\|U(t,\tau,u_\tau)\right\|_V^2 \le e^{-\sigma(t-\tau)} r_{\widehat{D}}^2 + \frac{\varepsilon}{\sigma}\int_{-\infty}^t e^{-\sigma(t-\xi)}\|f(\xi)\|_H^2 d\xi, \tag{48}$$

for all $u_\tau \in D(\tau)$, $t \ge \tau$.

Setting $e^{-\sigma(t-\tau)} r_{\widehat{D}}^2 \le (\varepsilon/\sigma)\int_{-\infty}^t e^{-\sigma(t-\xi)}\|f(\xi)\|_H^2 d\xi$, then we denote $R_\varepsilon(t)$ the nonnegative number given for each $t \in \mathbb{R}$ by

$$\left(R_\varepsilon(t)\right)^2 = \frac{2\varepsilon}{\sigma}\int_{-\infty}^t e^{-\eta(t-\xi)}\|f(\xi)\|_H^2 d\xi, \tag{49}$$

and consider the family $\widehat{B}_\varepsilon$ of closed balls in V defined by

$$B_\varepsilon(t) = \left\{v \in V \mid \|v\|_V \le 2R_\varepsilon(t)\right\}. \tag{50}$$

It is straightforward to check that $\widehat{B}_\varepsilon \in \mathscr{D}_\sigma$ and hence $\widehat{B}_\sigma$ is the $\mathscr{D}_\sigma$-pullback absorbing for the process $\{U(t,\tau,u_\tau)\}$. □

Setting

$$B_\varepsilon = \left\{u \in V \mid \|u\|_V \le R_\varepsilon(t)\right\}, \tag{51}$$

then we can check that family $\mathscr{B}_\varepsilon = \{B_\varepsilon(t)\}_{t\in\mathbb{R}}$ is pullback absorbing in V easily. Moreover,

$$\lim_{t\to-\infty} e^{\eta t} R_\varepsilon(t) = 0 \quad \text{for any } \varepsilon > 0. \tag{52}$$

Lemma 15. *Let $R_\varepsilon(t)$, $B_\varepsilon(t)$ be given as above. For any $t \in \mathbb{R}$, the solution $v(t) = U_{1,\varepsilon}(t,t-\tau)u(t-\tau)$ of (41) satisfies*

$$\left\|U_{1,\varepsilon}(t,t-\tau)u_{t-\tau}\right\|_V^2 \le e^{-\eta\tau} R_\varepsilon(t-\tau), \tag{53}$$

for all $\tau \ge 0$ and $u_{t-\tau} \in D_\varepsilon(t-\tau)$.

Proof. Multiplying equation in (41) with v and integrating over Ω, we derive

$$\frac{1}{2}\frac{d}{dt}\left(\|v(t)\|^2 + \|\nabla v(t)\|^2\right) + \nu\|\nabla v\|^2 \le 0. \tag{54}$$

Here we use the property of operator $B(\cdot)$ and $\mathscr{F}_i(0) = 0$ as

$$\begin{aligned}\int_\Omega \left(\nabla\cdot \vec{F}(u)\right) u\,dx &= -\int_\Omega \vec{F}(u)\cdot\nabla u\,dx \\ &= -\int_\Omega \nabla\cdot\vec{\mathscr{F}}(u)\,dx \\ &= -\int_{\partial\Omega}\vec{\mathscr{F}}(u)\cdot\vec{n}\,dx = 0,\end{aligned} \tag{55}$$

where $\vec{n}$ is the outer unit normal vector.

Using Poincaré's inequality, it follows

$$\frac{d}{dt}\left(\|v(t)\|^2 + \|\nabla v(t)\|^2\right) + \eta\left(\|v\|^2 + \|\nabla v\|^2\right) \le 0, \tag{56}$$

where we set $0 < \eta \le \min\{\lambda_1\nu, \nu\}$.

Integrating (56) from $t-\tau$ to t, we get

$$\begin{aligned}\left\|U_{1,\varepsilon}(t,t-\tau)u_{t-\tau}\right\|_V^2 &\le \|v(t)\|^2 + \|\nabla v(t)\|^2 \\ &\le \left(\|v_{t-\tau}\|^2 + \|\nabla v_{t-\tau}\|^2\right)e^{-\eta(t-\tau)} \\ &\le e^{-\eta\tau} R_\varepsilon(t-\tau)\end{aligned} \tag{57}$$

for all $t \ge \tau$, which completes our proof. □

Lemma 16. *Let $\mathscr{B}_\varepsilon(t) = \{B_\varepsilon(t)\}_{t\in\mathbb{R}}$ be given by (51) and (52). For any $t \in \mathbb{R}$, there exist a time $T_\varepsilon(t,\mathscr{B}) > 0$ and a function $I_\varepsilon(t) > 0$, such that the solution $U_{2,\varepsilon}(t,\tau)u_\tau = w(t)$ of (42) satisfies*

$$\left\|U_{2,\varepsilon}(t,t-\tau)u_{t-\tau}\right\|_V^2 \le I_\varepsilon(t), \tag{58}$$

for all $\tau \ge T_\varepsilon(t,\mathscr{B})$ and any $u_{t-\tau} \in B_\varepsilon(t-\tau)$.

Proof. Taking the inner product of equation in (42) with $A^\sigma w(t)$ in H, we derive

$$\begin{aligned}&\frac{1}{2}\frac{d}{dt}\left(\left\|A^{\sigma/2}w(t)\right\|^2 + \left\|A^{(\sigma+1)/2}w(t)\right\|^2\right) + \nu\int_\Omega\left|A^{(\sigma+1)/2}w(t)\right|^2 dx \\ &\quad = -\langle B(u), A^\sigma w\rangle + \langle B(v), A^\sigma w\rangle + \varepsilon\langle f(t,x), A^\sigma w\rangle.\end{aligned} \tag{59}$$

By Poincaré's inequality, Lemma 15, (51), and (34)–(36), we obtain

$$\begin{aligned}&-\langle B(u), A^\sigma w\rangle + \langle B(v), A^\sigma w\rangle \\ &\quad\le \left|\left\langle \nabla\cdot\left(\vec{F}(v) - \vec{F}(u)\right), A^\sigma w\right\rangle\right| \\ &\quad\le \left|\left(\sup_{i=1,2,3}\left(\left|\vec{F}_i'(v)\right| + \left|\vec{F}_i' u\right|\right)\right.\right. \\ &\qquad\left.\left.\times\,(\nabla v - \nabla u), A^\sigma w\right)\right| \\ &\quad= \left|\left(\sup_{i=1,2,3}\left(\left|\vec{F}_i'(v)\right| + \left|\vec{F}_i' u\right|\right)\nabla w, A^\sigma w\right)\right| \\ &\quad\le \left\|\sup_{i=1,2,3}\left(\left|\vec{F}_i'(v)\right| + \left|\vec{F}_i' u\right|\right)\right\|\left\|A^{(\sigma+(1/2))/2}w\right\|\end{aligned}$$

$$\begin{aligned}
&\leq \frac{C(\varepsilon)}{\lambda}\left\|\sup_{i=1,2,3}\left(\left|\vec{F}'_i(v)\right|+\left|\vec{F}'_i u\right|\right)\right\|^2 \\
&\quad + \nu\lambda\left\|A^{(\sigma+(1/2))/2}w\right\|^2 \\
&\leq \frac{C(\varepsilon)}{\lambda}\left\|\sup_{i=1,2,3}\left(\left|\vec{F}'_i(v)\right|+\left|\vec{F}'_i u\right|\right)\right\|^2 \\
&\quad + \nu\left\|A^{(\sigma+1)/2}w\right\|^2 \\
&\leq \frac{C}{\lambda}\left(2+\sigma^2\|u\|^2+\sigma^2\|v\|^2\right) \\
&\quad + \nu\left\|A^{(\sigma+1)/2}w\right\|^2 \\
&\leq C\left(2+\sigma^2 R_\varepsilon(t)+\sigma^2 e^{-\eta\tau}R_\varepsilon(t-\tau)\right) \\
&\quad + \nu\left\|A^{(\sigma+1)/2}w\right\|^2, \\
&\langle f(t,x), A^\sigma w\rangle \leq \frac{1}{\lambda}\left\|A^{(\sigma+1)/2}w(t)\right\|^2+\lambda\|f(t)\|_H^2.
\end{aligned} \tag{60}$$

Hence according to (59)–(60) and (31), we have

$$\begin{aligned}
&\frac{d}{dt}\left(\left\|A^{\sigma/2}w(t)\right\|^2+\left\|A^{(\sigma+1)/2}w(t)\right\|^2\right) \\
&\quad \leq C\left(1+\varepsilon\left\|A^{(\sigma+1)/2}w(t)\right\|^2+\varepsilon\|f(t)\|_H^2\right),
\end{aligned} \tag{61}$$

where the constant C depends on $\|u_{t-\tau}\|_V^2$, σ, and the first eigenvalue λ of the operator A.

Integrating (61) from $t-\tau$ to t, we conclude that

$$\begin{aligned}
&\left\|A^{\sigma/2}w(t)\right\|^2+\left\|A^{(\sigma+1)/2}w(t)\right\|^2 \\
&\quad \leq Ce^{Ct}\int_{t-\tau}^{t}\left(1+\varepsilon^2\|f(x,s)\|^2\right)e^{-Cs}ds \\
&\quad = I_\varepsilon(t)
\end{aligned} \tag{62}$$

for all $t>\tau$. This completes the proof of desiring lemma. □

Lemma 17. *For any $t\in\mathbb{R}$, any $\tau>0$, if u_0 varies in bounded sets, then the solution $u_\varepsilon(t)=U_\varepsilon(t,t-\tau)u_0$ of problem* (1) *converges to the solution $u(t)=S(t)u_0$ of the unperturbed problem* (1) *with $\varepsilon=0$ uniformly in V as $\varepsilon\to0^+$, which means*

$$\lim_{\varepsilon\to0^+}\sup_{u_0\in B}\|u_\varepsilon(t)-u(t)\|_V=0, \tag{63}$$

where B is a bounded subset in V.

Proof. Denote

$$y^\varepsilon(t)=u_\varepsilon(t)-u(t), \tag{64}$$

then we can verify that $y^\varepsilon(t)$ satisfies

$$y_t^\varepsilon+Ay_t^\varepsilon+\nu Ay^\varepsilon=-B(u^\varepsilon)+B(u)+\varepsilon f(x,t), \tag{65}$$

$$y_\varepsilon|_{\partial\Omega}=0, \tag{66}$$

$$y_\varepsilon|_{t=\tau}=(u_\varepsilon)_\tau-u_\tau. \tag{67}$$

Multiplying (65) by$y^\varepsilon(t)$, using (34)–(36) and noting the boundary value condition (66), we have

$$\begin{aligned}
&\frac{1}{2}\frac{d}{dt}\left(\|y^\varepsilon\|^2+\|\nabla y^\varepsilon\|^2\right)+\nu\|\nabla y^\varepsilon\|^2 \\
&\quad = \langle B(u),y^\varepsilon\rangle-\langle B(u^\varepsilon),y^\varepsilon\rangle+\langle\varepsilon f,y^\varepsilon\rangle \\
&\quad \leq |\langle B(u^\varepsilon)-B(u),y^\varepsilon)\rangle|+\langle\varepsilon f,y^\varepsilon\rangle \\
&\quad \leq \left|\left\langle\nabla\cdot\left(\vec{F}(u^\varepsilon)-\vec{F}(u)\right),y^\varepsilon\right\rangle\right| \\
&\qquad + \frac{\varepsilon^2}{4\nu}\|f(t)\|_H^2+\frac{\lambda\nu}{2}\|y^\varepsilon\|^2 \\
&\quad = \left|\left\langle\vec{F}(u^\varepsilon)-\vec{F}(u),\nabla y^\varepsilon\right\rangle\right| \\
&\qquad + \frac{\varepsilon^2}{4\lambda\nu}\|f(t)\|_H^2+\frac{\lambda\nu}{2}\|y^\varepsilon\|^2.
\end{aligned} \tag{68}$$

Using (34)–(36) and the Sobolev compact embedding theorem $V\hookrightarrow L^6\hookrightarrow L^4\hookrightarrow L^2$, we get

$$\begin{aligned}
&\left|\left\langle\vec{F}(u^\varepsilon)-\vec{F}(u),\nabla y^\varepsilon\right\rangle\right| \\
&\quad \leq \left|\left(C_1|u^\varepsilon|+C_2|u^\varepsilon|^2+C_1|u|+C_2|u|^2,\nabla y^\varepsilon\right)\right| \\
&\quad \leq \frac{C}{\nu}\left(\|u^\varepsilon\|^2+\|u^\varepsilon\|_{L^4}^2+\|u\|^2+\|u\|_{L^4}^2\right) \\
&\qquad + \frac{\nu}{2}\|\nabla y^\varepsilon\|^2 \\
&\quad \leq \frac{C}{\lambda\nu}\left(\|u^\varepsilon\|_V^2+\|u\|_V^2\right)+\frac{\nu}{2}\|\nabla y^\varepsilon\|^2.
\end{aligned} \tag{69}$$

Hence

$$\begin{aligned}
&\frac{1}{2}\frac{d}{dt}\left(\|y^\varepsilon\|^2+\|\nabla y^\varepsilon\|^2\right)+\nu\|\nabla y^\varepsilon\|^2 \\
&\quad \leq \frac{C}{\lambda\nu}\left(\|u^\varepsilon\|_V^2+\|u\|_V^2\right)+\frac{\nu}{2}\|\nabla y^\varepsilon\|^2 \\
&\qquad + \frac{\varepsilon^2}{4\lambda\nu}\|f(t)\|_H^2+\frac{\nu}{2}\|\nabla y^\varepsilon\|^2,
\end{aligned} \tag{70}$$

that is,

$$\begin{aligned}
\frac{d}{dt}\left(\|y^\varepsilon\|^2+\|\nabla y^\varepsilon\|^2\right) &\leq \frac{C}{\lambda\nu}\left(\|u^\varepsilon\|_V^2+\|u\|_V^2\right) \\
&\quad + \frac{\varepsilon^2}{4\lambda\nu}\|f(t)\|_H^2.
\end{aligned} \tag{71}$$

Using Lemmas 13, 14, 15, 16, and (31), noting that $\eta = \min\{\lambda\nu, \nu, \nu/((1/\lambda) + 2)\}$, we know

$$\begin{aligned}
&u^{\varepsilon}, \quad u \in C([\tau, +\infty), V), \\
&\int_{t-\tau}^{t} \left(\|u^{\varepsilon}(s)\|_V^2 + \|u(s)\|_V^2\right) ds \\
&\quad \le C\varepsilon \int_{t-\tau}^{t} e^{-\eta t} \int_{-\infty}^{t} e^{\eta s} \|f(s)\|_H^2 ds\, dt \\
&\quad + C\varepsilon \int_{t-\tau}^{t} e^{-\eta t} \int_{-\infty}^{t-\tau} e^{\eta s} \|f(s)\|_H^2 ds\, dt \\
&\quad \le C\varepsilon \iint_{-\infty}^{t} e^{\eta s} \|f(s)\|_H^2 ds\, dt \\
&\quad + C\varepsilon \iint_{-\infty}^{t} e^{\eta s} \|f(s)\|_H^2 ds\, dt \le C\varepsilon.
\end{aligned} \tag{72}$$

Applying the Gronwall inequality to (71) and noting that $f \in L^2_{\text{loc}}(\mathbb{R}, H)$, using Lemmas 14, 15, and 16, we conclude

$$\begin{aligned}
\|y^{\varepsilon}\|_V^2 &\le C\left(\|y^{\varepsilon}\|^2 + \|\nabla y^{\varepsilon}\|^2\right) \\
&\le C\varepsilon \left[\int_{t-\tau}^{t} \left(\|u^{\varepsilon}(s)\|_V^2 + \|u(s)\|_V^2\right) ds \right.\\
&\qquad \left. + \int_{t-\tau}^{t} \|f(s)\|_H^2 ds\right] \\
&\le C\varepsilon \left[\int_{t-\tau}^{t} e^{-\eta t} \int_{-\infty}^{t} e^{\eta s} \|f(s)\|_H^2 ds\, dt \right.\\
&\qquad \left. + \int_{t-\tau}^{t} e^{-\eta t} \int_{-\infty}^{t-\tau} e^{\eta s} \|f(s)\|_H^2 ds\, dt\right] \\
&\quad + C\varepsilon^2 \left[\int_{t-\tau}^{t} \|f(s)\|_H^2 ds\right] \\
&\le C'\varepsilon \longrightarrow 0
\end{aligned} \tag{73}$$

as $\varepsilon \to 0^+$, which implies (63). □

Proof of Theorem 11. Since the embedding $D(A^{s/2}) \hookrightarrow (L^{6/(3-2s)}(\Omega))^3$ is compact, combining Lemmas 13–17 with Theorem 9 and Lemma 10, we can obtain Theorem 11 easily. □

Conflict of Interests

The authors declare that there is no conflict of interests regarding the publication of this paper.

Acknowledgments

Xinguang Yang was in part supported by the NSFC (no. 11326154), the Innovational Scientists and Technicians Troop Construction Projects of Henan Province (no. 114200510011), the Key Scientific and Technological Project of Henan Province (no. 142102210448), and the Young Teacher Research Fund of Henan Normal University (qd12104). Juntao Li was in part supported by the NSFC (no. 61203293), the Foundation of Henan Educational Committee (no. 134120524), the Key Scientific and Technological Project of Henan Province (no. 122102210131), the College Young Teachers Program of Henan Province (no. 2012GGJS-063), and the Program for Science and Technology Innovation Talents in University of Henan Province (no. 13HASTIT040).

References

[1] T. B. Benjamin, J. L. Bona, and J. J. Mahony, "Model equations for long waves in nonlinear dispersive systems," *Philosophical Transactions of the Royal Society A*, vol. 272, pp. 47–48, 1972.

[2] J. M. Arrieta, A. N. Carvalho, and A. Rodríguez-Bernal, "Perturbation of the diffusion and upper semicontinuity of attractors," *Applied Mathematics Letters*, vol. 12, no. 5, pp. 37–42, 1999.

[3] J. Avrin and J. A. Goldstein, "Global existence for the Benjamin-Bona-Mahony equation in arbitrary dimensions," *Nonlinear Analysis: Theory, Methods & Applications*, vol. 9, no. 8, pp. 861–865, 1985.

[4] C. S. Q. Caldas, J. Limaco, and R. K. Barreto, "About the Benjamin-Bona-Mahony equation in domains with moving boundary," *Trends in Applied and Computational Mathematics*, vol. 8, no. 3, pp. 329–339, 2007.

[5] B. L. Guo, "Initial-boundary value problem for one class of systems of multidimensional inhomogeneous GBBM equations," *Chinese Annals of Mathematics. Series B*, vol. 8, no. 2, pp. 226–238, 1987.

[6] M. Hărăguş, "Stability of periodic waves for the generalized BBM equation," *Revue Roumaine de Mathématiques Pures et Appliquées*, vol. 53, no. 5-6, pp. 445–463, 2008.

[7] L. A. Medeiros and G. P. Menzala, "Existence and uniqueness for periodic solutions of the Benjamin-Bona-Mahony equation," *SIAM Journal on Mathematical Analysis*, vol. 8, no. 5, pp. 792–799, 1977.

[8] P. Biler, "Long time behaviour of solutions of the generalized Benjamin-Bona-Mahony equation in two-space dimensions," *Differential and Integral Equations*, vol. 5, no. 4, pp. 891–901, 1992.

[9] B. Wang, "Strong attractors for the Benjamin-Bona-Mahony equation," *Applied Mathematics Letters*, vol. 10, no. 2, pp. 23–28, 1997.

[10] B. Wang and W. Yang, "Finite-dimensional behaviour for the Benjamin-Bona-Mahony equation," *Journal of Physics A: Mathematical and General*, vol. 30, no. 13, pp. 4877–4885, 1997.

[11] B. Wang, D. W. Fussner, and C. Bi, "Existence of global attractors for the Benjamin-Bona-Mahony equation in unbounded domains," *Journal of Physics A: Mathematical and Theoretical*, vol. 40, no. 34, pp. 10491–10504, 2007.

[12] B. Wang, "Regularity of attractors for the Benjamin-Bona-Mahony equation," *Journal of Physics A: Mathematical and General*, vol. 31, no. 37, pp. 7635–7645, 1998.

[13] B. Wang, "Attractors and approximate inertial manifolds for the generalized Benjamin-Bona-Mahony equation," *Mathematical Methods in the Applied Sciences*, vol. 20, no. 3, pp. 189–203, 1997.

[14] B. Wang, "Random attractors for the stochastic Benjamin-Bona-Mahony equation on unbounded domains," *Journal of Differential Equations*, vol. 246, no. 6, pp. 2506–2537, 2009.

[15] M. Stanislavova, A. Stefanov, and B. Wang, "Asymptotic smoothing and attractors for the generalized Benjamin-Bona-Mahony equation on $\mathbb{R}^3$," *Journal of Differential Equations*, vol. 219, no. 2, pp. 451–483, 2005.

[16] M. Stanislavova, "On the global attractor for the damped Benjamin-Bona-Mahony equation," *Discrete and Continuous Dynamical Systems. Series A*, vol. 2005, pp. 824–832, 2005.

[17] C. Zhu, "Global attractor for the damped Benjamin-Bona-Mahony equations on $\mathbb{R}^1$," *Applicable Analysis*, vol. 86, no. 1, pp. 59–65, 2007.

[18] C. Zhu, "Asymptotic attractors of Benjamin-Bona-Mahony equations," *European Journal of Pure and Applied Mathematics*, vol. 1, no. 2, pp. 3–10, 2008.

[19] C. Zhu and C. Mu, "Exponential decay estimates for time-delayed Benjamin-Bona-Mahony equations," *Applicable Analysis*, vol. 87, no. 4, pp. 401–407, 2008.

[20] J. Y. Park and S. H. Park, "Pullback attractors for the non-autonomous Benjamin-Bona-Mahony equation in unbounded domains," *Science China Mathematics*, vol. 54, no. 4, pp. 741–752, 2011.

[21] Y. Qin, X. Yang, and X. Liu, "Pullback attractors for the non-autonomous Benjamin-Bona-Mahony equations in H^2," *Acta Mathematica Scientia. Series B*, vol. 32, no. 4, pp. 1338–1348, 2012.

[22] M. Zhao, X. Yang, and L. Zhang, "Averaging of the 3*D* non-autonomous Benjamin-Bona-Mahony equation with singularly oscillating forces," *Boundary Value Problems*, vol. 2013, article 111, 14 pages, 2013.

[23] A. O. Çelebi, V. K. Kalantarov, and M. Polat, "Attractors for the generalized Benjamin-Bona-Mahony equation," *Journal of Differential Equations*, vol. 157, no. 2, pp. 439–451, 1999.

[24] I. Chueshov, M. Polat, and S. Siegmund, "Gevrey regularity of global attractor for generalized Benjamin-Bona-Mahony equation," *Matematicheskaya Fizika, Analiz, Geometriya*, vol. 11, no. 2, pp. 226–242, 2004.

[25] T. Q. Bao, "Existence and upper semi-continuity of uniform attractors for nonautonomous reaction diffusion equations on $\mathbb{R}^n$," *Electronic Journal of Differential Equations*, vol. 203, pp. 1–18, 2012.

[26] J. K. Hale and G. Raugel, "Upper semicontinuity of the attractor for a singularly perturbed hyperbolic equation," *Journal of Differential Equations*, vol. 73, no. 2, pp. 197–214, 1988.

[27] A. N. Carvalho, H. M. Rodrigues, and T. Dlotko, "Upper semicontinuity of attractors and synchronization," *Journal of Mathematical Analysis and Applications*, vol. 220, no. 1, pp. 13–41, 1998.

[28] T. Caraballo and J. A. Langa, "On the upper semicontinuity of cocycle attractors for non-autonomous and random dynamical systems," *Dynamics of Continuous, Discrete and Impulsive Systems Series A*, vol. 10, no. 4, pp. 491–513, 2003.

[29] T. Caraballo, J. A. Langa, and J. C. Robinson, "Upper semicontinuity of attractors for small random perturbations of dynamical systems," *Communications in Partial Differential Equations*, vol. 23, no. 9-10, pp. 1557–1581, 1998.

[30] W. E. Fitzgibbon, M. E. Parrott, and Y. You, "Finite dimensionality and upper semicontinuity of the global attractor of singularly perturbed Hodgkin-Huxley systems," *Journal of Differential Equations*, vol. 129, no. 1, pp. 193–237, 1996.

[31] P. E. Kloeden, "Upper semi continuity of attractors of delay differential equations in the delay," *Bulletin of the Australian Mathematical Society*, vol. 73, no. 2, pp. 299–306, 2006.

[32] Y. Miyamoto, "Upper semicontinuity of the global attractor for the Gierer-Meinhardt model," *Journal of Differential Equations*, vol. 223, no. 1, pp. 185–207, 2006.

[33] Y. Wang and Y. Qin, "Upper semicontinuity of pullback attractors for nonclassical diffusion equations," *Journal of Mathematical Physics*, vol. 51, no. 2, Article ID 022701, 12 pages, 2010.

[34] A. Younsi, "Upper semicontinuous trajectory attractors for 3D hyperviscous flow," *Mediterranean Journal of Mathematics*, 2014.

[35] B. Wang, "Upper semi-continuity of random attractors for non-compact random dynamical systems," *Electronic Journal of Differential Equations*, vol. 139, pp. 1–18, 2009.

[36] S. Zhou, "Upper-semicontinuity of attractors for random lattice systems perturbed by small white noises," *Nonlinear Analysis: Theory, Methods & Applications*, vol. 75, no. 5, pp. 2793–2805, 2012.

Hindawi Publishing Corporation
The Scientific World Journal
Volume 2014, Article ID 794630, 8 pages
http://dx.doi.org/10.1155/2014/794630

Research Article

Numerical Modeling of the Photothermal Processing for Bubble Forming around Nanowire in a Liquid

Anis Chaari, Laurence Giraud-Moreau, Thomas Grosges, and Dominique Barchiesi

Group for Automatic Mesh Generation and Advanced Methods, Gamma3 (UTT-INRIA), University of Technology of Troyes, 12 rue Marie Curie, CS 42060, 10004 Troyes Cedex, France

Correspondence should be addressed to Thomas Grosges; thomas.grosges@utt.fr

Received 2 January 2014; Accepted 4 March 2014; Published 24 March 2014

Academic Editors: D. Baleanu and H. Jafari

An accurate computation of the temperature is an important factor in determining the shape of a bubble around a nanowire immersed in a liquid. The study of the physical phenomenon consists in solving a photothermic coupled problem between light and nanowire. The numerical multiphysic model is used to study the variations of the temperature and the shape of the created bubble by illumination of the nanowire. The optimization process, including an adaptive remeshing scheme, is used to solve the problem through a finite element method. The study of the shape evolution of the bubble is made taking into account the physical and geometrical parameters of the nanowire. The relation between the sizes and shapes of the bubble and nanowire is deduced.

1. Introduction

In the last years, many researchers are interested in the use of nanomaterials. In the chemical industry and in the manufactures of nanotubes and nanowires, the usually used materials are TiO_2 and ZnO [1–3]. Such a use of these nanomaterials (natural or artificial) increases and these are dispersed in air or in water [4]. Their impact on the environment and health must be evaluated (e.g., toxicity analysis) [5]. Therefore, the detection of the presence of such nanomaterials in the environment becomes crucial. Two modes of detections of such a nanowire/nanotube can be achieved. The first one consists in a direct detection of the nanowire by optical microscopy through the measurement of the scattering of light emitted by the nanomaterial. Due to a weak signal/noise ratio, such a detection mode can be difficult. The second mode is an indirect method and consists in studying the bubble created by the photothermal response of the nanowire immersed in a liquid and illuminated by an electromagnetic wave. In such an approach, the nanowire absorbs the electromagnetic radiation (energy) for a range of wavelengths and heats and, for temperature exceeding the threshold of vaporization of the liquid, induces the creation of a nanobubble [6, 7]. The created bubble grows before being detected. The analysis of the shape and size of the bubble should permit studying the morphology of the nanowire. The studied problem consists in solving a photothermic coupled system (light, nanowire, and heat) taking into account the physical parameters of the system (i.e., permittivity of materials, material conductivity, laser wavelength, and laser power).

In that context, a numerical multiphysic model, allowing studying the behavior of the nanowires illuminated by an incident laser field, is presented. The formation of the bubble, associated with a nanowire of TiO_2 immersed in water and illuminated by a laser pulse, is studied. An optimization process, including adaptive remeshing scheme, is used to detect the variations of the temperature, the bubble shape evolution, ensuring the convergence of the solution to the physical solution [8, 9]. The paper is organized as follows. Section 2 describes the equations of the model and the numerical resolution method. The adaptive remeshing process and the optimization steps are presented in Section 3. In Section 4, the results of numerical simulations are presented before concluding.

2. Model and Numerical Methods

The section is devoted to presenting the equation systems modeling the photothermic process and the numerical method used to solve the system.

2.1. Electromagnetic Problem. In electromagnetic system, the partial differential equations are derived from Maxwell's equations. The problem can be reduced to Helmholtz equation for the harmonic electric **E** and magnetic **H** fields (i.e., in the form $\exp(j\omega t)$, where ω is the angular frequency of the harmonic wave) [10]. In the 2D case of an infinity elliptical cylinder along the z-axis, the unknown field is the magnetic component and, for a polarized illumination in the transverse magnetic mode TM, the magnetic field can be written as $\mathbf{H}(x, y) = (0, 0, H_z(x, y))$. Therefore, the electromagnetic problem is reduced to a scalar problem and the computation of $\mathbf{H}(x, y)$, in a domain Ω, allows deducing the electric field $\mathbf{E}(x, y)$ by using the Maxwell-Ampere equation [10]:

$$\mathbf{E}(x, y) = \frac{-j}{\omega\epsilon_r\epsilon_0}\left[\nabla \times \mathbf{H}(x, y)\right], \quad \forall (x, y) \in \Omega, \qquad (1)$$

where $(\nabla \times \cdot)$ is the rotational operator, ω the angular frequency, ϵ_0 the permittivity of vacuum, and ϵ_r the relative complex permittivity of the considered materials which are functions of the spatial coordinates (x, y). The H_z component of the magnetic field satisfies the scalar equation

$$\left[\nabla.\left(\frac{1}{\epsilon_r}\nabla\right) + k_0^2\right] H_z(x, y) = 0, \quad \forall (x, y) \in \Omega, \qquad (2)$$

where $k_0 = \omega/c$ is the wave number of the monochromatic incoming wave and c the speed of light in vacuum. To compute the solution $H_z(x, y)$ of the electromagnetic problem, a set of conditions on the boundary Γ of the computational domain Ω must be imposed. The natural boundary condition at the interface between materials is the continuity of the normal component of the electromagnetic excitation:

$$\frac{1}{\epsilon_r}\frac{\partial H_z(x, y)}{\partial n} = -jk_0\left[H_z(x, y) - \left(n_y - 1\right)H_i(x, y)\right], \quad \forall (x, y) \in \Gamma, \qquad (3)$$

where $\partial/\partial n$ is the normal derivative operator, n_y is the normal vector component along the y-axis, and $H_i = H_0\exp(jk_0 y)$ is the incident illumination field along the y-axis with $H_0 = 1/(c\mu_0)$ and μ_0 being the permeability of vacuum. Such a boundary condition is used in problems of wave propagation [11–13].

2.2. Thermic Problem. Under illumination by an electromagnetic wave, the nanowire absorbs energy. That energy produces a heat source given by

$$Q(x, y) = \frac{\omega}{2}\epsilon_0 Im(\epsilon_r)\left|\mathbf{E}(x, y)\right|^2, \quad \forall (x, y) \in \Omega. \qquad (4)$$

The resolution of the thermal problem requires solving the heat equation which is a partial differential parabolic equation describing the evolution of the temperature T with a heat source Q. That equation is written as follows:

$$\left[\nabla \cdot (k(x, y)\nabla)\right] T(x, y) = Q(x, y), \quad \forall (x, y) \in \Omega, \qquad (5)$$

with a Dirichlet boundary condition $T = T_0$ and $k(x, y)$ is the thermal conductivity of the materials. The variation of the temperature depends on both imaginary part of the permittivity $\epsilon_r(x, y)$ and the intensity of the electric field $|\mathbf{E}(x, y)|^2$.

The resolution of the coupled electromagnetic and heat problems allows extracting the spatial distribution of the temperature in the computational domain. From the map of temperature and for a fixed threshold of vaporization α, the identification of the shape and size of the bubble around the nanowire can be achieved. Such information on shape and size of the bubble would be used to construct a relation between the geometric characteristics of the bubble and the nanowire.

2.3. The Finite Element Method. The objective is to solve (2) and (5) for the coupled system in a domain whose geometry can be complex. The Finite Element Method (FEM) was applied since the 1940s in mechanics, thermodynamics, electromagnetics, and electrical engineering [14, 15]. The method is used to solve partial differential equation systems with boundary conditions in open or close domains. The resolution of problem necessitates a discrete domain, generally named mesh of the domain [13]. The solutions of the problem are computed on the nodes of the mesh. In order to both control the error on the solution and to decrease the number of nodes, an improved method, including an iterative remeshing process, is developed and used. Such an improved FEM allows describing the complex structures with arbitrary shapes. Moreover, the stability of the FEM is also improved by using a weak formulation (or variational formulation) of (2) and (5). Therefore, the electromagnetic and thermic fields satisfy

$$\begin{aligned} &\int_\Omega \left[\nabla \cdot \left(\frac{1}{\epsilon_r}\nabla H_z(x, y)\right) + \frac{\omega^2}{c^2}H_z(x, y)\right] \cdot \nu d\Omega = 0, \\ &\int_\Omega \left[\nabla \cdot (k(x, y)\nabla) T(x, y) - Q(x, y)\right] \cdot \tilde{\nu} d\Omega = 0, \end{aligned} \qquad (6)$$

where ν and $\tilde{\nu}$ are test functions defined on $L^2(\Omega)$ (the linear space of the scalar functions ν and $\tilde{\nu}$, being 2-integrable on Ω). The basis of polynomial functions provides an approximation of the solutions H_z and T in each node [16]. The field H_z (resp., T) is a linear combination of such basic polynomial functions ν (resp., $\tilde{\nu}$) and the problem consists in solving a linear system [15, 17]. The solution verifies exactly the partial differential equations on each node for the given boundary conditions. Ritz's formulation of the variational problem is used to satisfy the continuity of the tangential components of the electromagnetic field [13].

3. Optimization Process and Adaptive Remeshing

Partial differential equations (electromagnetic and thermic) are formulated and solved on the mesh of the computational domain through the FEM. But the accuracy of the computed solution depends on the quality of the mesh [9, 18, 19].

A remeshing process and adaptive loops have been developed in order to improve the quality of the solutions by adapting the size of the mesh elements to the physical solution [9, 20]. The mesh adaption is required to converge to a stable solution, in particular where strong variation of the electromagnetic or temperature fields occurred. For each step of the adaption process, the approximate solution of the Helmholtz equation, the electric field $\mathbf{E}$, the heat source Q, and the temperature T are computed [20]. The interpolation error, based on an estimation of the discrete Hessian of the solution, is used to limit the maximum deviation between the exact solution and the solution associated with the mesh [21, 22]. The a posteriori error estimator, based on the interpolation error, allows defining a physical size map $C_p(\Omega)$ such as

$$C_p(\Omega) = \{h_p(x, y)\}, \quad \forall (x, y) \in \Omega, \tag{7}$$

where $h_p(x, y)$ is the physical size defined at each node and is proportional to the inverse of the deviation of the Hessian. For a given maximum tolerance on the physical error γ, the size $h_p(x, y)$ is given by

$$h_{\min} \leq h_p(x, y) = \frac{\gamma}{\eta(x, y)} \leq h_{\max}, \tag{8}$$

where $h_{\min}$ and $h_{\max}$ are the minimum and maximum sizes of the elements and $\eta(x, y)$ is an estimation of the maximum deviation obtained from the Hessian of the solution. The physical size map $C_p(\Omega)$ is used to govern the adaptive remeshing of the domain with the BL2D-V2 software (adaptive remeshing generating isotropic or anisotropic meshes) [23]. The domain is then entirely remeshed and a new mesh $M_p(\Omega)$ is obtained. The resolution of the multiphysics problem is based on the computation of two physical size maps: the first one $C_Q(\Omega)$ related to the heat source Q and the second one $C_T(\Omega)$ related to the temperature T. The adaptive computational scheme consists in iterative and adaptive loops:

A_1 initial mesh $M_{i=0}(\Omega)$ generated with triangular elements of the computational domain Ω,

A_2 computation of the field $(H_z)_i$ (solution of (2)) on $M_i(\Omega)$,

A_3 computation of the solutions $\mathbf{E}_i$ and Q_i on $M_i(\Omega)$,

A_4 physical error estimation: computation of the interpolation error of the physical solution Q_i; definition of a physical size map $C_{Q_i}(\Omega)$ connected to the field Q_i enabling relating the error to a given threshold δ,

A_5 remeshing of the domain conforming to the size map $C_{Q_i}(\Omega)$,

A_6 if the threshold δ is not satisfied loop to step A_2, with $i = i + 1$, in order to obtain a new mesh $M_i(\Omega)$,

else $M_Q(\Omega) = M_i(\Omega)$, and $M_{i=0}(\Omega) = M_Q(\Omega)$,

B_1 computation of the solutions T_i on $M_i(\Omega)$,

B_2 physical error estimation: computation of the interpolation error of the physical solution T_i; definition of a physical size map $C_{T_i}(\Omega)$ connected to the field T_i enabling relating the error to a given threshold δ,

B_3 remeshing of the domain conforming to the size map $C_{T_i}(\Omega)$,

B_4 if the threshold δ is not satisfied loop to step B_1, with $i = i + 1$, in order to compute the temperature T_i on the new adapted mesh $M_i(\Omega)$,

else $M_T(\Omega) = M_i(\Omega)$,

C_1 detection of the new domain (water vapor) on M_T for a fixed threshold of vaporization in order to produce a mesh $M_V(\Omega)$ and $M_{i=0}(\Omega) = M_V(\Omega)$,

C_2 computation of the physical solutions T_i on $M_i(\Omega)$,

C_3 physical error estimate: computation of the interpolation error of the physical solution T_i; definition of a physical size map $C_{V_i}(\Omega)$ connected to the field T_i enabling relating the error to a given threshold δ,

C_4 remeshing of the domain conforming to the size map $C_{V_i}(\Omega)$,

C_5 if the threshold δ is not satisfied loop to step C_2, with $i = i + 1$, in order to compute the temperature T_i on the last adapted mesh $M_i(\Omega)$,

else $M_F(\Omega) = M_i(\Omega)$.

4. Numerical Results and Discussion

Here, we consider a TiO_2 elliptical nanowire of semiaxes ($a = 45$ nm and $b = 10$ nm), with thermal conductivity $k(TiO_2) = 11.7\,\mathrm{W m^{-1} K^{-1}}$ immersed in water ($\epsilon_r(\text{water}) = 1.79$ and $k(\text{water}) = 0.6\,\mathrm{W m^{-1} K^{-1}}$) at temperature $T_0 = 25^\circ\mathrm{C}(298.15\,\mathrm{K})$. The nanowire is illuminated by a TM polarized laser pulse at wavelength $\lambda = 1050$ nm of complex permittivity $\epsilon_r(TiO_2)_{1050} = 5.4600 + j0.00148$ with a power density per area units $P_S = 1.75 \times 10^{12}\,\mathrm{W/m^2}$ [24, 25]. The materials of the system are considered isotropic and homogeneous.

The results of the adaptive process on mesh and on the temperature maps are illustrated in Figure 1. Figures 1(a) and 1(b) show the initial mesh M_0 and the associated temperature. The adaptive process on the temperature field T (with $\gamma = 0.0001$, $h_{\max} = 40$ nm, $h_{\min} = 0.03$ nm, and $\delta = 0.1$) produces the mesh M_T and the temperature map. The mesh is adapted on the outline of the nanowire that presents strong variations of the temperature. For a water vaporization threshold $\alpha = 100^\circ\mathrm{C}(373.15\,\mathrm{K})$, the detection of the new material (water vapor) is obtained from the temperature map computed on the mesh M_T. Figure 1(c) presents the areas of the three materials: TiO_2(red), vapor (green), and water (blue). The computation of the temperature on the domain that contains the water vapor requires including the physical parameters of the vapor (permittivity $\epsilon_r(\text{vap}) = 1.79$ and thermic conductivity $k(\text{vap}) = 0.05\,\mathrm{W m^{-1} K^{-1}}$). The spatial distribution of the temperature field T on the mesh M_{V_0} after detection of

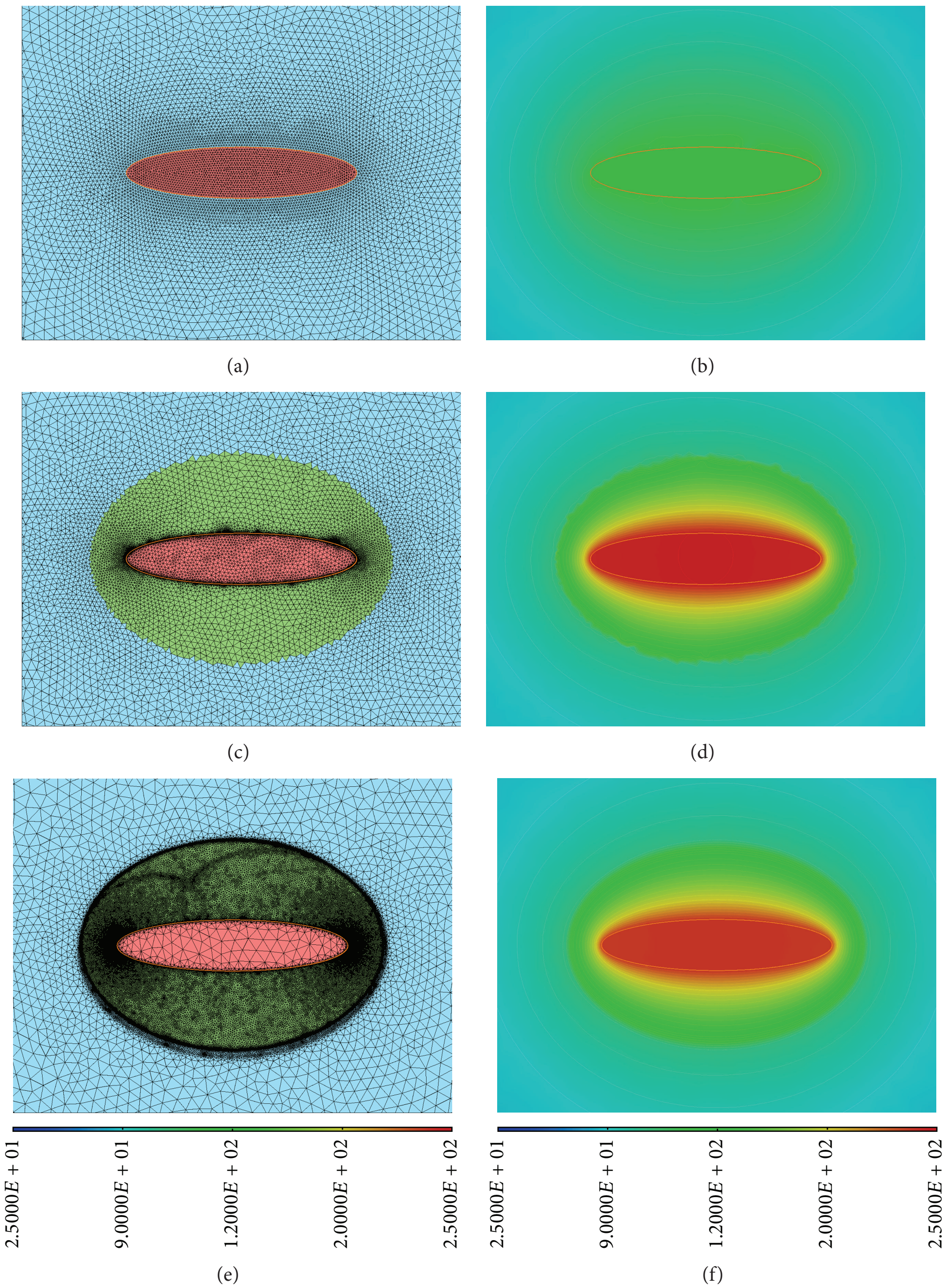

Figure 1: Initial mesh M_0 (a) and adaptive meshes M_{V_0} (c) and M_F (e) and the associated temperature maps on M_0 (b), M_{V_0} (d), and M_F (f) for nanowire illuminated at $\lambda = 1050$ nm.

the bubble produced around the nanowire is shown in Figure 1(d). The final mesh M_F is obtained, after eight iterations, by applying the adaptive process on the field T (with $\delta = 0.02$) taking into account the bubble. That mesh is adapted in the bubble especially on its outline where variations in the temperature occur and relaxed inside the nanowire where the temperature is almost constant (Figure 1(e)). The remeshing process takes into account the shape and size of the bubble. Figure 1(f) shows the temperature map T on the mesh M_F after convergence to a stable solution. The level curves are smooth where a strong variation of the temperature is shown (in the vicinity of the boundary of the bubble and the nanowire). The map also shows an increase of the temperature in the nanowire due to the creation of the bubble. Such an increase is due to the diffusion of the temperature, produced by the nanowire after detection of the bubble (i.e., the water vapor has a smaller thermal conductivity than water).

In order to study the evolution of the shape and size of the bubble, we also consider the nanowire illuminated

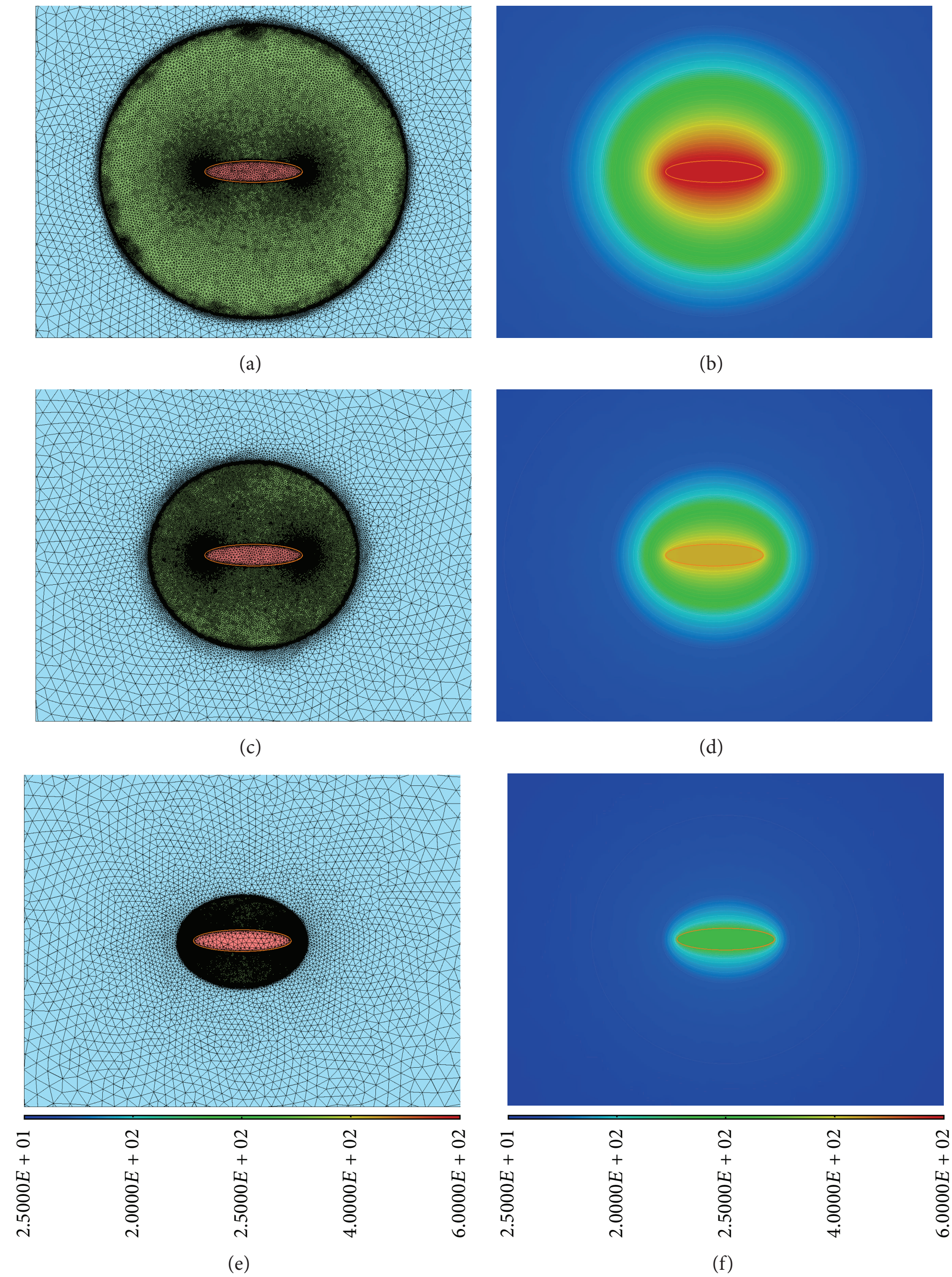

Figure 2: Adapted meshes M_F ((a), (c), and (e)) and temperature map T on M_F ((b), (d), and (f)) for wavelengths $\lambda = 950, 1000$, and 1050 nm, respectively.

at three wavelengths $\lambda = 950$ nm, $\lambda = 1000$ nm, and $\lambda = 1050$ nm with physical parameters ($\epsilon(TiO_2)_{950} = 5.500 + j0.00164$, $\epsilon_r(TiO_2)_{1000} = 5.475 + j0.00154$, and $\epsilon_r(TiO_2)_{1050} = 5.460 + j0.00148$). Figures 2(a), 2(b), 2(c), 2(d), 2(e), and 2(f) present the mesh M_F after bubble detection and distribution of the temperature T on the meshes for the three different wavelengths $\lambda = 950$ nm, $\lambda = 1000$ nm, and $\lambda = 1050$ nm, respectively. These show the evolution of the meshes (shape and size of the bubble) and the temperature as function of the wavelength. For λ increasing, the imaginary part of the complex permittivity of the TiO_2 decreases, leading to a decrease of the energy absorbed by the nanowire. Therefore, the temperature also decreases and the shape and size of bubble are changing. The created bubble follows the shape of the nanowire (elliptical) at the beginning and becomes circular with the increase of the temperature. Figure 3 shows the evolution of the mean temperature T in the nanowire as function of the aspect ratio $R_n = a/b$ for three wavelengths $\lambda = 950, 1000$, and 1050 nm on the mesh M_F.

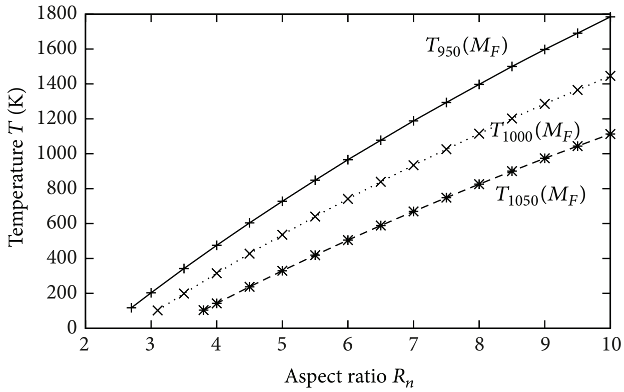

FIGURE 3: Evolution of the mean temperature as function of the nanowire aspect ratio R_n after formation of the bubble for the three wavelengths on M_F.

TABLE 1: Fit parameters of the f function.

λ	NDP	NDF	FNI	Set of parameters a_0	a_1	a_2	σ^2
950	42	39	32	1.0036	0.2418	2.2334	1.8111$e-5$
1000	38	35	15	1.0082	0.3659	2.6394	5.5850$e-5$
1050	31	28	23	1.0124	0.6529	3.2416	1.1106$e-4$

Figure 4(a) shows the evolution of the aspect ratio of the bubble $R_b = A/B$ (A and B being the semiaxes of the bubble) as function of the aspect ratio of the nanowire R_n for the three wavelengths. From the computed data, a function f, satisfying $R_b = f(R_n)$, can be obtained through a nonlinear least-squares fit method (LLS) by the Marquardt-Levenberg algorithm [26–29]. The method is used to find a set of the best parameters fitting the data. It is based on the sum of the squared differences or residuals (SSR) between the input data and the function evaluated at the data. The applied algorithm consists in minimizing the residual variance $\sigma^2 = \text{SSR/NDF}$ with NDF being the number of degrees of freedom (number of the data points (NDP) minus number of the estimated parameters) after a finite number of iterations (FNI). Therefore, the function can be written as follows:

$$f(x) = a_0 + \frac{a_1}{(x - a_2)^2}, \tag{9}$$

with a_0, a_1, and a_2 being set of parameters varying as function of the wavelength. The parameter a_0 concerns the asymptote value which is related to the maximum ratio for a circular bubble, a_1 is the inverse of the decay rate of the function f which is related to the speed tending to the circular shape, and a_2 is the initial ratio from which the bubble begins to form. Table 1 shows the fit parameters for each wavelength. The f function is continuous and strictly decreasing for R_n in the interval $]a_2, +\infty[$; therefore the inverse function f^{-1} exists. The measurement of the aspect ratio of the bubble R_b allows predicting the aspect ratio of the nanowire R_n through the relation $R_n = f^{-1}(R_b)$. Figure 4(b) presents the evolution of the bubble volume (in 2D: $V_b = \pi AB$) as function of the volume of the nanowire (i.e., $V_n = \pi ab$) for each wavelength. From the computed data (vapor bubble for each nanowire and for each wavelength) and by using the same method and the same algorithm, a function g can be obtained through a fit. That function g allows obtaining the relation between the volumes $\ln(V_b) = g(\ln(V_n))$. The g function is continuous and strictly increasing; therefore the inverse function g^{-1} also exists. The measurement of the bubble volume V_b can be used to determine the volume of the nanowire V_n through the relation $\ln(V_n) = g^{-1}(\ln(V_b))$. With the two functions f^{-1} and g^{-1}, the size and shape of the nanowire can be obtained from the information on the bubble:

$$\begin{aligned} \ln(V_n) &= \ln(\pi ba) = \ln\left(\pi b^2 R_n\right) \\ &= \ln\left(\pi b^2 f^{-1}(R_b)\right) = g^{-1}(\ln(V_b)); \end{aligned} \tag{10}$$

consequently,

$$\begin{aligned} b &= \left[\frac{\exp(g^{-1}(\ln(V_b)))}{\pi f^{-1}(R_b)}\right]^{1/2}, \\ a &= \left[\frac{f^{-1}(R_b)\exp(g^{-1}(\ln(V_b)))}{\pi}\right]^{1/2}. \end{aligned} \tag{11}$$

Therefore, the measurement of the size and shape of the bubble can be used to obtain information on the geometry of the nanowire and to reconstruct the size and shape of the nanowire.

5. Conclusion

The paper focuses on the forming and the evolution of the shape and size of the bubble through a photothermal process between a nanowire of TiO_2 immersed in water and an electromagnetic wave. The increase of temperature is related to the geometry of the nanowire which leads to an increase in the shape and size of the bubble. That solution is computed by developing an adaptive remeshing method. That allows to compute with accuracy the temperature by adapting the mesh to the evolution of the bubble. The coupled problem (light, matter, heat) is solved through an adaptive loop process allowing converging to a stable solution and decreasing the number of nodes. The influence of the laser source and the geometrical parameters (wavelength, size, and shape of the nanowire) related to the size and shape of the bubble are presented and analyzed. The aspect ratio and the volume of the bubble can be expressed as function of the aspect ratio and the volume of the nanowire. By solving the inverse problem, two functions are obtained enabling finding the size and shape of the nanowire from the size and shape of bubble.

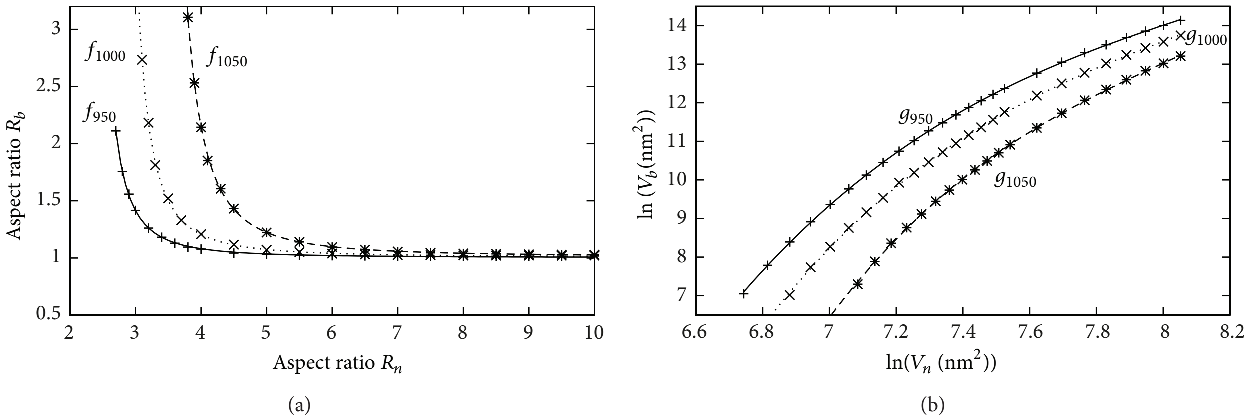

Figure 4: Evolution of (a) the aspect ratio of the bubble R_b as function of the aspect ratio of the nanowire R_n for the three wavelengths and (b) evolution of the volume of the bubble V_b as function of the volume of the nanowire V_n.

Conflict of Interests

The authors declare that there is no conflict of interests regarding the publication of this paper.

Acknowledgment

The authors thank the ANR-2011-NANO-008 NANOMORPH for financial support.

References

[1] M. Boroski, A. C. Rodrigues, J. C. Garcia, L. C. Sampaio, J. Nozaki, and N. Hioka, "Combined electrocoagulation and TiO_2 photoassisted treatment applied to wastewater effluents from pharmaceutical and cosmetic industries," *Journal of Hazardous Materials*, vol. 162, no. 1, pp. 448–454, 2009.

[2] D. Chatterjee and A. Mahata, "Demineralization of organic pollutants on the dye modified TiO_2 semiconductor particulate system using visible light," *Applied Catalysis B: Environmental*, vol. 33, no. 2, pp. 119–125, 2001.

[3] D. Karamanis, A. N. Ökte, E. Vardoulakis, and T. Vaimakis, "Water vapor adsorption and photocatalytic pollutant degradation with TiO_2-sepiolite nanocomposites," *Applied Clay Science*, vol. 53, no. 2, pp. 181–187, 2011.

[4] G. Bystrzejewska-Piotrowska, J. Golimowski, and P. L. Urban, "Nanoparticles: their potential toxicity, waste and environmental management," *Waste Management*, vol. 29, no. 9, pp. 2587–2595, 2009.

[5] B. Nowack, "The behavior and effects of nanoparticles in the environment," *Environmental Pollution*, vol. 157, no. 4, pp. 1063–1064, 2009.

[6] D. Lapotko and E. Lukianova, "Laser-induced micro-bubbles in cells," *International Journal of Heat and Mass Transfer*, vol. 48, no. 1, pp. 227–234, 2005.

[7] D. Lapotko, E. Lukianova, and A. Shnip, "Photothermal responses of individual cells," *Journal of Biomedical Optics*, vol. 10, no. 1, Article ID 014006, 2005.

[8] D. Barchiesi, T. Grosges, E. Kremer, and M. L. de la Chapelle, "Electromagnetic heat induced in meso-structures: computation of temperature in metallic dimers," *PIERS Online*, vol. 7, no. 5, pp. 406–410, 2011.

[9] T. Grosges, H. Borouchaki, and D. Barchiesi, "New adaptive mesh development for accurate near-field enhancement computation," *Journal of Microscopy*, vol. 229, no. 2, pp. 293–301, 2008.

[10] B. Born and E. Wolf, *Principle of Optics*, Pergamon Press, Oxford, UK, 1993.

[11] T. Grosges, S. Petit, D. Barchiesi, and S. Hudlet, "Numerical modeling of the subwavelength phase-change recording using an apertureless scanning near-field optical microscope," *Optics Express*, vol. 12, no. 24, pp. 5987–5995, 2004.

[12] T. Grosges, A. Vial, and D. Barchiesi, "Models of near-field spectroscopic studies: comparison between finite-element and finite-difference methods," *Optics Express*, vol. 13, no. 21, pp. 8483–8497, 2005.

[13] J. Jin, *The Finite Element Method in Electromagnetics*, John Wiley & Sons, New York, NY, USA, 1993.

[14] R. Courant, "Variational methods for the solution of problems of equilibrium and vibrations," *Bulletin of the American Mathematical Society*, vol. 49, no. 1, pp. 1–23, 1943.

[15] P. Silvester and G. Pelosi, *Finite Elements for Wave Electromagnetics: Methods and Techniques*, IEEE Press, New York, NY, USA, 1994.

[16] R. Fikri, D. Barchiesi, F. H'Dhili, R. Bachelot, A. Vial, and P. Royer, "Modeling recent experiments of apertureless near-field optical microscopy using 2D finite element method," *Optics Communications*, vol. 221, no. 1–3, pp. 13–22, 2003.

[17] I. Stakgold, *Boundary Value Problems of Mathematical Physics, Volumes I and II*, Macmillan, New York, NY, USA, 1969.

[18] P. G. Ciarlet, "Basic error estimates for elliptic problems," in *Handbook of Numerical Analysis*, vol. 2, pp. 17–351, North Holland, Amsterdam, The Netherlands, 1991.

[19] D. Xue and L. Demkowicz, "Modeling of electromagnetic absorption/scattering problems on curvilinear geometries using hp finite/infinite element method," *Finite Elements in Analysis and Design*, vol. 42, no. 7, pp. 570–579, 2006.

[20] T. Grosges, H. Borouchaki, and D. Barchiesi, "Improved scheme for accurate computation of high electric near-field gradients," *Optics Express*, vol. 15, no. 3, pp. 1307–1321, 2007.

[21] R. Radovitzky and M. Ortiz, "Error estimation and adaptive meshing in strongly nonlinear dynamic problems," *Computer Methods in Applied Mechanics and Engineering*, vol. 172, no. 1–4, pp. 203–240, 1999.

[22] M. Ainsworth and J. T. Oden, "A posteriori error estimation in finite element analysis," *Computer Methods in Applied Mechanics and Engineering*, vol. 142, no. 1-2, pp. 1–88, 1997.

[23] P. Laug and H. Borouchaki, "BL2D-V2: mailleur bidimensionnel adaptatif," Report INRIA RT-0275, 2003, http://hal.inria.fr/inria-00069902.

[24] T. L. Brown and J. A. Rice, "The effect of laser wavelength and power density on the laser desorption mass spectrum of fulvic acid," *Organic Geochemistry*, vol. 31, no. 7-8, pp. 627–634, 2000.

[25] A. O'Connor, O. Morris, and E. Sokell, "Angular and energy distribution of Sn ion debris ejected from a laser-produced plasma source, for laser power densities in the range suitable for extreme ultraviolet lithography," *Journal of Applied Physics*, vol. 109, no. 7, Article ID 073301, 2011.

[26] K. Levenberg, "A method for the solution of certain problems in least squares," *Quarterly of Applied Mathematics*, vol. 2, pp. 164–168, 1944.

[27] D. Marquardt, "An algorithm for least-squares estimation of nonlinear parameters," *SIAM Journal on Applied Mathematics*, vol. 11, no. 2, pp. 431–441, 1963.

[28] P. E. Gill and W. Murray, "Algorithms for the solution of the nonlinear least-squares problem," *SIAM Journal on Numerical Analysis*, vol. 15, no. 5, pp. 977–992, 1978.

[29] V. V. Vasin and G. Y. Perestoronina, "The Levenberg-Marquardt method and its modified versions for solving nonlinear equations with application to the inverse gravimetry problem," *Proceedings of the Steklov Institute of Mathematics*, vol. 280, no. 1, supplement, pp. 174–182, 2013.

Hindawi Publishing Corporation
The Scientific World Journal
Volume 2014, Article ID 826125, 7 pages
http://dx.doi.org/10.1155/2014/826125

Research Article

Mean-Variance Portfolio Selection for Defined-Contribution Pension Funds with Stochastic Salary

Chubing Zhang

School of Business, Tianjin University of Finance and Economics, Tianjin 300222, China

Correspondence should be addressed to Chubing Zhang; zcbhrj@163.com

Received 26 December 2013; Accepted 2 March 2014; Published 20 March 2014

Academic Editors: D. Baleanu and C. M. Khalique

This paper focuses on a continuous-time dynamic mean-variance portfolio selection problem of defined-contribution pension funds with stochastic salary, whose risk comes from both financial market and nonfinancial market. By constructing a special Riccati equation as a continuous (actually a viscosity) solution to the HJB equation, we obtain an explicit closed form solution for the optimal investment portfolio as well as the efficient frontier.

1. Introduction

There are two radically different methods to design a pension fund: defined-benefit plan (hereafter DB) and defined-contribution plan (hereafter DC). In DB, the benefits are fixed in advance by the sponsor and the contributions are adjusted in order to maintain the fund in balance, where the associated financial risks are assumed by the sponsor agent; in DC, the contributions are fixed and the benefits depend on the returns on the assets of the fund, where the associated financial risks are borne by the beneficiary. Historically, DB has been more popular. However, in recent years, owing to the demographic evolution and the development of the equity markets, DC plays a crucial role in the social pension systems.

Because the member of DC has some freedom in choosing the investment allocation of their pension fund in the accumulation phase, they have to solve an optimal investment portfolio problem. Traditionally, the usual method to deal with it has been the maximization of expected utility of final wealth. Consistently with the economics and financial literature, the most widely used utility function exhibits constant relative risk aversion (CRRA), that is, the power or logarithmic utility function (e.g., [1–4]). Some papers use the utility function that exhibits constant absolute risk aversion (CARA), that is, the exponential utility function (e.g., [5]). Some papers also adopt the CRRA and CARA utility functions simultaneously (e.g., [6, 7]). However, Zhou and Li [8] think that in these situations the resulting portfolio policies are often shown to be myopic optimal policies, the utility functions from the investors are difficultly elicited, and trade-off information between the risk and the expected return is implicit which makes an investment decision much less intuitive. The objective of mean-variance can effectively solve the weaknesses of utility maximization for the optimal investment of DC. But there have been few pieces of literature on the mean-variance portfolio selection for DC pension funds. Thus, this paper studies the optimal investment portfolio selection of DC pension funds under the mean-variance model.

Markowitz [9] firstly designed the mean-variance portfolio selection model based on a trade-off between their expected return and risk, which is measured as the variance of the return. The most important contribution of this model is that it quantifies the risk by using the variance, which enables investors to seek the highest return after specifying their acceptable risk level. However, the mean-variance portfolio selection by Markowitz [9, 10] is only a single-period investment model. There have been continuing efforts in extending portfolio selection from the static single period model to dynamic multiperiod (e.g., [11–13]) or continuous-time models (e.g., [8, 14–16]). In the dynamic setting, Merton [17] made the successful and fundamental works by stochastic control methods, but the Merton model does not exactly fit the structure of mean-variance model. Recently, Zhou and

Li [8] introduced a stochastic linear-quadratic (LQ) control framework to study the continuous-time version of the mean-variance problem without any constraints by the classical Riccati approach, where they derived closed-form strategy and obtained an explicit expression of the efficient frontier. After that, the stochastic LQ technique is widely used which is an effective method for mean-variance portfolio selection problems, for example, Li et al. [18], Chiu and Li [19], and Xie et al. [20]. This paper also adopts the stochastic LQ technique.

In addition, the optimal asset allocation for a pension fund involves quite a long period, generally from 20 to 40 years, so it follows that it becomes crucial to take into account the salary risk. Deelstra et al. [2] described the contribution flowed by a nonnegative, progressive measurable and square-integrable process and then studied optimal investment strategies for different examples of guarantees and contributions under the power utility. Battocchio and Menoncin [5] assumed that the stochastic salary's volatility came from both financial market and nonfinancial market and analyzed the behavior of the optimal portfolio with respect to salary under the exponential utility. Cairns et al. [3] considered the same assumption but used the member's final salary as a numeraire and then discussed various properties and characteristics of the optimal strategies with or without the presence of non-hedgeable salary risk under the power utility. Based on their researches, this paper also assumes that the stochastic salary risk comes from both financial market and nonfinancial market.

Our main objective in this paper is to find the optimal investment portfolio selection for DC pension funds with stochastic salary under the mean-variance model, which has not been reported in the existing literature. It is characterized by the following two aspects: (i) the optimal objective is not for the maximization of expected utility of final wealth but for the mean-variance of final wealth, so the decision-making process of weighing return and risk can be better understood; (ii) the stochastic salary's volatility contains both a hedgeable volatility whose risk source is the set of the financial market risk sources and a nonhedgeable whose risk source volatility does not the set of the financial market risk sources, so it is more suitable to the realistic economic background. We construct a special Riccati equation as a continuous (actually a viscosity) solution to the HJB equation and obtain an explicit closed form solution for the optimal investment portfolio as well as the efficient frontier.

2. Mathematical Model

In this section, we introduce the market structure and define the stochastic dynamics of the asset price and the salary.

We consider a complete and frictionless financial market which is continuously open over the fixed time interval $[0, T]$, where $T > 0$ denotes the retirement time.

2.1. The Financial Market. Given an n-dimensional standard Brownian motion $(w_1, \ldots, w_n)^T$, we consider the complete probability space (Ω, F, P) generated by it; that is, to say, F is the filtration $\{F_t\}_{t\geq 0}$, with $F_t = \sigma\{w_1(s), \ldots, w_n(s); 0 \leq s \leq t\}$.

The plan sponsor manages the fund in the planning interval $[0, T]$ by means of a portfolio formed by n risky assets $\{S^i\}_{i=1}^n$, which are correlated geometric Brownian motions, generated by $w = (w_1, \ldots, w_n)^T$, and a riskless asset S^0, as proposed in Merton [17]; that is, whose evolutions are given by the following equations:

$$dS^0(t) = rS^0(t)\,dt, \quad S^0(0) = 1,$$
$$dS^i(t) = S^i(t)\left(b_i dt + \sum_{j=1}^{n} \sigma_{ij} dw_j(t)\right), \tag{1}$$
$$S^i(0) = s_i > 0, \quad i = 1, 2, \ldots, n.$$

Here, $r > 0$ denotes the short risk-free rate of interest, $b_i > 0$ is the mean rate of return of the ith risky asset, and σ_{ij} is the covariance between asset i and j, for all $i, j = 1, 2, \ldots, n$. It is assumed that $b_i > r$ for all i, so the sponsor has incentives to invest with risk.

2.2. The Stochastic Salary. We denote the salary at time t by $L(t)$, which follows the stochastic differential equation (SDE):

$$dL(t) = \kappa L(t)\,dt + \eta L(t)\,dB(t), \quad L(0) = L_0 > 0, \tag{2}$$

where κ is an expected instantaneous growth rate of the salary and is a real constant. η is the instantaneous volatility of the salary, and both are constant parameters. Moreover, we assume that the instantaneous mean of salary is such that $\kappa = r + \nu$, where ν is a real constant.

We suppose that there exists correlation $q_i \in [-1, 1]$ between B and w_i, for $i = 1, 2, \ldots, n$. As a consequence, B is expressed in terms of $\{w_i\}_{i=0}^n$ as $B(t) = \sqrt{1 - q^T q}\, w_0(t) + q^T w(t)$, where $q^T q \leq 1$ for $q = (q_1, q_2, \ldots, q_n)^T$.

Remark 1. Equation (2) can be rewritten as $dL(t) = \kappa L(t)dt + \eta L(t) q^T w(t) + \eta L(t)\sqrt{1 - q^T q}\, w_0(t)$. ηq^T is a volatility scale vector measuring how the risk source of stocks affects the salary, while $\eta\sqrt{1 - q^T q}$ is a nonhedgeable volatility whose risk source does not the set of the financial market risk sources. This nonhedgeable risk source is represented by the one-dimensional standard Brownian motion $w_0(t)$ which is independent of $w(t)$. In addition, both Battocchio and Menoncin [5] and Cairns et al. [3] assumed that the salary was affected by hedgeable and nonhedgeable risk sources. However, Battocchio and Menoncin [5] just studied a risky asset, while Cairns et al. [3] extended the investment opportunity set to n risky assets. Obviously, our assumption is similar to Cairns et al. [3].

2.3. The Wealth Process. According to the viewpoint of Cairns et al. [3], we consider that the contributions are continuous in the pension fund at the rate of $kL(t)$.

Let $X(t)$ denote the wealth of pension fund at time t. $\pi_i(t)$, $i = 1, 2, \ldots, n$ represents the wealth amount invested in the ith risky asset at time t. We suppose that the investment strategy $\{\Lambda(t); t \geq 0\}$, with $\Lambda(t) = (\pi_1(t), \pi_2(t), \ldots, \pi_n(t))^T$, is a control process adapted to filtration $\{F_t\}_{t\geq 0}$, F-measurable, Markovian and stationary, stratifying $E\int_0^T \Lambda(t)^T\Lambda(t)dt < \infty$, where E is the expectation operator.

Therefore, the dynamics of the pension fund is given under the investment policy Λ by

$$dX(t) = \sum_{i=1}^{n}\pi_i(t)\frac{dS^i(t)}{S^i(t)} + \left(X(t) - \sum_{i=1}^{n}\pi_i(t)\right)\frac{dS^0(t)}{S^0(t)} + kL(t)\,dt, \quad X(0) = X_0, \tag{3}$$

where X_0 stands for an initial wealth.

By taking into (1), the evolution of pension wealth can be rewritten as

$$dX(t) = \left(rX(t) + \sum_{i=1}^{n}\pi_i(t)(b_i - r) + kL(t)\right)dt + \sum_{i=1}^{n}\sum_{j=1}^{n}\pi_i(t)\sigma_{ij}dw_j(t). \tag{4}$$

Next, we will assume the matrix notations $\sigma = (\sigma_{ij})$, $b = (b_1, b_2, \ldots, b_n)^T$, $1 = (1, 1, \ldots, 1)^T$, and $\Sigma = \sigma\sigma^T$. We take as given the existence of Σ^{-1}, that is, to say, σ^{-1}. Finally the vector of standardized risk premia or Sharpe ratio of the portfolio is denoted by $\theta = \sigma^{-1}(b - r1)$.

So, we can rewrite (4) as

$$dX(t) = \left(rX(t) + \Lambda^T(t)(b - r1) + kL(t)\right)dt + \Lambda^T(t)\sigma dw(t), \tag{5}$$

with the initial condition $X(0) = X_0$.

For a prescribed target expected terminal wealth $EX(T) = K$, mean-variance portfolio optimization consists of determining a dynamic portfolio satisfying all the constraints of a given framework and minimizing the risk as measured by the variance of the terminal wealth, that is, minimizing

$$\operatorname{Var}X(T) = E[X(T) - EX(T)]^2 = E[X(T) - K]^2. \tag{6}$$

Remark 2. The investor expects a return above the risk free investment consisting of $\pi_i(t) = 0$ for $i = 1, 2, \ldots, n$ and whose associated wealth process $X(\cdot)$ satisfies

$$dX(t) = (rX(t) + kL(t))\,dt, \quad X(0) = X_0,\ L(0) = L_0 \tag{7}$$

and has for solution $X(T) = X_0e^{rT} + \int_0^T kL(t)e^{r(T-t)}dt$, $L(0) = L_0$.

This leads to the following natural assumption:

$$K \geq X_0e^{rT} + \int_0^T kL(t)e^{r(T-t)}dt, \quad L(0) = L_0. \tag{8}$$

3. The Optimal Control Problem

In this section, we provide the mean-variance model and then derive the Hamilton-Jacobi-Bellman (HJB) equation.

3.1. Mean-Variance Model

Theorem 3. *A portfolio $\Lambda(\cdot)$ is said to be admissible if $\Lambda(\cdot) \in L_F^2(0, T; R^n)$ for any $T > 0$ and the corresponding linear stochastic differential equations (2) and (5) have a unique solution pair $(X(t), L(t))$ corresponding to $\Lambda(\cdot)$. In this case, $(X(\cdot), L(t), \Lambda(\cdot))$ is called an admissible (wealth, salary, and portfolio) triple.*

The following optimization problem parameterized by $K \geq X_0e^{rT} + \int_0^T kL(t)e^{r(T-t)}dt$, $L(0) = L_0$ is mean-variance portfolio selection:

$$\begin{aligned} &\min && \operatorname{Var}X(T) = E[X(T) - K]^2, \\ &\text{subject to} && EX(T) = K, \\ &&& (X(\cdot), L(t), \Lambda(\cdot)) \text{ is admissible.} \end{aligned} \tag{9}$$

Problem (9) is called feasible if there exists at least one admissible pair satisfying $EX(T) = K$. Given K, the optimal strategy $\Lambda^*(\cdot)$ of (9) is called an efficient strategy; this leads to a terminal wealth $X(T)$ and the pair $(K, \operatorname{Var}X(T))$ is called an efficient point. The set of all efficient points, when the parameter K runs over $[X_0e^{rT} + \int_0^T kL(t)e^{r(T-t)}dt, +\infty)$, $L(0) = L_0$, is called the efficient frontier.

Problem (9) is a dynamic quadratic convex optimization problem and hence has a unique solution. To find the optimal strategy corresponding to the constraint $EX(T) = K$, we introduce a Lagrange multiplier $2\mu \in R$ (the factor 2 is introduced for computational convenience) and after rearranging terms there arrives at the new cost function

$$\begin{aligned} \widehat{J}(\Lambda(\cdot), \mu) &= E\left[(X(T) - K)^2 + 2\mu(X(T) - K)\right] \\ &= E[X(T) - (K - \mu)]^2 - \mu^2. \end{aligned} \tag{10}$$

Letting $\gamma = K - \mu$ leads to the following optimal stochastic control problem (with the minimization over the set of strategies $\Lambda(\cdot)$):

$$\begin{aligned} &\min && \overline{J}(\Lambda(\cdot), \gamma) = E[X(T) - \gamma]^2 - (K - \gamma)^2, \\ &\text{subject to} && (X(\cdot), L(t), \Lambda(\cdot)) \text{ being admissible.} \end{aligned} \tag{11}$$

Note that, $\max_{\mu\in R}\min_{\Lambda(\cdot)}\widehat{J}(\Lambda(\cdot), \mu) = \max_{\gamma\in R}\min_{\Lambda(\cdot)}\overline{J}(\Lambda(\cdot), \gamma)$.

Remark 4. The link between problems (9) and (11) is provided by the Lagrange duality theorem; see, for example, Fu et al. [21]

$$\begin{aligned} \min \operatorname{Var}X(T) &= \max_{\mu\in R}\min_{\Lambda(\cdot)}\widehat{J}(\Lambda(\cdot), \mu) \\ &= \max_{\gamma\in R}\min_{\Lambda(\cdot)}\overline{J}(\Lambda(\cdot), \gamma). \end{aligned} \tag{12}$$

Obviously, for a fixed constant γ, problem (11) is clearly equivalent to

$$\begin{aligned} &\min && J(\Lambda(\cdot), \gamma) = E[X(T) - \gamma]^2, \\ &\text{subject to} && (X(\cdot), L(t), \Lambda(\cdot)) \text{ being admissible.} \end{aligned} \tag{13}$$

3.2. The Optimization Program. By using the classical tools of stochastic optimal control, we define the value function

$$H(t,X,L)=\inf_{\Lambda(\cdot)}\left\{(X(T)-\gamma)^2 \mid X(t)=x, L(t)=l;\text{s.t.}\,(2),(5)\right\},\quad 0<t<T. \tag{14}$$

The value function can be considered as a kind of utility function. Kramkov and Schachermayer [22] have demonstrated that the marginal utility of the value function is a constant. In addition, Jonsson and Sircar [23] have shown that the value function inherits the convexity of the utility function.

The maximum principle leads to the following Hamilton-Jacobi-Bellman (HJB) equation:

$$\begin{aligned}H_t+\inf_{\Lambda(\cdot)}\Big\{&\left(rx+\Lambda^T(t)(b-r1)+kl\right)H_x\\&+\kappa l H_l+\frac{1}{2}\eta^2 l^2 H_{ll}\\&+\frac{1}{2}\Lambda^T(t)\Sigma\Lambda(t)H_{xx}+\eta l\Lambda^T(t)\sigma q H_{xl}\Big\}=0\end{aligned}\tag{15}$$

with $H(T,x,l)=(x-\gamma)^2$, where $H_t, H_x, H_l, H_{xx}, H_{ll}$, and H_{xl} denote partial derivatives of first and second orders with respect to time, wealth, and salary.

The first order minimizing conditions for the optimal strategies $\Lambda^*(t)$ is

$$\Lambda^*(t)=-\Sigma^{-1}(b-r1)\frac{H_x}{H_{xx}}-\eta l\sigma^{-T}q\frac{H_{xl}}{H_{xx}}. \tag{16}$$

Putting this in (15), we obtain a partial differential equation (PDE) for the value function H

$$\begin{aligned}&H_t+(rx+kl)H_x-\frac{1}{2}\theta^T\theta\frac{H_x^2}{H_{xx}}+\kappa l H_l+\frac{1}{2}\eta^2 l^2 H_{ll}\\&\quad-\eta l\theta^T q\frac{H_x H_{xl}}{H_{xx}}-\frac{1}{2}\eta^2 l^2 q^T q\frac{H_{xl}^2}{H_{xx}}=0,\end{aligned}\tag{17}$$

with $H(T,x,l)=(x-\gamma)^2$.

4. Optimal Portfolio and Efficient Frontier

In this section, we find the optimal portfolio and the efficient frontier for the problems (9), (11), and (13).

4.1. Optimal Portfolio. We conjecture a solution to (17) with the following form:

$$\begin{aligned}H(t,x,l)=&\beta_0(t)+\beta_1(t)x+\beta_2(t)l\\&+\beta_3(t)x^2+\beta_4(t)l^2+\beta_5(t)xl,\end{aligned}\tag{18}$$

with the boundary conditions given by

$$\begin{aligned}&\beta_0(T)=\gamma^2,\qquad \beta_1(T)=-2\gamma,\qquad \beta_3(T)=1,\\&\beta_2(T)=\beta_4(T)=\beta_5(T)=0.\end{aligned}\tag{19}$$

Therefore,

$$\Lambda^*(t)=-\Sigma^{-1}(b-r1)\left(x+\frac{\beta_1}{2\beta_3}+\frac{\beta_5}{2\beta_3}l\right)-\eta l\sigma^{-T}q\frac{\beta_5}{\beta_3}. \tag{20}$$

The following ordinary differential equations are obtained for the above coefficients:

$$\begin{aligned}&\dot\beta_0=\frac{1}{4}\theta^T\theta\frac{\beta_1^2}{\beta_3},\qquad \beta_0(T)=\gamma^2,\\&\dot\beta_1=\left(\theta^T\theta-r\right)\beta_1,\qquad \beta_1(T)=-2\gamma,\end{aligned}\tag{21}$$

$$\begin{aligned}&\dot\beta_2=-\kappa\beta_l+\left(k+\frac{1}{2}\theta^T\theta\right)\beta_1+\frac{1}{2}\eta\theta^T q\frac{\beta_1\beta_5}{\beta_3},\qquad \beta_2(T)=0,\\&\dot\beta_3=\left(\theta^T\theta-2r\right)\beta_3,\qquad \beta_3(T)=1,\end{aligned}\tag{22}$$

$$\begin{aligned}&\dot\beta_4=-\left(2\kappa+\eta^2\right)\beta_4+\left(\theta^T\theta+2\eta\theta^T q+\eta^2 q^T q\right)\frac{\beta_5^2}{4\beta_3}-k\beta_5,\\&\beta_4(T)=0,\\&\dot\beta_5=-\left(2r+\kappa-\theta^T\theta-\eta\theta^T q\right)\beta_5-2k\beta_3,\qquad \beta_5(T)=0.\end{aligned}\tag{23}$$

Obviously, the method of resolution of this system is standard. Equation (21) has, for solution, $\beta_1(t)=-2\gamma e^{(r-\theta^T\theta)(T-t)}$; (22) also has, for solution, $\beta_3(t)=e^{(2r-\theta^T\theta)(T-t)}$.

Then, by substituting the expression for $\beta_3(t)$ into (23), we can obtain

$$\begin{aligned}\beta_5(t)=\frac{2k}{\kappa-\eta\theta^T q}&\left(e^{(2r-\theta^T\theta)(T-t)}\left(e^{-(\kappa-\eta\theta^T q)t}-1\right)\right.\\&\left.-e^{-(\kappa-\eta\theta^T q)T}+1\right).\end{aligned}\tag{24}$$

Finally, by substituting $\beta_1(t)$, $\beta_3(t)$, and $\beta_5(t)$ into (20), the optimal investment strategy in the risky assets is given by

$$\Lambda^*(t)=-\Sigma^{-1}(b-r1)\left(x-\gamma+\frac{1}{2}f(t)l\right)-\eta l\sigma^{-T}qf(t), \tag{25}$$

where

$$\begin{aligned}f(t)=\frac{2k}{\kappa-\eta\theta^T q}&\left(e^{-(2r-\theta^T\theta)(T-t)}\left(1-e^{-(\kappa-\eta\theta^T q)T}\right)\right.\\&\left.+e^{-(\kappa-\eta\theta^T q)t}-1\right).\end{aligned}\tag{26}$$

Proposition 5. *With the above notation and for a given* $\gamma, T > 0$ *and*

$$K \in \left[X_0 e^{rT} + \int_0^T kL(t)\, e^{r(T-t)} dt, +\infty\right), \quad L(0) = L_0, \tag{27}$$

an optimal investment strategy corresponding to the problems (11) *and* (13) *is*

$$\begin{aligned}\Lambda^*(t) = &-\Sigma^{-1}(b - r1)\left(X(t) - \gamma + \frac{1}{2} f(t) L(t)\right) \\ &- \eta \sigma^{-T} q f(t) L(t),\end{aligned} \tag{28}$$

where,

$$\begin{aligned}f(t) = \frac{2k}{\kappa - \eta\theta^T q}&\left(e^{-(2r-\theta^T\theta)(T-t)}\left(1 - e^{-(\kappa-\eta\theta^T q)T}\right)\right. \\ &\left. + e^{-(\kappa-\eta\theta^T q)t} - 1\right).\end{aligned} \tag{29}$$

Remark 6. The optimal portfolio in risky assets for the investor with mean-variance model can be divided into three parts.

The first part, $-\Sigma^{-1}(b - r1)X(t)$, is always negative and decreases with the wealth level, so we can denote it as a "pension wealth factor." The higher the wealth level the investor has the lower the capital amount are invested in risky assets.

The second part is $\Sigma^{-1}(b - r1)\gamma$. It is always positive, while the parameter γ depends on the equation $\gamma = K - \mu$. So we can denote it as a "terminal wealth expectation factor," which reflects the mean-variance intrinsic feature, that is, the weighing between mean and variance.

The third part, $-(1/2\Sigma^{-1}(b - r1) + \eta\sigma^{-T}q)f(t)L(t)$, is mainly relative to the salary and reflects how the plan member's salary affects the optimal investment strategy. So we call it a "stochastic salary factor." But we difficultly judge the sign of the "stochastic salary factor" for the several parameters' value that cannot be determined.

4.2. Efficient Frontier. In this section, we derive the efficient frontier for the portfolio selection problem (9); that is, we specify the relation between the variance and the expected value of the terminal wealth for every efficient strategy.

By substituting the optimal strategy (25) into the dynamics of the wealth equation (5), we obtain

$$\begin{aligned}dX(t) = \Bigg(&\left(r - \theta^T\theta\right) X(t) + kL(t) \\ &- \theta^T\theta\left(\frac{1}{2} f(t) L(t) - \gamma\right)\Bigg) dt \\ &- \Bigg(\theta^T\left(X(t) - \gamma + \frac{1}{2} f(t) L(t)\right) \\ &+ q^T \eta L(t) f(t)\Bigg) dw(t),\end{aligned} \tag{30}$$

with $X(0) = X_0$.

Next, by applying the Ito's formula to X^2, we obtain

$$\begin{aligned}dX^2(t) = \Bigg\{&\left(2r - \theta^T\theta\right) X^2(t) \\ &+ 2\left(k + \theta^T q\eta f(t)\right) L(t) X(t) + \theta^T\theta\gamma^2 \\ &- \theta^T(\theta + q\eta) f(t) L(t)\gamma \\ &+ \left(q^T q\eta^2 + \frac{1}{4\theta^T\theta} + \theta^T q\eta\right) f^2(t) L^2(t)\Bigg\} dt \\ &- 2X(t)\Bigg(\theta^T\left(X(t) - \gamma + \frac{1}{2} f(t) L(t)\right) \\ &+ q^T\eta L(t) f(t)\Bigg) dw(t),\end{aligned} \tag{31}$$

with $X^2(0) = X_0^2$.

In addition, according to (2), we have $EL(t) = L_0 e^{\kappa t}$, $EL^2(t) = L_0^2 e^{(2\kappa+\eta^2)t}$.

So, by taking expectations on both previous stochastic differential equations, we obtain that functions $m_1(t) = EX(t)$ and $m_2(t) = EX^2(t)$ satisfy the linear ordinary differential equations

$$\begin{aligned}\dot{m}_1(t) &= \left(r - \theta^T\theta\right) m_1(t) + kL_0 e^{\kappa t} \\ &\quad - \theta^T\theta\left(\frac{1}{2} f(t) L_0 e^{\kappa t} - \gamma\right), \\ m_1(0) &= X_0, \\ \dot{m}_2(t) &= \left(2r - \theta^T\theta\right) m_2(t) + 2\left(k + \theta^T q\eta f(t)\right) L_0 e^{\kappa t} m_1(t) \\ &\quad + \theta^T\theta\gamma^2 - \theta^T(\theta + 2q\eta) f(t) L_0 e^{\kappa t}\gamma \\ &\quad + \left(q^T q\eta^2 + \frac{1}{4\theta^T\theta} + \theta^T q\eta\right) f^2(t) L_0^2 e^{(2\kappa+\eta^2)t}, \\ m_2(0) &= X_0^2.\end{aligned} \tag{32}$$

By solving (32), we can express $m_1(T)$ and $m_2(T)$ as explicit functions of γ

$$m_1(T) = \alpha_T X_0 + \frac{\theta^T\theta}{r - \theta^T\theta}(\alpha_T - 1)\gamma + \alpha_T\beta_T, \tag{33}$$

with

$$\begin{aligned}\alpha_t &= e^{(r-\theta^T\theta)t}, \\ \beta_t &= L_0\int_0^t \left(k - \frac{1}{2}\theta^T\theta f(s)\right) e^{(\kappa - r + \theta^T\theta)s} ds,\end{aligned} \tag{34}$$

$$m_2(T) = \alpha_T e^{rT} X_0^2 + \phi\gamma^2 + \varphi\gamma + \varepsilon,$$

and with

$$\phi = -\frac{\theta^T\theta}{2r-\theta^T\theta}\left(1-\alpha_T e^{rT}\right),$$

$$\varphi = \alpha_T e^{rT}\left\{\frac{\theta^T\theta}{r-\theta^T\theta}\int_0^T \tau_t^1\lambda_t\left(1-\alpha_t^{-1}\right)dt - \int_0^T \tau_t^2\lambda_t\alpha_t dt\right\},$$

$$\varepsilon = \alpha_T e^{rT}\left\{X_0\int_0^T \tau_t^1\lambda_t dt + \int_0^T \tau_t^1\lambda_t\beta_t dt + \int_0^T \tau_t^3\alpha_t\lambda_t dt\right\},$$

$$\tau_t^1 = 2\left(k+\theta^T q\eta f(t)\right),$$

$$\tau_t^2 = \theta^T(\theta+2q\eta) f(t) L_0,$$

$$\tau_t^3 = \left(q^T q\eta^2 + \frac{1}{4\theta^T\theta} + \theta^T q\eta\right) f^2(t) L_0^2 e^{(\kappa+\eta^2)t}. \tag{35}$$

By using (33) and (34), we can thus give an explicit expression for problem (11), as a one parameter family in γ

$$\begin{aligned}\overline{J}(\Lambda^*(\cdot),\gamma) &= EX^2(T) - 2\gamma EX(T) + 2\gamma K - K^2\\ &= m_2(T) - 2\gamma m_1(T) + 2\gamma K - K^2\\ &= \alpha_T e^{rT}X_0^2 + \phi\gamma^2 - \frac{2\theta^T\theta}{r-\theta^T\theta}(\alpha_T-1)\gamma^2\\ &\quad - (2\alpha_T X_0 + 2\alpha_T\beta_T - 2K - \varphi)\gamma + \varepsilon - K^2;\end{aligned} \tag{36}$$

that is, to say,

$$\begin{aligned}\min_{\Lambda(\cdot)}\overline{J}(\Lambda(\cdot),\gamma) &= \alpha_T e^{rT}X_0^2 + \phi\gamma^2 - \frac{2\theta^T\theta}{r-\theta^T\theta}(\alpha_T-1)\gamma^2\\ &\quad - (2\alpha_T X_0 + 2\alpha_T\beta_T - 2K - \varphi)\gamma + \varepsilon - K^2.\end{aligned} \tag{37}$$

It then follows, using Remark 2, that minimum Var $X(T)$ is achieved for

$$\gamma^* = \frac{2\alpha_T X_0 + 2\alpha_T\beta_T - 2K - \varphi}{2\phi - \left(4\theta^T\theta/\left(r-\theta^T\theta\right)\right)(\alpha_T-1)}, \tag{38}$$

$$\begin{aligned}\min\ \mathrm{Var}\,X(T) &= \min_{\Lambda(\cdot)}\overline{J}(\Lambda(\cdot),\gamma^*)\\ &= \frac{(2\alpha_T X_0 + 2\alpha_T\beta_T - 2K - \varphi)^2}{4\left(\left(2\theta^T\theta/\left(r-\theta^T\theta\right)\right)(\alpha_T-1)-\phi\right)}\\ &\quad + \alpha_T e^{rT}X_0^2 - K^2 + \varepsilon.\end{aligned} \tag{39}$$

Proposition 7. *The efficient strategy of the portfolio selection problem* (9) *corresponding to the expected terminal wealth* $EX(T) = K$, *as a function of time* t, *wealth* $X(\cdot)$, *and* γ^* *is given by*

$$\begin{aligned}\Lambda^*(t) &= -\Sigma^{-1}(b-r1)\left(X(t)-\gamma^*+\frac{1}{2}f(t)L(t)\right)\\ &\quad - \eta\sigma^{-T}qf(t)L(t).\end{aligned} \tag{40}$$

Moreover, the efficient frontier is

$$\begin{aligned}\mathrm{Var}\,X(T) &= \frac{(2\alpha_T X_0 + 2\alpha_T\beta_T - 2EX(T) - \varphi)^2}{4\left(\left(2\theta^T\theta/\left(r-\theta^T\theta\right)\right)(\alpha_T-1)-\phi\right)}\\ &\quad + \alpha_T e^{rT}X_0^2 - EX^2(T) + \varepsilon.\end{aligned} \tag{41}$$

Remark 8. Expression (41) shows the familiar quadratic relation between the wealth and its variance. The minimum possible variance is attained when

$$EX(T) = \frac{2\alpha_T X_0 + 2\alpha_T\beta_T - \varphi}{2+2\left(\left(2\theta^T\theta/\left(r-\theta^T\theta\right)\right)(\alpha_T-1)-\phi\right)}. \tag{42}$$

Remark 9. Consider two wealth levels $\overline{K}$ and $\widetilde{K}$ ($\in [X_0e^{rT} + \int_0^T kL(t)e^{r(T-t)}dt, +\infty)$, $L(0) = L_0$) and their corresponding efficient portfolio $\overline{\Lambda}(\cdot)$ and $\widetilde{\Lambda}(\cdot)$ given by the explicit formula (40). Then, a portfolio $\Lambda^*(\cdot)$ is efficient if and only if $\Lambda^*(\cdot) = \lambda\overline{\Lambda}(\cdot) + (1-\lambda)\widetilde{\Lambda}(\cdot)$ for some $\lambda \in R$ and corresponding to the wealth $K = \lambda\overline{K} + (1-\lambda)\widetilde{K}$.

Proof. Suppose $\overline{\Lambda}(\cdot)$ and $\widetilde{\Lambda}(\cdot)$ are efficient and hence satisfy (40) corresponding to $\overline{K}$, $\widetilde{K}$, $\overline{\gamma}^*$, and $\widetilde{\gamma}^*$, respectively, and consider $\Lambda^*(\cdot) = \lambda\overline{\Lambda}(\cdot) + (1-\lambda)\widetilde{\Lambda}(\cdot)$, with the corresponding γ^*. By rearranging terms, $\Lambda^*(\cdot)$ can be expressed in the form $\Lambda^*(\cdot) = \lambda\overline{\Lambda}(\cdot)+(1-\lambda)\widetilde{\Lambda}(\cdot)$ corresponding to $K = \lambda\overline{K}+(1-\lambda)\widetilde{K}$ and $\gamma^* = \lambda\overline{\gamma} + (1-\lambda)\widetilde{\gamma}$ and is therefore efficient. Conversely, suppose that $\Lambda^*(\cdot)$ is efficient; that is, it satisfies (40) and corresponds to some K. Decompose K into $K = \lambda\overline{K}+(1-\lambda)\widetilde{K}$ for an appropriate $\lambda \in R$. Then, by using (38), write $\gamma^* = \lambda\overline{\gamma} + (1-\lambda)\widetilde{\gamma}$ and substitute back into (40) to arrive at the decomposition $\Lambda^*(\cdot) = \lambda\overline{\Lambda}(\cdot) + (1-\lambda)\widetilde{\Lambda}(\cdot)$. □

5. Conclusions

Defined-contribution pension funds play a crucial role in the social pension systems. The utility function is usually assumed to be a continuous, increasing, and strictly concave function such as a power, logarithm, exponential, or quadratic function. The risk and return relationship is implicit in the utility function approach and cannot be disentangled at the level of optimal strategies. In addition, the optimal asset allocation for a pension fund involves quite a long period, generally from 20 to 40 years, so it follows that it becomes crucial to take into account the salary risk. So this paper studies the optimal investment portfolio selection of DC pension funds with stochastic salary under the mean-variance model. We construct a special Riccati equation as a continuous (actually a viscosity) solution to the HJB equation and obtain an explicit closed form solution for the optimal investment portfolio as well as the efficient frontier.

In the future research, we will continue to concentrate on continuous-time portfolio selection problem under the mean-variance model. It would be interesting to extend our analysis to those more generalized situation, such as assuming the risky asset to follow constant elasticity of variance (CEV) models and introducing different stochastic interest rate model under the research framework. It is noteworthy that the optimal solver with the generalized situation is very difficult.

Conflict of Interests

The author declares that there is no conflict of interests regarding the publication of this paper.

Acknowledgments

The authors are grateful to the anonymous referee for careful reading of the paper and helpful comments and suggestions. C. Zhang was supported by the Young Scholar Program of Tianjin University of Finance and Economics (Grant no. TJYQ201201).

References

[1] J.-F. Boulier, S. Huang, and G. Taillard, "Optimal management under stochastic interest rates: the case of a protected defined contribution pension fund," *Insurance: Mathematics and Economics*, vol. 28, no. 2, pp. 173–189, 2001.

[2] G. Deelstra, M. Grasselli, and P.-F. Koehl, "Optimal investment strategies in the presence of a minimum guarantee," *Insurance: Mathematics and Economics*, vol. 33, no. 1, pp. 189–207, 2003.

[3] A. J. G. Cairns, D. Blake, and K. Dowd, "Stochastic lifestyling: optimal dynamic asset allocation for defined contribution pension plans," *Journal of Economic Dynamics and Control*, vol. 30, no. 5, pp. 843–877, 2006.

[4] J. Xiao, H. Zhai, and C. Qin, "The constant elasticity of variance (CEV) model and the Legendre transform-dual solution for annuity contracts," *Insurance: Mathematics and Economics*, vol. 40, no. 2, pp. 302–310, 2007.

[5] P. Battocchio and F. Menoncin, "Optimal pension management in a stochastic framework," *Insurance: Mathematics and Economics*, vol. 34, no. 1, pp. 79–95, 2004.

[6] J. Gao, "Optimal portfolios for DC pension plans under a CEV model," *Insurance: Mathematics and Economics*, vol. 44, no. 3, pp. 479–490, 2009.

[7] J. Gao, "Optimal investment strategy for annuity contracts under the constant elasticity of variance (CEV) model," *Insurance: Mathematics and Economics*, vol. 45, no. 1, pp. 9–18, 2009.

[8] X. Y. Zhou and D. Li, "Continuous-time mean-variance portfolio selection: a stochastic LQ framework," *Applied Mathematics and Optimization*, vol. 42, no. 1, pp. 19–33, 2000.

[9] H. M. Markowitz, "Portfolio selection," *Journal of Finance*, vol. 7, no. 1, pp. 77–91, 1952.

[10] H. M. Markowitz, *Portfolio Selection: Efficient Diversification of Investment*, John Wiley & Sons, New York, NY, USA, 1959.

[11] J. Y. Campbell, A. W. Lo, and A. C. MacKinlay, *The Econometrics of Financial Markets*, Princeton University Press, Princeton, NJ, USA, 1997.

[12] D. Li and W.-L. Ng, "Optimal dynamic portfolio selection: multiperiod mean-variance formulation," *Mathematical Finance*, vol. 10, no. 3, pp. 387–406, 2000.

[13] N. H. Hakansson, "Capital growth and the mean-variance approach to portfolio selection," *Journal of Financial and Quantitative Analysis*, vol. 6, pp. 517–557, 1971.

[14] R. C. Merton, "An analytic derivation of the efficient portfolio frontier," *Journal of Financial and Economics Analysis*, vol. 7, pp. 1851–1872, 1972.

[15] J. C. Cox and C.-F. Huang, "Optimal consumption and portfolio policies when asset prices follow a diffusion process," *Journal of Economic Theory*, vol. 49, no. 1, pp. 33–83, 1989.

[16] S. J. Grossman and Z. Zhou, "Equilibrium analysis of portfolio insurance," *Journal of Finance*, vol. 51, no. 4, pp. 1379–1403, 1996.

[17] R. C. Merton, "Optimum consumption and portfolio rules in a continuous-time model," *Journal of Economic Theory*, vol. 3, no. 4, pp. 373–413, 1971.

[18] X. Li, X. Y. Zhou, and A. E. B. Lim, "Dynamic mean-variance portfolio selection with non-shorting constraints," *SIAM Journal on Control and Optimization*, vol. 40, no. 5, pp. 1540–1555, 2002.

[19] M. C. Chiu and D. Li, "Asset and liability management under a continuous-time mean-variance optimization framework," *Insurance: Mathematics and Economics*, vol. 39, no. 3, pp. 330–355, 2006.

[20] S. Xie, Z. Li, and S. Wang, "Continuous-time portfolio selection with liability: mean-variance model and stochastic LQ approach," *Insurance: Mathematics and Economics*, vol. 42, no. 3, pp. 943–953, 2008.

[21] C. Fu, A. Lari-Lavassani, and X. Li, "Dynamic mean-variance portfolio selection with borrowing constraint," *European Journal of Operational Research*, vol. 200, no. 1, pp. 312–319, 2010.

[22] D. Kramkov and W. Schachermayer, "The asymptotic elasticity of utility functions and optimal investment in incomplete markets," *The Annals of Applied Probability*, vol. 9, no. 3, pp. 904–950, 1999.

[23] M. Jonsson and R. Sircar, "Optimal investment problems and volatility homogenization approximations," in *Modern Methods in Scientific Computing and Appllications*, A. Bourliux, M. Gander, and G. Sabidussi, Eds., vol. 75 of *NATO Science Series II*, pp. 255–281, Kluwer, 2002.

Hindawi Publishing Corporation
The Scientific World Journal
Volume 2014, Article ID 109128, 7 pages
http://dx.doi.org/10.1155/2014/109128

Research Article

A Note on the Solutions of Some Nonlinear Equations Arising in Third-Grade Fluid Flows: An Exact Approach

Taha Aziz[1] and F. M. Mahomed[1,2]

[1] *Differential Equations, Continuum Mechanics and Applications, School of Computational and Applied Mathematics, University of the Witwatersrand, Wits 2050, South Africa*
[2] *School of Mathematics and Statistics, University of New South Wales, Sydney, NSW 2052, Australia*

Correspondence should be addressed to Taha Aziz; tahaaziz77@yahoo.com

Received 21 January 2014; Accepted 17 February 2014; Published 17 March 2014

Academic Editors: H. Jafari and C. M. Khalique

In this communication, we utilize some basic symmetry reductions to transform the governing nonlinear partial differential equations arising in the study of third-grade fluid flows into ordinary differential equations. We obtain some simple closed-form steady-state solutions of these reduced equations. Our solutions are valid for the whole domain $[0,\infty)$ and also satisfy the physical boundary conditions. We also present the numerical solutions for some of the underlying equations. The graphs corresponding to the essential physical parameters of the flow are presented and discussed.

1. Introduction

The study of non-Newtonian fluids involves the modelling of materials with dense molecular structure such as polymer solutions, slurries, blood, and paints. These material exhibit both viscous behavior like liquids and elastic behavior like solids. Therefore, the understanding of the complex behavior and properties of non-Newtonian fluids is crucial these days. The problems dealing with the flow of non-Newtonian fluids have several technical applications in engineering and industry. Some of them are the extraction of crude oil from petroleum products, oil and gas well drilling, food stuff, extrusion of molten plastic, paper and textile industry, and so on. The flow properties of non-Newtonian fluids are quite different from those of the Newtonian fluids. Therefore, in practical applications, one cannot replace the behavior of non-Newtonian fluids with Newtonian fluids and it is very important to analyze and understand the flow behavior of non-Newtonian fluids in order to obtain a thorough understanding and improve utilization in various manufactures.

In the past couple of years, many nonlinear problems dealing with non-Newtonian fluids have been taken into account. Some important studies dealing with the flow of non-Newtonian fluids are due to the studies of Abd-el-Malek et al. [1], Ariel et al. [2], Chen et al. [3], C. Fetecau and C. Fetecau [4], Hayat et al. [5, 6], Rajagopal et al. [7], Fosdick and Rajagopal [8], Rajagopal [9], and many studies thereafter. Some researchers have utilized the numerical approaches [10–12] to tackle these sorts of problems and several nonlinear problems have recently been solved by the homotopy analysis method (HAM) [13–15]. The purpose of this study is to discuss some nonlinear equations arising in the study of third grade fluids [16–18] analytically in a simplest possible way instead of using the HAM or other difficult techniques. The third-grade fluid model represents a further although inconclusive attempt to study the physical structure of non-Newtonian fluids. This model is known to capture the very interesting phenomena like die-swell, rod climbing effect [19], shear thinning, and the shear thickening that many other non-Newtonian models do not exhibit. We consider three different problems, namely, (i) flow of a third grade fluid over a flat rigid plate within porous medium, (ii) flow of a third-grade fluid in a porous half space with suction/injection effects, and (iii) magnetohydrodynamic (MHD) flow of a third-grade fluid in a porous half space. We solve all of these problems by imposing the relevant boundary conditions to make the problems well posed.

The main focus in this work is to construct a class of closed-form solutions for boundary value problems for nonlinear diffusion equations arising in the study of non-Newtonian third- grade fluids thorough a porous medium with the principle of Lie group method for differential equations. We also obtain the numerical solutions for the underlying models to show how various physical parameters play their part in determining the properties of the flow.

2. Geometry of the Problems

We consider a Cartesian coordinate system $OXYZ$ with the y-axis in the vertically upward direction. The third-grade fluid occupies the porous space $y > 0$ and is in contact with an infinite moved plate at $y = 0$. Since the plate is infinite in the XZ-plane and therefore all the physical quantities except the pressure depend on y only. The flow is caused by the motion of the plate in its own plane with an arbitrary velocity. Far away from the plate, the fluid will be considered to be at rest. We have taken three different problems on the same flat plate geometry.

3. Problems to Be Investigated

3.1. Unsteady Flow of Third-Grade Fluid over a Flat Rigid Plate with Porous Medium. By following the methodology of References. [20, 21], the equation of motion for the unsteady flow of third-grade fluid over the rigid plate with porous medium is

$$\rho\frac{\partial U}{\partial t} = \mu\frac{\partial^2 U}{\partial y^2} + \alpha_1\frac{\partial^3 U}{\partial y^2\partial t} + 6\beta_3\left(\frac{\partial U}{\partial y}\right)^2\frac{\partial^2 U}{\partial y^2} - \frac{\phi}{\kappa}\left[\mu + \alpha_1\frac{\partial}{\partial t} + 2\beta_3\left(\frac{\partial U}{\partial y}\right)^2\right]U. \tag{1}$$

Here U is the velocity component, ρ is the density, μ the coefficient of viscosity, α_1 and β_3 are the material constants (for details on these material constants and the conditions that are satisfied by these constants, the reader is referred to [8]), ϕ the porosity and κ the permeability of the porous medium.

In order to solve (1) mentioned above, boundary conditions are specified as follows:

$$U(0,t) = U_0V(t), \quad t > 0, \tag{2}$$

$$U(\infty,t) = 0, \quad t > 0, \tag{3}$$

$$U(y,0) = 0, \quad y > 0, \tag{4}$$

where U_0 is the reference velocity. The first boundary condition (2) is the no-slip condition and the second boundary condition (3) says that the main stream velocity is zero. This is not a restrictive assumption since we can always measure velocity relative to the main stream. The initial condition (4) indicates that the fluid is initially at rest.

On introducing the nondimensional quantities

$$\overline{U} = \frac{U}{U_0}, \quad \overline{y} = \frac{U_0 y}{\nu}, \quad \overline{t} = \frac{U_0^2 t}{\nu}, \quad \overline{\alpha} = \frac{\alpha_1 U_0^2}{\rho\nu^2}, \quad \overline{\beta} = \frac{2\beta_3 U_0^4}{\rho\nu^3}, \quad \frac{1}{\overline{K}} = \frac{\phi\nu^2}{\kappa U_0^2}. \tag{5}$$

Equation (1) and the corresponding initial and the boundary conditions take the form

$$\frac{\partial U}{\partial t} = \frac{\partial^2 U}{\partial y^2} + \alpha\frac{\partial^3 U}{\partial y^2\partial t} + 3\beta\left(\frac{\partial U}{\partial y}\right)^2\frac{\partial^2 U}{\partial y^2} - \frac{1}{K}\left[U + \alpha\frac{\partial U}{\partial t} + \beta U\left(\frac{\partial U}{\partial y}\right)^2\right], \tag{6}$$

$$U(0,t) = V(t), \quad t > 0, \tag{7}$$

$$U(y,t) \longrightarrow 0 \quad \text{as } y \longrightarrow \infty, \quad t > 0, \tag{8}$$

$$U(y,0) = 0, \quad y > 0. \tag{9}$$

For simplicity, we ignore the bars of the nondimensional quantities. We rewrite (6) as

$$\frac{\partial U}{\partial t} = \mu_*\frac{\partial^2 U}{\partial y^2} + \alpha_*\frac{\partial^3 U}{\partial y^2\partial t} + 3\gamma\left(\frac{\partial U}{\partial y}\right)^2\frac{\partial^2 U}{\partial y^2} - \gamma_* U\left(\frac{\partial U}{\partial y}\right)^2 - \frac{1}{K_*}U, \tag{10}$$

where

$$\mu_* = \frac{1}{(1+\alpha/K)}, \quad \alpha_* = \frac{\alpha}{(1+\alpha/K)}, \quad \gamma = \frac{\beta}{(1+\alpha/K)}, \quad \gamma_* = \frac{\beta/K}{(1+\alpha/K)}, \quad \frac{1}{K_*} = \frac{1/K}{(1+\alpha/K)}. \tag{11}$$

We know that from the principal of Lie group theory that if a differential equation is explicitly independent of any dependent or independent variable, then this particular differential equation remains invariant under the translation symmetry corresponding to that particular variable. We notice that (10) is independent of t, so it is invariant under the Lie point symmetry generator $\mathbf{X} = \partial/\partial t$. So, by the theory of invariants, the solution of (10) corresponding to operator $\mathbf{X}$ is obtained by

$$\frac{dt}{1} = \frac{dy}{0} = \frac{dU}{0}, \tag{12}$$

implyingthe steady-state solution given by

$$U = F(\eta), \quad \text{where } \eta = y. \tag{13}$$

Inserting (13) into (10) yields

$$\mu_*\frac{\partial^2 F}{\partial \eta^2} + 3\gamma\left(\frac{\partial F}{\partial \eta}\right)^2\frac{\partial^2 F}{\partial \eta^2} - \gamma_* F\left(\frac{\partial F}{\partial \eta}\right)^2 - \frac{1}{K_*}F = 0, \tag{14}$$

and the transformed boundary conditions are given by

$$F(0) = l_1, \quad \text{where } l_1 \text{ is a constant}$$
$$F(\eta) \longrightarrow 0, \quad \text{as } y \longrightarrow \infty. \tag{15}$$

We have now transformed the governing nonlinear PDE (10) into a nonlinear ODE (14) as well as the boundary conditions (7)–(9) to the boundary conditions (15).

In order to solve (14) for $F(\eta)$, we assume a solution of the form

$$F(\eta) = A \exp(B\eta), \tag{16}$$

where A and B are the constants to be determined. Substituting (16) into (14), we obtain

$$\left(\mu_* B^2 - \frac{1}{K_*}\right) + e^{2B\eta}\left(3\gamma A^2 B^4 - \gamma_* A^2 B^2\right) = 0. \tag{17}$$

Separating (17) in the powers of e^0 and $e^{2B\eta}$, we deduce

$$e^0: \; \mu_* B^2 - \frac{1}{K_*} = 0, \tag{18}$$

$$e^{2B\eta}: \; 3\gamma A^2 B^4 - \gamma_* A^2 B^2 = 0. \tag{19}$$

From (19), we find

$$B = \pm\frac{\sqrt{\gamma_*}}{\sqrt{3\gamma}}. \tag{20}$$

We choose

$$B = -\frac{\sqrt{\gamma_*}}{\sqrt{3\gamma}}, \tag{21}$$

so that our solution would satisfy the second boundary condition at infinity. Using the value of B in (18), we obtain

$$\frac{\gamma_*}{3\gamma}\mu_* - \frac{1}{K_*} = 0. \tag{22}$$

Thus, the solution for $F(\eta)$ can be written as

$$U = F(\eta) = l_1 \exp\left(-\frac{\sqrt{\gamma_*}}{\sqrt{3\gamma}}\eta\right), \tag{23}$$

provided that condition (22) holds, where $A = l_1$ by using the first boundary condition.

3.2. Unsteady Flow of Third-Grade Fluid over a Flat Porous Plate with Porous Medium. By employing the same geometry as we have explained in Section 2, we extend the previous problem by incorporating the effects of plate suction or injection. We provide the closed-form solution of the problem by reducing the governing nonlinear PDE into an ODE with the aid of Lie groups.

The present analysis deals with a porous plate with suction or injection and thus the velocity field is given by

$$\mathbf{V} = [U(y,t), -W_0, 0], \tag{24}$$

where $W_0 > 0$ denotes the suction velocity and $W_0 < 0$ indicates blowing velocity. One can see that the incompressibility constraint is identically satisfied; that is,

$$\operatorname{div} \mathbf{V} = 0. \tag{25}$$

So, the unsteady flow through a porous medium and over a porous plate in the absence of the modified pressure gradient takes the form

$$\begin{aligned}
\rho\left[\frac{\partial U}{\partial t} - W_0\frac{\partial U}{\partial y}\right]
&= \mu\frac{\partial^2 U}{\partial y^2} + \alpha_1\frac{\partial^3 U}{\partial y^2 \partial t} \\
&\quad - \alpha_1 W_0\frac{\partial^3 U}{\partial y^3} + 6\beta_3\left(\frac{\partial U}{\partial y}\right)^2\frac{\partial^2 U}{\partial y^2} - \frac{\phi}{\kappa} \\
&\quad \times\left[\mu + \alpha_1\frac{\partial}{\partial t} - \alpha_1 W_0\frac{\partial}{\partial y} + 2\beta_3\left(\frac{\partial U}{\partial y}\right)^2\right]U.
\end{aligned} \tag{26}$$

The boundary conditions remain the same as given in (2)–(4). Defining the nondimensional parameters as

$$\begin{gathered}
\overline{U} = \frac{U}{U_0}, \qquad \overline{y} = \frac{U_0 y}{\nu}, \\
\overline{t} = \frac{U_0^2 t}{\nu}, \qquad \overline{\alpha} = \frac{\alpha_1 U_0^2}{\rho\nu^2}, \\
\overline{\beta} = \frac{2\beta_3 U_0^4}{\rho\nu^3}, \qquad \frac{1}{\overline{K}} = \frac{\phi\nu^2}{\kappa U_0^2}, \qquad \overline{W} = \frac{W_0}{U_0}.
\end{gathered} \tag{27}$$

Equation (28) becomes

$$\begin{aligned}
\left[\frac{\partial U}{\partial t} - W\frac{\partial U}{\partial y}\right] &= \frac{\partial^2 U}{\partial y^2} + \alpha\frac{\partial^3 U}{\partial y^2 \partial t} \\
&\quad - \alpha W\frac{\partial^3 U}{\partial y^3} + 3\beta\left(\frac{\partial U}{\partial y}\right)^2\frac{\partial^2 U}{\partial y^2} - \frac{1}{K} \\
&\quad \times\left[U + \alpha\frac{\partial U}{\partial t} - \alpha W\frac{\partial U}{\partial y} + \beta U\left(\frac{\partial U}{\partial y}\right)^2\right],
\end{aligned} \tag{28}$$

with the boundary conditions taking the form as given in (7)–(9). We rewrite (28) as

$$\begin{aligned}
\frac{\partial U}{\partial t} &= \mu_*\frac{\partial^2 U}{\partial y^2} + \alpha_*\frac{\partial^3 U}{\partial y^2 \partial t} - \alpha_* W\frac{\partial^3 U}{\partial y^3} \\
&\quad + 3\gamma\left(\frac{\partial U}{\partial y}\right)^2\frac{\partial^2 U}{\partial y^2} - \gamma_* U\left(\frac{\partial U}{\partial y}\right)^2 + W\frac{\partial U}{\partial y} - \frac{1}{K_*}U,
\end{aligned} \tag{29}$$

where $\mu_*, \alpha_*, \gamma_*, \gamma$, and $1/K_*$ are defined in (11). Now, we have to solve (29) subject to the boundary conditions (7)–(9).

As it can be seen, (29) is invariant under the time-translation symmetry generator $\mathbf{X} = \partial/\partial t$. The invariant solution corresponding to $\partial/\partial t$ is the steady-state solution given by

$$U = G(\eta), \quad \text{where } \eta = y. \tag{30}$$

Using (30) into (29) yields

$$\mu_* \frac{d^2G}{d\eta^2} - \alpha_* W \frac{d^3G}{d\eta^3} + 3\gamma\left(\frac{dG}{d\eta}\right)^2 \frac{d^2G}{d\eta^2} - \gamma_* G\left(\frac{dG}{d\eta}\right)^2 + W\frac{dG}{d\eta} - \frac{1}{K_*}G = 0, \tag{31}$$

with the transformed boundary conditions

$$G(0) = l_2, \quad \text{where } l_2 \text{ is a constant,}$$
$$G(\eta) \longrightarrow 0, \qquad \frac{dG}{d\eta} \longrightarrow 0 \quad \text{as } y \longrightarrow \infty. \tag{32}$$

Following the same methodology as adopted in solving the previous problem, (31) admits an exact solution of the form (which we require to be zero at infinity due to the condition $G(\infty) = 0$)

$$U = G(\eta) = l_2 \exp\left(-\frac{\sqrt{\gamma_*}}{\sqrt{3\gamma}}\eta\right), \tag{33}$$

provided that

$$\frac{\gamma_*}{3\gamma}\mu_* + \alpha W\sqrt{\frac{\gamma_*}{3\gamma}}\frac{\gamma_*}{3\gamma} - \sqrt{\frac{\gamma_*}{3\gamma}}W - \frac{1}{K_*} = 0. \tag{34}$$

Note that, if we set $W = 0$, we can recover the condition given in (22).

3.3. Unsteady Magnetohydrodynamic (MHD) Flow of Third-Grade Fluid over a Flat Porous Plate with Porous Medium. In this problem, we extend the previous one by considering the fluid to be electrically conducting under the influence of a uniform magnetic field applied transversely to the flow.

The unsteady MHD flow of a third-grade fluid in a porous half space with plate suction/injection is governed by

$$\begin{aligned}\rho\left[\frac{\partial U}{\partial t} - W_0\frac{\partial U}{\partial y}\right] &= \mu\frac{\partial^2 U}{\partial y^2} + \alpha_1\frac{\partial^3 U}{\partial y^2 \partial t} \\ &\quad - \alpha_1 W_0 \frac{\partial^3 U}{\partial y^3} + 6\beta_3\left(\frac{\partial U}{\partial y}\right)^2\frac{\partial^2 U}{\partial y^2} - \frac{\phi}{\kappa} \\ &\quad \times\left[\mu + \alpha_1\frac{\partial}{\partial t} - \alpha_1 W_0\frac{\partial}{\partial y} + 2\beta_3\left(\frac{\partial U}{\partial y}\right)^2\right] \\ &\quad \times U - \sigma B_0^2 U,\end{aligned} \tag{35}$$

where σ is the electrical conductivity and $\mathbf{B}_0$ the uniform applied magnetic field. Again the boundary conditions remain the same as given in (2)–(4). We define the dimensionless parameters as

$$\overline{U} = \frac{U}{U_0}, \quad \overline{y} = \frac{U_0 y}{\nu}, \quad \overline{t} = \frac{U_0^2 t}{\nu}, \quad \overline{\alpha} = \frac{\alpha_1 U_0^2}{\rho\nu^2},$$
$$\overline{\beta} = \frac{2\beta_3 U_0^4}{\rho\nu^3}, \quad \frac{1}{\overline{K}} = \frac{\phi\nu^2}{\kappa U_0^2},$$
$$\overline{M}^2 = \frac{\sigma B_0^2 \nu}{\rho U_0^2}, \quad \overline{W} = \frac{W_0}{U_0}. \tag{36}$$

Equation (26) takes the form

$$\begin{aligned}\left[\frac{\partial U}{\partial t} - W\frac{\partial U}{\partial y}\right] &= \frac{\partial^2 U}{\partial y^2} + \alpha\frac{\partial^3 U}{\partial y^2 \partial t} \\ &\quad - \alpha W\frac{\partial^3 U}{\partial y^3} + 3\beta\left(\frac{\partial U}{\partial y}\right)^2\frac{\partial^2 U}{\partial y^2} \\ &\quad - \frac{1}{K}\left[U + \alpha\frac{\partial U}{\partial t} - \alpha W\frac{\partial U}{\partial y} + \beta U\left(\frac{\partial U}{\partial y}\right)^2\right] \\ &\quad - M^2 U.\end{aligned} \tag{37}$$

We rewrite (37) as

$$\begin{aligned}\frac{\partial U}{\partial t} &= \mu_*\frac{\partial^2 U}{\partial y^2} + \alpha_*\frac{\partial^3 U}{\partial y^2 \partial t} - \alpha_* W\frac{\partial^3 U}{\partial y^3} \\ &\quad + 3\gamma\left(\frac{\partial U}{\partial y}\right)^2\frac{\partial^2 U}{\partial y^2} - \gamma_* U\left(\frac{\partial U}{\partial y}\right)^2 \\ &\quad + W\frac{\partial U}{\partial y} - \left(\frac{1}{K_*} + M_*^2\right)U,\end{aligned} \tag{38}$$

where μ_*, α_*, γ_*, γ, and $1/K_*$ are defined in (11) and

$$M_*^2 = \frac{M^2}{(1 + \alpha/K)}. \tag{39}$$

Now, we need to solve (38) subject to the boundary conditions (7)–(9). Since (38) is invariant under the time-translation symmetry generator $\mathbf{X} = \partial/\partial t$, the invariant solution corresponding to $\partial/\partial t$ is the steady-state solution. Consider

$$U = H(\eta), \quad \text{where } \eta = y. \tag{40}$$

Invoking (40) in (38) yields

$$\mu_*\frac{d^2H}{d\eta^2} - \alpha_* W\frac{d^3H}{d\eta^3} + 3\gamma\left(\frac{dH}{d\eta}\right)^2\frac{d^2H}{d\eta^2} - \gamma_* H\left(\frac{dH}{d\eta}\right)^2 + W\frac{dH}{d\eta} - \left(\frac{1}{K_*} + M_*^2\right)H = 0, \tag{41}$$

with the transformed boundary condition

$$H(0) = l_3, \quad \text{where } l_3 \text{ is a constant,}$$
$$H(\eta) \longrightarrow 0, \qquad \frac{dH}{d\eta} \longrightarrow 0 \quad \text{as } y \longrightarrow \infty. \tag{42}$$

Utilizing the same method adopted to solve the first problem, (41) admits an exact solution of the form (which we require to be zero at infinity due to the second boundary condition)

$$U = H(\eta) = l_3 \exp\left(-\frac{\sqrt{\gamma_*}}{\sqrt{3\gamma}}\eta\right), \tag{43}$$

provided that

$$\frac{\gamma_*}{3\gamma}\mu_* + \alpha W\sqrt{\frac{\gamma_*}{3\gamma}}\frac{\gamma_*}{3\gamma} - \sqrt{\frac{\gamma_*}{3\gamma}}W - \frac{1}{K_*} - M_*^2 = 0. \tag{44}$$

Note that, if we set $W = M_* = 0$, we can recover the previous two conditions given in (22) and (34).

Remark 1. We note that the similarity solutions (23), (33), and (43) are the same, but the imposing conditions (22), (34), and (44) under which these solutions are valid are different. These solutions do show the effects of the third-grade fluid parameters γ and γ_* on the flow. However, they do not directly contain the term which is responsible for showing the effects of suction/blowing and magnetic field on the flow. The imposing conditions do contain the magnetic field and suction/blowing parameters. Thus, these closed-form solutions are valid for the particular values of the suction/blowing and the magnetic field parameters. To show the effects of these interesting phenomena, we have solved the reduced (14), (31), and (41) with the boundary conditions (15), (32), and (42) numerically using the powerful numerical solver NDSolve in Mathematica. These numerical solutions are plotted in Figures 2–4 against the emerging parameters of the flow.

4. Analysis and Discussion

In order to analyze the behavior and properties of some of the essential physical parameters of the flow, we have plotted Figures 1–5.

In Figure 1, the closed-form solutions (23), (33), and (43) are plotted. Since these solutions physically behave in the same way, the restrictive conditions (22), (34), and (44) on the parameters under which these solutions are valid differ from each other. Therefore, the behavior of these solutions is indistinguishable in the graph.

In Figure 2, the numerical solution of the reduced ODE (14) is given. This numerical behavior of the velocity is exactly the same as observed previously in Figure 1 for the analytical solutions that velocity is a decreasing function of the dimensionless parameter η.

To examine the influence of plate suction/injection on the flow, Figures 3 and 5 have been plotted. In Figure 3, the reduced ODE (31) is plotted numerically for varying values of the parameter W_0 and in Figure 5 the reduced ODE (41) is plotted numerically for the varying values of the parameter W_0. The effect of the parameter W_0 on the velocity field is exactly the same in both of these figures. From these figures, it is clearly indicated that for the case of suction ($W_0 > 0$) the velocity field decreases as the boundary layer thickness and the effects of injection ($W_0 < 0$) are totally opposite to those of suction. This is in agreement with what is expected physically.

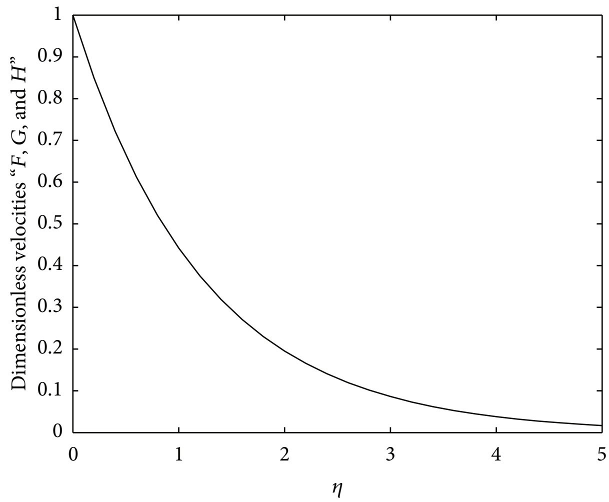

FIGURE 1: Profile of the analytical solutions F, G, and H as a function of dimensionless coordinate η, where we have chosen $\gamma = 1.5$, $\gamma_* = 1$, and $l_1 = l_2 = l_3 = 1$.

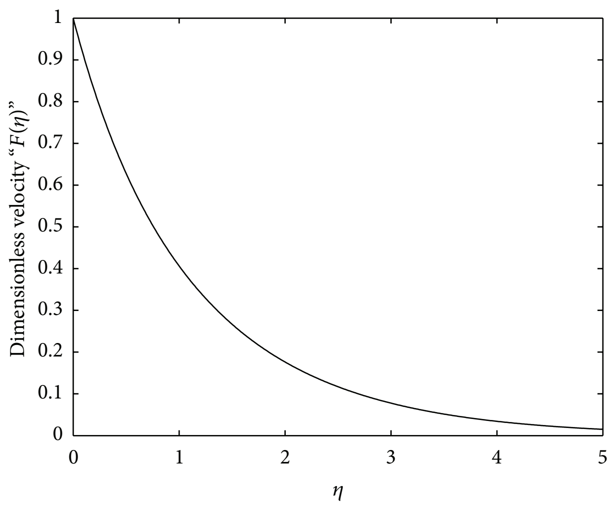

FIGURE 2: Numerical solution of ODE (14) subject to the boundary conditions (15), where we have chosen $\gamma = 0.5$, $\gamma_* = 0.75$, $\mu_* = 1.5$, and $K_* = \alpha_* = 1$.

Finally, the influence of the magnetic field on the structure on the velocity is analyzed in Figure 4. From the figure, it is observed quite clearly that with the increase of the Hartman number (magnetic field strength) M_*, the velocity field decreases. This is what we expect physically in this case as well.

5. Final Remarks

In this note, we have presented closed-form solutions for some nonlinear problems which describe the phenomena of third-grade fluids. In each case, the governing nonlinear PDEs reduced to nonlinear ODEs by using the Lie point

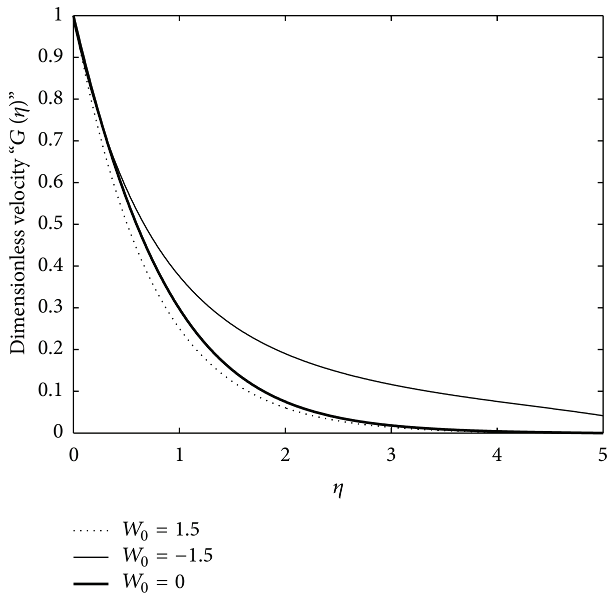

Figure 3: Numerical solution of ODE (31) subject to the boundary conditions (32) for varying values of W_0, where we have chosen $\gamma = 1.5$, $\gamma_* = 1$, $\mu_* = 0.5$, and $K_* = \alpha_* = 1$.

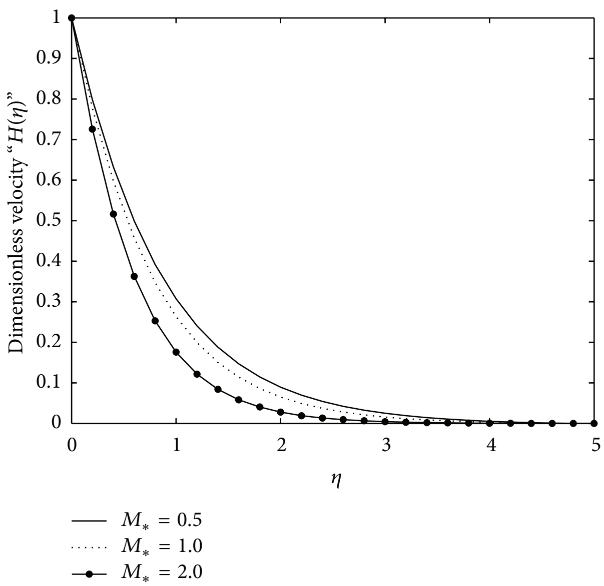

Figure 4: Numerical solution of ODE (41) subject to the boundary conditions (42) for varying values of M_*, where we have chosen $\gamma = 1.5$, $\gamma_* = 0.5$, $\mu_* = 0.5$, $W_0 = 0.75$, and $K_* = \alpha_* = 1$.

symmetry (which is translation) in the t direction. The reduced ODEs are then solved analytically by employing a very simple approach and also have been solved numerically to show the effects of some of the interesting emerging parameters of the flow. The method of solution that we have used here is helpful for solving a wide range of nonlinear problems in a simple way instead of using other difficult techniques.

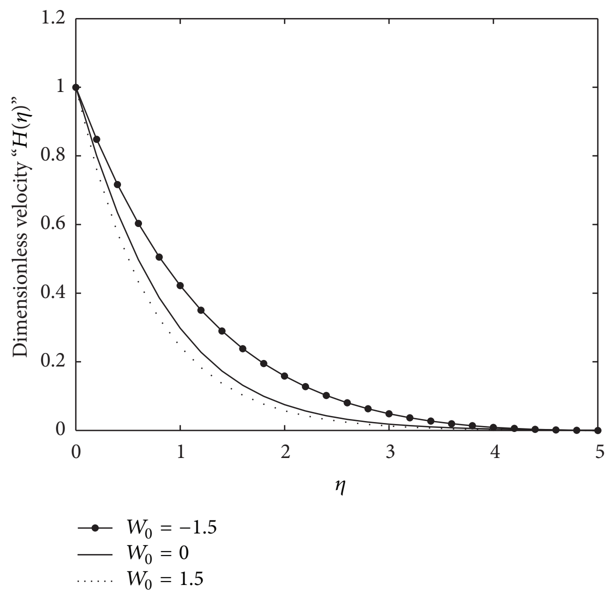

Figure 5: Numerical solution of ODE (41) subject to the boundary conditions (42) for varying values of W_0, where we have chosen $\gamma = 1.5$, $\gamma_* = 0.5$, $\mu_* = 0.5$, $M_* = 0.5$, $K_* = 0.75$, and $\alpha_* = 1$.

Conflict of Interests

The authors declare that there is no conflict of interests regarding the publication of this paper.

Acknowledgments

Taha Aziz and F. M. Mahomed acknowledge the financial support from the National Research Foundation (NRF) of South Africa. Taha Aziz also gratefully acknowledges the financial support from the School of Computational and Applied Mathematics and the Financial Aid and Scholarships Office, University of the Witwatersrand. F. M. Mahomed is a Visiting Professorial Fellow at UNSW.

References

[1] M. B. Abd-el-Malek, N. A. Badran, and H. S. Hassan, "Solution of the Rayleigh problem for a power law non-Newtonian conducting fluid via group method," *International Journal of Engineering Science*, vol. 40, no. 14, pp. 1599–1609, 2002.

[2] P. D. Ariel, T. Hayat, and S. Asghar, "The flow of an elastico-viscous fluid past a stretching sheet with partial slip," *Acta Mechanica*, vol. 187, no. 1–4, pp. 29–35, 2006.

[3] C. I. Chen, T. Hayat, and J. L. Chen, "Exact solutions for the unsteady flow of a Burgers' fluid in a duct induced by time-dependent prescribed volume flow rate," *Heat and Mass Transfer*, vol. 43, pp. 85–90, 2006.

[4] C. Fetecau and C. Fetecau, "Decay of a potential vortex in an Oldroyd-B fluid," *International Journal of Engineering Science*, vol. 43, no. 3-4, pp. 340–351, 2005.

[5] T. Hayat, A. H. Kara, and E. Momoniat, "The unsteady flow of a fourth-grade fluid past a porous plate," *Mathematical and Computer Modelling*, vol. 41, no. 11-12, pp. 1347–1353, 2005.

[6] T. Hayat, R. J. Moitsheki, and S. Abelman, "Stokes' first problem for Sisko fluid over a porous wall," *Applied Mathematics and Computation*, vol. 217, no. 2, pp. 622–628, 2010.

[7] K. R. Rajagopal, A. Z. Szeri, and W. Troy, "An existence theorem for the flow of a non-newtonian fluid past an infinite porous plate," *International Journal of Non-Linear Mechanics*, vol. 21, no. 4, pp. 279–289, 1986.

[8] R. L. Fosdick and K. R. Rajagopal, "Thermodynamics and stability of fluids of third grade," *Proceedings of the Royal Society A*, vol. 339, no. 1738, pp. 351–377, 1980.

[9] K. R. Rajagopal, "On the stability of third-grade fluids," *Archives of Mechanics*, vol. 32, no. 6, pp. 867–875, 1980.

[10] M. Sajid, R. Mahmood, and T. Hayat, "Finite element solution for flow of a third grade fluid past a horizontal porous plate with partial slip," *Computers and Mathematics with Applications*, vol. 56, no. 5, pp. 1236–1244, 2008.

[11] M. Khan, T. Hayat, and M. Ayub, "Numerical study of partial slip on the MHD flow of an Oldroyd 8-constant fluid," *Computers and Mathematics with Applications*, vol. 53, no. 7, pp. 1088–1097, 2007.

[12] C.-M. Chen, F. Liu, I. Turner, and V. Anh, "Numerical methods with fourth-order spatial accuracy for variable-order nonlinear Stokes' first problem for a heated generalized second grade fluid," *Computers and Mathematics with Applications*, vol. 62, no. 3, pp. 971–986, 2011.

[13] M. Sajid and T. Hayat, "The application of homotopy analysis method to thin film flows of a third order fluid," *Chaos, Solitons & Fractals*, vol. 38, no. 2, pp. 506–515, 2008.

[14] D. G. Domairry, A. Mohsenzadeh, and M. Famouri, "The application of homotopy analysis method to solve nonlinear differential equation governing Jeffery-Hamel flow," *Communications in Nonlinear Science and Numerical Simulation*, vol. 14, no. 1, pp. 85–95, 2009.

[15] S. J. Liao, *On the proposed homotopy analysis technique for nonlinear problems and its applications [Ph.D. dissertation]*, Shanghai Jiao Tong University, 1992.

[16] T. Hayat, H. M. Mamboundou, and F. M. Mahomed, "Unsteady solutions in a third-grade fluid filling the porous space," *Mathematical Problems in Engineering*, vol. 2008, Article ID 139560, 13 pages, 2008.

[17] B. Sahoo, "Hiemenz flow and heat transfer of a third grade fluid," *Communications in Nonlinear Science and Numerical Simulation*, vol. 14, no. 3, pp. 811–826, 2009.

[18] P. D. Ariel, "Flow of a third grade fluid through a porous flat channel," *International Journal of Engineering Science*, vol. 41, pp. 1267–1285, 2003.

[19] W. R. Schowalter, *Mechanics of Non-Newtonian Fluids*, Pergamon, New York, NY, USA, 1978.

[20] T. Hayat, F. Shahzad, and M. Ayub, "Analytical solution for the steady flow of the third grade fluid in a porous half space," *Applied Mathematical Modelling*, vol. 31, no. 11, pp. 2424–2432, 2007.

[21] M. Sajid and T. Hayat, "Series solution for steady flow of a third grade fluid through porous space," *Transport in Porous Media*, vol. 71, no. 2, pp. 173–183, 2008.

Hindawi Publishing Corporation
The Scientific World Journal
Volume 2014, Article ID 605376, 4 pages
http://dx.doi.org/10.1155/2014/605376

Research Article

A Novel Iterative Scheme and Its Application to Differential Equations

Yasir Khan,[1] F. Naeem,[2] and Zdeněk Šmarda[3]

[1] *Department of Mathematics, Zhejiang University, Hangzhou 310027, China*
[2] *Modern Textile Institute, Donghua University, Shanghai 200051, China*
[3] *Department of Mathematics, Faculty of Electrical Engineering and Communication, Brno University of Technology, Technicka 8, 61600 Brno, Czech Republic*

Correspondence should be addressed to Yasir Khan; yasirmath@yahoo.com

Received 18 December 2013; Accepted 18 February 2014; Published 16 March 2014

Academic Editors: H. Jafari and C. M. Khalique

The purpose of this paper is to employ an alternative approach to reconstruct the standard variational iteration algorithm II proposed by He, including Lagrange multiplier, and to give a simpler formulation of Adomian decomposition and modified Adomian decomposition method in terms of newly proposed variational iteration method-II (VIM). Through careful investigation of the earlier variational iteration algorithm and Adomian decomposition method, we find unnecessary calculations for Lagrange multiplier and also repeated calculations involved in each iteration, respectively. Several examples are given to verify the reliability and efficiency of the method.

1. Introduction

Over the last few decades several analytical/approximate methods have been developed to solve nonlinear ordinary and partial differential equations. For initial and boundary-value problems in ordinary and partial differential equations, some of these techniques include the perturbation method [1], the variational iteration method [2–4], the decomposition method [5–8], and the homotopy methods [9–11].

The Adomian decomposition method [12–16] for solving differential and integral equations, linear or nonlinear, has been the subject of extensive analytical and numerical studies. The method, well addressed in [12–16], has a significant advantage in which it provides the solution in a rapid convergent series with elegantly computable components. In recent years, a large amount of literature has been developed concerning the application of Adomian decomposition method in applied sciences. In addition, the method reveals the analytical structure of the solution which is absent in numerical solutions.

He's variational iteration method [2–4] is based on a Lagrange multiplier technique developed by Inokuti et al. [17]. This method is, in fact, a modification of the general Lagrange multiplier method into an iteration method, which is called correction functional. The method has been shown to solve effectively, easily, and accurately a large class of nonlinear problems [18–23]. Generally, one or two iterations lead to high accurate solutions.

In the present study, we have linked up variational iteration method and Adomian decomposition method through Lagrange multiplier, which shows that VIM is another form of expressing ADM and vice versa. This study reveals that there is no need to integrate the differential equation again and again as we do in Adomian decomposition method. Advantage of new iterative scheme over the variational iteration method is that it avoids the unnecessary calculations and we can construct Lagrange multiplier very easily without construction of the correctional functional.

2. New Formulation for Adomian Decomposition Method and Variational Iteration Algorithm II

In order to elucidate the solution procedure, we consider the following nth order partial differential equation:

$$L^n f(x,t) = Rf(x,t) + Nf(x,t) + g(x,t), \quad t > 0, \ x \in L, \tag{1}$$

where $L^n = \partial^n/\partial t^n, n \geq 1$, R is a linear differential operator, N is a nonlinear differential operator, R and N are free of partial derivative with respect to variable t, and g is the source term. As we are familiar with the fact that in all kinds of iteration techniques, except the operator rest of the terms, are treated as a known function on the behalf of initial guess. In this present newly proposed idea, we have used the same concept. We have bound all terms in one function except operator. Consider

$$g + Nf + Rf = F\left(t, x, g, f, \frac{\partial f}{\partial x}, \frac{\partial^2 f}{\partial x^2}, \ldots\right). \quad (2)$$

By incorporating (2) in (1), we get

$$L^n f = F\left(t, x, g, f, \frac{\partial f}{\partial x}, \frac{\partial^2 f}{\partial x^2}, \ldots\right). \quad (3)$$

On integrating (3), we obtain

$$L^{(n-1)} f = \int_0^t F\left(\xi, x, g, f, \frac{\partial f}{\partial x}, \frac{\partial^2 f}{\partial x^2}, \ldots\right) d\xi + c_1(x). \quad (4)$$

Again, by integrating (4), we have

$$L^{(n-2)} f = \int_0^t \int_0^\xi F\left(\tau, x, g, f, \frac{\partial f}{\partial x}, \frac{\partial^2 f}{\partial x^2}, \ldots\right) d\tau d\xi + c_1(x) t + c_2(x), \quad (5)$$

since we know that multiple integral can be reduce to a single integral by using integral property. Hence, we can write (5) in the following form:

$$L^{(n-2)} f = \int_0^t (t-\xi) F\left(\xi, x, g, f, \frac{\partial f}{\partial x}, \frac{\partial^2 f}{\partial x^2}, \ldots\right) d\xi + c_1(x) t + c_2(x). \quad (6)$$

If we continue this process of integration, we can get final form as follows:

$$f(x,t) = \int_0^t \frac{(t-\xi)^{n-1}}{(n-1)!} F\left(t, x, g, f, \frac{\partial f}{\partial x}, \frac{\partial^2 f}{\partial x^2}, \ldots\right) d\xi + \frac{c_1(x) t^{n-1}}{(n-1)!} + \frac{c_2(x) t^{n-2}}{(n-2)!} + \cdots c_n(x). \quad (7)$$

By writing the constant of integration in the form $c_k(x) = (\partial f^{n-k}(x, 0^+))/\partial t^{n-k}$, $k = 1, \ldots, n$ and substituting (2) in (7) then (7), we have

$$f(x,t) = \sum_{k=0}^{n-1} \frac{\partial^k f(x, 0^+)}{\partial t^k} \frac{t^k}{k!} + \int_0^t \frac{(t-\xi)^{n-1}}{(n-1)!} (Rf + Nf + g)\, d\xi. \quad (8)$$

In iteration form (8), it can be written as follows:

$$f_{j+1}(x,t) = f_0(x,t) + \int_0^t \frac{(t-\xi)^{n-1}}{(n-1)!} \left(Rf_j + Nf_j + g\right) d\xi, \quad j = 0, 1, 2, \ldots, \quad (9)$$

where $f_0(x,t) = \sum_{k=0}^{n-1}((\partial^k f(x, 0^+))/\partial t^k)(t^k/k!)$.

In (9), $(t-\xi)^{n-1}/(n-1)!$ is Lagrange multiplier of He's variational iteration method, denoted by λ, if n is an odd integer, and (9) can be written in standard variational iteration algorithm II [3]

$$f_{j+1}(x,t) = f_0(x,t) + \int_0^t \lambda \left(Rf_j + Nf_j + g\right) d\xi, \quad f_0(x,t) = \sum_{k=0}^{n-1} \frac{\partial^k f(x, 0^+)}{\partial t^k} \frac{t^k}{k!}, \quad \lambda = \frac{(t-\xi)^{n-1}}{(n-1)!}. \quad (10)$$

Equation (10) is exactly the same as the standard He's variational iteration algorithm II [3]. Here is a point to be noted, if we change our initial guess by adding source term in it, the resulting formulation will give the results obtained by well-known Adomian decomposition method by decomposing the nonlinear term in (10). Consider

$$f_{j+1}(x,t) = \int_0^t \lambda \left(Rf_j + Nf_j\right) d\xi, \quad f_0(x,t) = H(x,t), \quad \lambda = \frac{(t-\xi)^{n-1}}{(n-1)!}, \quad H(x,t) = \sum_{k=0}^{n-1} \frac{\partial f(x, 0^+)}{\partial t^k} \frac{t^k}{k!} + \int_0^t \lambda g(x, \xi)\, d\xi. \quad (11)$$

Equation (11) is an alternative approach of Adomian decomposition method, where $H(x,t)$ is a term which arises from prescribed initial condition and source term. Furthermore, if we decompose the term $H(x,t)$ in (11) and write the resulting equation in the form

$$f_1(x,t) = H_1(x,t) + \int_0^t \lambda (Rf_0 + Nf_0)\, d\xi, \quad H(x,t) = \sum_{k=0}^{n-1} \frac{\partial f(x, 0^+)}{\partial t^k} \frac{t^k}{k!} + \int_0^t \lambda g(x, \xi)\, d\xi, \quad H(x,t) = H_0(x,t) + H_1(x,t), \quad \lambda = \frac{(t-\xi)^{n-1}}{(n-1)!}, \quad (12)$$

$$f_0(x,t) = H_0(x,t),$$

$$f_{j+1}(x,t) = \int_0^t \lambda \left(Rf_j + Nf_j\right) d\xi, \quad j \geq 1, \quad (13)$$

equation (12) is an alternative form of modified Adomian decomposition method.

3. Illustrative Examples

In order to illustrate the solution procedure, we consider the following examples for ordinary and partial differential equations.

Example 1. Consider the Blasius equation

$$u'''(x) + \frac{1}{2}u(x)u''(x) = 0, \tag{14}$$

subject to the boundary conditions

$$u(0) = 0, \qquad u'(0) = 1, \quad u' \longrightarrow 0, \ x \longrightarrow \infty. \tag{15}$$

To solve the above given problem, we consider an extra initial condition; that is, $u''(0) = \alpha$. In order to solve (14) with this extra initial condition, we follow the formulation given in (10). Consider

$$\begin{gathered} u_{j+1}(x) = u_0(x) - \int_0^x \frac{\lambda}{2}\left(u_j(\xi)u_j''(\xi)\right)d\xi, \\ u_0(x) = u(0) + xu'(0) + \frac{x^2}{2!}u''(x) = x + \frac{x^2\alpha}{2!}, \end{gathered} \tag{16}$$

$$\lambda = \frac{(x-\xi)^2}{2!}. \tag{17}$$

By using (16), we obtain the following successive approximations:

$$\begin{gathered} u_1(x) = x + \frac{\alpha x^2}{2} - \frac{\alpha x^4}{48} - \frac{\alpha^2 x^5}{240}, \\ u_2(x) = x + \frac{\alpha x^2}{2} - \frac{\alpha x^4}{48} - \frac{\alpha^2 x^5}{240} + \frac{\alpha x^6}{960} + \frac{11\alpha^2 x^7}{20160} \\ + \frac{11\alpha^3 x^8}{161280} - \frac{\alpha^2 x^9}{193536} - \frac{\alpha^3 x^{10}}{518400} - \frac{\alpha^4 x^{11}}{5702400}, \\ \vdots \end{gathered} \tag{18}$$

Equation (18) is the exactly the same as obtained by using classical VIM in [20] and one can find the value of α by using Padé approximant [21].

Example 2. Consider the nonhomogeneous wave equation

$$\frac{\partial^2 u(x,t)}{\partial t^2} = \frac{\partial^2 u(x,t)}{\partial x^2} + \eta(x,t), \tag{19}$$

where $\eta(x,t) = 2e^{-\pi t}\sin \pi x$, subject to the initial conditions

$$u(x,0) = \sin \pi x, \qquad u_t(x,0) = -\pi \sin \pi x, \tag{20}$$

whose exact solution is

$$u(x,t) = e^{-\pi t}\sin \pi x. \tag{21}$$

To solve (19), we follow the formulation, given in (11). Consider

$$\begin{gathered} u_{j+1}(x,t) = \int_0^t \lambda\left(\frac{\partial^2 u_j}{\partial x^2}\right)d\xi, \\ u_0(x,t) = H(x,t), \qquad \lambda = (t-\xi), \\ H(x,t) = \sin \pi x - t\pi \sin \pi x \\ + \int_0^t (t-\xi)\left(2\pi^2 e^{-\pi\xi}\sin \pi x\right)d\xi, \\ u_0(x,t) = H(x,t) = -\sin \pi x + t\pi \sin \pi x \\ + 2e^{-\pi t}\sin \pi x \\ u_{j+1}(x,t) = \int_0^t (t-\xi)\left(\frac{\partial^2 u_j}{\partial x^2}\right)d\xi, \\ u_1(x,t) = \left(2 - 2\pi t + \frac{\pi^2 t^2}{2!} - \frac{\pi^3 t^3}{3!}\right)\sin \pi x - 2e^{-\pi t}\sin \pi x, \\ u_2(x,t) = \left(-2 + 2\pi t - \pi^2 t^2 + \frac{\pi^3 t^3}{3} - \frac{\pi^4 t^4}{4!} + \frac{\pi^5 t^5}{5!}\right)\sin \pi x \\ - 2e^{-\pi t}\sin \pi x, \\ u_3(x,t) = \left(2 - 2\pi t + \pi^2 t^2 - \frac{\pi^3 t^3}{3} + \frac{\pi^4 t^4}{3(4)}\right. \\ \left. - \frac{\pi^5 t^5}{3(4)(5)} + \frac{\pi^6 t^6}{6!} - \frac{\pi^7 t^7}{7!}\right)\sin \pi x \\ - 2e^{-\pi t}\sin \pi x, \\ \vdots \end{gathered} \tag{22}$$

Upon summing these iterations, we observe that

$$\begin{gathered} u(x,t) = \left(1 - \pi t + \frac{\pi^2 t^2}{2!} - \frac{\pi^3 t^3}{3!} + \frac{\pi^4 t^4}{4!} - \frac{\pi^5 t^5}{5!}\right. \\ \left. + \frac{\pi^6 t^6}{6!} - \frac{\pi^7 t^7}{7!} + \cdots\right)\sin \pi x \approx e^{-\pi t}\sin \pi x. \end{gathered} \tag{23}$$

Solution (23) is exactly the same as obtained by using ADM in [22].

4. Conclusion

This paper helps us to gain insight into the idea of Adomian decomposition method and variational iteration method. By keeping in view both methods, we propose more simplified forms to calculate Lagrange multipliers. By introducing this Lagrange multiplier in ADM and VIM following the observations that have been made,

(i) there is no need to do integration process again and again like we do in Adomian decomposition method and one can get the same results of Adomian method.

(ii) It is easy to calculate the Lagrange multiplier of He's variational iteration method.

(iii) This new approach avoids the unnecessary calculations like we did in He's variational iteration method and Adomian decomposition method.

(iv) This study shows that VIM is another form of expressing ADM and vice versa.

So we can say that the present method is parallel form of ADM and can give good results of VIM with less effort.

Conflict of Interests

The authors declare that there is no conflict of interests regarding the publication of this paper.

Authors' Contribution

The authors have made the same contribution. All authors read and approved the final paper.

Acknowledgments

The authors are grateful to the reviewers for their comments and useful suggestions and the third author was supported by Project no. FEKT-S-14-2200 of Faculty of Electrical Engineering and Communication, Brno University of Technology, Czech Republic.

References

[1] J. Kevorkian and J. D. Cole, *Multiple Scale and Singular Perturbation Methods*, Springer, New York, NY, USA, 1996.

[2] J.-H. He, "Variational iteration method—a kind of non-linear analytical technique: some examples," *International Journal of Non-Linear Mechanics*, vol. 34, no. 4, pp. 699–708, 1999.

[3] J. H. He, G. C. Wu, and F. Austin, "The variational iteration method which should be followed," *Nonlinear Science Letters A*, vol. 1, no. 1, pp. 1–30, 2009.

[4] N. Faraz, Y. Khan, and F. Austin, "An alternative approach to differential-difference equations using the variational iteration method," *Zeitschrift fur Naturforschung A*, vol. 65, no. 12, pp. 1055–1059, 2010.

[5] Y. Khan, "An effective modification of the laplace decomposition method for nonlinear equations," *International Journal of Nonlinear Sciences and Numerical Simulation*, vol. 10, no. 11-12, pp. 1373–1376, 2009.

[6] Y. Khan and N. Faraz, "Application of modified Laplace decomposition method for solving boundary layer equation," *Journal of King Saud University*, vol. 23, no. 1, pp. 115–119, 2011.

[7] Y. Khan and F. Austin, "Application of the laplace decomposition Method to Nonlinear Homogeneous and Non-Homogenous Advection Equations," *Zeitschrift fur Naturforschung A*, vol. 65, no. 10, pp. 849–853, 2010.

[8] Y. Khan and H. Latifizadeh, "Application of new optimal homotopy perturbation method and Adomian decomposition methods to MHD non-Newtonian fluid flow over a stretching sheet," *International Journal of Numerical Methods for Heat and Fluid Flow*, vol. 24, pp. 124–136, 2014.

[9] C. Chun, H. Jafari, and Y.-I. Kim, "Numerical method for the wave and nonlinear diffusion equations with the homotopy perturbation method," *Computers and Mathematics with Applications*, vol. 57, no. 7, pp. 1226–1231, 2009.

[10] Y. Khan, Q. Wu, N. Faraz, and A. Yildirim, "The effects of variable viscosity and thermal conductivity on a thin film flow over a shrinking/stretching sheet," *Computers and Mathematics with Applications*, vol. 61, no. 11, pp. 3391–3399, 2011.

[11] Y. Khan and Q. Wu, "Homotopy perturbation transform method for nonlinear equations using He's polynomials," *Computers and Mathematics with Applications*, vol. 61, no. 8, pp. 1963–1967, 2011.

[12] G. Adomian, *Solving Frontier Problems of Physics: The Decomposition Method*, Kluwer Academic Publishers, Boston, Mass, USA, 1994.

[13] R. Rach, "On the Adomian (decomposition) method and comparisons with Picard's method," *Journal of Mathematical Analysis and Applications*, vol. 128, no. 2, pp. 480–483, 1987.

[14] A.-M. Wazwaz, "The decomposition method applied to systems of partial differential equations and to the reaction-diffusion Brusselator model," *Applied Mathematics and Computation*, vol. 110, no. 2-3, pp. 251–264, 2000.

[15] H. Jafari and V. Daftar-Geijji, "Revised Adomian decomposition method for solving a system of nonlinear equations," *Applied Mathematics and Computation*, vol. 189, pp. 541–548, 2007.

[16] R. C. Rach, "A new definition of the Adomian polynomials," *Kybernetes*, vol. 37, no. 7, pp. 910–955, 2008.

[17] M. Inokuti, H. Sekine, and T. Mura, "General use of the Lagrange multiplier in nonlinear mathematical physics," in *Variational Method in the Mechanics of Solids*, S. Nemat-Naseer, Ed., pp. 156–162, Pergamon Press, New York, NY, USA, 1978.

[18] L. Xu, J.-H. He, and A.-M. Wazwaz, "Variational iteration method-Reality, potential, and challenges," *Journal of Computational and Applied Mathematics*, vol. 207, no. 1, pp. 1–2, 2007.

[19] J.-H. He, "Variational iteration method-Some recent results and new interpretations," *Journal of Computational and Applied Mathematics*, vol. 207, no. 1, pp. 3–17, 2007.

[20] A.-M. Wazwaz, "The variational iteration method for solving linear and nonlinear systems of PDEs," *Computers and Mathematics with Applications*, vol. 54, no. 7-8, pp. 895–902, 2007.

[21] A.-M. Wazwaz, "The variational iteration method for solving two forms of Blasius equation on a half-infinite domain," *Applied Mathematics and Computation*, vol. 188, no. 1, pp. 485–491, 2007.

[22] M. El-Gamel, "Comparison of the solutions obtained by Adomian decomposition and wavelet-Galerkin methods of boundary-value problems," *Applied Mathematics and Computation*, vol. 186, no. 1, pp. 652–664, 2007.

[23] H. Jafari, H. Tajadodi, and D. Baleanu, "A modified variational iteration method for solving fractional Riccati differential equation by Adomian polynomials," *Fractional Calculus and Applied Analysis*, vol. 16, pp. 109–122, 2013.

Hindawi Publishing Corporation
The Scientific World Journal
Volume 2014, Article ID 792829, 15 pages
http://dx.doi.org/10.1155/2014/792829

Research Article

On the Iterative Methods of Linearization, Decrease of Order and Dimension of the Karman-Type PDEs

A. V. Krysko,[1] J. Awrejcewicz,[2] S. P. Pavlov,[3] M. V. Zhigalov,[3] and V. A. Krysko[3]

[1] *Engels Institute of Technology (Branch), Saratov State Technical University, Department of Higher Mathematics and Mechanics, Russian Federation, Ploschad Svobodi 17, Engels, Saratov 413100, Russia*
[2] *Department of Automation and Biomechanics, Lodz University of Technology, and Department of Vehicles, Warsaw University of Technology, 84 Narbutta Street, 02-524 Warszawa, Poland*
[3] *Saratov State Technical University, Department of Mathematics and Modeling, Russian Federation, Polytehnicheskaya 77, Saratov 410054, Russia*

Correspondence should be addressed to J. Awrejcewicz; awrejcew@p.lodz.pl

Received 8 November 2013; Accepted 30 December 2013; Published 16 March 2014

Academic Editors: D. Baleanu and H. Jafari

Iterative methods to achieve a suitable linearization as well as a decrease of the order and dimension of nonlinear partial differential equations of the eighth order into the biharmonic and Poisson-type differential equations with their simultaneous linearization are proposed in this work. Validity and reliability of the obtained results are discussed using computer programs developed by the authors.

1. Introduction

Mathematical models of continuous mechanical structures are described by nonlinear partial differential equations which may be solved analytically only in a few rare cases. However, a direct application of the numerical methods is associated also with big difficulties regarding a high order of both dimension and differential operator, as well as nonlinearity of the PDEs studied.

This is why it is tempting to develop approaches that offer a reduction of the input differential equations. The mentioned methods can be divided into three groups: (1) linearization; (2) order decrease of the PDEs; (3) order decrease of a differential operator.

The so far existing methods of solutions of nonlinear problems, depending on the introduced linearization level, can be divided into two groups. The first one deals with the linearization of PDEs, whereas the second one is dedicated to the linearization of algebraic equations obtained through the discretization procedures applied to the input PDEs. Below, we consider the methods associated with the first group. This group contains the Newton and Newton-Kantorovich methods [1].

One of the linearization methods is the method of quasi-linearization, widely illustrated in monograph [2]. It presents a further development of Newton's method, and it generalizes the method proposed by Kantorovich.

On the other hand, there is a seminal approach known as the Agmon-Douglis-Nirenberg (ADN) theory for elliptic PDEs still attracting a large number of imitators [3, 4]. In particular, the abstract least squares theory is developed satisfying the ADN elliptic theory assumptions [5–7].

Furthermore, in the case of corners in plane domains the ADN system exhibits singularities, which imply a need for construction of singular exponents and angular functions [8]. Our approach does not have this disadvantage and it is simple in direct applications to the real world systems.

The so far briefly addressed approaches linearize the input problem; that is, they reduce it to the solution of linear problems. However, there is one more important question to be solved, that is, a reduction of the space dimension of the initial problem.

One of the methods to solve the stated problem is focused on averaging (integration) along such a coordinate on which the object dimension is lesser in comparison to the two remaining coordinates. On the other hand, it is well known that mathematical problems related to the theory of material strength can be formulated as variational problems, that is, the problems of finding extrema of a certain functional. Variational statements create a foundation for the construction of direct difference and variational methods, as it is widely described in monograph [9].

We mention only a few works [10–12] devoted to the third group, that is, aiming at a decrease of the PDE order.

Note that the so far presented state of the art of the proposed and applied methods allows us to solve each of the mentioned problems separately: either a decrease of the system order or its linearization. However, we show how all these problems can be solved simultaneously.

Our paper is focused mainly on the method of dimension decrease and linearization of the Karman-type PDEs. However, the presented approach can be successfully applied to other nonlinear PDEs. In particular, in the modified version two variants of the proposed method are presented:

(i) the first iterative method consists of the reduction of the eighth order linear PDEs to a successive solution of linear PDEs of the fourth order biharmonic equations; that is, the system dimension is reduced twice with simultaneous linearization of the problem;

(ii) the applied second iterative procedure includes a further order decrease of the earlier obtained (first iterative method) linear system of biharmonic PDEs of the fourth order to the successive solution to the system of the second order Poisson-type equations.

In other words, the application of these two iterative procedures implies a fourfold reduction of the PDEs order with the linearization procedure carried out simultaneously.

The proposed iterative procedures regarding the nonlinear PDEs order decrease and linearization can also be applied to PDEs with a curvilinear boundary. The application of FDM (finite difference method) to solve biharmonic equations and PDEs of the Poisson-type requires a solution to the so-called Sapondzhyan-Babuška problem. The paradox of Sapondzhyan-Babuška (see [13–15]) was discovered when studying the asymptotic behavior of solutions to an elasticity system in a thin polygonal plate (inscribed in the plate with smooth boundary) as the length of the side of the polygon tends to zero and the number of sides goes to infinity. In Section 2 of our work we prove the proposed iterative procedure to remove this paradox (this problem concerns smoothness of the curvilinear boundary).

In Section 3 of our work the reliability and validity of the method of variational iterative procedure to solve PDEs described by positively defined operators are illustrated and discussed. Namely, the convergence of the method of variational iterations generalizes the Kantorovich-Vlasov method [16] aimed at the reduction of PDEs to ODEs. On the other hand, as it was pointed out by Vorovich [17], the Kantorovich-Vlasov method generalizes the Galerkin method. It should be emphasized that the choice of approximating functions referring either to two variables in the Galerkin method or to one variable in the Kantorovich-Vlasov method cannot be applied in the method of variational iterations. The system of functions being sought is provided by a solution of the PDEs with regard to two variables assuming that we deal with the 2D problem. Furthermore, the proposed approach can be applied to 3D elliptic equations.

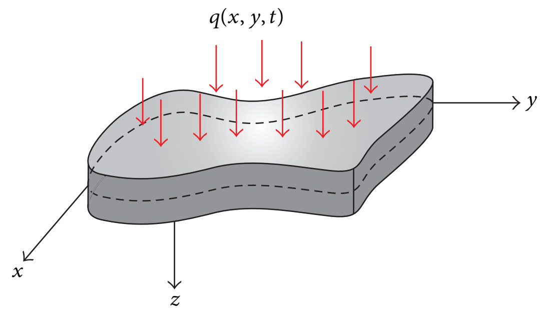

FIGURE 1: A studied plate.

Section 6 of the paper deals with a comparison of the solutions to the Karman equations obtained via our proposed iterative procedures with those offered by FEM and FDM, as well as with experimental results. Good coincidence of the results is achieved.

2. Mathematical Model of a Flexible Karman-Type Plate (Hypotheses, Differential Equations, and Boundary Conditions)

The objects of our investigation are plates of different shapes (in particular, rectangular ones), representing a closed 3D part of space R^3 (Figure 1). The following hypotheses are introduced: (i) plate material is elastic and isotropic; (ii) the following Karman relations between deformations and displacements are introduced:

$$\varepsilon_{xx} = \frac{\partial u}{\partial x} + \frac{1}{2}\left(\frac{\partial w}{\partial x}\right)^2, \quad \varepsilon_{xy} = \frac{\partial u}{\partial y} + \frac{\partial v}{\partial x} + \frac{\partial w}{\partial x}\frac{\partial w}{\partial y}, \quad (u, v, w), (x, y). \tag{1}$$

Equations governing the deflection $w(x, y, t)$ and stress function $F(x, y)$ have the following form [15]:

$$\begin{gathered} \Delta^2 w - L(w, F) - q = 0, \\ \Delta^2 F + \frac{1}{2} L(w, w) = 0. \end{gathered} \tag{2}$$

The following operators are introduced:

$$\begin{gathered} \Delta^2(\cdot) = \frac{1}{\lambda^2}\frac{\partial^4(\cdot)}{\partial x^4} + \lambda^2\frac{\partial^4(\cdot)}{\partial y^4} + 2\frac{\partial^4(\cdot)}{\partial x^2 \partial y^2}, \\ L(\cdot,\cdot) = \frac{\partial^2(\cdot)}{\partial x^2}\frac{\partial^2(\cdot)}{\partial y^2} - 2\frac{\partial^2(\cdot)}{\partial x \partial y}\frac{\partial^2(\cdot)}{\partial x \partial y} + \frac{\partial^2(\cdot)}{\partial x^2}\frac{\partial^2(\cdot)}{\partial y^2}. \end{gathered} \tag{3}$$

Here and further on the following nondimensional quantities are introduced: $w = h\overline{w}$; $F = Eh^2\overline{F}$; $t = t_0\overline{t}$; $\varepsilon = \overline{\varepsilon}/\tau$; $x = a\overline{x}$; $y = b\overline{y}$; $q = \overline{q}(12(1-\nu^2)Eh^4/a^2b^2)$;

$\tau = (ab/h)\sqrt{\rho/Eg}$; $\lambda = a/b$, where a, b are the maximal plate dimensions regarding x and y, respectively; h is thickness; g is acceleration due to gravity; $\rho = \gamma h$; γ is specific gravity of volume plate material; ν is Poisson's coefficient; E is the Young modulus; w, F are deflection and stress functions, respectively.

Let us add boundary conditions of the support on flexible nonstretched (noncompressed) ribs to the system of plates [18, 19]:

$$w|_\Gamma = \left.\frac{\partial^2 w}{\partial n^2}\right|_\Gamma = F|_\Gamma = \left.\frac{\partial^2 F}{\partial n^2}\right|_\Gamma = 0, \tag{4}$$

where Γ stands for the space boundary occupied by the plate. The following initial conditions are attached to (2):

$$w|_{t=0} = w_0, \qquad \dot{w}|_{t=0} = \dot{w}_0. \tag{5}$$

System of (2) is composed of nonlinear PDEs of the eighth order. Finding a reliable solution to this problem is still a serious problem in spite of achievements of the numerical methods. It should be emphasized that the solution to the mentioned problem was found earlier via either FDM (finite difference method) or FEM (finite element method), or by the Bubnov-Galerkin method. Below, we propose a novel method of order reduction and linearization of PDEs (2).

3. Methods of Order Decrease and Linearization of the Karman Equation

There are two ways for construction of the fundamental iterative procedure to solve system (2): (i) system reduction to a successive solution to the Germain-Lagrange type equations, in this case the system order is decreased twice; (ii) system reduction to a Poisson-type equation (in this case the system order is reduced four times). In both mentioned cases the linearization procedure of the input PDEs is carried out.

3.1. Iterative Linearization Procedure and Reduction of the Karman Equation into Germain-Lagrange Equations. We keep the biharmonic operator in each of (2), and we shift nonlinear terms into their right-hand sides. Assuming that functions on the right-hand sides are computed with respect to their previous step and that the equations are solved successively, the following iterative procedure is proposed:

$$\begin{gathered}\Delta^2 w^{(k)} = L\left(w^{(k-1)}, F^{(k-1)}\right) + q,\\ \Delta^2 F^{(k)} = -\frac{1}{2}L\left(w^{(k)}, w^{(k)}\right), \quad \{x, y\} \in \Omega.\end{gathered} \tag{6}$$

On the first step of the iterative procedure the following biharmonic equation for a given load $q(x, y)$ is solved:

$$\Delta^2 w^{(1)}(x, y) = q(x, y). \tag{7}$$

The value of $w^{(1)}(x, y)$ is substituted into the right-hand side of equation system (6), and as a result a biharmonic equation for $F^{(1)}(x, y)$ with the known right-hand side is obtained. The value of the stress function found so far is substituted to the first system equation. The process of finding solutions is continued to achieve the required accuracy.

Let us note that as a result of the application of the iterative procedure, the Germain-Lagrange type system of equations are obtained.

Let us prove convergence of the constructed iterative procedure. Let $H^2(\Omega)$ refer to a Sobolev space of functions $\xi = \{w, F\}$ such that

$$\begin{gathered}\xi \in L^2(\Omega), \qquad \frac{\partial \xi}{\partial x_i} \in L^2(\Omega),\\ \frac{\partial^2 \xi}{\partial x_i \partial x_j} \in L^2(\Omega); \quad i, j = 1, 2,\end{gathered} \tag{8}$$

where $L^2(\Omega)$ denotes the space of functions being summed with a square in Ω.

Let $H_0^2(\Omega)$ denote the closure of functions from $D(\Omega)$ (space of functions of class C^∞ in Ω, having compact carrier in Ω) in norm $H^2(\Omega)$:

$$H_0^2(\Omega) = \overline{D(\Omega)}^{H^2(\Omega)} = \left\{\xi \in H^2(\Omega) \mid \xi|_\Gamma = \left.\frac{\partial \xi}{\partial n}\right|_\Gamma = 0\right\}. \tag{9}$$

Since space Ω is bounded and its boundary Γ is efficiently regular, then map $\xi \to \|\Delta\xi\|_{0,\Omega}$ defines the norm in $H_0^2(\Omega)$ being equivalent to the norm generated by spaces $H^2(\Omega)$.

Assume that $q \in H^{-2}(\Omega)$ ($H^{-2}(\Omega)$ denotes a conjugation to $H^2(\Omega)$). It is known [17] that in this case problems (2) and (4) have a solution (it may happen that it shall be nonunique).

Novel Variation Formulation of the Problem. Let us denote by $(\cdot,\cdot)$ a scalar product in $L^2(\Omega)$: $(\xi, \eta) = \int_\Omega \xi\eta\, d\Omega$, and by $\beta(w, F, \mu)$ a three linear form defined on $(H_0^2(\Omega))^3$:

$$\beta(w, F, \mu) = (\Delta F, \Delta\mu) + \frac{1}{2}(L(w, w), \mu). \tag{10}$$

Let us define the set

$$M = \left\{w, F \in H_0^2(\Omega) \mid \forall\mu \in H_0^2(\Omega), \beta(w, F, \mu) = 0\right\}, \tag{11}$$

and square function $J(w, F) : M \to R$

$$J(w, F) = \frac{1}{2}\|\Delta w\|_{0,\Omega}^2 + \frac{1}{2}\|\Delta F\|_{0,\Omega}^2 - (q, w). \tag{12}$$

Theorem 1. *The problem of minimizing* (12) *on set* (11) *has, at least, one solution.*

Proof. Let $\{w_n, F_n\} \in M$ be the minimizing series; that is, we have

$$J(w_n, F_n) \longrightarrow \inf_{\{w,F\}\in M} J(w, F), \tag{13}$$

which exists, since J is a square functional.

For arbitrary $w, F \in H_0^2(\Omega)$ the following inequality holds:

$$J(w, F) \geq c_1\|w\|_{2,\Omega}^2 + c_2\|F\|_{2,\Omega}^2 - c_3 \cdot \|w\|_{2,\Omega}, \tag{14}$$

where $\|\cdot\|_{2,\Omega}$ denotes the norm in $H^2(\Omega)$ and c_i are certain positive constants. Then, (13) yields $c_1\|w_n\|_{2,\Omega}^2 + c_2\|F_n\|_{2,\Omega}^2 - c_3\|w_n\|_{2,\Omega} \le J(w_n, F_n) \le J(w_0, F_0) = A$, where w_0, F_0 are the arbitrary functions (initial approximation).

Then, the following estimation holds:

$$c_1\left(\|w_n\|_{2,\Omega}^2 - \frac{c_3}{2c_1}\right)^2 + c_2\|F_n\|_{2,\Omega}^2 \le A + \frac{c_3^2}{4c_1},$$
$$\|w_n\|_{2,\Omega} \le c_4, \qquad \|F_n\|_{2,\Omega} \le c_5. \tag{15}$$

Therefore, series $\{w_n, F_n\}$ is bounded in $(H_0^2(\Omega))^2$. Consequently, one may choose a series $\{w_k, F_k\}$ that $w_k \to \widetilde{w}$, $F_k \to \widetilde{F}$ is weak in $H_0^2(\Omega)$. Since $H_0^2(\Omega) \to L^2(\Omega)$ is compact, then $w_k \to \widetilde{w}$, $F_k \to \widetilde{F}$ is strong in $L^2(\Omega)$.

We show that interval $\{\widetilde{w}, \widetilde{F}\}$ of the minimized series belongs to M; that is, $\beta(\widetilde{w}, \widetilde{F}, \mu) = 0$, for all $\mu \in H_0^2(\Omega)$.

Since $(L(w_k, w_k), \mu) = (L(w_k, \mu), w_k)$ $\forall\mu \in H_0^2(\Omega)$, $L(w_k, \mu) \to L(\widetilde{w}, \mu)$ is weak in $H_0^2(\Omega)$, and $w_k \to \widetilde{w}$ is strong in $L^2(\Omega)$, we get $(L(w_k, w_k), \mu) = (L(\widetilde{w}, \widetilde{w}), \mu)$ and consequently, $\beta(\widetilde{w}, \widetilde{F}, \mu) = 0$ for all $\mu \in H_0^2(\Omega)$. This means that

$$\{\widetilde{w}, \widetilde{F}\} \in M. \tag{16}$$

However, $J(w, F)$ is half-continuous from below in weak topology on $(H^2(\Omega))^2$, and therefore the following inequality holds: $\underline{\lim}_{k\to\infty} J(w_k, F_k) \ge J(\widetilde{w}, \widetilde{F})$.

Then (13) and (16) imply that $J(\widetilde{w}, \widetilde{F}) \le \inf_{(w,F)\in M} J(w, F)$. Therefore, the following equation holds: $J(\widetilde{w}, \widetilde{F}) = \inf_{(w,F)\in M} J(w, F)$, which means that $\{\widetilde{w}, \widetilde{F}\} \in M$ is a solution to the minimization problem. □

Let us explain how points of the minimum of functional (12) are linked with solutions to problems (6) and (4). For this purpose a notation of weak solution shall be introduced.

A weak solution to problems (6) and (4) is defined by the pair of functions $\{w, F\} \in M$, satisfying the following:

$$(\Delta w, \Delta\mu) - (L(w, F), \mu) = (q, \mu) \quad \forall\mu \in H_0^2(\Omega). \tag{17}$$

Theorem 2. *Points of the functional minimum* (12) *are weak solutions to problems* (6) *and* (4).

Proof. Let $\{w, F\} \in M$ be one of the functional (12) minimum points. Let us take $\eta = w + t\,\delta w \quad \delta w \in H_0^2(\Omega)$ and let us choose $\xi = F + \delta F \quad \delta F \in H_0^2(\Omega)$ such that $\{\eta, \xi\} \in M$, that is, in the way that $\beta(w, F, \mu) = 0$ for all $\mu \in H_0^2(\Omega)$. Then $J(w, F) \le J(\eta, \xi)$. This yields

$$t(\Delta w, \Delta\delta w) + (\Delta F, \Delta\delta F) - t(q, \delta w) + \frac{t_2}{2}\|\Delta\delta w\|_{2,\Omega}^2$$
$$+ \frac{1}{2}\|\Delta\delta F\|_{2,\Omega}^2 \ge 0, \quad \forall t \in R,\ \delta w \in H_0^2(\Omega), \tag{18}$$

and by taking $\mu = F$, condition $\beta(\eta, \xi, \mu) = 0$ yields

$$(\Delta F, \Delta\delta F) = -t(L(w, \delta w), F) - \frac{t^2}{2}(L(\delta w, \delta w), F). \tag{19}$$

Substituting (19) into (18), dividing the obtained expression by t and going to the limit for $t \to 0$, the following inequality is obtained:

$$(\Delta w, \Delta\delta w) - (L(w, F), \delta w) \ge (q, \mu). \tag{20}$$

Substituting δw by $-\delta w$ in (20), one obtains equality, that is, (17).

Let us use the following notation $(\Phi(w, F), \mu) = a_1(\Delta w, \Delta\mu) - (L(w, F), \mu) - (q, \mu)$.

Equation (17) can be given in the following form:

$$(\Phi(w, F), \mu) = 0, \tag{21}$$

and it is clear that $\Phi(w, F) \in H^{-2}(\Omega)$.

Therefore, each point of the minimum of functional (17) on M satisfies (21), and hence it is a weak solution to problems (6) and (4). □

Therefore, it has been shown that finding a solution to problems (6) and (4) is equivalent to finding a solution to the problem of minimization (13) with the occurrence of constraints $\{w, F\} \in M$. The reduced problem can be solved by various methods to find a minimum taking into account the mentioned constarints. Once a solution to the problem of finding an extreme is chosen, various algorithms to solve problems (6) and (4) can be applied.

Below, we focus on the method of gradient projection with a restoring constraint [18], which for linear constraints allows for essential simplification of finding a solution to the stated problem.

Let us construct an iteration process of minimizing $J(w, F)$ on M using the following scheme:

(a) element $w_0 \in H_0^2(\Omega)$ is taken arbitrarily;

(b) after computation of w_n, $F_n \in H_0^2(\Omega)$ and $w_{n+1} \in H_0^2(\Omega)$ is defined successively by solutions to the following problems:

$$\beta(w_n, F_n, \mu) = 0, \quad F_n \in H_0^2(\Omega) \quad \forall\mu \in H_0^2(\Omega), \tag{22}$$

$$(\Delta w_{n+1}, \Delta\mu) = (\Delta w_n, \Delta\mu) - \rho_n(\Phi(w_n, F_n), \mu) \quad \forall\mu \in H_0^2(\Omega); \tag{23}$$

(c) coefficient ρ_n on step (b) is defined by the condition

$$J(w_{n+1}, F_{n+1}) - J(w_n, F_n) \le \varepsilon(\Phi(w_n, F_n), w_{n+1} - w_n), \quad 0 < \varepsilon < 1, \tag{24}$$

where ε stands for a parameter of the method.

Theorem 3. *For the iteration process* (22) *to* (25) $(\Phi(w_n, F_n), \mu) \to 0$ *for* $n \to 0$ *an arbitrary initial point* $\{w_0, F_0\} \in M$*, obtained through this procedure series* $\{w_n, F_n\}$ *includes a subseries convergent to the weak solution to the problem ((*6*) and* (4)*).*

Proof. A possibility of constructing the series $\{w_n, F_n\}$ is yielded by an observation that for all ρ_n $w_{n+1} \in H_0^2(\Omega)$ and, consequently, $L(w_{n+1}, w_{n+1}) \in H^{-2}(\Omega)$, $\nabla_k^2 w_{n+1} \in H^{-2}(\Omega)$ [19]. It means that the coupling equation $\beta(w_{n+1}, F_{n+1}, \mu) = 0$ is solvable. Consider the following difference:

$$\begin{aligned}\Delta J_n &= J(w_{n+1}, F_{n+1}) - J(w_n, F_n)\\ &= \frac{1}{2}(\Delta(w_{n+1} - w_n), \Delta(w_{n+1} + w_n))\\ &\quad + \frac{1}{2}(\Delta(F_{n+1} - F_n), \Delta(F_{n+1} + F_n))\\ &\quad - (q, w_{n+1} - w_n).\end{aligned} \tag{25}$$

Owing to $\{w_n, F_n\} \in M$, $\{w_{n+1}, F_{n+1}\} \in M$, (25) gives

$$\Delta J_n = (\Phi(w_n, F_n), \delta w) + \frac{1}{2}\|\Delta\delta w\|_{0,\Omega}^2 + \frac{1}{2}\|\Delta\delta F\|_{0,\Omega}^2, \tag{26}$$

where $\delta w = w_{n+1} - w_n$, $\delta F = F_{n+1} - F_n$. Taking (23) into account, one observes that δw serves as a general solution to the boundary value problem:

$$\Delta^2 \delta w = -\rho_n \Phi(w_n, F_n), \quad \delta w \in H_0^2(\Omega). \tag{27}$$

Further on it means that

$$\delta w = -\rho_n G[\Phi(w_n, F_n)], \tag{28}$$

where $G[\bullet] : H^{-2}(\Omega) \to H_0^2(\Omega)$ stands for the linear bounded operator being inversed to operator $\Delta^2(\bullet)$. Therefore

$$\begin{aligned}\Delta J_n &= -\rho_n(\Phi(w_n, F_n), G[\Phi(w_n, F_n)])\\ &\quad + \frac{1}{2}\|\Delta\delta w\|_{0,\Omega}^2 + \frac{1}{2}\|\Delta\delta F\|_{0,\Omega}^2.\end{aligned} \tag{29}$$

Let us proceed to the second order terms. Taking in (11) $\mu = \delta w$ and applying (28), one gets

$$\begin{aligned}\|\Delta\delta w\|_{0,\Omega}^2 &= -\rho_n(\Phi(w_n, F_n), \delta w)\\ &= \rho_n^2(\Phi(w_n, F_n), G[\Phi(w_n, F_n)]).\end{aligned} \tag{30}$$

Let us estimate the last term in (29). Since $\{w_n, F_n\} \in M$ and $\{w_{n+1}, F_{n+1}\} \in M$, then for δF the following equation should be satisfied:

$$\begin{gathered}(\Delta\delta F, \Delta\mu) + (L(w_n, \delta w), \mu) + (\nabla_k^2 \delta w, \mu)\\ + \frac{1}{2}(L(\delta w, \delta w), \mu) = 0\\ \delta F \in H_0^2(\Omega), \quad \forall\mu \in H_0^2(\Omega).\end{gathered} \tag{31}$$

This, in particular, yields

$$\begin{aligned}\|\Delta\delta F\|_{0,\Omega} &\le c_7\left(\|L(w_n, \delta w)\|_{L^1(\Omega)}\right.\\ &\quad \left.+ \|L(\delta w, \delta w)\|_{L^1(\Omega)} + \|\nabla_k^2 \delta w\|_{L^1(\Omega)}\right).\end{aligned} \tag{32}$$

However, w_n belongs to the bounded set in $H_0^2(\Omega)$ for arbitrary n. It implies that $\|\Delta\delta F\|_{0,\Omega} \le c_8\|\Delta\delta w\|_{0,\Omega}^2$ or equivalently

$$\|\Delta\delta F\|_{0,\Omega}^2 \le c_9\rho_n^4(\Phi(w_n, F_n), G[\Phi(w_n, F_n)])^2. \tag{33}$$

Substituting (30), (33) into (29), and taking into account both positive defiantness (in the sense of $(\Phi(w_n, F_n), G[\Phi(w_n, F_n)]) \ge \alpha\|\Phi(w_n, F_n)\|^2$) and the constraints of operator $G[\bullet]$, one gets

$$\begin{aligned}\Delta J_n &\le -\rho_n c_{10}\|\Phi(w_n, F_n)\|^2\\ &\quad \times\left(-1 + \frac{\rho_n}{2} + c_1\frac{\rho_n^3}{2}\|\Phi(w_n, F_n)\|^2\right).\end{aligned} \tag{34}$$

The latter estimation shows that the values $\rho_n \neq 0$ are responsible for the satisfaction of inequality (24). For this purpose ρ_n should be chosen in the following way:

$$\frac{\rho_n}{2} + c_1\frac{\rho_n^3}{2}\|\Phi(w_n, F_n)\|^2 \le 1 - \varepsilon. \tag{35}$$

It can always be done, since $0 < \varepsilon < 1$.

Taking ρ_n in accordance with the algorithm applied so far, the following estimations are obtained on each step:

$$\Delta J_n \le -\rho_n\varepsilon\|\Phi(w_n, F_n)\|^2, \tag{36}$$

which means that for the arbitrarily taken n we have $J_{n+1} - J_n \le 0$. Since functional J is bounded from below, the last inequality yields for $n \to \infty$ $\Delta J_n \to 0$. Besides, (36) gives

$$\|\Phi(w_n, F_n)\|^2 \le \frac{-\Delta J_n}{\varepsilon\rho_n}. \tag{37}$$

Let us emphasize that the so far introduced algorithm of the choice of ρ_n guarantees that for arbitrary n we have $\rho_n \ge \rho_0 > 0$. In fact, because $\Delta J_n \le 0$, then

$$J(w_n, F_n) \le J(w_0, F_0) = A. \tag{38}$$

Owing to (38), norms $\|w_n\|_{2,\Omega}$, $\|F_n\|_{2,\Omega}$ are bounded. Therefore, also the norm $\|\Phi(w_n, F_n)\|$ is bounded. In addition, taking (37) into account, we have $\|\Phi(w_n, F_n)\| \to 0$ for $n \to \infty$, and consequently, also $(\Phi(w_n, F_n), \mu) \to 0$ for $n \to \infty$ for all $\mu \in H_0^2(\Omega)$. The occurrence of a convergent subseries follows now from a bound of norms $\|w_n\|_{2,\Omega}$, $\|F_n\|_{2,\Omega}$ (see proof of Theorem 1). □

We have shown in the above the convergence of the reduction procedure of system (2) to the successive solution to the biharmonic Germain-Lagrange type equation. The applied procedure linearizes and decreases the order of the input equations. We have proposed a further development of this approach on the basis of reduction of the biharmonic equation to that of the Poisson-type. The latter approach allows us to decrease four times the order of system (2).

3.2. Iterative Procedure of Reduction of the Germain-Lagrange Equations Type to the Poisson Equations Type. The following original iterative procedure is proposed.

We consider a biharmonic equation given in the bounded convex space $\Omega \in R^2$:

$$\Delta^2 w(x, y) = g(x, y). \tag{39}$$

On the space boundary the following boundary conditions are given:

$$w|_\Gamma = 0, \qquad \Delta w - \chi \frac{\partial w}{\partial n}\bigg|_\Gamma = 0, \tag{40}$$

where χ denotes the curvature of boundary Γ.

Let us introduce the following new function $M_w = \Delta w$. Substituting this function into (39) the following system of two Poisson-type equations is obtained:

$$\begin{gathered}\Delta M_w(x, y) = g(x, y), \\ \Delta w(x, y) = M_w(x, y), \quad x, y \in \Omega.\end{gathered} \tag{41}$$

Boundary conditions have the following form:

$$w(x, y)|_{x,y\in\Gamma} = 0, \qquad M_w(x, y)|_{x,y\in\Gamma} = 0. \tag{42}$$

Therefore, a solution of the biharmonic equation is divided into a solution of two Poisson-type equations. Below, we prove convergence of the proposed procedure.

Let us define the following set for the function $\xi = \{w, M_w\}$:

$$E = \{\xi \in \rho^\infty(\Omega) \mid \xi|_\Gamma = 0\}, \tag{43}$$

where $\rho^\infty(\Omega)$ is the set of functions infinitely many times differentiable on $\overline{\Omega} \in R^2$. Closure of set (43) in norm $H^2(\Omega)$ is a subspace in $H^2(\Omega)$ which is denoted by $V(\Omega)$. It is clear that $V(\Omega) = H^2(\Omega) \cap H_0^1(\Omega)$.

It is known (see [13]) that a solution to problems (39) and (40) is equivalent to minimization on $V(\Omega)$ of the following functional:

$$J(v) = \frac{1}{2}\int_\Omega |\Delta\xi|^2 d\Omega - \int_\Omega g\xi \, d\Omega - \frac{1}{2}\int_\Gamma \chi\left|\frac{\partial\xi}{\partial n}\right|^2 ds. \tag{44}$$

Hybrid Variation Problem Formulation. We assume that instead of functional (44) the following one is minimized:

$$\Phi(\xi, \psi, \alpha) = \frac{1}{2}\int_\Omega |\psi|^2 d\Omega - \int_\Omega g\xi \, d\Omega - \frac{1}{2}\int_\Gamma \chi|\alpha|^2 ds, \tag{45}$$

on such triads $(\xi, \psi, \alpha) \in V(\Omega) \times L^2(\Omega) \times L^2(\Gamma)$ that their elements are coupled through equalities $-\Delta\xi = \psi$, $(\partial w/\partial n)|_\Gamma = \alpha$.

Let us define the space of the following functions:

$$\begin{aligned}P(\Omega) = \big\{&(\xi, \psi, \alpha) \in H_0^1(\Omega) \times L^2(\Omega) \times L^2(\Gamma) \mid \\ &\forall\mu \in H^1(\Omega), \beta[(\xi, \psi, \alpha), \mu] = 0\big\},\end{aligned} \tag{46}$$

where the bilinear form $\beta[\cdot, \cdot]$ is defined as

$$\beta[(\xi, \psi, \alpha), \mu] = \frac{1}{2}\int_\Omega \nabla\xi\nabla\mu \, d\Omega - \int_\Omega \psi\mu \, d\Omega - \int_\Gamma \alpha\mu \, ds. \tag{47}$$

Theorem 4. *If the space Ω is convex and has a Lipschitz continuous boundary Γ, then, first, the map $(\xi, \psi, \alpha) \in P(\Omega) \to |\psi|_{0,\Omega}^2$, now and later $|\xi|_{m,\Omega} = (\sum_{|k|=m} \int_\Omega |\partial^k\xi|^2 d\Omega)^{1/2}$, $\|\xi\|_{m,\Omega} = (\sum_{|k|\le m} \int_\Omega |\partial^k\xi|^2 d\Omega)^{1/2}$) is the norm on space $P(\Omega)$ equivalent to the real dot product form $(\xi, \psi, \alpha) \in P(\Omega) \to (|\xi|_{1,\Omega}^2 + |\psi|_{0,\Omega}^2 + |\alpha|_{0,\Gamma}^2)^{1/2}$ transforming $P(\Omega)$ into a Hilbert space; second, if $(\xi, \psi, \alpha) \in P(\Omega)$, then*

$$(\xi, \psi, \alpha) \in V \times L^2(\Omega) \times L^2(\Gamma), \quad -\Delta\xi = \psi, \quad \frac{\partial w}{\partial n}\bigg|_\Gamma = \alpha, \tag{48}$$

and if (48) is satisfied, then $(\xi, \psi, \alpha) \in P(\Omega)$.

Proof. In the beginning we show the second statement. Since Ω has a continuous boundary, then the following Green formula holds:

$$\begin{gathered}\int_\Omega \nabla\xi\nabla\mu d\Omega = -\int_\Omega \Delta\xi\mu d\Omega + \int_\Gamma \frac{\partial\xi}{\partial n}\mu ds, \\ \forall\xi \in H^2(\Omega), \ \forall\mu \in H^1(\Omega).\end{gathered} \tag{49}$$

Let $(\xi, \psi, \alpha) \in P(\Omega)$. Then $\xi \in H_0^1(\Omega)$, $\psi \in L^2(\Omega)$, $\alpha \in L^2(\Gamma)$, and $\beta[(\xi, \psi, \alpha), \mu] = 0$ for all $\mu \in H^1(\Omega)$.

The last condition, in particular for $\forall\mu \in H_0^1(\Omega)$ yields

$$\int_\Omega \nabla\xi\nabla\mu \, d\Omega = \int_\Omega \psi\mu \, d\Omega. \tag{50}$$

It follows from (50) that v appears as a solution to the Dirichlet problem for the operator $-\Delta$ for $\xi|_\Gamma = 0$. Since space Ω is convex, therefore $\xi \in H^2(\Omega)$ ([13], Section 7.1, page 373), and consequently $\xi \in H^2(\Omega) \cap H_0^1(\Omega)$. Using now (50) for $\mu \in H_0^1(\Omega)$, we get $-\Delta\xi = \psi$. Using the Green formula for $\mu \in H^1(\Omega)$, we find that $(\partial\xi/\partial n)|_\Gamma = \alpha$. Assume that (48) holds. We show that $(\xi, \psi, \alpha) \in P(\Omega)$. Since $\xi \in V(\Omega) \subset H^2(\Omega)$ and $-\Delta\xi = \psi$, $(\partial\xi/\partial n)|_\Gamma = \alpha$, then (49) yields $\int_\Omega \nabla\xi\nabla\mu \, d\Omega = \int_\Omega \psi\mu \, d\Omega + \int_\Gamma \alpha\mu \, ds$ for all $\mu \in H^1(\Omega)$; that is, $\beta[(\xi, \psi, \alpha), \mu] = 0$ for all $\mu \in H^1(\Omega)$. Besides $\xi \in V(\Omega) \subset H_0^1(\Omega)$ and the second statement is proved.

Let us prove the first statement. Endowed with the multiplication norm $P(\Omega)$ is a Hilbert space. Let $(\xi, \psi, \alpha) \in P(\Omega)$. Then, as it has been shown, $\xi \in H^2(\Omega) \cap H_0^1(\Omega)$. For $\mu = \xi$ condition $\beta[(\xi, \psi, \alpha), \mu] = 0$ yields

$$|\xi|_{1,\Omega}^2 \le C_1|\psi|_{0,\Omega}|\xi|_{0,\Omega}. \tag{51}$$

Let us introduce space $M \subset H^1(\Omega)$ such that $H^1(\Omega) = H_0^1(\Omega) \oplus M$. Besides, let us introduce the following operator $B : H^1(\Omega) \to L^2(\Omega)$ defined in the following way: for all $\psi \in L^2(\Omega)$ $\alpha = B\psi \in L^2(\Gamma)$ we have a unique solution to the following equation:

$$\int_\Gamma \alpha\mu \, ds = \int_\Omega \nabla\xi\nabla\mu \, d\Omega - \int_\Omega \psi\mu \, d\Omega \quad \forall\mu \in M. \tag{52}$$

Under the condition that $\xi \in H_0^1(\Omega)$ satisfies the following:

$$\int_\Omega \nabla\xi\nabla\mu \, d\Omega = \int_\Omega \psi\mu \, d\Omega \quad \mu \in H_0^1(\Omega). \tag{53}$$

It is not difficult to verify that under the theorem conditions, $B\psi = -B\Delta\xi = (\partial\xi/\partial n)|_\Gamma$; that is, B stands for the operator of external normal derivative for $\xi \in H^2(\Omega) \cap H_0^1(\Omega)$. This operator is bounded; that is, $\xi \in H^2(\Omega) \cap H_0^1(\Omega)$. We denote its norm by $\|B\|$. Then $\|B\| = \sup_{v\in H^2(\Omega)\cap H_0^1(\Omega)}(\|\partial\xi/\partial n\|_{0,\Gamma}/|\Delta\xi|_{0,\Omega})$, where $\| \bullet \|_{0,\Gamma}$ denotes the norm associated with the scalar product $(\alpha,\beta)_{L^2(\Gamma)} = \int_\Gamma \alpha\beta \, ds$. Therefore, for all $\psi \in L^2(\Omega)$ $\|\alpha\|_{0,\Gamma} \le \|B\||\psi|_{0,\Omega}$. Hence, taking (52) into account we get $(\|\xi\|_{1,\Omega} + \|\psi\|_{0,\Omega} + \|\alpha\|_{0,\Gamma}) \le C_2\|\psi\|_{0,\Omega}$ and the theorem is proved. □

Results of this theorem allow us to transit from minimization of functional (45) on space $V(\Omega)$ to minimization of functional (45) on space $P(\Omega)$.

Theorem 5. *Let $w \in V(\Omega)$ be a solution to problem* (44)*, then*

$$\Phi\left(w, -\Delta w, \frac{\partial w}{\partial n}\right) \longrightarrow \inf_{(v,\psi,\alpha)\in \underline{P}(\Omega)} \Phi(\xi,\psi,\alpha). \tag{54}$$

In this case the triad $(w, -\Delta w, \partial w/\partial n) \in P(\Omega)$ is the unique solution to the problem of minimization of (54).

Proof. We prove that a symmetric bilinear form $a([(\xi,\psi,\alpha),(\eta,\varphi,\beta)]) = \int_\Omega \psi\varphi \, d\Omega - \int_\Gamma \chi\alpha\beta \, ds$, $(\xi,\psi,\alpha),(\eta,\varphi,\beta) \in P(\Omega)$ is continuous and elliptic on $P(\Omega)$.

Owing to Theorem 4, if $(\xi,\psi,\alpha),(\eta,\varphi,\beta) \in P(\Omega)$, then $-\Delta\xi = \psi$; $(\partial\xi/\partial n)|_\Gamma = \alpha$; $-\Delta\eta = \varphi$; $(\partial\eta/\partial n)|_\Gamma = \beta$. Then we have

$$a([(\xi,\psi,\alpha),(\eta,\phi,\beta)]) = \int_\Omega \Delta\xi\Delta\eta \, d\Omega - \int_\Gamma \frac{\partial\xi}{\partial n}\frac{\partial\eta}{\partial n} ds. \tag{55}$$

For $\eta = \xi$, $\varphi = \psi$, $\beta = \alpha$ from (55) we obtain ([13], Section 1.2, page 38)

$$\begin{aligned} &a([(\xi,\psi,\alpha),(\eta,\psi,\alpha)]) \\ &= \int_\Omega \left[\left(\frac{\partial^2\xi}{\partial x^2}\right)^2 + 2\frac{\partial^2\xi}{\partial x^2}\frac{\partial^2\xi}{\partial y^2} + \left(\frac{\partial^2\xi}{\partial x^2}\right)^2 + 2\left(\frac{\partial^2\xi}{\partial x\,\partial y}\right)^2\right] d\Omega \\ &\ge |\psi|_{0,\Omega}^2. \end{aligned} \tag{56}$$

Then, elliptic property has been proved by P. Continuity of the bilinear form is evident. It means that the problem of minimization

$$\Phi(\xi^*,\psi^*,\alpha^*) \longrightarrow \inf_{(u,\varphi,\beta)\in P(\Omega)} \Phi(\eta,\varphi,\beta) \tag{57}$$

has a solution which is unique. Let us find a link between a solution to problem (37) as well as problems (41) and (42). If $(\xi^*,\psi^*,\alpha^*) \in P(\Omega)$ is a solution to problem (57), then the following relations should hold:

$$\begin{gathered} \int_\Omega \psi^*\varphi \, d\Omega - \int_\Omega \eta g \, d\Omega - \int_\Gamma \chi\alpha^*\beta \, ds = 0 \\ \forall (\eta,\varphi,\beta) \in P(\Omega). \end{gathered} \tag{58}$$

Since $(\xi^*,\psi^*,\alpha^*) \in P(\Omega)$, then $-\Delta\xi^* = \psi^*$, $(\partial\xi^*/\partial n)|_\Gamma = \alpha^*$, and $\xi^* \in P(\Omega)$. Therefore, taking (58) into account we get $\int_\Omega \Delta\xi^*\Delta\eta d\Omega - \int_\Gamma \chi(\partial\xi^*/\partial n)(\partial\eta/\partial n) \, ds = \int_\Gamma \eta g ds$. Therefore, ξ^* coincides with the solution w to problems (39) and (40), and $\psi^* = -\Delta w$, $\alpha^* = (\partial w/\partial n)|_\Gamma$. □

Remark 6. Since the space is convex and its boundary is regular, then for $g \in H^{-1}(\Omega)$ a solution to problems (39) and (40),

$$w \in H^3(\Omega) \cap H_0^1(\Omega), \qquad \Delta w \in H^1(\Omega). \tag{59}$$

Solution to the Minimization Problem (44). We show that a solution to problem (44) can be reduced to a solution of successive Dirichlet problems for the operator $-\Delta$.

For further analysis it is suitable to introduce a linear transformation $A : L^2(\Omega) \to H_0^1(\Omega)$ in the following way: if $\psi \in L^2(\Omega)$ is a given function, then the function $\xi = A\psi \in H_0^1(\Omega)$ is a unique solution to the equation $\int_\Omega \nabla\xi\nabla\mu \, d\Omega = \int_\Omega \psi\mu \, d\Omega$ $\forall\mu \in H_0^1(\Omega)$, for $\xi \in H_0^1(\Omega)$. This means that space $P(\Omega)$, defined by (43), can be presented in the following form:

$$\begin{aligned} P(\Omega) = \{&(\xi,\psi,\alpha) \in H_0^1(\Omega) \times L^2(\Omega) \times L^2(\Gamma) \mid \\ &\xi = A\psi,\ \alpha = B\psi\}. \end{aligned} \tag{60}$$

Problem (44) is equivalent to the following problem of optimal control:

$$\min_{\psi\in L^2(\Omega)} \left[\frac{1}{2}\int_\Omega |\psi|^2 d\Omega - \int_\Omega g\xi \, d\Omega - \frac{1}{2}\int_\Gamma \chi|\alpha|^2 ds\right], \tag{61}$$

where the state function ξ and α are coupled via control $\psi \in L^2(\Omega)$ through the following state equations:

$$\begin{gathered} \xi \in H_0^1(\Omega), \quad \xi = A\psi, \\ \alpha \in L^2(\Gamma), \quad \alpha = B\psi. \end{gathered} \tag{62}$$

As it follows from Remark 6, although the optimal control ψ is sought on $L^2(\Omega)$, its regularity is higher for $g \in H^{-1}(\Omega)$ $\psi \in H^1(\Omega)$. In this case the following trace is defined: $\psi|_\Gamma = \lambda$, $\lambda \in M$. Furthermore, besides (62), we require that $\int_\Omega \nabla\psi_\lambda\nabla\mu \, d\Omega = \int_\Omega g\mu \, d\Omega$ for all $\mu \in H_0^1(\Omega)$ and $\psi_\lambda - \lambda \in H_0^1(\Omega)$. Then, if $\xi_\lambda = A\psi_\lambda$ and $\alpha_\lambda = B\psi_\lambda$, (61) implies that $\min_{\psi\in L^2(\Omega)}\Phi(\xi,\psi,\alpha) = \min_{\lambda\in M} D(\lambda)$, where

$$\begin{aligned} D(\lambda) = &-\frac{1}{2}\int_\Omega |\psi_\lambda|^2 d\Omega - \int_\Gamma \lambda\alpha_\lambda \, ds \\ &- \frac{1}{2}\int_\Gamma \chi|\alpha_\lambda|^2 ds \quad \forall\lambda \in M. \end{aligned} \tag{63}$$

The fundamental idea consists now in the application of a gradient method to the problem of minimization (63).

Let us take M' as a dual space for space M, and let $\langle\cdot,\cdot\rangle$ denote the relation of duality between spaces M and M'. We denote by $D' \in M'$ a derivative of the functional $D(\lambda)$. Let us introduce a map $S : M \to H^1(\Omega)$ in the following way: for $\lambda \in M$ $\mathring{\varphi}_\lambda = S(\lambda)$ is a unique function from $H^1(\Omega)$ satisfying the condition

$$\int_\Omega \nabla\mathring{\phi}_\lambda \nabla\mu\, d\Omega = 0, \quad \forall\mu \in H_0^1(\Omega), \qquad \mathring{\phi}_\lambda - \lambda \in H_0^1(\Omega). \tag{64}$$

Theorem 7. *For an arbitrary $\lambda \in M$ defined in* (63), *the functional is differentiable and its derivative is defined by the relation*

$$\forall\mu \in M \quad \left\langle D'(\lambda), \mu\right\rangle = \int_\Omega \mathring{\varphi}_\theta \mathring{\varphi}_\mu\, d\Omega, \quad \text{where } \mathring{\varphi}_\mu = S(\mu),\ \mathring{\varphi}_\theta = S(\theta_\lambda), \quad \theta_\lambda = \lambda + \chi\alpha_\lambda, \quad \theta_\lambda \in M. \tag{65}$$

Proof. Differentiating (63) yields

$$\left\langle D'(\lambda), \mu\right\rangle = -\int_\Omega \psi_\lambda \mathring{\phi}_\mu d\Omega - \int_\Gamma \alpha_\lambda \mu\, d\Omega - \int_\Gamma (\lambda + \chi\, \alpha_\lambda)\, \mathring{\beta}_\mu ds, \tag{66}$$

where $\mathring{\varphi}_\mu = S(\mu)$, $\mathring{\beta}_\mu = B\mathring{\varphi}_\mu$.

From (66) and taking (52) into account we get

$$\left\langle D'(\lambda), \mu\right\rangle = -\int_\Omega \nabla v_\lambda \nabla\mathring{\phi}_\mu d\Omega - \int_\Gamma (\lambda + \chi\alpha_\lambda)\, \mathring{\beta}_\mu ds. \tag{67}$$

First term in (67) is equal to zero due to (64). Let us introduce the function $\mathring{\varphi}_\theta = S(\theta_\lambda)$, where θ_λ is defined by (66) and let $\mathring{u}_\mu = A\mathring{\varphi}_\mu$. Then, (66) implies $\langle D'(\lambda), \mu\rangle = \int_\Omega \mathring{\phi}_\theta \mathring{\phi}_\mu d\Omega - \int_\Gamma \nabla\mathring{\phi}_\theta \nabla\mathring{u}_\mu d\Omega$.

However, the last term in this equality is equal to zero due to (64), which ends the proof. The gradient method applied to minimization (63) consists now in the determination of a series $\{\lambda_n\}_{n=0}^\infty$ of functions $\lambda^n \in M$ via the following iteration scheme:

$$\mu \in M \quad \left(\lambda^{n+1} - \lambda^n, \mu\right)_M = -\rho_n \left\langle D'(\lambda^n), \mu\right\rangle, \tag{68}$$

where $(\cdot,\cdot)_M$ is the arbitrary scalar product in space M, ρ is the positive parameter, and λ^0 is the arbitrary function of M.

Therefore, one iteration (68) corresponds to successive solutions of the following problems:

(a) find for a given function $\lambda^n \in M$ a unique function $\psi^n \in H^1(\Omega)$, satisfying the following relations:

$$\psi^n - \lambda^n \in H_0^1(\Omega), \tag{69}$$

$$\forall\mu \in H_0^1(\Omega) \quad \int_\Omega \nabla\psi^n \nabla\mu\, d\Omega = \int_\Omega g\mu\, d\Omega; \tag{70}$$

(b) find a function $\xi^n \in H_0^1(\Omega)$, satisfying the following relation:

$$\forall\mu \in H_0^1(\Omega) \quad \int_\Omega \nabla\xi^n \nabla\mu\, d\Omega = \int_\Omega \psi^n \mu\, d\Omega; \tag{71}$$

(c) find a function $\alpha^n \in L^2(\Gamma)$, satisfying the following relation:

$$\forall\mu \in M \quad \int_\Gamma \alpha^n \mu\, d\Omega = \int_\Omega \nabla\xi^n \nabla\mu\, d\Omega - \int_\Omega \psi^n \mu\, d\Omega; \tag{72}$$

(d) find a function $\lambda^{n+1} \in M$, satisfying the following relation:

$$\forall\mu \in M \quad \left(\lambda^{n+1} - \lambda^n, \mu\right)_M = -\rho \int_\Omega \mathring{\phi}_\theta^n \mathring{\phi}_\mu d\Omega; \tag{73}$$

where $\mathring{\varphi}_\theta^n = S\theta_\lambda^n$, $\theta_\lambda^n = \lambda^n - \chi B\psi^n$, and $\mathring{\varphi}_\mu = S\mu$. □

We show that by a proper choice of parameter $\rho > 0$ the iteration process ((69)–(73)) is convergent for arbitrarily taken initial approximation.

Let us first define the map $C : H^1(\Omega) \to M$ in the following way: for any function $\psi \in H^1(\Omega)$ function $C\psi \in M$ is unique satisfying the following condition:

$$\forall\mu \in M \quad (C\psi, \mu)_M = \int_\Omega \psi\mathring{\phi}_\mu d\Omega. \tag{74}$$

Let us take $\|C\| = \sup_{\psi\in H^1(\Omega)}(|C\psi|_\mu/|\psi|_{0,\Omega})$, where $|\cdot|_M$ denotes the norm associated with the scalar product $(\cdot,\cdot)_M$. It is clear that this norm exists, since the map $\mu \in M \to \mathring{\varphi}_\mu \in H^1(\Omega)$ is bounded.

Theorem 8. *If parameter ρ satisfies the following condition:*

$$0 < \rho < \frac{2}{\|C\|^2\left(1 - |\chi|_{L^\infty(\Omega)}\, \|S\|\, \|B\|\right)^2}, \tag{75}$$

then the iteration process (69)–(73) *is convergent in the sense that*

$$\lim_{n\to\infty} \psi^n = \psi \text{ в } L^2(\Omega), \qquad \lim_{n\to\infty} \xi^n = \xi \text{ в } H_0^1(\Omega), \qquad \lim_{n\to\infty} \alpha^n = \alpha \text{ в } L^2(\Gamma). \tag{76}$$

Proof. It is sufficient to show that $\lim_{n\to\infty}\psi^n = 0$ in $L^2(\Omega)$ in the particular case when $g = 0$. If we use the definition (74) of map C, then the recurrent formula (73) gives

$$\lambda^{n+1} = \lambda^n - \rho C\mathring{\varphi}_\theta^n, \quad \text{where } \mathring{\varphi}_\theta^n = S\theta_\lambda^n,\ \theta_\lambda^n = \lambda^n + \chi B\psi^n, \tag{77}$$

and therefore

$$\left|\lambda^{n+1}\right|_M^2 = \left|\lambda^n\right|_M^2 - 2\rho\left(C\mathring{\phi}_\theta^n, \lambda^n\right)_M + \rho^2\left|C\mathring{\phi}_\theta^n\right|_M^2. \tag{78}$$

Consider the term $(C\overset{\circ}{\varphi}{}^n_\theta, \lambda^n)_M$:

$$\left(C\overset{\circ}{\varphi}{}^n_\theta, \lambda^n\right)_M = \int_\Omega \overset{\circ}{\varphi}{}^n_\theta \psi^n d\Omega = -\int_\Gamma \left(\lambda^n + \chi B\psi^n\right) B\psi^n ds$$
$$= \int_\Omega \left|\psi^n\right|^2 d\Omega - \int_\Gamma \chi\left|B\psi^n\right|^2 ds \geq \left|\psi^n\right|^2_{0,\Omega}. \quad (79)$$

Let us estimate the norm $|\overset{\circ}{\varphi}{}^n_\theta|$:

$$\left|\overset{\circ}{\varphi}{}^n_\theta\right|_{0,\Omega} = \left|S(\lambda^n + \chi B\psi^n)\right|_{0,\Omega} \leq \left|\psi^n\right|_{0,\Omega}$$
$$+ \|S\| \left|\chi\right|_{L^\infty(\Omega)} \|B\| \left|\psi^n\right|_{0,\Omega} \quad (80)$$
$$\leq \left(1 + \left|\chi\right|_{L^\infty(\Omega)} \|S\| \|B\|\right) \left|\psi^n\right|_{0,\Omega}.$$

The latter inequalities and (78) imply the following estimation:

$$\left|\lambda^{n+1}\right|^2_M - \left|\lambda^n\right|^2_M$$
$$\leq -\rho\left[2\eta - \|C\|^2\left(1 + \left|\chi\right|_{L^\infty(\Omega)} \|S\| \|B\|\right)^2 \rho\right] \left|\psi^n\right|^2_{0,\Omega}. \quad (81)$$

Hence, in particular, we get

$$\lim_{n\to\infty} \left|\psi\right|^n_{0,\Omega} = 0, \quad (82)$$

if ρ satisfies inequalities (75). Besides, we have

$$\lim_{n\to\infty} \xi^n = \lim_{n\to\infty} A\psi^n = 0 \text{ в } H^1_0(\Omega),$$
$$\lim_{n\to\infty} \alpha^n = \lim_{n\to\infty} B\psi^n = 0 \text{ в } L^2(\Gamma), \quad (83)$$

which finishes the proof. □

Since convergence of the considered method is guaranteed, any choice of subspace M, satisfying the condition $H^1(\Omega) = H^1_0(\Omega) \oplus M$ and any choice of scalar product $(\cdot,\cdot)_M$ on space is allowed. However, the choice influences parameter ρ, as well as the computation time on each iterations. Finally, we point out a few remarks regarding practical computations of $\lambda^{n+1} \in M$.

If the scalar product in M is defined via the following formula:

$$(\lambda, \mu)_M = \int_\Omega S\lambda \cdot S\mu \, d\Omega, \quad (84)$$

then as λ^{n+1} any function from M can be taken, assuming that the following condition is satisfied:

$$\lambda^{n+1}\Big|_\Gamma = \left(\lambda^n - \rho\theta^n_\lambda\right)\Big|_\Gamma. \quad (85)$$

Equality (85) can be understood in the sense of trace equality on a boundary. In fact, if (85) is satisfied, then

$$\left(\lambda^{n+1} - \lambda^n, \mu\right)_M = -\rho\int_\Omega S\theta^n \cdot S\mu \, d\Omega = -\rho\int_\Omega \overset{\circ}{\varphi}{}^n_\theta \overset{\circ}{\varphi}_\mu d\Omega, \quad (86)$$

which means that conditions of Theorem 7 are satisfied.

We may choose also the following scalar product:

$$\text{either } (\lambda, \mu)_M = \int_\Omega \nabla\lambda\nabla\mu \, d\Omega.$$
$$\text{or } (\lambda, \mu)_M = \int_\Omega \lambda\mu \, d\Omega. \quad (87)$$

However, in the latter case one needs to compute gradient $\langle D'(\lambda), \mu\rangle$ on each step, which extends the computational time.

Final Remarks. (1) The proof has been carried out for equations in the hybrid form (2). It can be relatively easily extended into equations regarding displacements. (2) Results can be extended on other types of the differential equations, including nonlinear ones, consisting of a biharmonic operator.

3.3. Iterative Procedure for the Reduction of the Karman Equation into the Poisson Equation. In the preceding sections we have proved convergence of the iterative procedures for linearization of (2) by reducing the solution of the eighth order system of nonlinear differential equations into that of the solution to a biharmonic equation, as well as the reduction of the biharmonic equation to the Poisson-type equation in the case of a curvilinear boundary using the finite element method (FEM).

While considering a space with the rectangular boundary, we may extend the procedure reported in Section 3.1 by introduction of new variables into the iterative procedure of solution to the Poisson-type equations without difficulties.

In the case of spaces with the curvilinear boundary, the procedure described in Section 3.2 can be applied to solve (2) using the iterative procedure, whose convergence has been proved in Section 3.1.

For this purpose new variables $M_w(x, y)$ and $M_F(x, y)$ are introduced

$$M_w(x, y) = \Delta w(x, y), \qquad M_F(x, y) = \Delta F(x, y). \quad (88)$$

Then each of differential equations (2) is divided into two Poisson-type equations. The iterative procedure of solution of the obtained system of four Poisson-type equations has the following form:

$$\Delta M^{(k)}_w = q + L\left(w^{(k-1)}, F^{(k-1)}\right),$$
$$\Delta w^{(k)} = M^{(k)}_w,$$
$$\Delta M^{(k)}_F = L\left(w^{(k)}, w^{(k)}\right), \quad (89)$$
$$\Delta F^{(k)} = M^{(k)}_F, \quad \{x, y\} \in \Omega.$$

Boundary conditions (4) are transformed to the following form:

$$w|_\Gamma = M_w|_\Gamma = F|_\Gamma = M_F|_\Gamma = 0. \quad (90)$$

The given procedure (89) has advantages over procedure (6), while solving each equation since instead of the fourth order equation that of the second order is solved. Because equations are solved by numerical methods (FDM, FEM) and the approximation of the biharmonic operator has high requirements on the approximating functions, then for the Poisson-type equation one may simplify the procedure (89) of finding a solution by choosing simple approximating functions.

In the FDM case, an order of algebraic equations system, after a discretization of the biharmonic equation, is higher for the second order equation, and hence higher expectations are required from computer abilities while solving the problem numerically.

4. The Method of Variational Iterations (MVI) of PDEs Solutions

4.1. Validation of Convergence. The method of variational iterations (MVI) was applied first in 1933 by Shunok who considered a deflection of cylindrical panels. However, this work did not meet with the response of others, and then it was rediscovered in the sixties of the previous century by Kantorovich and Krylov [20], who applied it in his investigation of rectangular plates. Then the MVI found wide application in solving various problems of plates and shells (see the list of references reported in [21]).

Here we prove validity and reliability of the mentioned method for a class of equations with positively defined operators, that is, biharmonic and harmonic ones. In other words, we prove a theorem on convergence of the MVI for iterative procedures (6) and (89).

Formally, the MVI scheme is as follows. Assume that our aim is to find a solution to the following:

$$T\omega(x,y) = g(x,y), \qquad x, y \in \Omega(x,y), \tag{91}$$

where T stands for a certain operator defined on set $D(T)$ of the Hilbert space $L_2(\Omega)$; $g(x,y)$ is the function given for two variables x and y; $\omega(x,y)$ is the function of these two variables being sought; $\Omega(x,y)$ is the space of changes of variables x and y.

If $\Omega(x,y) = X \times Y$ (X is the certain bounded set of variables x, Y is the bounded set of y), then a solution to (91) can be given in the following form:

$$\omega_N(x,y) = \sum_{i=1}^{N} u_i(x)\, v_i(y), \tag{92}$$

where functions $u_i(x)$ and $v_i(y)$ are defined by the following system of equations:

$$\begin{gathered}\int_X (T\omega_N - g)\, u_1(x)\, dx = 0,\\ \vdots\\ \int_X (T\omega_N - g)\, u_N(x)\, dx = 0,\\ \int_Y (T\omega_N - g)\, v_1(y)\, dy = 0,\\ \vdots\\ \int_Y (T\omega_N - g)\, v_N(y)\, dy = 0.\end{gathered} \tag{93}$$

It is found in the following way: we have a certain system composed of N functions regarding one variable, for instance, $u_1^0(x), u_2^0(x), \ldots, u_N^0(x)$, and then from the first N equations of system (93) the system of N functions $v_1^1(x), v_2^1(x), \ldots, v_N^1(x)$ is defined. Then, the so far obtained functions represent a new choice of the functions regarding the variable x – $u_1^2(x), u_2^2(x), \ldots, u_N^2(x)$, and the latter serves to get a new set of functions regarding variable y – $v_1^3(x), v_2^3(x), \ldots, v_N^3(x)$, and so forth.

Definition 9. We say that a process of computation, when one given system of functions is replaced by the second system, is the MVI step. The number of steps needed to define a certain choice of functions corresponds to the superscript (number) of functions being considered. Truncating the process of finding functions $u_i(x)$ and $v_i(y)$ on the kth step, which, for example, corresponds to the choice of functions $v_1^k(y), v_2^k(y), \ldots, v_N^k(y)$, we define the function

$$\omega_N^k = \sum_{i=1}^{N} u_i^{k-1}(x)\, v_i^k(y), \tag{94}$$

taken as the approximating solution of (91) obtained by MVI.

Remark 10. Here and further on, we shall take as operator T a certain differential operator defined on set $D(T)$ of the Hilbert space $L_2(\Omega)$. Then, on each step system (93) shall be transformed to a system of ODEs which can be solved further.

Remark 11. We call function $\omega_N(x,y)$ the Nth approximation to (91) if the number of series terms in (92) is equal to N.

Let us study the case of first approximation; that is, the following solution of (91) is sought:

$$\omega_1(x,y) = u(x)\, v(y), \tag{95}$$

where functions $u(x)$ and $v(y)$ are defined through the illustrated way from the following system of equations:

$$\begin{gathered}\int_X (Tu(x)\cdot v(y) - g)\, u(x)\, dx = 0,\\ \int_Y (Tu(x)\cdot v(y) - g)\, u(y)\, dy = 0.\end{gathered} \tag{96}$$

Let the operator T in (91) be positive definite. Let us introduce the following notation: $H_T(X \times Y)$ is the energy space of the operator T; $[\cdot,\cdot]$ is the scalar product of elements in H_T; ω_0 is the exact solution to (91).

Theorem 12. *If T is a positive definite operator with the space of action $D(T) \subset H_T$, then the sequence of elements $\alpha_k = \|\omega_1^k(x,y) - \omega_0\|_{H_T}$ is monotonously decreasing; that is, for arbitrary i and j if $i \geq j$, then*

$$\left\|\omega_1^i - \omega_0\right\|_{H_T} \leq \left\|\omega_1^j - \omega_0\right\|_{H_T}. \tag{97}$$

Proof. We consider a subset M_1^1 of the space H_T which has the following form:

$$\begin{aligned} M_1^1 = \{&\omega(x,y) \mid \omega(x,y) = u^0(x)\,v(y), \\ &u^0(x) \in H_T(x), v(y) \in H_T(Y)\}. \end{aligned} \tag{98}$$

It is clear, that set M_1^1 represents a subspace of space $H_T(X \times Y)$ (generally, of infinite dimension). Therefore, one may define ω_0 projection onto space M_1^1. As it is known that element $u^0(x)v^*(y) \in M_1^1$ stands for the projection of ω_0 onto M_1^1 if the following condition is satisfied:

$$\left[u^0(x)\,v^*(y) - \omega_0, u^0(x)\,v(y)\right]_{H_T} = 0 \tag{99}$$

for arbitrary elements $u_0(x)v(y) \in M_1^1$. It is clear that if $u^0(x)v^*(y) \in M_1^1$, then (99) coincides with the first equation of system (97).

Since the element $u^0(x)v^1(y)$ obtained through the first step of MVI is a projection of element ω_0 onto the subspace M_1^1, hence the following inequality holds:

$$\left\|\omega_1^1(x,y) - \omega_0\right\|_{H_T} \leq \left\|u^0(x)\,v(y) - \omega_0\right\|_{H_T} \tag{100}$$

for arbitrary elements $u^0(x)v(y) \in M_1^1$. An analogous construction allows us to get a similar inequality for the subspaces; that is, we have

$$\begin{aligned} M_2^1 = \{&\omega(x,y) \mid \omega(x,y) = u^0(x)\,v^1(y), \\ &u(x) \in H_T(x), v^1(y) \in H_T(Y)\}. \end{aligned} \tag{101}$$

In the case corresponding to the second MVI step,

$$\left\|u^2(x)\,v^1(y) - \omega_0\right\|_{H_T} \leq \left\|u(x)\,v^1(y) - \omega_0\right\|_{H_T} \tag{102}$$

for arbitrary elements $u(x)v^1(y) \in M_2^1$. It follows from (100) and (102) that $\|u^2(x)v^1(y) - \omega_0\|_{H_T} \leq \|u^0(x)v^1(y) - \omega_0\|_{H_T}$. Considerations similar to those so far provided and obtained for the kth MVI step prove the theorem as well as inequality (97) with the help of induction. □

Remark 13. Results of Theorem 12 are extended into the case of Nth approximation, and therefore inequality (97) is given in the following form:

$$\|\omega_N^n(x,y) - \omega_0\|_{H_T} \leq \|\omega_N^n(x,y) - \omega_0\|_{H_T}, \quad m \geq n. \tag{103}$$

In order to prove the theorem we introduce the following lemma.

Lemma 14. *Let each of elements of the basis system of space H_T have the following form:*

$$\theta_i(x,y) = \varphi_i(x)\,\psi_i(y), \quad \forall^i \varphi_i(x) \in H_T(X), \ \varphi_i(y) \in H_T(Y). \tag{104}$$

If for the initial MVI approximation one takes any component of a certain basis function θ_i, that is, $u^0(x) \equiv \varphi_i(x)$, then for an arbitrary number k of the MVI steps the following inequality holds:

$$\left\|\omega_1^k(x,y) - \omega_0\right\|_{H_T} \leq \left\|c\varphi_i(x)\,\psi_i(y) - \omega_0\right\|_{H_T}, \tag{105}$$

where c is the arbitrarily taken real number.

Proof. Since $u^0(x)v^1(y) \equiv \varphi_i(x)v^1(y)$, then Theorem 12 yields

$$\begin{aligned} \left\|\omega_1^k(x,y) - \omega_0\right\|_{H_T} &\leq \left\|\varphi_i(x)\,v^1(y) - \omega_0\right\|_{H_T} \\ &\leq \left\|c\varphi_i(x)\,\psi_i(y) - \omega_0\right\|_{H_T}. \end{aligned} \tag{106}$$

On the basis of the given lemma we formulate one of the MVI convergence criterions. Initially, we identify space H_T with space $\overset{0}{W}{}_2^m(\Omega)$ which is generated through a closure regarding the norm

$$\|\omega\|_{W_2^m} = \left\{\int_\Omega \sum_{k=0}^{m} \sum_{(k)} \left|\frac{\partial^k \omega}{\partial^{k_1} x \partial^{k_2} y}\right| dx\,dy\right\}^2 \tag{107}$$

of a set of infinitely differentiable functions $\overset{0}{C}{}^\infty(\Omega)$ with a compact carrier in Ω. □

Theorem 15. *Let each of elements of the basis system of space $\overset{0}{W}{}_2^m(X \times Y)$ have the following form:*

$$\theta_i(x,y) = \varphi_i(x)\,\psi_i(y), \tag{108}$$

where $\{\varphi_i(x)\}$ stands for the basis system in space $\overset{0}{W}{}_2^m(X)$ and $\{\psi_i(y)\}$ in space $\overset{0}{W}{}_2^m(Y)$, and in order to get an arbitrary Nth order approximation of the MVI we take components of the elements of the basis system $\{\theta_i(x,y)\}$ as the initial functions. Then, for sufficiently large N the MVI gives a unique approximate solution ω_N, and the sequence $\{\omega_N\}$ is convergent with respect to the norm of space $\overset{0}{W}{}_2^m(X \times Y)$ to the exact solution ω_0 irrespectively of the number of steps k. This construction can be carried out for each Nth approximation; that is,

$$\left\|\omega_N^k - \omega_0\right\|_{\overset{0}{W}{}_2^m} \longrightarrow 0, \quad N \longrightarrow \infty. \tag{109}$$

Proof. If we prove the theorem regarding approximations obtained via the first step of MVI, then owing to the Lemma the obtained results shall be valid for the arbitrary kth step. Therefore, let us consider the Nth approximation of problem (91), obtained on the first step. In a way similar to considerations regarding Theorem 12, one may show that each ω_N^1 stands for a projection of element ω_0 onto the following subspace:

$$M_N^1 = \left\{ \omega(x,y) \mid \omega(x,y) = \sum_{i=1}^{N} u^0(x)\, v^1(y) \right\}, \qquad (110)$$

where $u_i^0(x)$ denotes N the fixed elements from system $\{\varphi_i(x)\}$, and for arbitrary i and $v_i(y)$ they cover the whole space $\overset{0}{W}{}_2^m(Y)$. Therefore, $\omega_N^1 = P_N\omega_0$, where P_N stands for the operator of an orthogonal projection onto subspace M_N^1 which is bounded. Since elements of the basis system $\theta_i(x,y)$ have form (108), it is limiting dense ([20], page 191) in $\overset{0}{W}{}_2^m(X\times Y)$. Then the proof is carried out in a way similar to that of Theorem 16.2 (see [20], page 216), since all conditions of its application are satisfied. □

Remark 16. Results of Theorem 12 and the Lemma indicate that using the MVI one may get an approximate solution to (91) in a way not worse than that obtained via the Ritz method in accordance with the corresponding subspace.

The MVI can be extended also on the case of a large number of variables. For instance, a sought solution to (91) is the function of three variables x, y, z, and hence the approximate solution of MVI can be sought in the following form:

$$\omega(x,y,z) = u(x)\, v(y,z). \qquad (111)$$

Remark 17. Note that during application of the MVI there is no need to construct the initial condition, satisfying, say, boundary conditions of the stated problem. Let us assume that operator T defines a certain boundary value problem. Let us introduce an arbitrary function from a space of the definition of the differential operator of the studied problem. Then on the first (second) step we get a system of functions satisfying boundary conditions regarding one (two) of the variables.

Observe that the MVI, on each step, defines only one of the functions appearing in the representation of solution (108). The following method develops MVI and allows us, using only a first step, to estimate at once two functions regarding two directions of the coordinates.

4.2. Numerical Results. Let us consider the following rectangular plate

$$\Delta^2\omega = \frac{g(x,y)}{D}, \qquad (112)$$

where $\omega(x,y)$ is the normal plate deflection in point x, y; $g(x,y)$ is the intensity of the normal load; $D = Eh^3[12(1-\nu^2)]^{-1}$; E, ν are the Young modulus and Poisson constant, respectively; $2h$ is the plate thickness, $\overline{y} = 0; 1, \overline{x} = 0; 1$, where $\overline{y} = y/b$, $\overline{x} = x/a$; a and b are the plate dimensions; and $\overline{g}(x,y) = ga^2b^2[Eh^4]^{-1}$. Plate space in the plane x, y is denoted by Ω, and its contour is Γ. Below, we study two types of boundary conditions.

Table 1: Solution methods.

Reduction to the Poisson-type equation (MVI)	Bubnov's method	Solution in series
0.004054	0.00416	0.00406

In the case of a simple support $w = \partial^2 w/\partial n^2|_\Gamma = 0$, a solution obtained via variational iterations is compared with that obtained through the first order approximation of the Bubnov method and with the solution represented by double trigonometric series. The following deflection function has been assumed: $W(x,y) = A\sin(\pi x)\sin(\pi y)$, which satisfies the boundary conditions. Substituting this into (112) and applying the Bubnov procedure we obtain $A = (4/\pi^6)q$, and for $q = 1$ we have $A = 0.00416$. The deflection function $w(x,y) = \sum_{m,n} A_{m,n}\sin(m\pi x/a)\sin(n\pi y/b)$ is substituted into (20) then multiplied by $\sin(m\pi x/a)$, $\sin(n\pi y/b)$, and integrated regarding the plate surface. The following deflection value is obtained:

$$\begin{aligned} w(x,y) &= \frac{q}{24D}\left(x^4 - 2ax^3 + a^3x\right) \\ &\quad - \frac{4qa^4}{\pi^5 D}\sin\frac{m\pi x}{a} \\ &\quad \times \sum_{m,n}\frac{1}{m^5}\left[\frac{a_m th(\alpha_m)+2}{2ch(\alpha_m)} ch\left(\frac{2\alpha_m y}{b}\right)\right. \\ &\qquad\left. - \frac{\alpha_m}{2ch(\alpha_m)}\frac{2y}{b} sh\left(\frac{2\alpha_m y}{b}\right)\right]. \end{aligned} \qquad (113)$$

It should be emphasized that the obtained series converges fast, and in practice it is sufficient to keep only its first term. For the square plate, the deflection measured in its center is 0.00406 (Table 1).

In the second case the plate contours are clamped; that is, $w = (\partial w/\partial n)|_\Gamma = 0$. Here computations are carried out in the first approximation, where owing to Remark 16, we take $\sin(\pi x)$ as the input function; that is, this function does not satisfy damping conditions on the plate's contour. A solution to the obtained ODEs was carried out via the difference method (FDM) with the plate partition 60×60 and successive solution to the obtained algebraic equations by the Gauss method.

Results of the quarter plate deflection function obtained on the line $\overline{y} = 0.5$ are given in Table 2. These results coincide with the conclusion of Theorem 12 regarding monotonous series $\{a_k\}$ behavior. The exact value of deflection equal to 0.0138 is taken from monograph [20].

5. Numerical Study of the Karman Equations

5.1. Iterative Procedure of Linearization and Variational Iteration for System (6). A simultaneous use of the iterative procedure is described in Section 3 and the method of

Table 2: Deflection of the plate quarter.

Step	$\overline{y}=0.5,\ \overline{x}=0.1$	$\overline{y}=0.5,\ \overline{x}=0.3$	$\overline{y}=0.5,\ \overline{x}=0.5$
1	$0.55543336\cdot 10^{-3}$	$0.19404364\cdot 10^{-2}$	$0.22896260\cdot 10^{-2}$
2	$0.16923198\cdot 10^{-2}$	$0.79178517\cdot 10^{-2}$	$0.10638649\cdot 10^{-1}$
3	$0.21179814\cdot 10^{-2}$	$0.10124784\cdot 10^{-1}$	$0.13723563\cdot 10^{-1}$
4	$0.21349905\cdot 10^{-2}$	$0.102096\cdot 10^{-1}$	$0.13840985\cdot 10^{-1}$
5	$0.21349905\cdot 10^{-2}$	$0.10211107\cdot 10^{-1}$	$0.13842917\cdot 10^{-1}$
6	$0.21352879\cdot 10^{-2}$	$0.10211157\cdot 10^{-1}$	$0.13843016\cdot 10^{-1}$

variational iterations of system (6) allows us to carry out three remarkable procedures:

(1) decrease of the order of the system twice (from the 8th to 4th order);

(2) linearization of the sought nonlinear systems;

(3) transition from PDEs to ODEs with constant coefficients.

This result is particularly important in the analysis of elliptic type PDEs.

Next, we present numerical results of our method using an example of the computation of flexible isotropic square plates of constant thickness for three types of boundary conditions (114)–(116).

Consider the following:

$$w=\frac{\partial^2 w}{\partial n^2}=F=\frac{\partial^2 F}{\partial n^2}=0,\quad x=y=0,\quad x=y=1, \tag{114}$$

$$w=\frac{\partial^2 w}{\partial n^2}=F=\frac{\partial F}{\partial n}=0;\quad x=y=0;\quad x=y=1, \tag{115}$$

$$w=\frac{\partial w}{\partial n}=F=\frac{\partial F}{\partial n}=0;\quad x=y=0;\quad x=y=1. \tag{116}$$

For simplicity, we apply the MVI using its first approximation $N=1$. ODEs are reduced to AE (algebraic equations) through FDM with approximation $0(h^2)$, which is solved using the Gauss method. The interval of integration [0, 1] was divided into 100 parts. Relation $q[w(0.5,0.5)]$ is illustrated in Figure 2. Curves (1), (2), and (3) refer to boundary conditions (114), (115), and (116), respectively. Curves (2) and (3) are obtained for the Poisson coefficient $\nu=0.33$ and curve (1) for $\nu=0.1$. Circles refer to experimental results [21]; stars refer to the solution obtained by FDM [22], where FDM was applied directly to (2) and nonlinear AEs was solved by Newton's method. Plane mesh step is 20×20. Computations were carried out with step $\Delta q=10$, where in order to accelerate convergence of the iterative procedure, w and F were taken from the previous step.

Dependence of the deflection change in the plate center on the number of iterations is shown in Figure 3 (curve (1)). Boundary conditions correspond to the plate support on flexible noncompressed ribs (114). The remaining parameters are $N=20$, $q=60$, $\nu=0.28$, and $\varepsilon=10^{-3}$. We require 16 iterations to achieve a priori given accuracy.

One may see from Figure 3 that the deflection oscillates in the vicinity of a certain averaged value, and it tends to it with an increase of the iteration number. It can be explained in the following way. Since the initial approximation is given by the linear equations, the observed deflection shall be larger than a real one. Substitution of w into the second equation of system (6) shows that the stress function value is also larger than a real one. Therefore, taking into account the obtained values of the stress function F, the deflection estimated through the

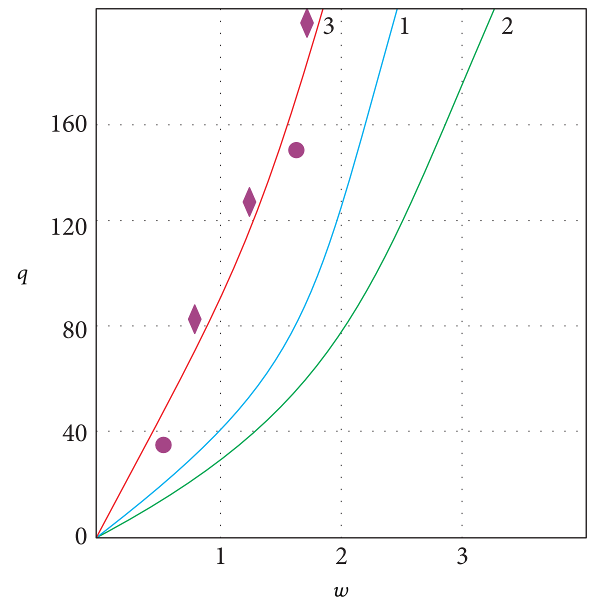

Figure 2: q versus w.

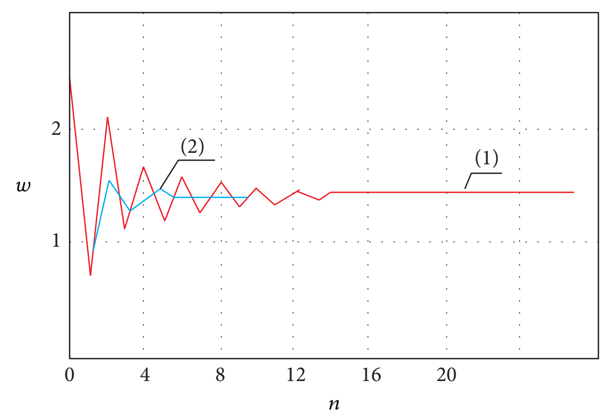

Figure 3: w versus n.

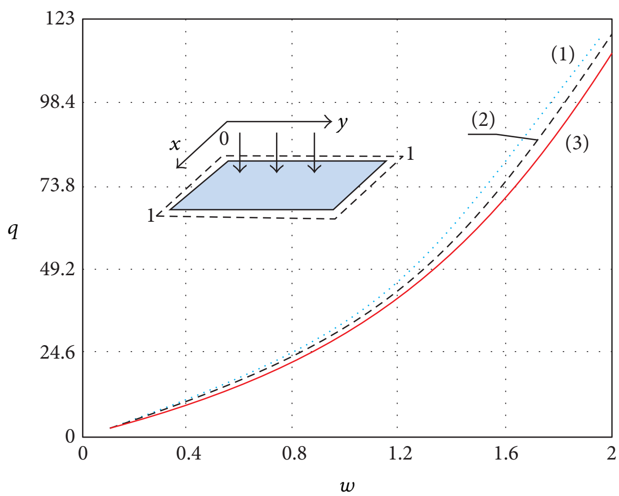

Figure 4: Load deflection function.

first equation of system (6) is lesser than the real one. In other words, the deflection obtained via odd (even) iteration is lesser (larger) than the real one, and it can be estimated by the following formula:

$$w = \frac{w_{\text{odd}} + w_{\text{even}}}{2}. \tag{117}$$

Formula (117) allowed us to reduce the number of iterations up to seven (see Figure 3, curve (2)). However, an increase of the load implies the convergence decrease.

5.2. Iterative Linearization Procedure (Poisson-Type Equations). In order to solve system (89) we used the MVI and FDM. Results of a comparison of solutions for systems (6) and (89), using the MVI and FDM applied to system (2) in the case of a square plate, are shown in Figure 4. One may see that the result obtained by the application of procedure (6)—curve (2)—and (89)—curve (3)—differs slightly from the result obtained via the FDM—(1). Furthermore, a comparison of the results obtained through iterative procedures (6) (dot curve) and (89) (dashed curve) shows that the compared results for small deflection practically coincide.

The use of formula (117), in order to increase the convergence, implies that the function "load-deflection" practically remains unaffected, but the number of iterations increases. Figure 5 shows results regarding the procedure (89): (i) without the application of (117)—curve (1)—and (ii) with the application of formula (117)—curve (2). One may observe that the iterative process converges twice as fast.

6. Summary

In this work we have proposed and theoretically established (theorems with proofs) some iterative procedures dedicated to a decrease of the order and then linearization of the Karman nonlinear PDEs. It has been shown that the result obtained via the modified Kantorovich-Vlasov method coincides with the exact solution. Furthermore, the theoretical

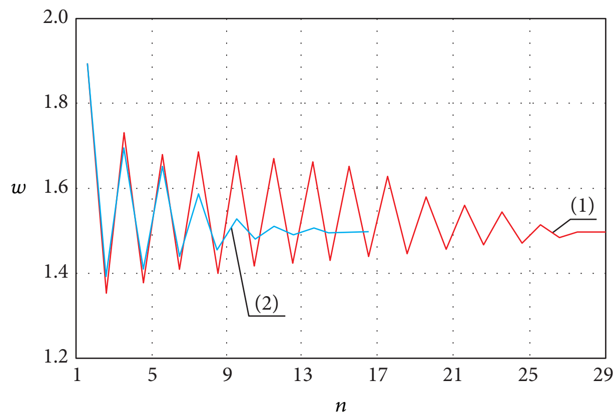

Figure 5: Plate deflection versus number of iterations.

considerations have been supported by the numerical analysis of the Karman equations using two introduced iterative procedures.

Conflict of Interests

The authors declare that there is no conflict of interests regarding the publication of this paper.

Acknowledgment

This work has been partially supported by the National Science Foundation of Poland under Grant MAESTRO2 no. 2012/04/A/ST8/00738 for years 2010–2016.

References

[1] L. V. Kantorovich and V. I. Krylov, *Approximate Methods of Higher Analysis*, Interscience Publishers, New York, NY, USA, 1958.

[2] R. E. Bellman and R. E. Kalaba, *Quasi Linearization and Nonlinear Boundary-Value Problems*, Elsevier, New York, NY, USA, 1965.

[3] S. Agmon, A. Douglis, and L. Nirenberg, "Estimates near the boundary for solutions of elliptic partial differential equations satisfying general boundary conditions II," *Communications on Pure and Applied Mathematics*, vol. 17, pp. 35–92, 1964.

[4] S. Agmon, A. Douglis, and L. Nirenberg, "Estimates near the boundary for solutions of elliptic partial differential equations satisfying general boundary conditions I," *Communications on Pure and Applied Mathematics*, vol. 12, pp. 623–727, 1959.

[5] G. J. Fix and E. Stephan, "On the finite element-least squares approximation to higher order elliptic systems," *Archive for Rational Mechanics and Analysis*, vol. 91, no. 2, pp. 137–151, 1986.

[6] P. B. Bochev and M. D. Gunzburger, "Accuracy of least-squares methods for the Navier-Stokes equations," *Computers and Fluids*, vol. 22, no. 4-5, pp. 549–563, 1993.

[7] P. B. Bochev and M. D. Gunzburger, *Least-Squares Finite Element Methods*, Springer, New York, NY, USA, 2009.

[8] M. Costabel and M. Dauge, "Construction of corner singularities for Agmon-Douglis-Nirenberg elliptic systems," *Mathematische Nachrichten*, vol. 162, pp. 209–237, 1993.

[9] K. Washizu, *Variational Methods in Elasticity and Plasticity*, Pergamon Press, Oxford, UK, 1974.

[10] D. K. Bazaj and J. H. Kissel, "Use of polar finite-difference approximation for solving bi-harmonic equation for plates," *International Journal of Mechanical Sciences*, vol. 12, no. 1, pp. 51–60, 1970.

[11] O. L. Bowie, "Application of partitioning to problem-solving in elasticity," in *Proceedings of the International Conference on Fracture Mechanics and Technology*, pp. 1109–1126, Hong Kong, 1977.

[12] M. Stippes and D. Shadman, "Traction problems in plane elasticity," *SIAM Journal on Applied Mathematics* , vol. 15, pp. 1130–1135, 1975.

[13] P. G. Ciarlet, *The Finite Element Method for Elliptic Problems*, North-Holland, Amsterdam, The Netherlands, 1978.

[14] C. A. J. Fletcher, *Computational Galerkin Methods*, Springer, New York, NY, USA, 1984.

[15] A. S. Volmir, *The Nonlinear Dynamics of Plates and Shells*, Nauka, Moscow, Russia, 1972, Russian.

[16] M. S. Kornishin, *Nonlinear Problems of Plate and Shallow Shell Theory and Methods of Solution*, Nauka, Moscow, Russia, 1964, Russian.

[17] I. I. Vorovich, "On the existence of solutions in the nonlinear theory of shells," *News Academy of Sciences USSR*, vol. 19, pp. 173–186, 1955.

[18] P. E. Gill, W. Murray, and M. H. Wright, *Practical Optimization*, Academic Press, London, UK, 1981.

[19] J. L. Lions, *Methods of Nonlinear Boundary Problems Solving*, Dunod and Gauthier-Villars, Paris, France, 1969, French.

[20] L. V. Kantorovich and V. I. Krylov, *Approximate Methods of Higher Analysis*, Interscience, New York, NY, USA, 1958.

[21] W. Ramberg, A. E. Pherson, and S. Levy, *Normal-Pressure Tests of Rectangular Plates*, NACAT, 1942.

[22] V. A. Krysko, *Nonlinear Statics and Dynamics of Non-Homogeneous Shells*, Saratov University Press, Saratov, Russia, 1976, Russian.

Hindawi Publishing Corporation
The Scientific World Journal
Volume 2014, Article ID 563084, 4 pages
http://dx.doi.org/10.1155/2014/563084

Research Article

An Osgood Type Regularity Criterion for the 3D Boussinesq Equations

Qiang Wu,[1,2] Lin Hu,[2] and Guili Liu[3]

[1] *School of Resources and Safety Engineering, Central South University, Changsha, Hunan 410075, China*
[2] *Jiangxi University of Science and Technology, Ganzhou, Jiangxi 341000, China*
[3] *Department of Basic Teaching, Harbin Finance University, Harbin 150030, Heilongjiang, China*

Correspondence should be addressed to Guili Liu; guili2005_liu@126.com

Received 2 November 2013; Accepted 2 February 2014; Published 11 March 2014

Academic Editors: D. Baleanu and H. Jafari

We consider the three-dimensional Boussinesq equations, and obtain an Osgood type regularity criterion in terms of the velocity gradient.

1. Introduction

In this paper, we consider the following three-dimensional (3D) Boussinesq equations with the incompressibility condition:

$$\begin{gathered} \mathbf{u}_t + (\mathbf{u}\cdot\nabla)\,\mathbf{u} - \Delta\mathbf{u} + \nabla\pi = \theta\mathbf{e}_3, \\ \theta_t + (\mathbf{u}\cdot\nabla)\,\theta - \Delta\theta = 0, \\ \nabla\cdot\mathbf{u} = 0, \\ \mathbf{u}(x,0) = \mathbf{u}_0, \quad \theta(x,0) = \theta_0, \end{gathered} \tag{1}$$

where $\mathbf{u} = (u_1(x,t), u_2(x,t), u_3(x,t))$ is the fluid velocity, $\pi = \pi(x,t)$ is a scalar pressure, and $\theta = \theta(x,t)$ is the scalar temperature, while $\mathbf{u}_0$ and θ_0 are the prescribed initial velocity and temperature, respectively, with $\nabla\cdot\mathbf{u}_0 = 0$.

In case $\theta = 0$, (1) reduces to the incompressible Navier-Stokes equations. The regularity of its weak solutions and the existence of global strong solutions are important open problems; see [1–3]. Starting with [4, 5], there have been a lot of literatures devoted to finding sufficient conditions (which now are called regularity criteria) to ensure the smoothness of the solutions; see [6–16] and so forth. Since the convective terms $(\mathbf{u}\cdot\nabla)\mathbf{u}$ are the same in the Navier-Stokes equations and Boussinesq equations, the authors also consider the regularity conditions for (1). In particular, Qiu et al. [17] obtained Serrin type regularity condition:

$$\mathbf{u} \in L^p\left(0,T;L^q\left(\mathbb{R}^3\right)\right), \qquad \frac{2}{p}+\frac{3}{q}=1, \quad 3<q\leqslant\infty. \tag{2}$$

The extension to the multiplier spaces was established by the same authors in [18]. For the Besov-type regularity criterion, Fan and Zhou [19] and Ishimura and Morimoto [20] showed the following regularity conditions:

$$\begin{gathered} \nabla\times\mathbf{u} \in L^1\left(0,T;\dot{B}^0_{\infty,\infty}\left(\mathbb{R}^3\right)\right), \\ \nabla\mathbf{u} \in L^1\left(0,T;L^\infty\left(\mathbb{R}^3\right)\right). \end{gathered} \tag{3}$$

Zhang [21, 22] then considers the regularity criterion in terms of the pressure or its gradient. The readers are also referred to [23] for generalized models.

Motivated by [24–26], we will improve (3) as in the following.

Theorem 1. *Let $(\mathbf{u}_0,\theta_0) \in H^1(\mathbb{R}^3)$. Assume that $(\mathbf{u},\theta)$ is the smooth solution to (1) with the initial data $(\mathbf{u}_0,\theta_0)$ for $0 \leqslant t < T$. If*

$$\sup_{2\leqslant q<\infty}\int_0^T \frac{\left\|\overline{S}_q\nabla\mathbf{u}\right\|_{L^\infty}}{q\ln q} < \infty, \tag{4}$$

then the solution $(\mathbf{u},\theta)$ *can be extended after time* $t = T$. *Here,* $\dot{\Delta}_k$ *denotes the Fourier localization operator and* $\Delta S_q = \sum_{l=-q}^{q} \dot{\Delta}_l$.

Remark 2. The Osgood type condition (4) is weaker than (3). Notice that, for $q \in [2,\infty)$, we have

$$\frac{\|\overline{S}_q \nabla \mathbf{u}\|_{L^\infty}}{q\ln q} \leqslant \frac{1}{q\ln q}\sum_{l=-q}^{q}\left\|\dot{\Delta}_l(\nabla\times\mathbf{u})\right\|_{L^\infty} \leqslant C\|\nabla\times\mathbf{u}\|_{\dot{B}^0_{\infty,\infty}}. \quad (5)$$

The rest of this paper is organized as follows. In Section 2, we recall the definition of Besov spaces and some interpolation inequalities. Section 3 is devoted to proving Theorem 1.

2. Preliminaries

Let $\mathcal{S}(\mathbb{R}^3)$ be the Schwartz class of rapidly decreasing functions. For $f \in \mathcal{S}(\mathbb{R}^3)$, its Fourier transform $\mathcal{F}f = \widehat{f}$ is defined by

$$\widehat{f}(\xi) = \int_{\mathbb{R}^3} f(x)\, e^{-ix\cdot\xi} dx. \quad (6)$$

Let us choose a nonnegative radial function $\varphi \in \mathcal{S}(\mathbb{R}^3)$ such that

$$0 \leqslant \widehat{\varphi}(\xi) \leqslant 1, \qquad \widehat{\varphi}(\xi) = \begin{cases} 1, & \text{if } |\xi| \leqslant 1, \\ 0, & \text{if } |\xi| \geqslant 2, \end{cases} \quad (7)$$

and let

$$\psi(x) = \varphi(x) - 2^{-3}\varphi\left(\frac{x}{2}\right),$$
$$\varphi_j(x) = 2^{3j}\varphi\left(2^j x\right), \qquad \psi_j(x) = 2^{3j}\psi\left(2^j x\right), \qquad j \in \mathbb{Z}. \quad (8)$$

For $j \in \mathbb{Z}$, the Littlewood-Paley projection operators S_j and $\dot{\Delta}_j$ are, respectively, defined by

$$S_j f = \varphi_j * f, \qquad \dot{\Delta}_j f = \psi_j * f. \quad (9)$$

Observe that $\dot{\Delta}_j = S_j - S_{j-1}$. Also, it is easy to check that if $f \in L^2(\mathbb{R}^3)$, then

$$S_j f \longrightarrow 0, \quad \text{as } j \longrightarrow -\infty; \qquad S_j f \longrightarrow f, \quad \text{as } j \longrightarrow +\infty, \quad (10)$$

in the L^2 sense. By telescoping the series, we thus have the following Littlewood-Paley decomposition:

$$f = \sum_{j=-\infty}^{+\infty} \dot{\Delta}_j f, \quad (11)$$

for all $f \in L^2(\mathbb{R}^3)$, where the summation is the L^2 sense. Notice that

$$\dot{\Delta}_j f = \sum_{l=j-2}^{j+2} \dot{\Delta}_l \dot{\Delta}_j f = \sum_{l=j-2}^{j+2} \psi_l * \psi_j * f; \quad (12)$$

then from Young's inequality, it readily follows that

$$\left\|\dot{\Delta}_j f\right\|_{L^q} \leqslant C 2^{3j(1/p-1/q)}\left\|\dot{\Delta}_j f\right\|_{L^p}, \quad (13)$$

where $1 \leqslant p \leqslant q \leqslant \infty$ and C is an absolute constant independent of f and j.

Let $-\infty < s < \infty$, $1 \leqslant p, q \leqslant \infty$; the homogeneous Besov space $\dot{B}^s_{p,q}$ is defined by the full-dyadic decomposition such that

$$\dot{B}^s_{p,q} = \left\{ f \in \mathcal{Z}'\left(\mathbb{R}^3\right); \|f\|_{\dot{B}^s_{p,q}} < \infty \right\}, \quad (14)$$

where

$$\|f\|_{\dot{B}^s_{p,q}} = \left\| \left\{ 2^{js}\left\|\dot{\Delta}_j f\right\|_{L^p} \right\}_{j=-\infty}^{+\infty} \right\|_{\ell^q}, \quad (15)$$

and $\mathcal{Z}'(\mathbb{R}^3)$ is the dual space of

$$\mathcal{Z}\left(\mathbb{R}^3\right) = \left\{ f \in \mathcal{S}\left(\mathbb{R}^3\right);\ D^\alpha \widehat{f}(0) = 0,\ \forall \alpha \in \mathbb{N}^3 \right\}. \quad (16)$$

Also, it is well known that

$$\dot{H}^s\left(\mathbb{R}^3\right) = \dot{B}^s_{2,2}\left(\mathbb{R}^3\right), \quad \forall s \in \mathbb{R}. \quad (17)$$

We refer to [27] for more detailed properties.

3. Proof of Theorem 1

This section is devoted to proving Theorem 1. From standard continuity arguments, we need to only provide the uniform H^1 bounds of the solution $(\mathbf{u},\theta)$.

Taking the inner products of $(1)_1$ with $-\Delta\mathbf{u}$, $(1)_2$ with $-\Delta\theta$, we obtain by adding together that

$$\begin{aligned} &\frac{1}{2}\frac{d}{dt}\|\nabla(\mathbf{u},\theta)\|_{L^2}^2 + \|\Delta(\mathbf{u},\theta)\|_{L^2}^2 \\ &\quad = \int_{\mathbb{R}^3} [(\mathbf{u}\cdot\nabla)\mathbf{u}]\cdot\Delta\mathbf{u}\, dx - \int_{\mathbb{R}^3} \theta\Delta u_3\, \mathrm{d}x \\ &\qquad + \int_{\mathbb{R}^3} [(\mathbf{u}\cdot\nabla)\theta]\cdot\Delta\theta\, \mathrm{d}x \\ &\quad = \int_{\mathbb{R}^3} \partial_k\theta\partial_k u_3\, \mathrm{d}x \\ &\qquad - \int_{\mathbb{R}^3} \partial_k u_j\left(\partial_j u_i \partial_k u_i + \partial_j\theta\partial_k\theta\right) \mathrm{d}x \\ &\quad \equiv I + J. \end{aligned} \quad (18)$$

For I, we use Hölder's inequality to get

$$I_1 \leqslant \frac{1}{2}\|\nabla(\mathbf{u},\theta)\|_{L^2}^2. \quad (19)$$

For J, applying the Littilewood-Paley decomposition as in (11), we get

$$\nabla\mathbf{u} = \sum_{l<-q} \dot{\Delta}\nabla\mathbf{u} + \sum_{l=-q}^{q} \dot{\Delta}\nabla\mathbf{u} + \sum_{l>q} \dot{\Delta}\nabla\mathbf{u}, \quad (20)$$

where q is positive integral to be determined later on. Plugging (20) into J, we see that

$$\begin{aligned} J &\leqslant \sum_{l<-q} \int_{\mathbb{R}^3} \left|\dot{\Delta}_l \nabla \mathbf{u}\right| \cdot |\nabla (\mathbf{u},\theta)|^2 \, \mathrm{d}x \\ &\quad + \int_{\mathbb{R}^3} \left|\sum_{l=-q}^{q} \dot{\Delta}_l \nabla \mathbf{u}\right| \cdot |\nabla (\mathbf{u},\theta)|^2 \, \mathrm{d}x \\ &\quad + \sum_{l>q} \int_{\mathbb{R}^3} \left|\dot{\Delta}_l \nabla \mathbf{u}\right| \cdot |\nabla (\mathbf{u},\theta)|^2 \, \mathrm{d}x \\ &\equiv J_1 + J_2 + J_3. \end{aligned} \tag{21}$$

For J_1, we dominate as

$$\begin{aligned} J_1 &\leqslant \sum_{l<-q} \left\|\dot{\Delta}_l \nabla \mathbf{u}\right\|_{L^\infty} \|\nabla (\mathbf{u},\theta)\|_{L^2}^2 \\ &\leqslant C \sum_{l<-q} 2^{3l/2} \left\|\dot{\Delta}_l \nabla \mathbf{u}\right\|_{L^2} \|\nabla (\mathbf{u},\theta)\|_{L^2}^2 \quad (\text{by } (13)) \\ &\leqslant C \left(\sum_{l<-q} 2^{(3l/2)\cdot 2}\right)^{1/2} \cdot \left(\sum_{l<-q} \left\|\dot{\Delta}_l \nabla \mathbf{u}\right\|_{L^2}^2\right)^{1/2} \|\nabla (\mathbf{u},\theta)\|_{L^2}^2 \\ &\leqslant C 2^{-3q/2} \|\nabla \mathbf{u}\|_{L^2} \|\nabla (\mathbf{u},\theta)\|_{L^2}^2 \quad (\text{by } (17)) \\ &= \left[C 2^{-q/2} \|\nabla (\mathbf{u},\theta)\|_{L^2}\right]^3. \end{aligned} \tag{22}$$

For J_2, we have

$$\begin{aligned} J_2 &= \int_{\mathbb{R}^3} \left|\overline{S}_q \nabla \mathbf{u}\right| \cdot |\nabla (\mathbf{u},\theta)|^2 \, \mathrm{d}x \\ &\leqslant \left\|\overline{S}_q \nabla \mathbf{u}\right\|_{L^\infty} \|\nabla (\mathbf{u},\theta)\|_{L^2}^2. \end{aligned} \tag{23}$$

Finally, for J_3, we estimate as

$$\begin{aligned} J_3 &\leqslant \sum_{l>q} \left\|\Delta_l \nabla \mathbf{u}\right\|_{L^3} \|\nabla (\mathbf{u},\theta)\|_{L^3}^2 \\ &\leqslant C \sum_{l>q} 2^{l/2} \left\|\Delta_l \nabla \mathbf{u}\right\|_{L^2} \|\nabla (\mathbf{u},\theta)\|_{L^2} \|\Delta (\mathbf{u},\theta)\|_{L^2} \\ &\quad (\text{by } (13) \text{ and Gagliardo-Nireberg inequality}) \\ &\leqslant C \left(\sum_{l>q} 2^{-(l/2)\cdot 2}\right)^{1/2} \cdot \left(\sum_{l>q} 2^{l\cdot 2} \left\|\dot{\Delta}_l \nabla \mathbf{u}\right\|_{L^2}^2\right)^{1/2} \\ &\quad \times \|\nabla (\mathbf{u},\theta)\|_{L^2} \|\Delta (\mathbf{u},\theta)\|_{L^2} \\ &\leqslant \left[C 2^{-q/2} \|\nabla (\mathbf{u},\theta)\|_{L^2}\right] \|\Delta (\mathbf{u},\theta)\|_{L^2}^2 \quad (\text{by } (17)). \end{aligned} \tag{24}$$

Gathering (22), (23), and (24) together and plugging them into (21), we deduce

$$\begin{aligned} J &\leqslant \left[C 2^{-q/2} \|\nabla (\mathbf{u},\theta)\|_{L^2}\right]^3 \\ &\quad + \left\|\overline{S}_q \nabla \mathbf{u}\right\|_{L^\infty} \|\nabla (\mathbf{u},\theta)\|_{L^2}^2 \\ &\quad + \left[C 2^{-q/2} \|\nabla (\mathbf{u},\theta)\|_{L^2}\right] \|\Delta (\mathbf{u},\theta)\|_{L^2}^2. \end{aligned} \tag{25}$$

Substituting (19) and (25) into (18), we find

$$\begin{aligned} &\frac{1}{2}\frac{d}{dt} \|\nabla (\mathbf{u},\theta)\|_{L^2}^2 + \|\Delta (\mathbf{u},\theta)\|_{L^2}^2 \\ &\quad \leqslant \frac{1}{2} \|\nabla (\mathbf{u},\theta)\|_{L^2}^2 + \left[C 2^{-q/2} \|\nabla (\mathbf{u},\theta)\|_{L^2}\right]^3 \\ &\qquad + \frac{\left\|\overline{S}_q \nabla \mathbf{u}\right\|_{L^\infty}}{q \ln q} \cdot q \ln q \|\nabla (\mathbf{u},\theta)\|_{L^2}^2 \\ &\qquad + \left[C 2^{-q/2} \|\nabla (\mathbf{u},\theta)\|_{L^2}\right] \|\Delta (\mathbf{u},\theta)\|_{L^2}^2. \end{aligned} \tag{26}$$

Taking

$$q = \left[\frac{2}{\ln 2 \ln^+ \left(C \|\nabla (\mathbf{u},\theta)\|_{L^2}\right)}\right] + 1, \tag{27}$$

where $[t]$ is the largest integer smaller than $t \in \mathbb{R}$ and $\ln^+ t = \ln(e+t)$, then (26) implies that

$$\begin{aligned} &\frac{d}{dt} \|\nabla (\mathbf{u},\theta)\|_{L^2}^2 \\ &\quad \leqslant \|\nabla (\mathbf{u},\theta)\|_{L^2}^2 + C \\ &\qquad + \frac{\left\|\overline{S}_q \nabla \mathbf{u}\right\|_{L^\infty}}{q \ln q} \ln^+ \left(\|\nabla (\mathbf{u},\theta)\|_{L^2}\right) \ln^+ \ln^+ \left(\|\nabla (\mathbf{u},\theta)\|_{L^2}\right) \\ &\qquad \times \|\nabla (\mathbf{u},\theta)\|_{L^2}^2. \end{aligned} \tag{28}$$

Applying Gronwall inequality three times, we deduce

$$\begin{aligned} &\|\nabla (\mathbf{u},\theta)\|_{L^2}^2 + \int_0^t \|\Delta (\mathbf{u},\theta)\|_{L^2} \, \mathrm{d}\tau \\ &\quad \leqslant C \exp \exp \exp \left(\int_0^t \frac{\left\|\overline{S}_q \nabla \mathbf{u}\right\|_{L^\infty}}{q \ln q} \, \mathrm{d}\tau\right). \end{aligned} \tag{29}$$

Recalling (4), we see the solution $(\mathbf{u},\theta)$ is uniformly bounded in $L^\infty(0,T;H^1(\mathbb{R}^3))$. This completes the proof of Theorem 1.

Conflict of Interests

The authors declare that there is no conflict of interests regarding the publication of this paper.

Acknowledgments

This work was supported by the NSF of China (no. 11326238, no. 11326138, and no. 11101101), the Science Foundation of Jiangxi Provincial Department of Education (no. GJJ13374 and no. GJJ13658), and the Youth Natural Science Foundation of Jiangxi Province (20132BAB211007).

References

[1] E. Hopf, "Über die Anfangswertaufgabe für die hydrodynamischen Grundgleichungen," *Mathematische Nachrichten*, vol. 4, pp. 213–231, 1951.

[2] P. G. Lemarié-Rieusset, *Recent Developments in the Navier–Stokes Problem*, vol. 431, Chapman & Hall/CRC, Boca Raton, Fla, USA, 2002.

[3] J. Leray, "Sur le mouvement d'un liquide visqueux emplissant l'espace," *Acta Mathematica*, vol. 63, no. 1, pp. 193–248, 1934.

[4] J. Serrin, "On the interior regularity of weak solutions of the Navier–Stokes equations," *Archive for Rational Mechanics and Analysis*, vol. 9, no. 1, pp. 187–195, 1962.

[5] J. Serrin, "The initial value problem for the Navier–Stokes equations," in *Nonlinear Problems*, R. E. Langer, Ed., pp. 69–98, University of Wisconsin Press, Madison, Wis, USA, 1963.

[6] X. W. He and S. Gala, "Regularity criterion for weak solutions to the Navier–Stokes equations in terms of the pressure in the class $L^2(0,T;B^{-1}_{\infty,\infty}(\mathbb{R}^3))$," *Nonlinear Analysis, Real World Applications*, vol. 12, no. 6, pp. 3602–3607, 2011.

[7] J. Neustupa, A. Novotný, and P. Penel, "An interior regularity of a weak solution to the Navier–Stokes equations in dependence on one component of velocity," in *Topics in Mathematical Fluid Mechanics*, vol. 10 of *Quaderni di Matematica*, pp. 163–183, Seconda Università degli Studi di Napoli, Caserta, Italy, 2002.

[8] Z. J. Zhang, "A Serrin-type regularity criterion for the Navier–Stokes equations via one velocity component," *Communications on Pure and Applied Analysis*, vol. 12, no. 1, pp. 117–124, 2013.

[9] Z. J. Zhang, "A remark on the regularity criterion for the 3D Navier–Stokes equations involving the gradient of one velocity component," *Journal of Mathematical Analysis and Applications*, vol. 414, no. 1, pp. 472–479, 2014.

[10] Z. J. Zhang, Z.-A. Yao, P. Li, C. C. Guo, and M. Lu, "Two new regularity criteria for the 3D Navier–Stokes equations via two entries of the velocity gradient," *Acta Applicandae Mathematicae*, vol. 123, no. 1, pp. 43–52, 2013.

[11] Z. J. Zhang, D. X. Zhong, and L. Hu, "A new regularity criterion for the 3D Navier–Stokes equations via two entries of the velocity gradient tensor," *Acta Applicandae Mathematicae*, vol. 129, no. 1, pp. 175–181, 2014.

[12] Z. J. Zhang, Z. A. Yao, M. Lu, and L. D. Ni, "Some Serrin-type regularity criteria for weak solutions to the Navier–Stokes equations," *Journal of Mathematical Physics*, vol. 52, no. 5, Article ID 053103, 2011.

[13] Z. J. Zhang, P. Li, and D. X. Zhong, "Navier–Stokes equations with regularity in two entries of the velocity gradient tensor," *Applied Mathematics and Computation*, vol. 228, pp. 546–551, 2014.

[14] Y. Zhou, "A new regularity criterion for weak solutions to the Navier–Stokes equations," *Journal des Mathematiques Pures et Appliquees*, vol. 84, no. 11, pp. 1496–1514, 2005.

[15] Y. Zhou and M. Pokorný, "On a regularity criterion for the Navier–Stokes equations involving gradient of one velocity component," *Journal of Mathematical Physics*, vol. 50, no. 12, Article ID 123514, 11 pages, 2009.

[16] Y. Zhou and M. Pokorný, "On the regularity of the solutions of the Navier–Stokes equations via one velocity component," *Nonlinearity*, vol. 23, no. 5, pp. 1097–1107, 2010.

[17] H. Qiu, Y. Du, and Z. A. Yao, "Serrin-type blow-up criteria for 3D Boussinesq equations," *Applicable Analysis*, vol. 89, no. 10, pp. 1603–1613, 2010.

[18] H. Qiu, Y. Du, and Z. Yao, "Blow-up criteria for 3D Boussinesq equations in the multiplier space," *Communications in Nonlinear Science and Numerical Simulation*, vol. 16, no. 4, pp. 1820–1824, 2011.

[19] J. S. Fan and Y. Zhou, "A note on regularity criterion for the 3D Boussinesq system with partial viscosity," *Applied Mathematics Letters*, vol. 22, no. 5, pp. 802–805, 2009.

[20] N. Ishimura and H. Morimoto, "Remarks on the blow-up criterion for the 3-D Boussinesq equations," *Mathematical Models and Methods in Applied Sciences*, vol. 9, no. 9, pp. 1323–1332, 1999.

[21] Z. J. Zhang, "A remark on the regularity criterion for the 3D Boussinesq equations via the pressure gradient," *Abstract and Applied Analysis*, vol. 2014, Article ID 510924, 4 pages, 2014.

[22] Z. J. Zhang, "A logarithmically improved regularity criterion for the 3D Boussinesq equations via the pressure," *Acta Aplicandae Mathematicae*, 2013.

[23] B. Mehdinejadiani, H. Jafari, and D. Baleanu, "Derivation of a fractional Boussinesq equation for modelling uncon-fined groundwater," *The European Physical Journal Special Topics*, vol. 222, no. 8, pp. 1805–1812, 2013.

[24] Q. Zhang, "Refined blow-up criterion for the 3D magnetohydrodynamics equations," *Applicable Analysis*, vol. 92, no. 12, pp. 2590–2599, 2013.

[25] Z. J. Zhang and S. Gala, "Osgood type regularity criterion for the 3D Newton-Boussinesq equation," *Electronic Journal of Differential Equations*, vol. 2013, no. 223, pp. 1–6, 2013.

[26] Z. J. Zhang, T. Tang, and L. H. Liu, "An Osgood type regularity criterion for the liquid crystal flows," *Nonlinear Differerntial Equations and Applications*, 2013.

[27] H. Triebel, *Interpolation Theory, Function Spaces, Differential Operators*, vol. 18, North-Holland, Amsterdam, The Netherlands, 1978.

Hindawi Publishing Corporation
The Scientific World Journal
Volume 2013, Article ID 540705, 6 pages
http://dx.doi.org/10.1155/2013/540705

Research Article

Cotton-Type and Joint Invariants for Linear Elliptic Systems

A. Aslam[1,2] and F. M. Mahomed[1]

[1] *Differential Equations, Continuum Mechanics and Applications, School of Computational and Applied Mathematics, University of the Witwatersrand, Wits 2050, South Africa*
[2] *School of Natural Sciences (SNS), National University of Sciences and Technology, Campus H-12, Islamabad 44000, Pakistan*

Correspondence should be addressed to F. M. Mahomed; fazal.mahomed@wits.ac.za

Received 9 October 2013; Accepted 26 November 2013

Academic Editors: D. Baleanu, H. Jafari, and C. M. Khalique

Cotton-type invariants for a subclass of a system of two linear elliptic equations, obtainable from a complex base linear elliptic equation, are derived both by spliting of the corresponding complex Cotton invariants of the base complex equation and from the Laplace-type invariants of the system of linear hyperbolic equations equivalent to the system of linear elliptic equations via linear complex transformations of the independent variables. It is shown that Cotton-type invariants derived from these two approaches are identical. Furthermore, Cotton-type and joint invariants for a general system of two linear elliptic equations are also obtained from the Laplace-type and joint invariants for a system of two linear hyperbolic equations equivalent to the system of linear elliptic equations by complex changes of the independent variables. Examples are presented to illustrate the results.

1. Introduction

The general scalar linear second order partial differential equation (PDE) in two independent variables (x, y) is of the form

$$aw_{xx} + 2bw_{xy} + cw_{yy} + dw_x + ew_y + fw = g, \tag{1}$$

where a, b, c, d, e, f, and g are given C^2 functions of x and y. All linear PDEs of the form (1) are hyperbolic, elliptic, or parabolic depending on whether $b^2 - ac$ is positive, negative, or zero, respectively, and thus can be simplified to one of the three canonical forms by introducing new coordinates [1]. The general linear second-order PDE (1) was first classified by Lie [2] in terms of its symmetry properties. He obtained seven canonical forms according to their point symmetries and types of equations. Of these, four belonged to the hyperbolic class and three to the parabolic class.

The scalar linear second order elliptic equation in two independent variables in canonical form is

$$u_{xx} + u_{yy} + au_x + bu_y + cu = 0. \tag{2}$$

It is well known that by means of the linear complex transformations [1, 3]

$$x = \frac{1}{2}(t + z), \qquad y = \frac{-i}{2}(t - z), \tag{3}$$

the elliptic equation (2) can be mapped to the linear hyperbolic equation

$$u_{tz} + Au_t + Bu_z + Cu = 0, \tag{4}$$

where

$$A = \frac{1}{4}(a + ib), \qquad B = \frac{1}{4}(a - ib), \qquad C = \frac{1}{4}c. \tag{5}$$

In 1773, Laplace [4] in his fundamental memoir deduced two semi-invariants

$$\begin{aligned} h &= A_t + AB - C, \\ k &= B_Z + AB - C, \end{aligned} \tag{6}$$

for (4), known as the Laplace invariants.

These Laplace invariants (6) can be transformed, by use of the inverse of the transformations (3) as well as after the substitution of (5) into (6) and then splitting the real and imaginary parts, to arrive at the Cotton invariants

$$\mu = a_y - b_x,$$
$$H = a_x + b_y + \frac{1}{2}\left(a^2 + b^2\right) - 2c. \quad (7)$$

These invariants (7) were first derived by Cotton [5]. Laplace and Cotton invariants remain unaltered under linear transformations of the dependent variable which, respectively, map the linear hyperbolic and elliptic equations into themselves. The corresponding invariant quantities for the linear parabolic equations can be found in [6–8]. Ovsiannikov [9] used the Laplace invariants in the group classification of the hyperbolic equation (4) by writing the determining equations for the symmetries of (4) in terms of these invariants. The solution of the equivalence problem for scalar linear (1 + 1) hyperbolic equations and some new invariants are given in [10, 11]. Laplace-type and joint invariants for a system of two linear hyperbolic equations are derived in [12] and Laplace-type invariants for a subclass of a system of two linear hyperbolic equations obtained from a complex linear hyperbolic equation are presented in [13]. The approach of complex symmetry analysis (CSA), was utilized in [14]. This method provides a connection between a complex scalar ordinary differential equation (ODE)/PDE and a system of real ODEs/PDEs by a complex split of the base complex equation into real and imaginary parts. In this work, we derive Cotton-type invariants for a subclass of a system of two linear hyperbolic PDEs. Cotton-type and joint invariants for a general linear system of elliptic equations are also determined. Examples are provided as illustration.

The outline of this note is as follows. In Section 2, Cotton-type invariants are derived for a subsystem of two linear elliptic equations by split of the complex Cotton invariants for the corresponding scalar complex linear elliptic equation. Cotton-type invariants for the same class are also obtained by transforming the Laplace-type invariants for the corresponding system of two linear hyperbolic equations which are equivalent to the system of two linear elliptic equations by means of complex linear transformations of the independent variables. These are shown to be the same. Moreover, Cotton-type and joint invariants for a general linear system of two elliptic equations are derived in Section 3. Then in Section 4 some examples are given to illustrate the results. Finally, in Section 5, a brief conclusion is given.

2. Cotton Invariants for a Subclass

In this section, Cotton-type invariants for a subsystem of two linear elliptic equations are first obtained from a complex scalar linear elliptic equation by splitting the complex Cotton invariants of the base complex equation into real and imaginary parts. Then for such a system, we determine invariants from the Laplace-type invariants for the equivalent system of two linear hyperbolic equations. This is achieved by performing complex splits of the Laplace-type invariants. It is concluded, as a proposition, that the Cotton-type invariants are the same for both the approaches. The subsystem of two elliptic equations

$$u_{xx} + u_{yy} + \alpha_1 u_x - \alpha_2 v_x + \beta_1 u_y - \beta_2 v_y + \gamma_1 u - \gamma_2 v = 0,$$
$$v_{xx} + v_{yy} + \alpha_2 u_x + \alpha_1 v_x + \beta_2 u_y + \beta_1 v_y + \gamma_2 u + \gamma_1 v = 0 \quad (8)$$

is obtained by splitting of the complex linear elliptic equation

$$w_{xx} + w_{yy} + a w_x + b w_y + c w = 0, \quad (9)$$

where

$$a = \alpha_1 + i\alpha_2, \qquad b = \beta_1 + i\beta_2,$$
$$c = \gamma_1 + i\gamma_2, \qquad w = u + iv. \quad (10)$$

The Cotton invariants, corresponding to the complex elliptic equation (9), are (7) which split into the four invariants

$$\mu_1 = \alpha_{1y} - \beta_{1x},$$
$$\mu_2 = \alpha_{2y} - \beta_{2x},$$
$$H_1 = \alpha_{1x} + \beta_{1y} + \frac{1}{2}\left(\alpha_1^2 + \beta_1^2\right) - \frac{1}{2}\left(\alpha_2^2 + \beta_2^2\right) - 2\gamma_1, \quad (11)$$
$$H_2 = \alpha_{2x} + \beta_{2y} + \alpha_1\alpha_2 + \beta_1\beta_2 - 2\gamma_2.$$

These are precisely the Cotton-type invariants for the linear elliptic system (8). The simplest case is when the semiinvariants (11) are zero. In this case the elliptic PDE system (8) reduces to the Laplace system by linear transformation of the dependent variables. This is similar to the scalar linear elliptic PDE case.

Now for the system of elliptic equations (8), we derive the Cotton-type invariants by transforming the system of equations to the corresponding linear hyperbolic equations and then using the inverse transformations of the independent variables to convert the Laplace-type invariants to the Cotton-type invariants. By means of the transformations (3), the system of elliptic equations (8) can be mapped to the system of two linear hyperbolic type equations as follows:

$$u_{tz} + A_1 u_t - A_2 v_t + B_1 u_z - B_2 v_z + C_1 u - C_2 v = 0,$$
$$v_{tz} + A_2 u_t + A_1 v_t + B_2 u_z + B_1 v_z + C_2 u + C_1 v = 0, \quad (12)$$

where

$$A_1 = \frac{1}{4}\left(\alpha_1 + i\beta_1\right), \qquad B_1 = \frac{1}{4}\left(\alpha_1 - i\beta_1\right), \qquad C_1 = \frac{1}{4}\gamma_1,$$
$$A_2 = \frac{1}{4}\left(\alpha_2 + i\beta_2\right), \qquad B_2 = \frac{1}{4}\left(\alpha_2 - i\beta_2\right), \qquad C_2 = \frac{1}{4}\gamma_2. \quad (13)$$

The system of hyperbolic equations (12) has four Laplace-type invariants [13]:

$$h_1 = A_{1t} + A_1 B_1 - A_2 A_2 - C_1,$$
$$h_2 = A_{2t} + A_1 B_2 + A_2 B_1 - C_2,$$
$$k_1 = B_{1z} + A_1 B_1 - A_2 B_2 - C_1, \quad (14)$$
$$k_2 = B_{2z} + A_1 B_2 + A_2 B_1 - C_2.$$

Now by the application of the transformations (3) and complex splits, the Laplace-type invariants (14) become the Cotton-type invariants (11). We therefore conclude the following result.

Proposition 1. *For a class of a system of two linear elliptic equations* (8) *obtained from a complex base linear elliptic equation* (9) *or equivalent to a subsystem of two linear hyperbolic equations* (12) *by complex linear transformations of the independent variables* (3)*, Cotton-type invariants either constructed by splitting of the complex Cotton invariants* (7) *of the complex base elliptic equation into real and imaginary parts or those computed by split of the Laplace-type invariants* (14) *of the system of linear hyperbolic equations are identical to* (11).

3. Cotton-Type and Joint Invariants in General

In this section, Cotton-type and joint invariants for a general system of two linear elliptic equations are obtained. A general system of two linear elliptic equations is

$$\begin{aligned} &u_{xx} + u_{yy} + a_1 u_x + a_2 v_x + b_1 u_y + b_2 v_y + c_1 u + c_2 v = 0, \\ &v_{xx} + v_{yy} + a_3 u_x + a_4 v_x + b_3 u_y + b_4 v_y + c_3 u + c_4 v = 0. \end{aligned} \tag{15}$$

By means of the complex transformations of the independent variables (3), this system (15) is transformed into the system of two linear hyperbolic equations as follows:

$$\begin{aligned} &u_{tz} + A_1 u_t + A_2 v_t + B_1 u_z + B_2 v_z + C_1 u + C_2 v = 0, \\ &v_{tz} + A_3 u_t + A_4 v_t + B_3 u_z + B_4 v_z + C_3 u + C_4 v = 0, \end{aligned} \tag{16}$$

where

$$\begin{aligned} A_1 &= \frac{1}{4}\left(a_1 + ib_1\right), & B_1 &= \frac{1}{4}\left(a_1 - ib_1\right), & C_1 &= \frac{1}{4}c_1, \\ A_2 &= \frac{1}{4}\left(a_2 + ib_2\right), & B_2 &= \frac{1}{4}\left(a_2 - ib_2\right), & C_2 &= \frac{1}{4}c_2, \\ A_3 &= \frac{1}{4}\left(a_3 + ia_3\right), & B_3 &= \frac{1}{4}\left(a_3 - ib_3\right), & C_3 &= \frac{1}{4}c_3, \\ A_4 &= \frac{1}{4}\left(a_4 + ib_4\right), & B_4 &= \frac{1}{4}\left(a_4 - ib_4\right), & C_4 &= \frac{1}{4}c_4. \end{aligned} \tag{17}$$

This system of linear hyperbolic equations (16) has five semi-invariants [12] under the linear change of dependent variables. They are [12]

$$\begin{aligned} I_1 &= k_1 + k_4, \qquad I_2 = k_5 + k_8, \\ I_3 &= k_1 k_4 - k_2 k_3, \qquad I_4 = k_5 k_8 - k_6 k_7, \\ I_5 &= k_1 k_5 + k_2 k_7 + k_3 k_6 + k_4 k_8, \end{aligned} \tag{18}$$

where

$$\begin{aligned} k_1 &= A_1 B_1 + A_3 B_2 + A_{1t} - C_1, \\ k_2 &= A_1 B_3 + A_3 B_4 + A_{3t} - C_3, \\ k_3 &= A_2 B_1 + A_4 B_2 + A_{2t} - C_2, \\ k_4 &= A_2 B_3 + A_4 B_4 + A_{4t} - C_4, \\ k_5 &= A_1 B_1 + A_2 B_3 + B_{1z} - C_1, \\ k_6 &= A_3 B_1 + A_4 B_3 + B_{3z} - C_3, \\ k_7 &= A_1 B_2 + A_2 B_4 + B_{2z} - C_2, \\ k_8 &= A_3 B_2 + A_4 B_4 + B_{4z} - C_4. \end{aligned} \tag{19}$$

The system of linear hyperbolic equations (16) also has the four joint invariants [12]

$$J_1 = \frac{I_2}{I_1}, \qquad J_2 = \frac{I_3}{I_1^2}, \qquad J_3 = \frac{I_4}{I_1^2}, \qquad J_4 = \frac{I_5}{I_1^2}. \tag{20}$$

We utilize the same approach as in the previous section. Indeed via the transformations (3), the Laplace-type invariants (18) transform to the five Cotton-type invariants

$$\begin{aligned} H_1 &= \operatorname{Im}\left(K_1 + K_4\right) = \operatorname{Im}\left(K_5 + K_8\right), \\ H_2 &= \operatorname{Re}\left(K_1 + K_4\right) = \operatorname{Re}\left(K_5 + K_8\right), \\ H_3 &= \operatorname{Im}\left(K_1 K_4 - K_2 K_3\right) = \operatorname{Im}\left(K_5 K_8 - K_6 K_7\right), \\ H_4 &= \operatorname{Re}\left(K_1 K_4 - K_2 K_3\right) = \operatorname{Re}\left(K_5 K_8 - K_6 K_7\right), \\ H_5 &= \operatorname{Re}\left(K_1 K_5 + K_2 K_7 + K_3 K_6 + K_4 K_8\right). \end{aligned} \tag{21}$$

And the invariant equation is

$$\operatorname{Im}\left(K_1 K_5 + K_2 K_7 + K_3 K_6 + K_4 K_8\right) = 0, \tag{22}$$

where

$$\begin{aligned} K_1 = {} & \frac{1}{4^2}\left(a_1^2 + b_1^2 + a_2 a_3 + b_2 b_3 + 2a_{1x} + 2b_{1y} - 4c_1\right) \\ & + \frac{i}{4^2}\left(a_2 b_3 - a_3 b_2 - 2a_{1y} + 2b_{1x}\right), \\ K_2 = {} & \frac{1}{4^2}\left(a_1 a_3 + b_1 b_3 + a_3 a_4 + b_3 b_4 + 2a_{3x} + 2b_{3y} - 4c_3\right) \\ & + \frac{i}{4^2}\left(a_3 b_1 - a_1 b_3 + a_4 b_3 - a_3 b_4 - 2a_{3y} + 2b_{3x}\right), \\ K_3 = {} & \frac{1}{4^2}\left(a_1 a_2 + b_1 b_2 + a_2 a_4 + b_2 b_4 + 2a_{2x} + 2b_{2y} - 4c_2\right) \\ & + \frac{i}{4^2}\left(a_1 b_2 - a_2 b_1 + a_2 b_4 - a_4 b_2 - 2a_{2y} + 2b_{2x}\right), \\ K_4 = {} & \frac{1}{4^2}\left(a_2 a_3 + b_2 b_3 + a_4^2 + b_4^2 + 2a_{4x} + 2b_{4y} - 4c_4\right) \\ & + \frac{i}{4^2}\left(a_3 b_2 - a_2 b_3 - 2a_{4y} + 2b_{4x}\right), \end{aligned}$$

$$
\begin{aligned}
K_5 &= \frac{1}{4^2}\left(a_1^2 + b_1^2 + a_2a_3 + b_2b_3 + 2a_{1x} + 2b_{1y} - 4c_1\right)\\
&\quad + \frac{i}{4^2}\left(a_3b_2 - a_2b_3 + 2a_{1y} - 2b_{1x}\right),\\
K_6 &= \frac{1}{4^2}\left(a_1a_3 + b_1b_3 + a_3a_4 + b_3b_4 + 2a_{3x} + 2b_{3y} - 4c_3\right)\\
&\quad + \frac{i}{4^2}\left(a_1b_3 - a_3b_1 + a_3b_4 - a_4b_3 + 2a_{3y} - 2b_{3x}\right),\\
K_7 &= \frac{1}{4^2}\left(a_1a_2 + b_1b_2 + a_2a_4 + b_2b_4 + 2a_{2x} + 2b_{2y} - 4c_2\right)\\
&\quad + \frac{i}{4^2}\left(a_2b_1 - a_1b_2 + a_4b_2 - a_2b_4 + 2a_{2y} - 2b_{2x}\right),\\
K_8 &= \frac{1}{4^2}\left(a_2a_3 + b_2b_3 + a_4^2 + b_4^2 + 2a_{4x} + 2b_{4y} - 4c_4\right)\\
&\quad + \frac{i}{4^2}\left(a_2b_3 - a_3b_2 + 2a_{4y} - 2b_{4x}\right).
\end{aligned}
\tag{23}
$$

Note that we have an invariant equation here. This differs from the invariants of the split elliptic system of Section 2. We therefore have the following result.

Proposition 2. *A general system of two linear elliptic equations* (15) *has the five Cotton-type invariants* (21) *and its coefficients satisfy the invariant condition* (22).

Now the four joint invariants (20) reduce to the four invariants of the elliptic equations (15) and they are

$$
\begin{aligned}
\mu_1 &= \frac{\left(H_1^2 - H_2^2\right)H_3 + 2H_1H_2H_4}{\left(H_1^2 - H_2^2\right)^2 + 4H_1^2H_2^2},\\
\mu_2 &= \frac{\left(H_1^2 - H_2^2\right)H_4 - 2H_1H_2H_3}{\left(H_1^2 - H_2^2\right)^2 + 4H_1^2H_2^2},\\
\mu_3 &= \frac{\left(H_1^2 - H_2^2\right)H_5}{\left(H_1^2 - H_2^2\right)^2 + 4H_1^2H_2^2},\\
\mu_4 &= \frac{-2H_1H_2H_5}{\left(H_1^2 - H_2^2\right)^2 + 4H_1^2H_2^2},
\end{aligned}
\tag{24}
$$

where the semi-invariants H_1^2 and H_2^2 are both not zero. The situation when both are zero occur for the Laplace system discussed earlier. We have thus obtained the Cotton-type and joint invariants for a general linear elliptic system of two equations (15) by using the Laplace-type and joint invariants of the general system of linear hyperbolic equations (16) by utilizing the known semi- and joint invariants of [12]. We thus state the following proposition.

Proposition 3. *A general system of two linear elliptic equations* (15) *has the four joint invariants* (24).

4. Applications

Here we present some examples for illustration. We consider u, v, $\overline{u}$, and $\overline{v}$ as dependent variables and x, y, s, and t as independent variables.

Example 4. Consider the system of two linear elliptic equations

$$
\begin{aligned}
&u_{xx} + u_{yy} + \frac{2}{x}u_x + \frac{4}{y}u_y + \frac{2}{y^2}u = 0,\\
&v_{xx} + v_{yy} - \frac{4}{x}v_x - \frac{2}{y}v_y + 2\left(\frac{1}{y^2} + \frac{3}{x^2}\right)v = 0.
\end{aligned}
\tag{25}
$$

This system transforms to the simplest elliptic equations

$$
\overline{u}_{xx} + \overline{u}_{yy} = 0, \qquad \overline{v}_{xx} + \overline{v}_{yy} = 0, \tag{26}
$$

under the transformation

$$
\overline{u} = xy^2u, \qquad \overline{v} = \frac{v}{x^2y}. \tag{27}
$$

The systems of elliptic equations (25) and (26) are transformable into each other as these systems have the same Cotton-type semi-invariants

$$
H_1 = H_2 = H_3 = H_4 = H_5 = 0. \tag{28}
$$

Example 5. The system of elliptic equations

$$
\begin{aligned}
&u_{xx} + u_{yy} + (1-2y)\,u_x + (1-2x)\,u_y\\
&\quad + \left(x^2 + y^2 - x - y\right)u = 0,\\
&v_{xx} + v_{yy} + (1-2y)\,v_x + (1-2x)\,v_y\\
&\quad + \left(x^2 + y^2 - x - y\right)v = 0,
\end{aligned}
\tag{29}
$$

with the Cotton-type invariants

$$
\begin{aligned}
&H_1 = 0, \qquad H_2 = \frac{1}{4},\\
&H_3 = 0, \qquad H_4 = \frac{1}{64}, \qquad H_5 = \frac{1}{32},
\end{aligned}
\tag{30}
$$

reduces to the simple system of elliptic equations

$$
\begin{aligned}
&\overline{u}_{xx} + \overline{u}_{yy} + \overline{u}_x + \overline{u}_y = 0,\\
&\overline{v}_{xx} + \overline{v}_{yy} + \overline{v}_x + \overline{v}_y = 0,
\end{aligned}
\tag{31}
$$

by the application of the transformation

$$
\overline{u} = \exp(-xy)\,u, \qquad \overline{v} = \exp(-xy)\,v. \tag{32}
$$

The system (31) also has the Cotton-type invariants (30).

Example 6. The uncoupled system two of elliptic equations

$$\begin{aligned}
&u_{xx}+u_{yy}+\left(\frac{2}{x}+1\right)u_x+\left(1-\frac{4}{y}\right)u_y \\
&\quad+\left(\frac{1}{x}+\frac{6}{y^2}-\frac{2}{y}\right)u=0, \\
&v_{xx}+v_{yy}+\left(1-\frac{2}{x}\right)v_x+\left(1+\frac{4}{y}\right)v_y \\
&\quad+\left(\frac{2}{y^2}+\frac{2}{y}-\frac{1}{x}+\frac{2}{x^2}\right)v=0,
\end{aligned} \tag{33}$$

has the Cotton-type invariants

$$\begin{gathered}
H_1=0, \qquad H_2=\frac{1}{4}, \\
H_3=0, \qquad H_4=\frac{1}{64}, \qquad H_5=\frac{1}{32}.
\end{gathered} \tag{34}$$

Therefore it is reducible to the simple system

$$\begin{aligned}
\bar{u}_{xx}+\bar{u}_{yy}+\bar{u}_x+\bar{u}_y=0, \\
\bar{v}_{xx}+\bar{v}_{yy}+\bar{v}_x+\bar{v}_y=0,
\end{aligned} \tag{35}$$

by means of the transformation

$$\bar{u}=\frac{x}{y^2}u, \qquad \bar{v}=\frac{y^2}{x}v. \tag{36}$$

Example 7. Consider now the linear system of elliptic equations

$$\begin{aligned}
&u_{xx}+u_{yy}+\left(\frac{2}{x}+\frac{1}{2}\right)u_x+\left(\frac{1}{2}-\frac{2}{y}\right)u_y \\
&\quad+\frac{1}{2}\left(\frac{4}{y^2}-\frac{1}{y}+\frac{1}{x}\right)u=0, \\
&v_{xx}+v_{yy}+\left(\frac{2}{x}+\frac{1}{2}\right)v_x+\left(\frac{1}{2}-\frac{2}{y}\right)v_y \\
&\quad+\frac{1}{2}\left(\frac{4}{y^2}-\frac{1}{y}+\frac{1}{x}\right)v=0,
\end{aligned} \tag{37}$$

which has the joint invariants

$$\mu_1=0, \qquad \mu_2=-\frac{1}{4}, \qquad \mu_3=-\frac{1}{2}, \qquad \mu_4=0. \tag{38}$$

By using the transformation

$$s=\frac{x}{2}, \qquad t=\frac{y}{2}, \qquad \bar{u}=\frac{x}{y}u, \qquad \bar{v}=\frac{x}{y}v, \tag{39}$$

the above system reduces to the simple system

$$\begin{aligned}
\bar{u}_{ss}+\bar{u}_{tt}+\bar{u}_s+\bar{u}_t=0, \\
\bar{v}_{ss}+\bar{v}_{tt}+\bar{v}_s+\bar{v}_t=0,
\end{aligned} \tag{40}$$

because this system has the joint invariant identical to the system (37).

Example 8. Finally, the coupled system of elliptic equations

$$\begin{aligned}
&u_{xx}+u_{yy}+\left(2+\frac{1}{x}\right)u_x+2y^3x^{-3/2}v_x-\frac{2}{y}u_y \\
&\quad+\left(\frac{1}{x}-\frac{1}{4x^2}+\frac{2}{y^2}\right)u-2y^3x^{-5/2}v=0, \\
&v_{xx}+v_{yy}+\frac{2x^{3/2}}{y^3}u_x+2\left(1-\frac{1}{x}\right)v_x+\frac{4}{y}v_y \\
&\quad+\frac{x^{1/2}}{y^3}u+2\left(\frac{1}{y^2}-\frac{1}{x}+\frac{1}{x^2}\right)v=0,
\end{aligned} \tag{41}$$

with the joint invariants

$$\mu_1=0, \qquad \mu_2=0, \qquad \mu_3=-1, \qquad \mu_4=0, \tag{42}$$

simplifies to the system

$$\begin{aligned}
\bar{u}_{ss}+\bar{u}_{tt}+\bar{u}_s+\bar{u}_t+\bar{v}_s+\bar{v}_t=0, \\
\bar{v}_{ss}+\bar{v}_{tt}+\bar{u}_s+\bar{u}_t+\bar{v}_s+\bar{v}_t=0,
\end{aligned} \tag{43}$$

which has the same joint invariants as the system (41). The transformation that does this reduction is

$$\begin{gathered}
s=x+y, \qquad t=x-y, \\
\bar{u}=\frac{\sqrt{x}}{y}u, \qquad \bar{v}=\frac{y^2}{x}v.
\end{gathered} \tag{44}$$

5. Conclusion

In this paper, we have derived the Cotton-type invariants for a special class of a system of two linear elliptic equations in two independent variables which arises from the complex split of a base complex linear elliptic equation. Moreover, the Cotton-type and joint invariants for a general system of two linear elliptic equations are also obtained. Laplace 1773, in his fundamental memoir, discussed two semi-invariants under the change of dependent variables of the scalar linear hyperbolic equation, known as Laplace invariants. Later, Cotton 1900 derived semi-invariants for the scalar linear elliptic equation, known as Cotton invariants. Linear hyperbolic and elliptic equations can be transformed into each other by the application of linear complex transformation of the independent variables. So do Laplace and Cotton invariants.

By a complex split, a complex scalar linear elliptic equation has been transformed into a system of two linear elliptic equations, which is a subclass of the general system of two linear elliptic equations. Cotton-type semi-invariants for this system of elliptic equations are obtained by two approaches. One is by splitting of the complex Cotton invariants that correspond to the complex base scalar linear elliptic equation into real and imaginary parts and the second by transformation of the subsystem of the linear elliptic equations into linear hyperbolic equations and application of the linear inverse transformations on the Laplace-type semi-invariants of the hyperbolic equations to deduce the Cotton-type invariants for the required subsystem of linear elliptic equations. It is found that the Cotton-type invariants by both approaches are the same. For a general system of linear elliptic equations, the Cotton-type and joint invariants have been constructed by transformation of the system of two linear elliptic equations into a system of two linear hyperbolic equations and thereafter applying the linear inverse transformations on the Laplace-type and joint invariants of [12] to deduce the Cotton-type and joint invariants for the linear system of elliptic equations.

Conflict of Interests

It is declared by the authors that there is no conflict of interests in the publication of this paper.

Acknowledgments

A. Aslam is grateful to DECMA for hospitality and financial support for his stay at DECMA during which this work was completed as well as NUST for travel support. FMM is thankful to the NRF of South Africa for a research grant support.

References

[1] J. Kevorkian, *Partial Differential Equations: Analytical Solution Techniques*, The Wadsworth and Brooks/Cole Mathematics Series, Pacific Grove, Calif, USA, 1990.

[2] S. Lie, "Uber die Integration durch bestimmte Integrale von einer Klasse linear partieller differentialgleichungen," *Archiv der Mathematik*, vol. 6, Article ID -, pp. 328–368, 1881.

[3] S. J. Farlow, *Partial Differential Equations For Scientists and Engineers*, John Wiley and Sons, New York, NY, USA, 1982.

[4] P. S. Laplace, "Recherches sur le calcul integral aux differences partielles," in *Memoires De Lacad Emie Royale Des Sciences De Paris 1773*, pp. 341–402, 1777.

[5] E. Cotton, "Sur les invariants différentiels de quelques équations linéaires aux dérivées partielles du second ordre," *Annales Scientifiques de l'École Normale Supérieure*, vol. 17, pp. 211–244, 1900.

[6] N. H. Ibragimov, "Laplace type invariants for parabolic equations," *Nonlinear Dynamics*, vol. 28, no. 2, pp. 125–133, 2002.

[7] I. K. Johnpillai and F. M. Mahomed, "Singular invariant equation for the (1+1) Fokker-Planck equation," *Journal of Physics A*, vol. 34, no. 49, pp. 11033–11051, 2001.

[8] F. M. Mahomed, "Complete invariant characterization of scalar linear (1+1) parabolic equations," *Journal of Nonlinear Mathematical Physics*, vol. 15, supplement 1, pp. 112–123, 2008.

[9] L. V. Ovsiannikov, *Group Analysis of Differential Equations*, Academic Press, New York, NY, USA, 1982.

[10] N. H. Ibragimov, "Invariants of hyperbolic equations: a solution of the Laplace problem," *Journal of Applied Mechanics and Technical Physics*, vol. 45, no. 2, pp. 158–166, 2004.

[11] I. K. Johnpillai and F. M. Mahomed, "Equivalence problem for scalar linear (1+1) hyperbolic equations," *Problems of Nonlinear Analysis in Engineering Systems*, vol. 11, no. 22, pp. 63–74, 2005.

[12] C. Tsaousi and C. Sophocleous, "Differential invariants for systems of linear hyperbolic equations," *Journal of Mathematical Analysis and Applications*, vol. 363, no. 1, pp. 238–248, 2010.

[13] F. M. Mahomed, A. Qadir, and A. Ramnarain, "Laplace-type semi-invariants for a system of two linear hyperbolic equations by complex methods," *Mathematical Problems in Engineering*, vol. 2011, Article ID 202973, 15 pages, 2011.

[14] S. Ali, F. M. Mahomed, and A. Qadir, "Complex Lie symmetries for scalar second-order ordinary differential equations," *Nonlinear Analysis: Real World Applications*, vol. 10, no. 6, pp. 3335–3344, 2009.